



University
of Glasgow

Rao, Ravulaparti Rama (1978) *A study of swelling clay*. PhD thesis.

<http://theses.gla.ac.uk/6340/>

Copyright and moral rights for this thesis are retained by the author

A copy can be downloaded for personal non-commercial research or study, without prior permission or charge

This thesis cannot be reproduced or quoted extensively from without first obtaining permission in writing from the Author

The content must not be changed in any way or sold commercially in any format or medium without the formal permission of the Author

When referring to this work, full bibliographic details including the author, title, awarding institution and date of the thesis must be given

A S T U D Y O F S W E L L I N G C L A Y

by

RAVULAPARTI RAMA RAO B.E; M. Tech.

A thesis submitted for the degree of

Doctor Of Philosophy

Department of Civil Engineering

University of Glasgow

October, 1978

TABLE OF CONTENTS

<u>CONTENTS</u>	<u>PAGE</u>
Acknowledgements	i
Notation	ii
Summary	v
<u>Chapter 1 : STATEMENT OF PROBLEM</u>	1
1.1 Introduction	1
1.2 Expansive Soils in India	2
1.3 Definition of Swelling and Related Properties	3
1.3.1 Swelling	3
1.3.2 Swell Potential	5
1.3.3 Swell Pressure	6
1.4 Statement of Problem	7
<u>Chapter 2 : CHOICE AND DESIGN OF APPARATUS</u>	12
2.1 Introduction	12
2.1.1 General Objectives	12
2.1.2 Properties to be Measured	13
2.2 Previous Methods	16
2.2.1 Introduction	16
2.2.2 Holtz and Gibbs (1956)	18
2.2.3 Lambe (1960)	19
2.2.4 Uppal and Palit (1969)	21
2.2.5 Double Oedometer Tests	22
2.2.6 Multiple Consolidometer Method	28
2.2.7 Single Consolidometer Tests	29
2.2.8 Seed et al (1962) ^a - Swell Pressure	32
2.2.9 Seed et al (1962) - Swelling Potential	34

2.2.10	Katti et al (1969)	35
2.2.11	Finn et al (1958)	37
2.2.12	Agarwal and Sharma (1973)	39
2.2.13	Alpan (1957)	40
2.2.14	Summary of Previous Attempts	41
2.3	Points of Detail	44
2.3.1	Apparatus Friction	44
2.3.2	Compressibility of Apparatus	46
2.3.3	Compressibility of Filter Paper	48
2.3.4	Seating of the Porous Stones and Soil Sample	49
2.3.5	Summary	50
2.4	Design of Apparatus	50
2.4.1	Introduction	50
2.4.2	Compaction Mould	52
2.4.3	Isotropic Swell Pressure	53
2.4.4	Laterally Confined Swell Pressure	55
2.4.5	Laterally Confined Swell Potential	56
2.5	Design Details	57
2.5.1	Isotropic Swell Pressure	57
2.5.2	Laterally Confined Swell Pressure	60
2.5.3	Summary of the Design of Apparatus	62
<u>Chapter 3 : MATERIALS, METHODS AND RESULTS</u>		65
3.1	Introduction	65
3.2	Materials	66
3.2.1	Soils for Artificial Mixtures	66
3.2.2	Artificial Mixtures	68
3.2.3	Natural Soils	68
3.3	Methods	71

3.3.1	Limit Tests	71
3.3.2	Allophane Tests	71
3.3.3	Particle Size Distribution Tests	72
3.3.4	Organic Matter Tests	73
3.3.5	pH Value Tests	73
3.3.6	X-Ray Diffraction Tests	73
3.3.7	Compaction Tests	75
3.3.8	Sample Preparation for Swell Tests	76
3.3.9	Swell Potential Tests	77
3.3.10	Laterally Confined Swell Pressure Tests	78
3.3.11	Isotropic Swell Pressure Tests	80
3.4	Results	82
3.4.1	Introduction	82
3.4.2	Results on Artificial Mixtures	82
3.4.3	Results on Natural Soils	83
3.4.4	Effect of Temperature on Swell Pressure	85
3.4.5	Variation of Swell Properties With Time	87
	3.4.5.1 Swell Potential Vs Time	88
	3.4.5.2 Swell Pressure Vs Time	89
3.4.6	Maximum and Ultimate Swell Pressure	89
3.5	Summary and Conclusions	91
<u>Chapter 4 : PREDICTION OF SWELL PROPERTIES</u>		93
4.1	Introduction	93
4.2	Theories Based on Soil Properties	94
	4.2.1 Introduction	94
	4.2.2 Holtz and Gibbs (1956)	94
	4.2.3 Williams (1957)	95
	4.2.4 Dinesh Mohan (1957)	95
	4.2.5 Seed et al (1962)	96

4.2.6	Roderick and Jin (1963)	98
4.2.7	Da Nilov (1964)	99
4.2.8	Ranganatham and Satyanarayana (1965)	100
4.2.9	Komornik and David (1969)	101
4.2.10	Livneh et al (1969)	103
4.2.11	Nayak and Christinsen (1971)	104
4.2.12	Vajayavergiya and Ghazzaley (1973)	105
4.2.13	Chen (1975)	106
4.2.14	Comments	106
4.3	Simple Mixing Laws	107
4.3.1	Introduction	107
4.3.2	Linear Relationship	107
4.3.3	Quadratic Mixing Law	108
4.3.4	Smart's (1970) Bounds	109
4.3.5	S-shaped Relationship	110
4.3.6	Summary	111
<u>Chapter 5 : DISCUSSION OF RESULTS</u>		112
<u>Part I : Artificial Mixtures</u>		112
5.1	Introduction	112
5.2	Atterberg Limits	115
5.3	Compaction and Swell Properties	118
5.3.1	Introduction	118
5.3.2	Bentonite-Sand Mixtures	118
5.3.3	Illite-Sand Mixtures	121
5.3.4	Bentonite-Illite Mixtures	123
5.3.5	Summary of Discussion on Artificial Mixtures	124
<u>Part II : Natural Soils</u>		127
5.4	Introduction	127

5.4.1	Variation of Properties with Clay Content	128
5.4.2	Analysis of Particle Size Distribution Curves	129
5.4.3	Effect of Clay Content For First Family of Soils	131
5.4.4	Multiple Regression Analysis For Prediction of Soil Properties	135
5.4.5	Summary of Discussions on Natural Soils	138
Part III : Earlier Predictive Theories		141
5.5	Introduction	141
5.5.1	Holtz and Gibbs (1956)	141
5.5.2	Williams (1957)	142
5.5.3	Dinesh Mohan (1957)	142
5.5.4	Seed et al (1962)	143
5.5.5	Da Nilov (1964)	144
5.5.6	Ranganatham et al (1965)	144
5.5.7	Komornik and David (1969); Livneh et al (1969)	145
5.5.8	Nayak and Christinsen (1971)	146
5.5.9	Vijayvergiya and Ghazzaley (1973)	147
5.5.10	Chen (1975)	147
5.5.11	Summary of Earlier Predictive Theories	148
<u>Chapter 6 : CONCLUSIONS AND RECOMMENDATIONS</u>		150
6.1	Introduction	150
6.2	Conclusions	151
6.3	Recommendations	155
APPENDICES		
<u>Appendix 1 : Design Calculations</u>		157
A1.1	Introduction	157
A1.2	Isotropic Swell Pressure	158

A1.2.1	Introduction	158
A1.2.2	Compressibility of Water	158
A1.2.3	Expansion of Chamber	159
A1.2.4	Compressibility of Membrane	163
A1.2.5	Expansion of 'O'-Ring	165
A1.2.6	Compressibility and Bedding Error of Porous Stones	167
A1.2.7	Compressibility of Filter Paper	170
A1.2.8	Preliminary Test of Apparatus	170
A1.2.9	Expansion of a Typical Sample	171
A1.2.10	Discussion	172
A1.3	Laterally Confined Swell Pressure	173
A1.3.1	Introduction	173
A1.3.2	Use of Strain Gauges	174
A1.3.3	Use Of Proving Bar	177
A1.3.4	Compressibility and Bedding Error of Porous Stones	179
A1.3.5	Summary	179
A1.4	Conclusions	180
<u>Appendix 2 : Specific Gravity</u>		181
A2.1	Introduction	181
A2.2	Artificial Mixtures	181
A2.3	Natural Soils	182
<u>Appendix 3 : Cation Exchange Capacity</u>		184
A3.1	Introduction	184
A3.2	Experimental Procedure	184
A3.3	Results	185
<u>Appendix 4 : Isotronic Swell Potential</u>		187
A4.1	Definition and Principle	187
A4.2	Apparatus	187

A4.3	Test Procedure	188
A4.4	Results and Comments	189
<u>Appendix 5 : Non-Dimensional Compaction Curves</u>		192
<u>Appendix 6 : Elastic Mixing Laws</u>		194
A6.1	Introduction	194
A6.2	Voigt and Reuss	194
A6.3	Paul's Theory	195
A6.4	HSH Bounds	195
A6.5	Logarithmic Mixing Law	196
A6.6	Summary	196
<u>Appendix 7 : Laterally Confined Swell Pressure of Bentonite-Illite Mixtures</u>		197
<u>Appendix 8 : Analysis of Particle Size Distribution Curves</u>		199
<u>Appendix 9 : Calculation of Sample Expansion, etc.</u>		201
<u>Appendix 10: Tan ϕ_r VS Clay Content, Montmorillonite</u>		203
<u>Appendix 11: Additional Regression Equations</u>		204
<u>References</u>		205

ACKNOWLEDGEMENTS

The work described in this thesis was carried out in the Civil Engineering Laboratories at the University of Glasgow.

The author wishes to record his grateful thanks to his supervisor, Professor Hugh B. Sutherland, F.R.S.E., Cormack Professor of Civil Engineering at the University of Glasgow, for his encouragement and advice throughout the course of the investigation. The author expresses his sincere thanks and gratitude to Dr P. Smart, Lecturer in the Department of Civil Engineering, for his able guidance, constant assistance, encouragement, and for his keen interest in the research work of this thesis.

The author thanks Messrs C.M. and J. Darlow for supplying the soil samples for this study; Messrs A. McKay, R. Thornton and I. Todd for constructing apparatus; and Messrs M. Hind, W. Nisbet, and W. Henderson and Mrs Pauline A. MacLean for their assistance with experimental work.

The author extends his gratitude:

- to the Commonwealth Scholarship Commission in the U.K. for awarding the scholarship;
- to the British Council for the financial support;
- to the Ministry of Education, Government of India, for giving the opportunity to pursue higher studies;
- to his wife, Subhadra, for her encouragement over the period of this work and for typing the Tables and Figure captions of this thesis;
- to Miss S.J. Pollock for typing the draft of this thesis;
- and to Mr C.Vassie for his assistance in tracing the diagrams of this thesis.

NOTATION

(NOTE : f in right hand column means fraction.)

a	: air voids content = $\frac{\text{volume of air}}{\text{total volume}}$	%
a _i	: initial air voids content	%
a _f	: final air voids content	%
A	: Skempton's activity	%/%
C (or c)	: clay content = $\frac{\text{mass of clay}}{\text{mass of solids}}$ or = $\frac{\text{volume of clay}}{\text{volume of solids}}$	f or %
CEC	: cation exchange capacity	$\frac{\text{meq}}{100 \text{ gm}}$
DW	: volumetric water content = $\frac{\text{change in volume of water}}{\text{volume of solids}}$	%
e _i	: initial void ratio	f or %
e _f	: final void ratio	f or %
G _s	: specific gravity of solids	-
LI	: liquidity index	-
LL	: liquid limit	%
OMC (or omc)	: optimum moisture content	%
ORG	: organic matter content by weight	%
PL	: plastic limit	%
PI	: plasticity index	%
P _c	: laterally confined swell pressure	psi or KN/m ²

P_i	:	isotropic swell pressure	psi or KN/m ²
r	:	simple correlation coefficient	-
R	:	multiple regression coefficient	-
S (or s)	:	sand content = $\frac{\text{mass of sand}}{\text{mass of solids}}$ or = $\frac{\text{volume of sand}}{\text{volume of solids}}$	f or %
S_c	:	laterally confined swell potential = $\frac{\text{volume increase}}{\text{initial total volume}}$	%
S_i	:	isotropic swell potential = $\frac{\text{volume increase}}{\text{initial total volume}}$	%
S_{cs}	:	laterally confined swell amount = $\frac{\text{volume increase}}{\text{volume of solids}}$	%
S_{is}	:	isotropic swell amount	%
W	:	water content = $\frac{\text{weight of water}}{\text{weight of solids}}$	%
W_i	:	initial water content	%
W_f	:	final water content	%
Z	:	silt content = $\frac{\text{mass of silt}}{\text{mass of solids}}$	%
α	:	volumetric air content = $\frac{\text{volume of air}}{\text{volume of solids}}$	%
α_i	:	initial volumetric air content	%
α_f	:	final volumetric air content	%
v	:	volumetric water content = $\frac{\text{volume of water}}{\text{volume of solids}}$	%
v_i	:	initial volumetric water content	%

w_f	:	final volumetric water content	%
γ_d	:	optimum dry density	lb/cft or kg/m ³
ϕ_r	:	residual angle of internal friction	deg

SUMMARY

The primary concern of this thesis is to measure the swell properties of compacted soils (swell potential and swell pressure) and to predict these and related properties using more easily measured parameters such as soil composition, organic matter content, and plasticity characteristics. These predictions are required for reconnaissance studies and for the design of minor works. Several methods of prediction were already available, but they are shown to disagree, and some attention was paid to the reasons for this disagreement.

Apparatus were designed and constructed for both isotropic and laterally confined swell pressure measurement. Calculations and observations suggested that all known swell pressure apparatus lead to underestimates of the order of 15% or more. The effect of temperature fluctuations on measurements was also demonstrated. Strain gauges were found to be superior to proving bars for the laterally confined swell pressure apparatus. In an extra-long term isotropic swell pressure test it was found that the swell pressure rose to a maximum and then fell to a steady value, this phenomena being attributed to the stress relaxation of the sample.

Measurement of swell pressure and swell potential were made on three artificial mixtures comprising bentonite-sand, illite-sand, and bentonite-illite; and on one series of 10 natural samples.

In the clay-sand mixtures, whilst the swell potential

itself was found to be non-linear with composition, the transformation of data to a volumetric basis (i.e. swell amount) showed that swell amount was proportional to clay content apart from weak interaction effects in the illite-sand mixtures. The swell pressure variation of both clay-sand mixtures was found to be non-linear. Algebraic models were found which do represent the (observed) data accurately, and consideration of these models suggested certain physical phenomena as causes of the non-linearity. In the bentonite-sand mixtures, the bentonite dominated the behaviour over the entire range of the composition, whilst in illite-sand mixtures the predominant component in the mixture dominated the behaviour. It was noted that Kenny's (1967) results for $\tan \phi_r$ followed a similar pattern of behaviour, and it was suggested that the differences in behaviour between the bentonite and the illite were due to the relative importance of physico-chemical effects and mechanical-friction effects for the two clay minerals.

It was found that prediction of the Atterberg limits, and compaction, and swell properties of natural soils can be based on clay content alone only in severely limited circumstances, in which there is a close similarity (geological, mineralogical, textural, etc) between the samples. However, linear multiple regressions were sufficient to predict reasonably accurately these soil properties, when the correct choice of independent parameters was made.

Chapter 1

STATEMENT OF PROBLEM

1.1 INTRODUCTION

Experience and research in many parts of the world have shown the special nature of problems associated with structures built on expansive soils. Most of the foundation problems of residential, light commercial and industrial buildings, buried pipes, side-walks and roadways on expansive clays, do not result from excessive loading of the subsoil but from the seasonal swelling or shrinking of the soil itself.

Clay soils with low water content exhibit an increase in their volume change when they come into contact with water and this phenomena is known as swelling. A decrease in water content is associated with a decrease in volume and this is shrinking. Some clay soils are very sensitive to variation in water content and such soils are classified as expansive or swelling soils. These types of soils have been encountered in many parts of the world, including India, Canada, U.S.A., South Africa, Israel and Australia. Expansive soils are encountered in parts of England also, where they are sometimes troublesome. In tropical countries, like India, where there is a large seasonal variation in soil moisture and rainfall, the volume changes in the soil cause cracking of light structures built on them. Chen (1975) reports that in the U.S.A. alone the loss caused by these soils comes to around 2300 million dollars per year.

Although soil physicists have developed theories to explain the behaviour of swelling soils, it is only within the past two decades that engineers have attempted to interpret these in an engineering sense. As expected, these interpretations have varied widely and in some instances there has been disagreement. The identification of swelling soils and the quantitative prediction of the magnitude of the potential swelling pressure and volume change are still problems for soil engineers.

1.2 EXPANSIVE SOILS IN INDIA

In India, large tracts are covered by expansive soil known as Black Cotton Soil, also referred to sometimes as 'Regur' soils. The major area of their occurrence is the south of the Vindhya Range covering almost the entire Deccan Plateau. These soils cover an area of about 200,000 sq. miles and thus form about 20% of the total area of the country.

Indian Black Cotton Soils are generally heavy soils of montmorillonitic origin, exhibiting characteristic properties of swelling and shrinking as the moisture content varies, resulting in high volume changes. Vertical cracks up to about 4 in (100 mm) wide at ground level extending up to 10 ft (3 m) depth are noted on these soils. These soils are sometimes classified as belonging to the 'Chernozem' group (Dinesh Mohan, 1973) because of their dark colour, suggesting organic matter; and of the typical horizon of calcium carbonate concentrations known as 'Kankar' in India. Soils similar to Indian Black Cotton soils are known to occur in

other parts of the world also, e.g.: 'Badole' of the Sudan, 'Pampus' of Argentina, 'Tirs' of Morocco, 'Margilatic Soils' of Indonesia, 'Black Earths' of Java, Sumatra and Australia and many other places in Africa.

Geologically their formation is usually associated with basalts. However, they can occur in association with granitegneiss, slate, shale, sandstone and limestone. These soils occur both as residual and transported soils. In the latter case the strata are usually found to be thicker, up to about 26 ft (8 m) deep.

Although the Black Cotton soils are ascribed geologically to diverse parent rocks for their origin; from an engineering point of view, however, it is their volume change properties and subsequent swell pressure and differential movements of the ground that are of significance. The range of liquid limit for Indian Black Cotton soils is 40 to 100, plasticity index 20 to 60, and shrinkage limit 9 to 14 (Dinesh Mohan, 1973).

The present study was intended as a preliminary to a study of Indian Black Cotton soils. In particular, it was intended to establish methods of assessment and of analysis which could be used for these, and to collect detailed information for comparative purposes.

1.3 DEFINITION OF SWELLING AND RELATED PROPERTIES

1.3.1 Swelling

According to Mielenz and King (1955), two mechanisms are

involved in the swelling of soils:

- (1) a relaxation of effective compressive stress related to an enlargement of capillary films,
- (2) osmotic imbibition of water by clay minerals that have an expanding lattice.

These two definitions are widely accepted as explaining swelling and can be elaborated as follows:

If a saturated sample is removed from the ground, the total stresses that acted in-situ are reduced to zero and a negative pore pressure or capillary tension, u_k , is set up in the sample.

$$\text{Since } \sigma' \doteq \sigma - u \quad (1.1)$$

where, σ' = effective stress

σ = total stress

u = pore water pressure.

It follows:

$$\begin{aligned} \sigma' &\doteq \sigma - (-u_k) \\ &= \sigma + u_k \end{aligned} \quad (1.2)$$

When the total stress is zero, it is seen that $\sigma' \doteq u_k$, i.e. the effective stress in the sample is approximately equal to the capillary tension. If the sample is submerged in water, the menisci are destroyed and u_k becomes zero, there must be a tendency for the sample to swell. This is

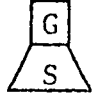
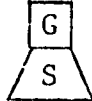
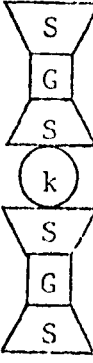
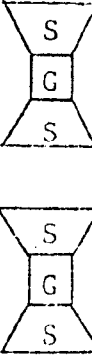
the first mechanism defined by Mielenz and King.

With no confining stress, additional swelling will occur in some clays depending on the kind and amount of clay minerals present, their exchangeable ions, electrolyte content of the aqueous phase, particle size distribution, void size and distribution, the initial structure, water content and possibly other factors (Mielenz and King, 1955). Published data indicate that the magnitude of volume change (swelling) decreases with the type of clay mineral present, in the order montmorillonite, illite and kaolinite. The schematic structure and properties of these minerals are given (Gromko, 1974) in Table 1.1. For a relatively inactive kaolinite clay, therefore, one would not expect any appreciable additional swelling due to osmotic imbibition. On the other hand, a montmorillonitic clay which has a readily expandable lattice would swell considerably following the release of capillary tension, the adsorption of water being due primarily to osmotic imbibition. This is the second mechanism defined by Mielenz and King.

1.3.2 Swell Potential

In order to standardise the quantification of swell, Seed et al (1962) defined 'swell potential' as the percentage volume change under a 1 psi (6.895 KN/m^2) surcharge of a laterally confined sample, compacted at optimum water content to maximum dry density in the standard A.A.S.H.O. (DSIR, 1972) compaction test. This definition is adopted here.

The percent swell of an unconfined sample is defined as

Property (1)	Mineral		
	Kaolinite (2)	Illite (3)	Montmorillonite (4)
Schematic structure*	 		
Particle thickness	0.5 μ -2 μ	0.003 μ -0.1 μ	9.5 \AA
Particle diameter, in microns	0.5 μ -4 μ	0.5 μ -10 μ	0.5 μ -10 μ
Specific (Ref. 37) surface, in sq meters per gram	5-30	50-100	600-800
Cation exchange (Ref. 18) capacity, in milliequivalents per 100 g of clay	3-15	10-40	80-150
Maximum swelling (Ref. 7), as a percentage, for surcharge load, in tons per square foot			
0.1	Negligible	350	1,500
0.2	Negligible	150	350

*G = Gibbsite sheet; S = Silica sheet; k = Potassium ion.

Table 1.1 Diagrams and Properties of Clay Minerals (reproduced from Gromko, 1974).

'isotropic swell potential' in the present study. The other conditions imposed in the definition of 'swell potential' are kept unaltered.

1.3.3 Swell Pressure

There are at least three possible definitions that can be attributed to swell pressure. They are:

- (1) Swell pressure may be defined as the pressure to compress a fully swollen sample back to its original void ratio,
- (2) Swell pressure may be defined as that pressure developed by dead load, for which, there will be neither compression nor expansion of the sample on saturation,
- (3) Swell pressure may be defined as the pressure which must be developed to prevent volume change when free water is supplied.

Definition (1) has the disadvantage of changing the initial structure of the sample during swelling, and the sample may not attain the initial particle orientation when brought back to its original void ratio. In order to determine the swell pressure by definition (2), it is necessary to test a series of identical samples with exactly the same initial conditions and then resort to interpolation or even extrapolation. This serves as an indirect means of measuring swell pressure.

In the present study, swell pressure was measured in accordance with definition (3), by attempting to prevent any

volume change in the sample.

Many of the apparatus used for swell pressure measurement at constant volume also maintain the shape of the sample constant. In this study, however, two types of test were made in accordance with the following terms:

1. Laterally confined swell pressure, neither shape nor volume may change;
2. Isotropic swell pressure, shape may change, volume may not.

In all these tests free water was supplied to the sample until it developed a maximum pressure, and no attempt was made to saturate the sample.

1.4 STATEMENT OF PROBLEM

When substantial and expensive structures are to be built on expansive soils, the swell properties of the soils should be carefully measured directly, and the design arranged accordingly. When the structures to be built are either small and inexpensive or extensive such as roads, the cost of these careful direct measurements would represent too high a proportion of the total cost of the works and recourse must be made to indirect prediction of the swell properties from more easily available parameters. These indirect methods are also required for preliminary reconnaissance studies. Many studies of prediction methods have been made previously. However, they are unreliable for general validity, e.g. from the data of Ranganatham et al (1965), for a Black Cotton Soil with a clay content

equal to 38%, plasticity index equal to 36.6%, Seed et al (1962) predict a swell potential of 8.9%, whilst Chen (1975) predicts a value of 5.4% against a measured value of 20.2%. The general problem with which this thesis is concerned is the measurement of swell properties and the prediction of these properties from more easily measured parameters such as the texture of the soil, type of clay, and the organic matter content.

The following individual factors and their various combinations reflect the major soil characteristics relative to susceptibility to swell:

- (1) Solid phase: soil type and physico-chemical properties related to such.
- (2) Granulometric parameters: variations in grain size distribution and texture of soil particles.
- (3) Structure and fabric: Arrangement, surface and water retention characteristics of soil pore space.
- (4) History related to apparent loading-unloading stresses to which the soil media have been subjected, and the technique of sample preparation.
- (5) Time, environmental changes, and the thixotropic properties of the soil media.
- (6) Type and electrolytic properties of pore fluid.

Although the original interest of this study had been concerned with the influence of the type of clay minerals in swelling, it is necessary to have a better understanding

of the effect of the quantity of clay (i.e. of clay size particles) on the geotechnical properties of expansive soils. There have been few studies in which the various geotechnical properties of expansive soils are studied over the full range of clay content in either artificial mixtures or natural swelling soils. Therefore, a series of 10 closely related natural soils were selected for this study spanning a wide range of clay content (9 to 87%), and these were supplemented by two series of artificial mixtures in which the clay content was varied from 0 to 100%, viz, bentonite-sand and illite-sand; and a third series of mixtures of bentonite-illite. In order to isolate the effect of clay type and content, it is necessary to standardise the factors (3), (4), (5) and (6) listed above; and inclusion of these four factors would have required a testing programme of unreasonable length. In order to achieve this, the initial conditions of testing were fixed at the optimum compaction conditions and distilled water was used as the pore fluid for all tests in this study.

Since there are neither Indian, nor British, nor American standard tests for the measurement of swell properties, it was necessary to choose or design suitable apparatus for this study. The design of the apparatus used is described in the following chapter together with a review of apparatus which had been used for similar measurements by other workers.

The experimental programme is reported in Chapter 3.

The variation of soil properties with clay content for the artificial mixtures are explained either by a linear mixing law, or if interaction between the components was present, by suitable non-linear mixing laws. In particular it will be shown that if swell amount is referred to the volume of solids, then to a first approximation swell amount is proportional to the clay content in both series of clay-sand mixtures considered, apart from a relatively small interaction effect. No previous investigation of this simple hypothesis has been found, presumably because most investigators have expressed their results only in terms of swell potential, which will be shown here to be a strongly non-linear function of clay content. It will also be shown here that swell pressure is a non-linear function of clay content; a parallel will then be drawn between the patterns of behaviour of swell pressure and of the tangent of the angle of residual friction, $\tan \phi_r$, and on the strength of this observation it will be suggested that whereas physico-chemical forces control the swell pressure of montmorillonitic clays, mechanical-frictional forces are more important in illitic clays, this suggestion being in agreement with the analysis which Olson and Mesri (1970) made of the pattern of behaviour of consolidation. The non-linear laws which were considered are reviewed in Chapter 4, and the analyses are presented in Chapter 5.

The analyses presented in Chapter 5 will also show that two courses of action are possible if accurate predictions of the swell properties are to be obtained for natural soils.

In the first course of action, the soils must be placed into closely defined "families", and separate sets of predictive equations used for each family. It will be shown in Chapter 5 that accurate predictions can be obtained in this way, but that the criteria for inclusion in a family are very strict indeed. In the second course of action, the predictions must be made by using a relatively large number of carefully chosen independent variables; for the soils studied here clay content, silt content, organic matter content, and plasticity index were used. Somewhat surprisingly, plasticity index was not required for predicting swell pressure for these particular soils. Silt content was definitely required, although no previous investigation of its influence had been reported.

The main part of this thesis is concerned with the fundamental points mentioned above, viz, the patterns of behaviour of swell pressure and swell amount, and the proper choice of independent variables for use in predictive equations. However, the data collected does permit both direct and indirect investigation to be made of some of the predictive equations which had been proposed earlier. These are reviewed in Chapter 4 and analysed in Chapter 5.

All the series of measurements made in this study were designed with a view to using statistical analysis to determine between alternative hypotheses.

Chapter 2

CHOICE AND DESIGN OF APPARATUS

2.1 INTRODUCTION

2.1.1 General Objectives

The present objective is to study the relationships between the swell properties, the mineralogical properties and the simple index properties of swelling clays. Even though this approach is not new and has been examined by many previous researchers, there has been hardly any reported instance in which the factors affecting swelling have been tested statistically in order to assess their level of significance. Aitchison (1969) pointed out that the literature covering this subject, although voluminous, tends to be vague and discontinuous. It is vague because it is not expressed in a uniform technical language. It is discontinuous because, engineers have been disposed to consider their own problems of expansive soil behaviour more in the light of their own experience than in terms of any general pattern of recorded knowledge. This situation appears to be a consequence of three reasons:

- a) Even when similar equipment and testing procedures have been employed to measure swell properties, some investigations concentrated on undisturbed clays, a few on sedimented natural samples, and some on compacted natural soils, in some cases only artificial clays were studied.
- b) Even for one type of sample preparation, the methods and procedures of measuring the swell properties varied considerably in many instances. Although swelling phenomena

have been fully recognised for many years a standard method of measuring the swell properties of clay has not been established to date. One difficulty in providing a suitable yardstick for measuring the swelling characteristics is that numerous variables are involved. Chen (1975) rightly stressed the urgent need for uniformity in testing expansive soils.

c) In some instances, points of detail affecting the measurement of the swell properties were not previously taken into account. For example, Fredlund (1969) has shown how erroneous the consolidometer could be unless corrections were applied for a number of procedural effects, and yet the consolidometer had been the most widely used equipment between 1956 and 1969 to measure both the amount of swell and swell pressure.

To achieve the present object of studying the relationships between various swell properties and the numerous factors influencing them, it is not only important to subject these factors to statistical analysis to assess their level of significance, but it is equally important to choose or design suitable equipment for measuring the swell properties selected for study. Whilst the accuracy and reliability of the measured values is important, it should be emphasised at this stage that the equipment should be simple and direct and should be suitable for repetitive use on a large number of samples.

2.1.2 Properties to be Measured

The important swell properties selected for measurement

in this investigation are the swell potential and swell pressure. It was decided to measure these properties (a) on an unconfined sample, which is allowed to swell or develop swell pressure freely in all directions, and (b) on a laterally confined sample, which is allowed to swell or develop swell pressure only in the vertical direction. The sample in the former case is expected to swell with no shear strain in the ideal case, if it is isotropic. The sample in the latter case is expected to swell, ideally, under zero lateral strain. In deciding on these conditions, it was thought that the in-situ swelling is partly 'volumetric' and partly 'with shear'. The two cases (volumetric with no shear and shear with no volume change) are the two extremes that can occur in-situ. The case of lateral confinement falls somewhere in between the two extreme cases mentioned. Even though the swelling in-situ is partly 'volumetric' and partly 'with shear', the two extreme cases may occur approximately in the following situations. If a relatively small "building" is underlain by swelling soil, there is no rigid lateral restraint, which leads to 'volumetric' swell; and, in the case of a large "building" of the same type of soil, a one-dimensional situation tends to prevail so leading to swelling with lateral restraint. Logically swelling with shear and swelling with volumetric change are separate in that, there will be no volume change in the former case, whilst it is a case of free swelling with no shear in the latter case. Mathematically, these two cases correspond to the deviatoric component of the strain tensor,

$(\epsilon_{11} - \frac{\epsilon_{11} + \epsilon_{22} + \epsilon_{33}}{3})$ and to the volumetric component of the strain tensor $(\epsilon_{11} + \epsilon_{22} + \epsilon_{33})$, small strain version), respectively. In practice it is difficult to conduct a test of pure shear with no volume change, and it is not a swelling case either. Therefore, it was decided to measure the swell properties in the two confinement conditions, viz, (i) soil allowed to swell freely against equal all-round pressure, and (ii) soil laterally confined and allowed to swell only in the vertical direction.

At this stage, it was necessary to choose suitable equipment in order to measure the following dependent parameters.

- (i) swell potential on a sample which is allowed to swell freely in all directions without any confinements (For brevity, this will be referred to here as 'isotropic swell potential'),
- (ii) isotropic swell pressure,
- (iii) swell potential on a sample, which is laterally confined and allowed to swell only in the vertical direction. (For brevity this will be referred to hereafter as 'laterally confined swell potential' or simply as swell potential),
- (iv) laterally confined swell pressure.

The next section is a review of previous work by earlier researchers on the design and use of equipment for measuring the swell properties. This review throws some light on the merits and limitations of the earlier equipment and assisted in the choice and design of suitable apparatus with which reliable measurements of the above mentioned four parameters could be

made for the present investigation. Points of detail of the apparatus are reviewed in section 2.3. The design of apparatus is reported in section 2.4.

2.2 PREVIOUS METHODS

2.2.1 Introduction

Holtz and Gibbs (1956) were probably the first to measure swell properties in the laboratory, and subsequently several attempts were made by other research workers to improve upon their method. The available methods of measurement in the laboratory vary in complexity of concept and accuracy. Even in a consolidometer, which has been used to a large extent for these purposes, the procedures of testing vary greatly from worker to worker. A review of the earlier attempts is given in the following section, and it becomes apparent from the review that there is still a need for the design of some simple apparatus that will permit the measurement of the four selected swell parameters (mentioned in the previous section) with the least amount of procedural effect and on a large number of samples.

Whilst there are many different test methods and equipment for determining the swell properties of expansive soils in the laboratory, these methods and equipment may be divided into two general groups. The first group includes all tests in which a soil specimen is soaked or immersed in water during the test. In this group of tests the soil water suction at the end of the test is exactly or nearly equal to zero. The second group embraces all tests in which the suction can be controlled during the test. The first group of tests, which

are less expensive than those of the second group, are used for economy when it is not necessary to consider conditions other than the extreme case of 'full swell' given by soaking or immersion. The main advantage of the first group of tests is the relatively simple equipment and test procedure. The swell potential and swell pressure determined from these tests usually represent the highest possible values. The equipment and test procedure for the second group of tests are necessarily more complicated and time consuming than those of the first group of tests and are dependent upon the kind and range of suctions to be applied during the test. The use of the second group of tests would be essential if it were desired to make a precise evaluation of the volume change characteristics of expansive soils or for a quantitative analysis of heave or other problems related to soil moisture changes. In so far as the engineering applications in practice are concerned, these two groups of tests may be used to supplement each other in order to achieve the maximum efficiency in conducting the desired soil investigation and analysis (Chu et al, 1973). However, for the present purpose, in which a simple apparatus is required to test a large number of samples, apparatus of the first group is appropriate.

In the first group of tests discussed above (i.e. where free water is supplied until the soil water suction of the sample finally reaches zero), both the swell and swell pressure develop gradually over a length of time and ultimately reach their maximum values. The time required to record these maximum values of swell properties depends mainly on the thickness of the sample employed for testing. Thus, even simple tests are slow to complete, e.g. 2 - 12 weeks each

in the present work. In consequence, (1) care must be taken that the maximum swell pressure is developed, and (2) the number of samples which can be tested will be restricted.

The equipment and test procedures of the earlier workers are presented below one by one. Some significant points of detail that contribute to the measurement of various swell properties are then discussed in section 2.3. Consideration was given to these factors in choosing and designing the necessary equipment for the present study. From these considerations, the methods finally adopted in this study to measure four selected swell properties were: (1) the isotropic swell pressure equipment based on the design of Finn et al's (1958) apparatus; (2) the isotropic swell potential measured using a triaxial cell under an equal all-round back pressure of 1 psi (6.895 KN/m^2); (3) the laterally confined swell pressure apparatus based on the equipment used by Seed et al (1962)^a; and (4) the laterally confined swell potential measured in a pot somewhat similar to that of a consolidometer pot, the procedure of measurement being in accordance with the original definition of swelling potential (Seed et al, 1962).

2.2.2 Holtz and Gibbs (1956)

Holtz and Gibbs (1956) proposed a simple test called the free-swell test. This test is performed by slowly pouring 10 cm^3 (0.61 in^3) of dry soil passing the No 40 sieve into a 100 cm^3 (6.1 in^3) graduated cylinder filled with water and noting the swollen volume of the soil after it comes to rest at the bottom. The free-swell value in percentage is

determined by using the expression:

$$\text{Percentage free-swell} = \frac{\text{final volume} - \text{initial volume}}{\text{initial volume}} \times 100$$

This value of percentage free-swell was used empirically to express the degree of expansion.

The main drawbacks of this free-swell test are:

- (a) air may be entrapped in the sample during swelling;
- (b) the method of test has not been standardised.

This test has been superseded by the use of consolidometers, etc, to measure the swell properties.

It was pointed out (Dawson, 1956) that the volume readings may be terminated before the sample has had sufficient time to swell completely, and as a result use of this test might lead to an underestimation of the free-swell value. This cannot be taken as a serious objection, as it would always be possible to define a suitable period of test if the test were to be standardised.

The free-swell test was intended essentially to measure the material properties by estimating the degree of expansion. This test, in fact, might still be useful to give a preliminary idea of the nature of the soil during field reconnaissance.

2.2.3 Lambe (1960)

According to Chen (1975), the determination of the Potential Volume Change (PVC) of soil was developed by Lambe(1960) in order to identify the degree of expansion of a swelling clay. The sample is first compacted in a fixed ring consolidometer with compactive effort of 55,000 ft-lb per cu. ft (2632 KN - m per cu.m). Then an initial pressure of 200 psi

(1379 KN/m²) is applied and the sample is submerged in water. During this process the sample is partially restrained from vertical expansion by a proving ring. The proving ring reading is taken at the end of 2 hrs. The reading, expressed as pressure, is designated as swell index. Using Fig. 2.1, the swell index can be converted to Potential Volume Change. Chen (1975) does not give full details on the use of this graph. Lambe established the following categories of PVC rating:

<u>PVC rating</u>	<u>Category</u>
less than 2	Non-Critical
2 - 4	Marginal
4 - 6	Critical
greater than 6	Very Critical.

Since almost all of the swell potential and swell pressure tests carried out in the present study took at least 2 weeks to develop maximum values, the time period of 2 hr given for the PVC test is too short; the sizes of the present samples were comparable to those of Lambe. This test also suffers from the drawback that there is no unique relation between swell index (i.e. swell pressure) and potential volume change. For example, it can be seen from Fig. 2.1, that for a swell index value of 2000 lb/sq.ft, the potential swell can be categorised anywhere between 'marginal' and 'very critical', unless the soil exists precisely in one of the two extreme conditions mentioned in Fig. 2.1.

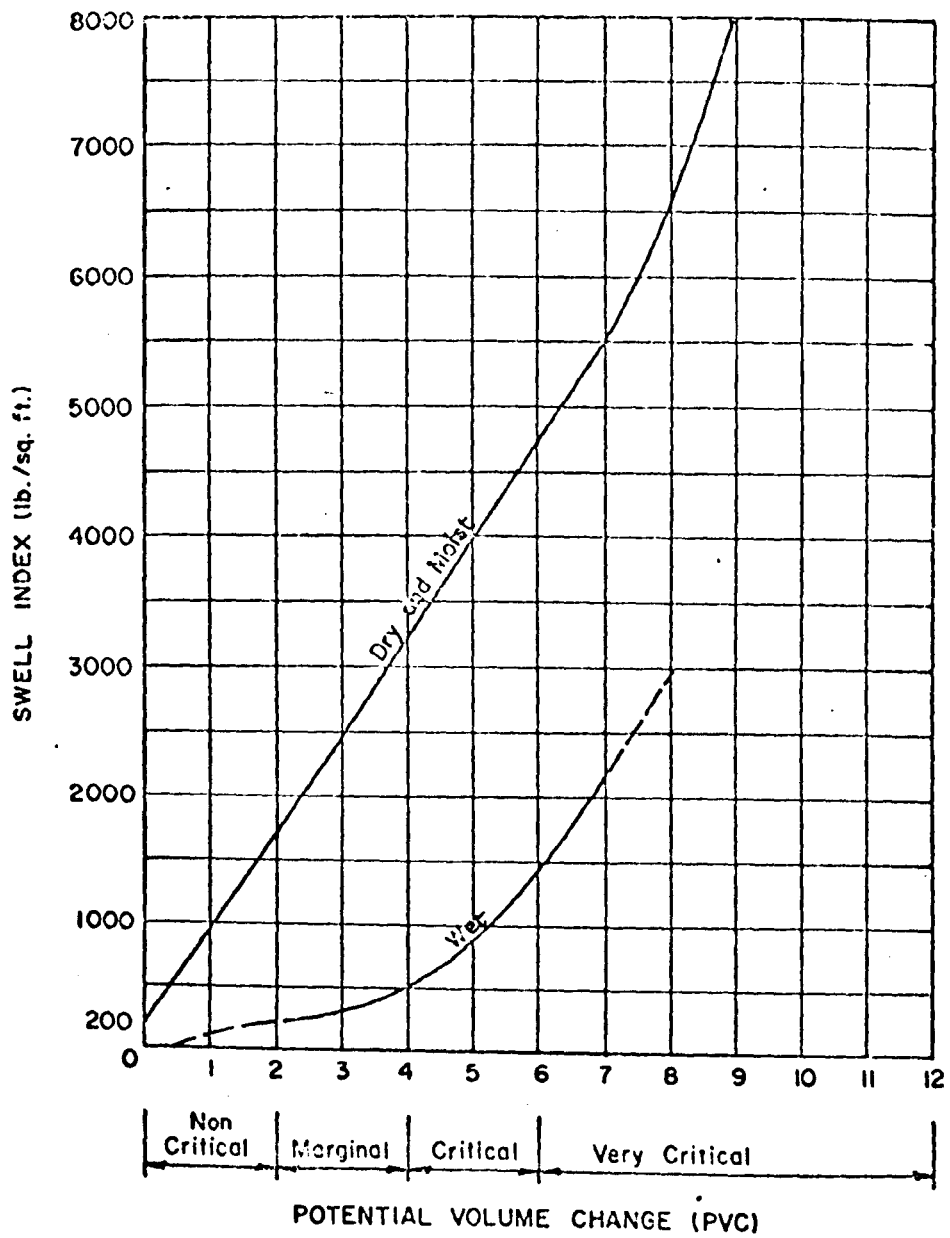


Fig. 2.1 Swell Index versus Potential Volume Change (reproduced from Chen, 1975).

Although Chen (1975) commented that the PVC meter test should be used only as a comparison between various swelling soils, it is really a swell pressure test from an unusual initial condition; and Seed et al's (1962) procedure described below was preferred for the present work.

2.2.4 Uppal and Palit (1969)

In the absence of any particular procedure being standardised to measure swell pressure, one general procedure, in view of its simplicity, has been widely used in soil laboratories around the world. This simple procedure is to measure the vertical pressure from the deflection of a proving ring fixed over the top of the sample, which is enclosed in a cylindrical mould, the mould being filled with water till the sample is completely submerged. Sufficient time is allowed until the sample develops its maximum value of swell pressure. In many instances, the mould designed for performing the California Bearing Ratio test is used as the enclosing mould. This method is not free from criticism, because a fraction of the potential total upward pressure will not be recorded because a certain amount of swelling is accommodated within the deformation of the proving ring.

To avoid errors which may be caused due to the deformation of the proving ring, Uppal and Palit (1969) suggested a modification to this method, which consisted in enclosing the sample, compacted at a particular moisture content to a certain density, into a metallic mould with

a perforated base to enable the sample to absorb moisture to saturation. A number of such samples are taken and various dead loads are applied to the samples. The swelling (taken as the volume change in vertical direction and recorded with a dial gauge) is recorded when the sample is completely swollen and plotted against increasing overburden pressure. From this relationship, Fig. 2.2, the overburden for no swell is extrapolated. The overburden for the no swell condition divided by the cross-sectional area of the sample is taken as the swell pressure of the sample. Presumably, this procedure could be modified so that interpolation is used instead of extrapolation.

This procedure is similar to multiple consolidometer test used by Noble (1966). Comments on Uppal and Palit's method are deferred until the multiple consolidometer method has been described in the next section but one.

2.2.5 Double Oedometer Tests

Of the many methods available to predict the amount of total heave under a given structural load, the double oedometer technique developed by Jennings and Knight (1958) based on the concept of effective stress has received wide attention. The general test procedure is as follows:

Two consolidometer rings are filled with undisturbed samples from adjacent locations. The first sample is kept at its natural moisture content, and a confined compression test is performed. The second sample is submerged in water under a small nominal pressure of 20 lb/sq.ft (0.96 KN/m^2) and is allowed to swell. When the swelling is complete, a

Note :- The Curve is for a set of Samples with identical initial conditions. Different Curves will be obtained with different initial conditions.

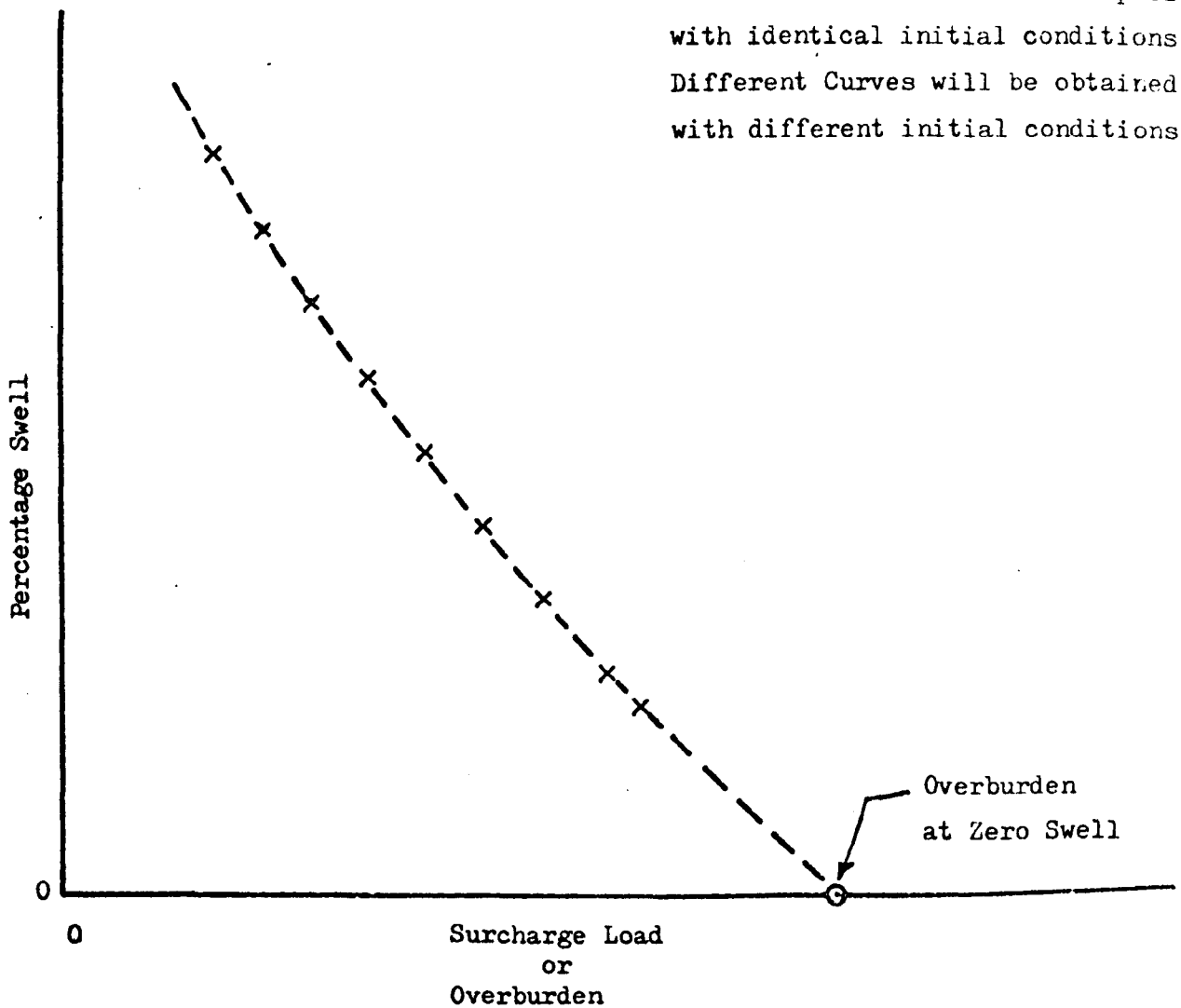


Fig. 2.2 Sketch to Illustrate The Principle of Swell Pressure Measurement by Uppal and Palit, 1969.

consolidation test is performed in the conventional manner. The two compression curves are plotted on the same diagram, and one of the curves is selected for vertical adjustment in order to bring the virgin sections of both curves into agreement as shown in Fig. 2.3.

The basic principle involved in this method is given below and illustrated in Fig. 2.3.

A soil sample taken at a depth Z has an overburden pressure $P_0 = \gamma Z$, where γ is the unit weight of the soil. In this expression, P_0 is the total pressure. The void ratio at the overburden pressure is e_0 . The settlement due to a load increment Δp can be calculated from the corresponding change in void ratio, $e_0 - e_1$. If no load is applied, the soil under a covered area will gain moisture and swelling will take place. The condition will alter P_0 , resulting in a new effective pressure $P_0 + U_L$ represented in the upper saturated curve by $P_0 + U_L$ and e_2 (Fig. 2.3). If D is the depth of the water table, and γ_w is the unit weight of water, $U_L = \gamma_w (D - Z)$. Jennings and Knight (1958) seem to treat $P_0 + U_L$ as the effective pressure and to assume that any changes in γ are negligible. The effect of the load increment is then again taken into consideration, and the final values are $(P_0 + U_L + \Delta p)$ and e_3 . The final conditions of movement may then be predicted by adding the effects of the void ratio changes, $e_3 - e_0$, over the whole profile. The method is essentially based on the assumption that there is a point during compression at which the initially unsaturated soils pass from an applied pressure to an effective phenomenon and the compression curve joins with the

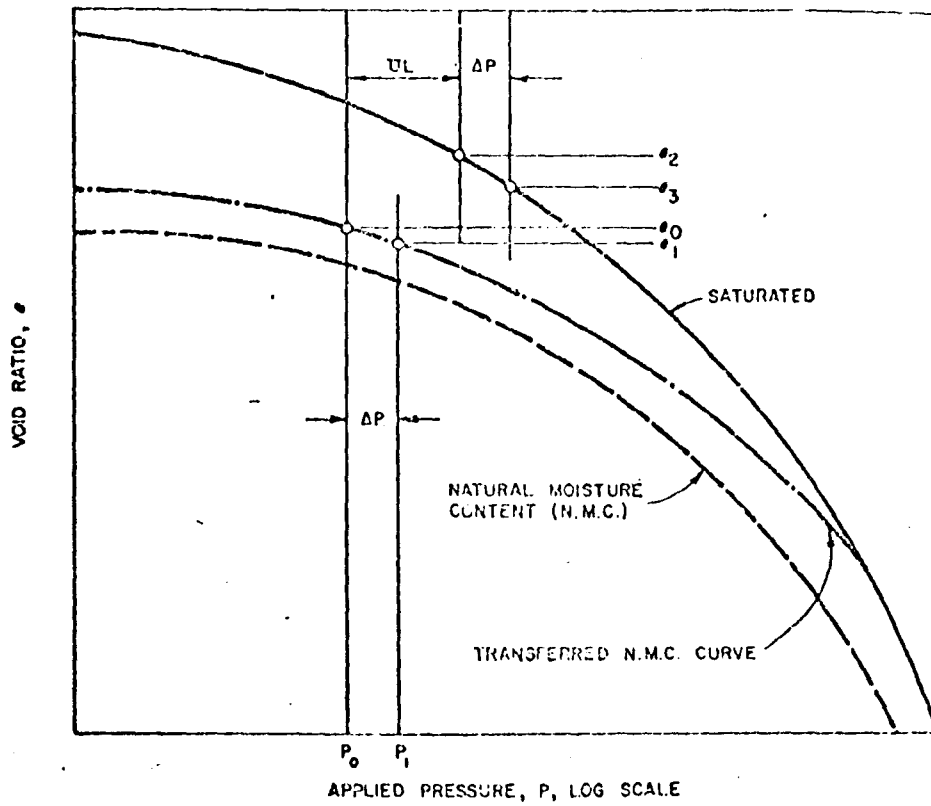


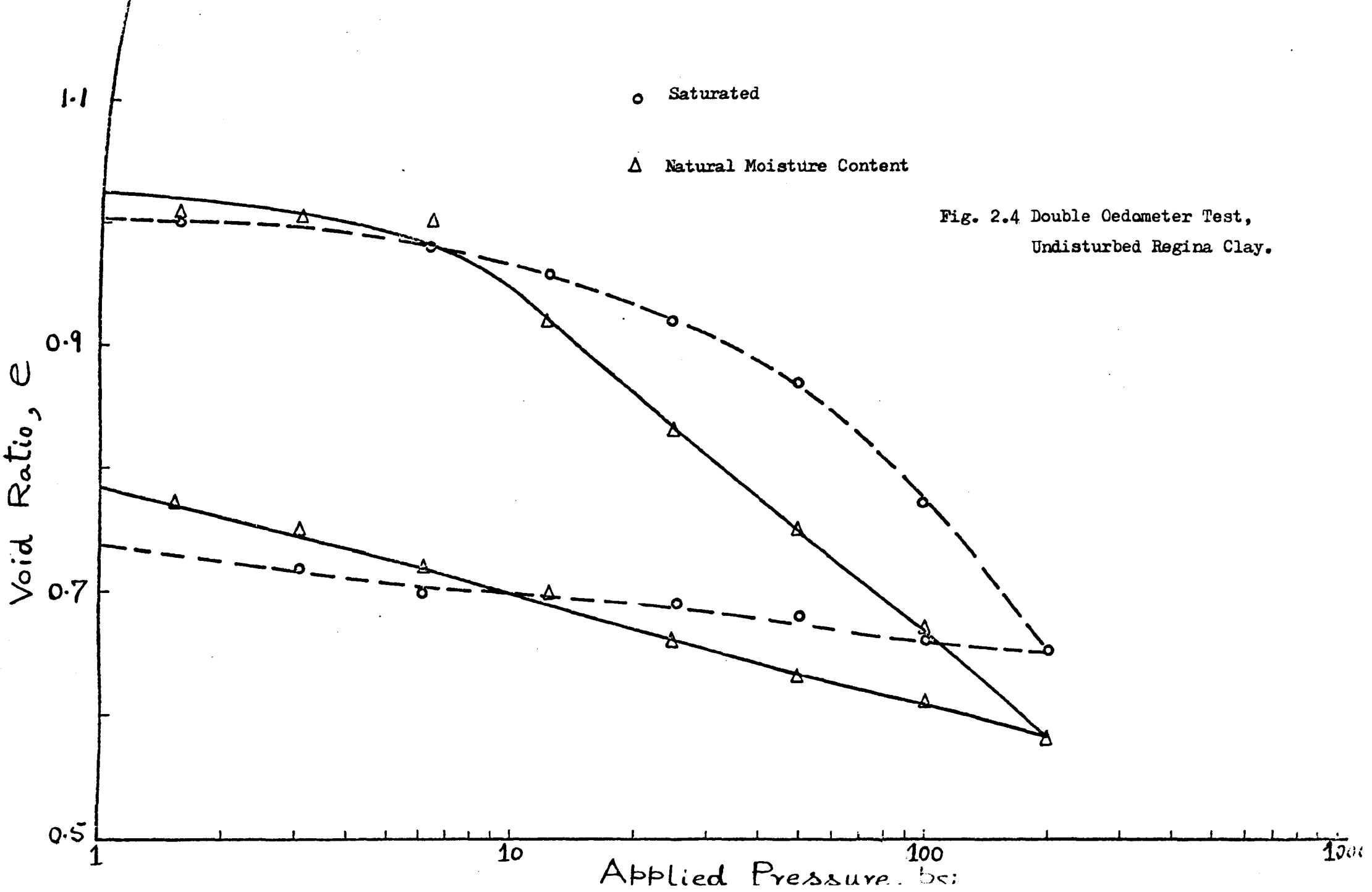
Fig. 2.3 e - log P Curves showing adjustment to bring Straight Line portions coincident (reproduced from Jennings and Knight, 1958).

virgin consolidation curve.

The double oedometer test takes account of many of the factors determining soil volume change, but it does not include the effect of horizontal stresses. While the results of this test have correlated fairly well with field measurements of heave, this test seems generally to overestimate heave by about 16% (Chen, 1975). Care must be taken in this test to avoid testing partially saturated samples with such small degrees of saturation that upon wetting and application of load, the soil will tend to collapse; otherwise heave will be overestimated (Jennings, 1961). An error would occur if there were significant initial in-situ water pressures. Usually, water is allowed access under relatively small loads in this test, because insufficient water may otherwise enter the sample. Since water enters in-situ soil under overburden loads, it is assumed that the same soil conditions occur whether inundation occurs prior to or following loading, i.e. the path of heave is not significant.

Fig. 2.4 illustrates a practical difficulty which sometimes arises with double oedometer tests. Fig. 2.4 is for a double oedometer test performed in this investigation on undisturbed Regina clay. It can be seen that the slopes of the straightline portions of the two curves are different, resulting in some difficulty in bringing the straightline portions into coincidence. A Wykeham-Farrance oedometer was employed for these tests.

The difference in the slope of the straightline portions for the Regina clay was unexpected but was confirmed by



repeating the tests on a compacted bentonite-kaolinite (1:1) mixture and employing the same oedometers as above (Fig. 2.5).

As a further check, two pairs of tests were simultaneously performed on Bearsden soil (a collapsing type of soil, but low swelling), one pair being tested in a Wykeham-Farrance oedometer, and the other pair in a clockhouse oedometer. The results of these tests are shown in Figs. 2.6 and 2.7. Although there are slight differences in the overall results on the two machines, it can be seen however, that the difference in the slope of the two straightline portions in each test, is much smaller than observed in the other two soils mentioned above. The results on Bearsden soil are almost in full agreement with the results published elsewhere on other soils for the double oedometer technique.

It appears from the above results that in highly swelling soils it may not be uncommon to observe considerably different slopes for straightline portions of the two curves thereby invalidating the technique of overlapping. Therefore other test procedures were considered for the present work.

The following comments (Smart, 1975) draw attention to some further points of the double oedometer technique for predicting the heave of the expansive soils:

(1) Whilst performing the oedometer tests at natural water content, the samples should neither take up water by absorption of vapour from the atmosphere; nor should they lose water by evaporation; nor should they exchange water with the porous stones, until the later stages of the test, when

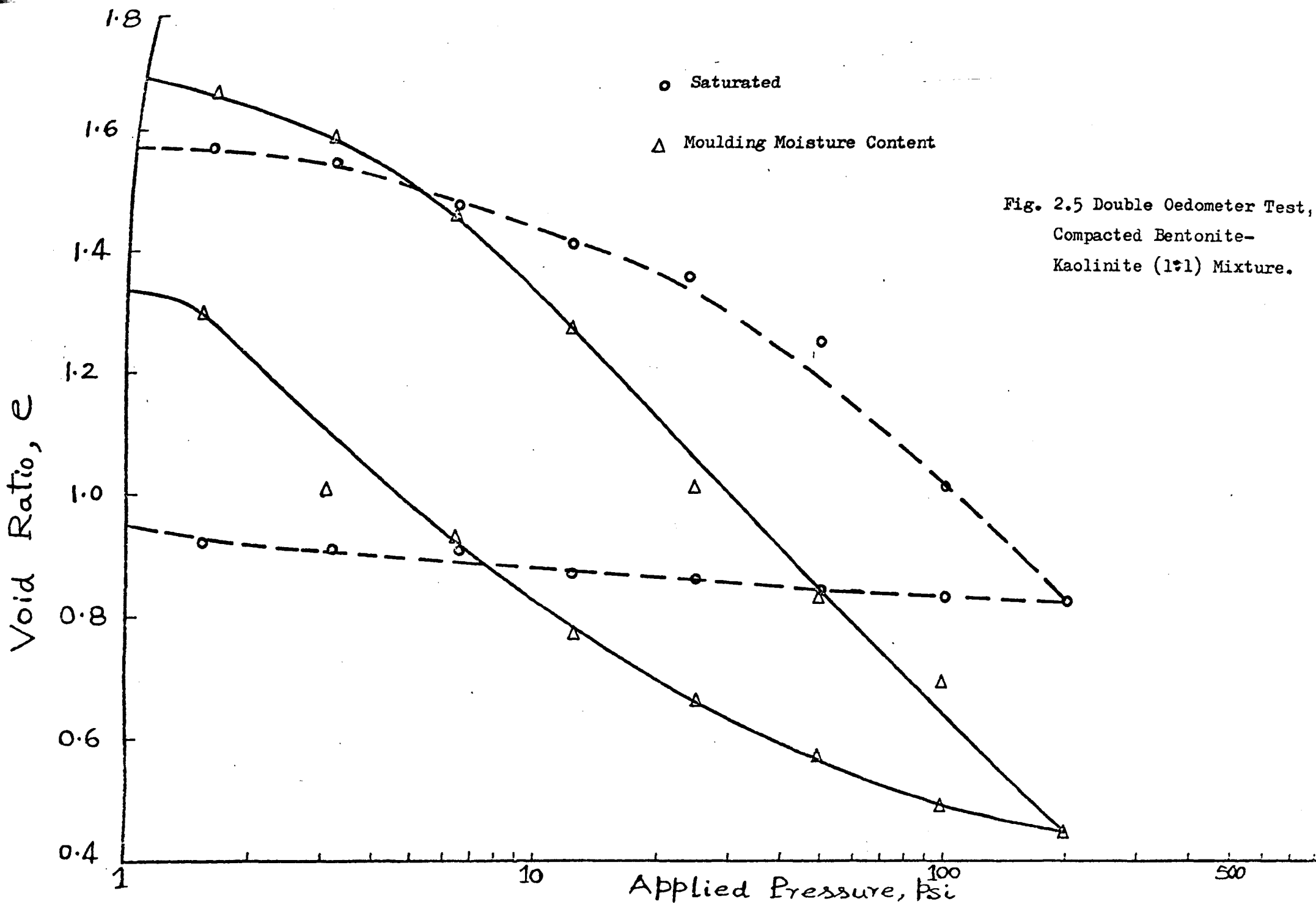
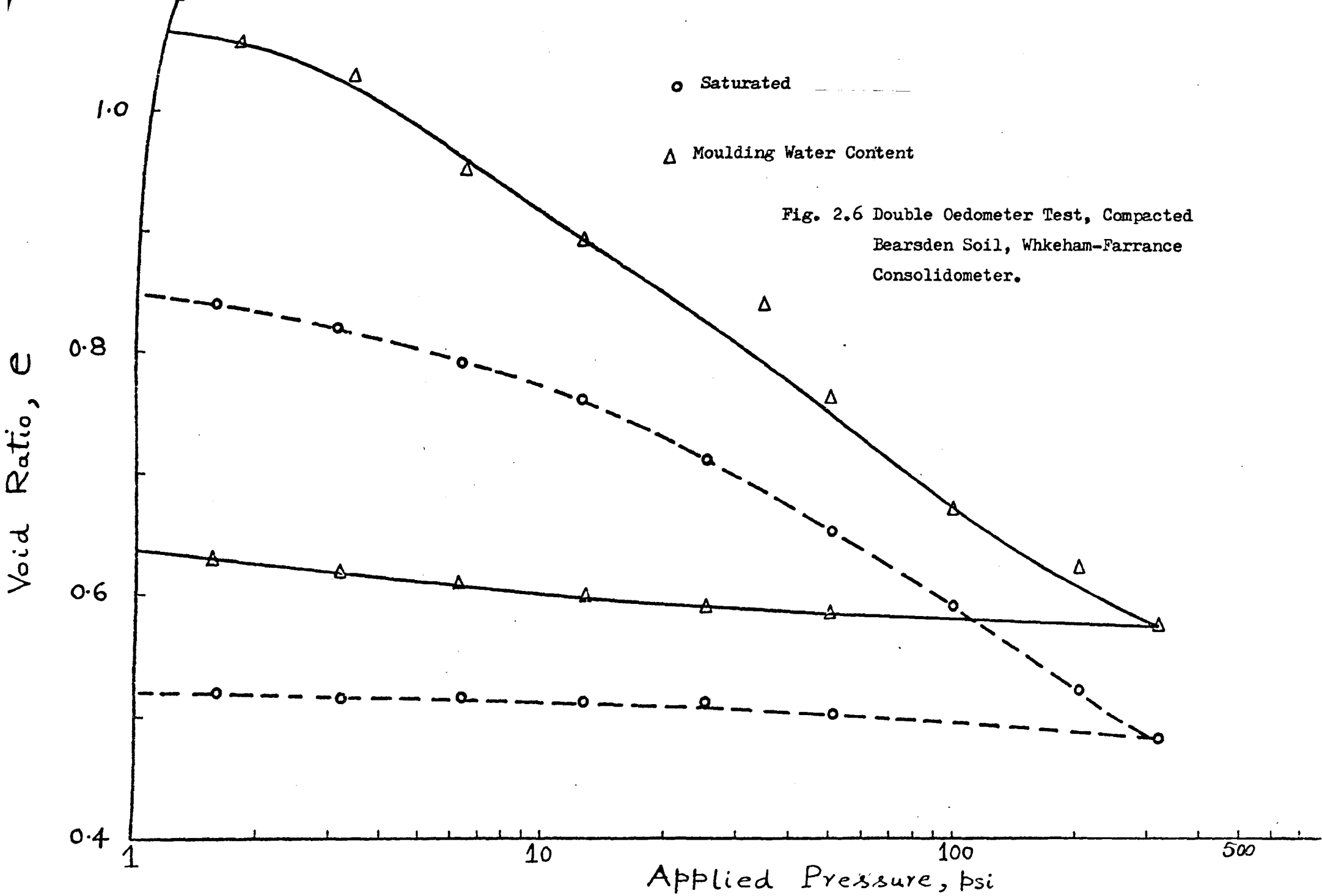


Fig. 2.5 Double Oedometer Test, Compacted Bentonite-Kaolinite (1:1) Mixture.



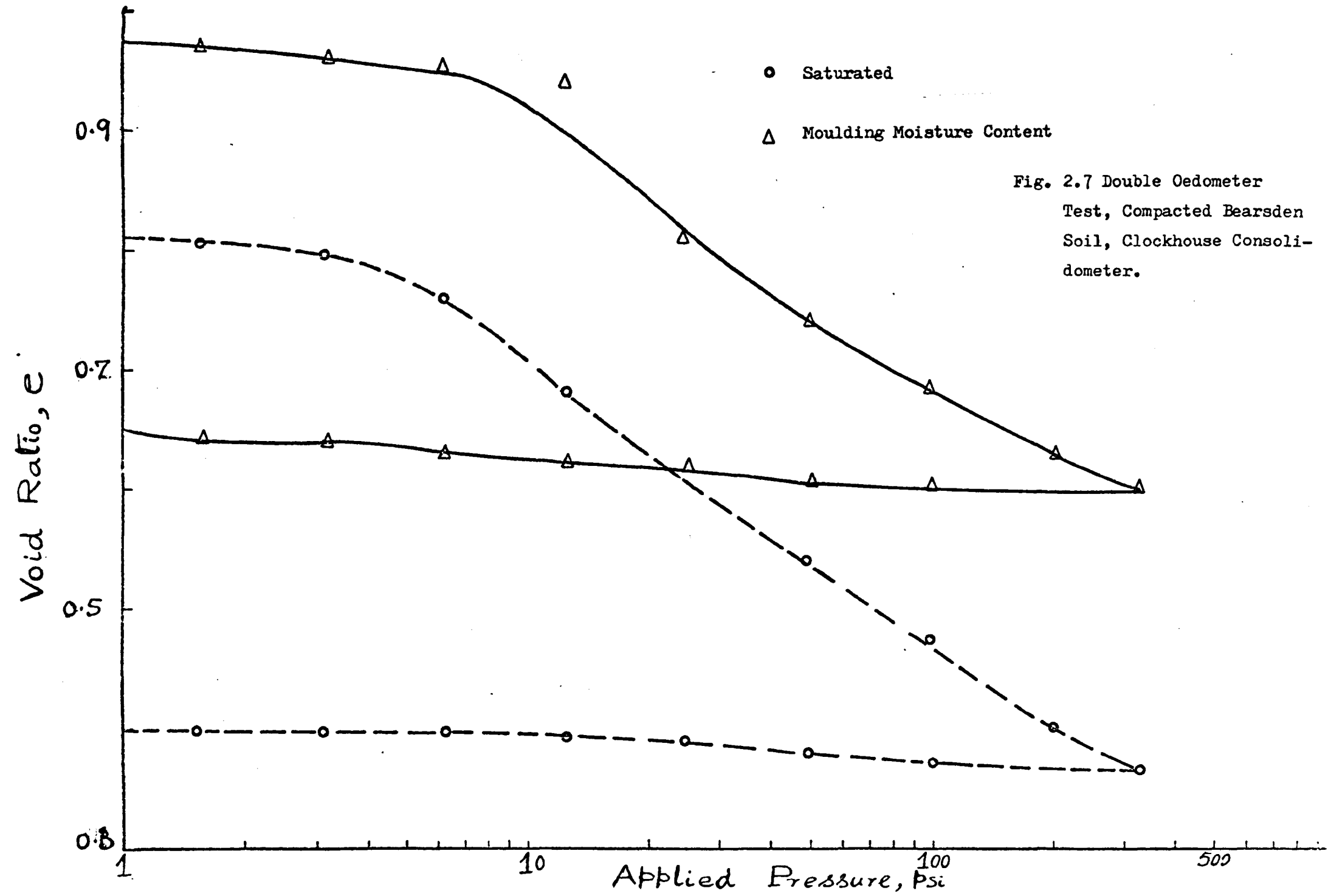


Fig. 2.7 Double Oedometer Test, Compacted Bearsden Soil, Clockhouse Consolidometer.

some water will be squeezed out. A reasonable compromise may be to test in a Rowe's cell (Rowe et al, 1960), in which the sample is almost totally confined, adjusting the initial moisture content of the porous stone to suit the particular sample being tested. Alternatively, the pore water tension of the sample might be controlled by applying suction to the porous stone, but it would be necessary to determine the correct tension to be applied, and this would vary from both stage-to-stage of one test and from test-to-test.

(2) During the tests at natural moisture content, during the early stages, the existence of a pore-water tension within the samples results in these tests being total-pressure tests, as is perhaps appropriate for partially-saturated samples. Towards the end of the test, so much air may be squeezed out that the samples become nearly saturated, and the tests then become effective pressure tests. Thus, a slight complication may arise in the estimation of e_0 for the strata lower (or higher) than that for which the sample was taken.

(3) The correctness of the estimation of e_0 rests on the assumption that when the samples are reloaded to the in-situ total overburden pressures, P_0 , whilst at their natural moisture contents, the correct values of pore water tension are restored, which may or may not be the case.

(4) The correctness of the estimation of e_1 depends on the appropriateness of the Natural Water Content curve; but, in-situ, the load increment, Δ_p , will change the pore-water tension, causing a change in the moisture content profile, and a further change in the pore-water tension profile, much as happens to the pore-pressure during the consolidation of

saturated clays. Unless the stones in the consolidometer accurately represent the layers of soil above and below the layer of the soil being considered, which is unlikely, the changes in the sample in the oedometer will not accurately represent the changes in the soil in-situ. Thus, there is likely to be a slight approximation in the estimation of settlement (which occurs in the intermediate calculations).

(5) The correctness of the estimation of $P_2 (= P_0 + \Delta_u)$ depends largely on the estimation of the pore-water pressure, Δ_u . This is difficult and the formula given earlier for pore water pressure when swollen, $[\Delta_u = -\gamma_w(D - Z)]$, should be reviewed in the light of the circumstances of every particular case.

The general procedure suggested for the double oedometer test is quite appropriate to a structure for which construction and settlement are relatively rapid and swelling is relatively slow. This would frequently seem to be so for swelling clays in the narrow sense, i.e. montmorillonitic surface soils in dry climates. However, in wet climates, in heavily overconsolidated clays, foundation excavations both unload and expose the sub-foundation strata, which may swell rapidly before the structure is constructed. It is necessary to make appropriate adjustments when predicting heave in the latter cases.

Prudence suggests that the consolidometer samples which are to swell should be say 2 mm less in height than the ring of the consolidometer at the start of the tests.

2.2.6 Multiple Consolidometer Method

Noble (1966) studied the swelling characteristics of a post-glacial lacustrine clay by means of standard consolidation apparatus. In Noble's method a number of identical samples are subjected to various oedometer tests, in order to determine a single swell parameter (i.e. laterally confined swell pressure). This method is therefore called the multiple consolidometer method.

Noble allowed various specimens (prepared to constant initial conditions) to swell under various surcharge loads in the standard consolidation apparatus. An empirical relationship was obtained between volume change, surcharge load and initial water content. Swell pressure for no volume change was obtained by interpolation or extrapolation. A plot of volume change versus surcharge load, obtained from multiple consolidometer test data, is shown in Fig. 2.8. Uppal and Palit (1969) followed a similar procedure (presented earlier) except that they used a mould and dial gauge instead of the consolidometer.

Both Noble's (1966) and Uppal and Palit's (1969) procedures are useful for design purposes, and the stress path can be adjusted to give a closer approximation to that encountered in-situ than is obtained in the double oedometer test. Many of the points of detail presented later will apply to these tests, so that the final value of the measured swell pressure may be erroneous unless a number of corrections are applied to the experimental data. However, a series of tests is necessary in both cases in order to estimate the swell pressure of a single soil, so neither

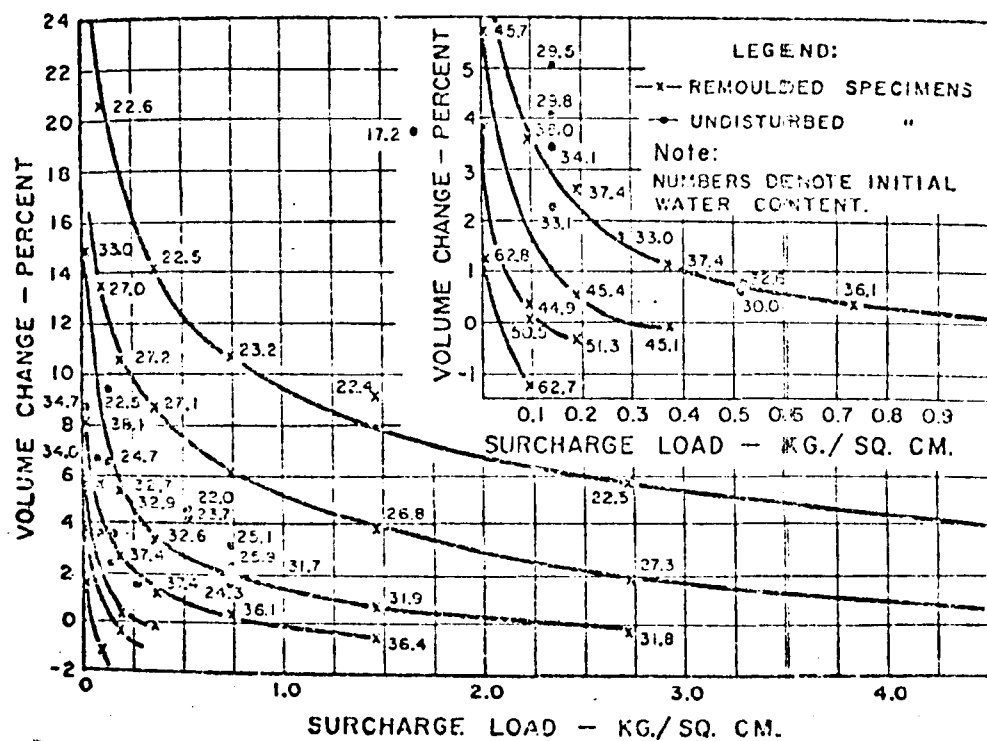


Fig. 2.8 Volume Change versus Surcharge Load from Experimental data (reproduced from Noble, 1966).

procedure was appropriate here.

2.2.7 Single Consolidometer Tests

Fredlund (1969) studied the procedures for swell pressure tests carried out in a single consolidometer. Although various procedures are used, he noted that two types of tests have been common to measure laterally confined swell pressure. These are the free swell test and constant volume tests. In either test, the sample is placed in a consolidometer and subjected to a nominal pressure of 1 psi (6.895 KN/m²). The samples are then submerged in water. In the free swell test, the sample is allowed to change volume until equilibrium is reached. The sample is then loaded and unloaded in the conventional manner. The pressure required to reduce the volume of the sample to its original volume is termed the swell pressure of the soil. In the constant volume test, the total stress on the sample is increased after submersion in order to keep it at constant volume. In this case, the pressure at which the volume tends neither to increase nor to decrease is termed the swell pressure of the soil.

The two procedures outlined above produce swell pressure values that are considerably different. Fredlund (1969) presented and discussed a set of typical free swell and constant volume test results. His results are shown in Fig. 2.9 and are plotted using dashed and solid lines to show those portions of the curve which are only total stresses and those portions which are effective stresses respectively. Additional construction lines are shown to demonstrate the

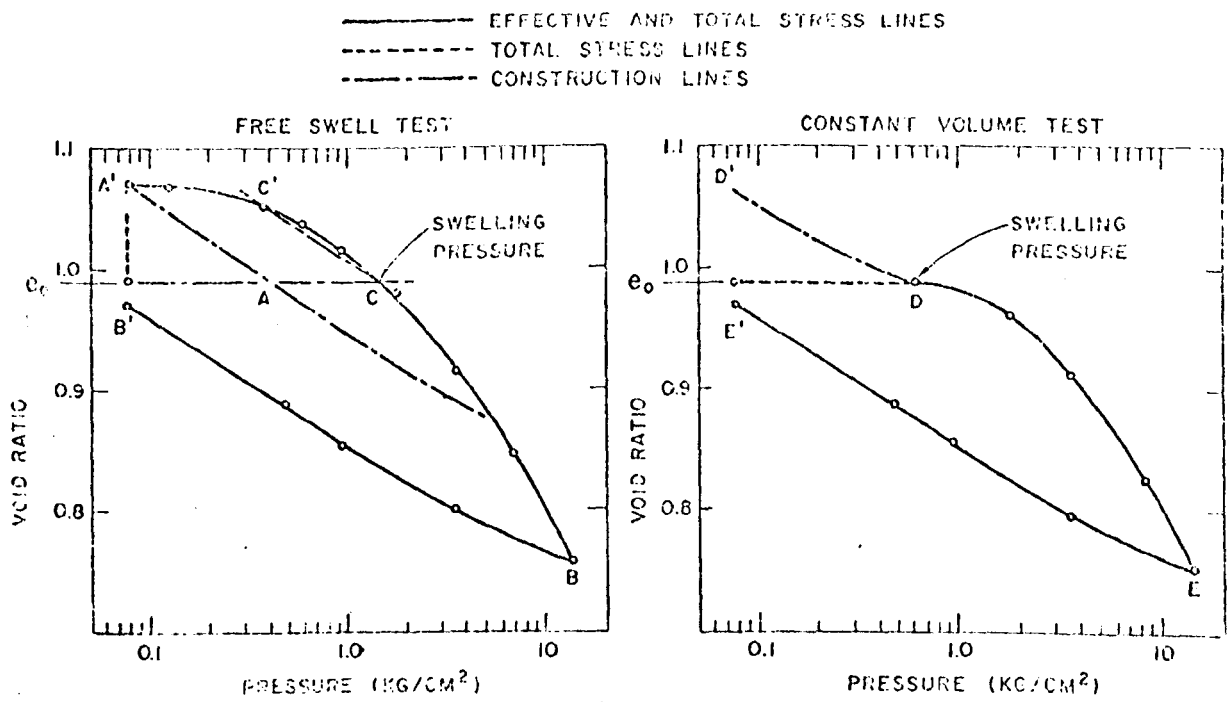


Fig. 2.9 Typical Free Swell and Constant Volume Consolidation Test Results (reproduced from Fredlund, 1969).

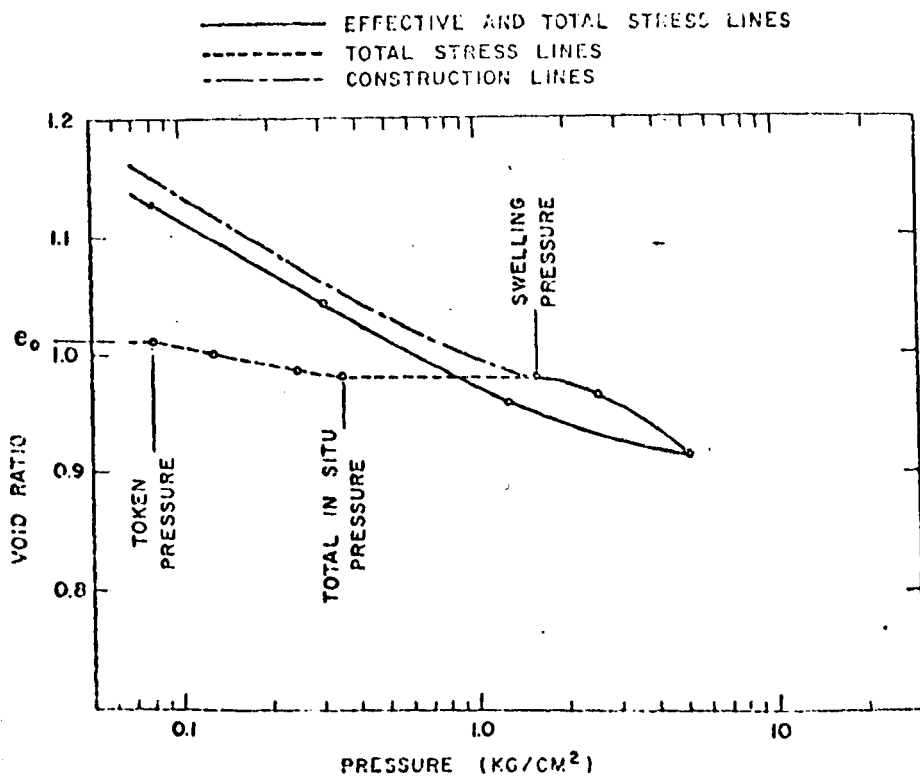


Fig. 2.10 Modified Constant Volume Consolidation Test Results (reproduced from Fredlund, 1969).

interpretation of the results. The construction is based primarily on the assumption that the rebound curves remain parallel when shifted vertically on the void ratio versus effective pressure plot. On the constant volume test, the initial effective stress in the soil is assumed to be equal to the value at point D. During submersion in water, the negative stresses in the pore water were released until atmospheric pressure was attained. Release of the total stress on the sample would allow rebound along line D-D¹. Using the same line of reasoning for the free swell test leads us to assume that point A should be of similar magnitude to point D from the constant volume test. However, a prediction of heave, based upon the free swell test, generally assumes the initial field effective stress equal to point C.

The swell pressure obtained from the free swell test (point C) appears to be incorrectly interpreted; however, the results continue to be used in practice because they produce a more conservative design. Skempton (1961) stated that the value obtained for swell pressure from a constant volume test gives an indication of negative pore pressures in-situ if the sample had not been disturbed or allowed to dry after sampling. Applying this reasoning to the interpretation of constant volume tests performed on dessicated lacustrine clays in Western Canada would indicate that in many cases the in-situ pore pressure was actually positive (Fredlund, 1969). Since the water table there is well below the depth under consideration, the most logical error would appear to be in the measurement of swell pressure. In other

words, the measured swell pressure is too low. However, this does not mean that the free swell test is a more accurate simulation of the field conditions but, rather, that procedural factors have produced an underestimation of the swell pressure measured in the constant volume test. One cause for a difference in these two tests may also be due to changes in soil structure during the recompression stage of the free swell test.

Fredlund (1969) observed that most of the points of detail presented later will be significant only at small pressures, and in the light of this observation modified the constant volume test. In the modified constant volume test the sample is trimmed, placed in a consolidation pot, and a token pressure applied for an initial dial reading. The sample is covered to prevent evaporation, and the load on the sample is doubled in increments (allowing each to come to equilibrium) until the load on the sample is equal to the total vertical pressure existing in the field. The sample is then submerged in water, and the test continued according to a constant volume test procedure. The typical results of a modified constant volume test presented by Fredlund are shown in Fig. 2.10. It is, however, important to note that a correction should be made for the compressibility of the apparatus, which otherwise underestimates the measured values to a considerable extent even with the modified procedure. The modified constant volume test is superior to either the free swell or constant volume tests in that the sample is allowed to consolidate under the total in-situ pressure. In other words, this test approximates

the same stress path as in the field, at least in some cases.

The modified constant volume test, with a nominal value of in-situ pressure would be fairly simple; but it would not correspond to the definition adopted here, which requires that all change of volume be prevented. Thus, the simpler test described in the next section, was preferred here.

2.2.8 Seed et al (1962)^a - Swell Pressure

Seed et al (1962)^a while studying the factors influencing swell potential and swell pressure, used an expansion pressure device (Fig. 2.11) that is commonly employed by the State Highways Departments in U.S.A., in connection with the design of pavements. The procedure used for preparing the specimen and measuring the expansion pressures is described below:

Samples are mixed to the desired water content and compacted in 4 in (102 mm) diameter moulds, using a kneading compactor to form specimens approximately 2.5 in (64 mm) high. The samples are then subjected to static pressure until moisture is exuded. The pressure is then released and the sample allowed to stand for half an hour. A perforated plate with a vertical stem is placed on top of the sample, and the mould containing the sample is placed in an expansion pressure device so that the stem of the plate firmly contacts the centre of a horizontal proving bar fixed at each end. A seating load of 0.4 psi (2.8 KN/m²) is used at the ends. A dial gauge is mounted to record subsequent deflections of the proving bar. Water is poured on the

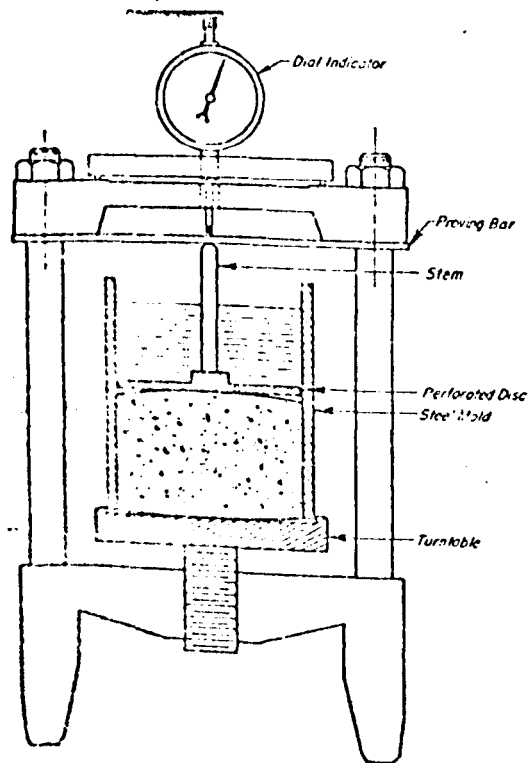


Fig. 2.11 Swell Pressure Measuring Apparatus on a Laterally Confined Sample (reproduced from Seed et al, 1962)^a.

upper face of the sample and the pressure that developed is observed by noting the proving bar deflection. Calibration of the proving bar permitted computation of the expansion pressure.

It should be noted, however, in this procedure the sample is not maintained at constant volume, in as much as the proving bar must deflect upwards to measure the expansion pressures, and the sample is thus allowed to expand by an amount equal to the deflection of the proving bar. Thus, while the actual sample expansion is quite small (0.0004 inch per 1 psi for a $\frac{1}{4}$ " thick proving bar), the true swell pressure at zero volume change is not measured, but rather a swell pressure corresponding to a small amount of swell is determined. The investigators noted that even this small volume increase has a marked effect on the observed pressures.

At this stage it appears certain that one either has to use sophisticated systems like electrical relay systems or servo-mechanisms to maintain zero volume change or resort to the simple equipment (like the one discussed above) by trying to bring the sample expansion to the lowest possible minimum. It can be seen later that even sophisticated equipment using electrical relay systems does not yield precise values of swell pressure unless a small correction is made. As the objective of this study was to test a large number of samples in a simple, direct and reliable apparatus, it was felt that the apparatus used by Seed et al (1962)^a should serve as an ideal piece for further modification and improvement. It also appeared desirable to change the means of measuring the swell pressure by fixing some

strain gauges to the tie bars and avoiding the proving bars, proving rings and dial gauges. The apparatus redesigned and constructed in the present study is presented later under the section 'Design of Apparatus'. Care was taken in the design to bring down the volumetric strain of the sample to the lowest possible value.

2.2.9 Seed et al(1962) - Swelling Potential

Seed et al (1962) classified the degree of expansion of a swelling clay as low, medium, high and very high on the basis of magnitudes of swelling potential. Seed et al defined swelling potential as the percentage swell of a laterally confined sample on soaking under 1 psi (6.895 KN/m²) surcharge, after the sample had been compacted to maximum density at optimum moisture content in the standard A.A.S.H.O. compaction test. The main purpose of evaluating swelling potential is the identification of those soils on which swelling tests may be necessary for design purposes. In order to compare the swelling potential of different soils, it is necessary to compare the amounts of swell that would develop under some standard conditions of placement and test.

Samples 1 in (25.4 mm) in height were used for the determination of the swelling potential, and in order to achieve this a special mould was constructed having the same dimensions as the standard A.A.S.H.O. mould but divided into three parts. The central part, designed to yield a 1 in(25.4 mm) high sample, also serves as a confining ring during the swell test. The soil in the ring was trimmed from the compacted sample, covered top and bottom with

porous stones, and then allowed to swell by providing free water whilst the sample was maintained under a surcharge pressure of 1 psi (6.895 KN/m^2). Seed et al determined the percentage swell at different moulding water contents (both dry and wet of optimum), and from the plot (see Fig. 2.12) of moulding water content versus percentage swell, interpolated the percentage swell at optimum water content. This value was taken as the swelling potential. It may be interesting to note from Fig. 2.12 that the maximum swell is obtained on the dry side of optimum water content.

In this study, the swell potential is adopted as a measure of the 'laterally confined swell', and the measurement is made in accordance with the original definition. The apparatus for the measurement is described under the section 'Design of Apparatus'.

2.2.10 Katti et al (1969)

Katti et al (1969) measured a large number of swell properties by using triaxial equipment. The measured properties include, (i) vertical and lateral swell pressure, (ii) vertical and lateral swell amount, and (iii) volumetric swell amount (defined as the amount of swell when the sample is allowed to swell freely with neither lateral nor vertical restraints, i.e. in the same way as in this study)

In order to measure the vertical swell pressure, the ram butting against the proving ring system and resting on the sample was modified to have the same diameter as that of the sample. This modification was done in order to prevent cell water pressure from acting in the vertical

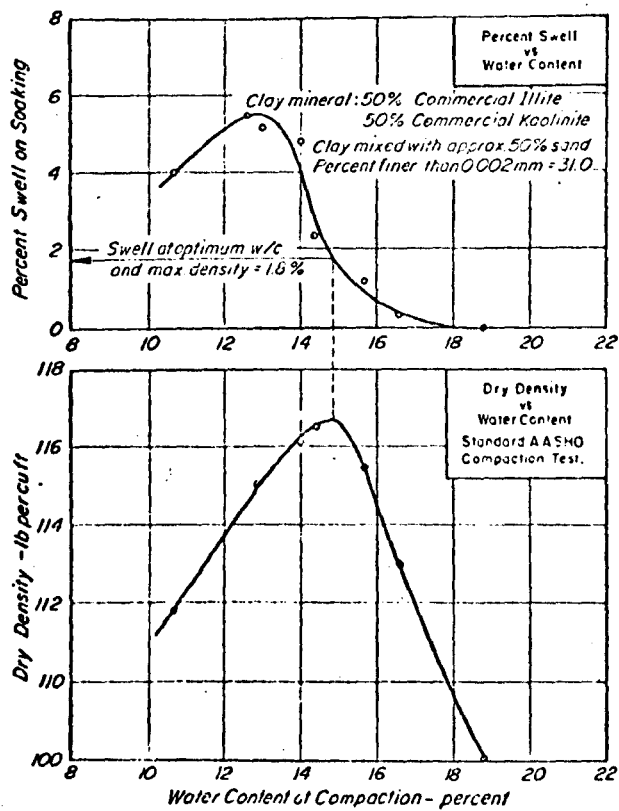


Fig. 2.12 Swelling Test Data for Compacted Samples
 (reproduced from Seed et al, 1962).

direction. The lateral pressure was controlled to maintain no lateral swell of the sample while measuring the vertical swell pressure. The lateral swell pressure was measured with the help of Bishop's pore pressure apparatus; and while doing so, the sample was maintained under no vertical swell by raising the triaxial bench and thus increasing the force in the proving ring to hold the ram down.

The set-up to measure the swell amount (lateral) is shown in Fig. 2.13. Katti et al report that volumetric swelling was measured by recording the quantity of water displaced by the swollen specimen into a scaled perspex tubing. However, some details of the apparatus are not mentioned, for example, the height of water maintained in the burette which supplies 'free' water to the sample; and the height above the cell of the perspex tubing and the magnitude of the back pressure on the sample resulting from the height of the tubing. The vertical swelling was prevented, while measuring the lateral swell (Fig. 2.13), but again the exact details of measuring are not reported.

Even though triaxial equipment is widely used today to study the strength and deformation characteristics of soils, great care has to be exercised in correcting for points of detail, section 2.3, while applying it to study swell properties. Katti et al did correct for the expansion of the cell and for the ram friction, but they seem to have not accounted for other factors, viz, the compressibility of filter papers and the seating of the porous stones and of the sample. Even the proving ring that was used for measuring the vertical swell pressure

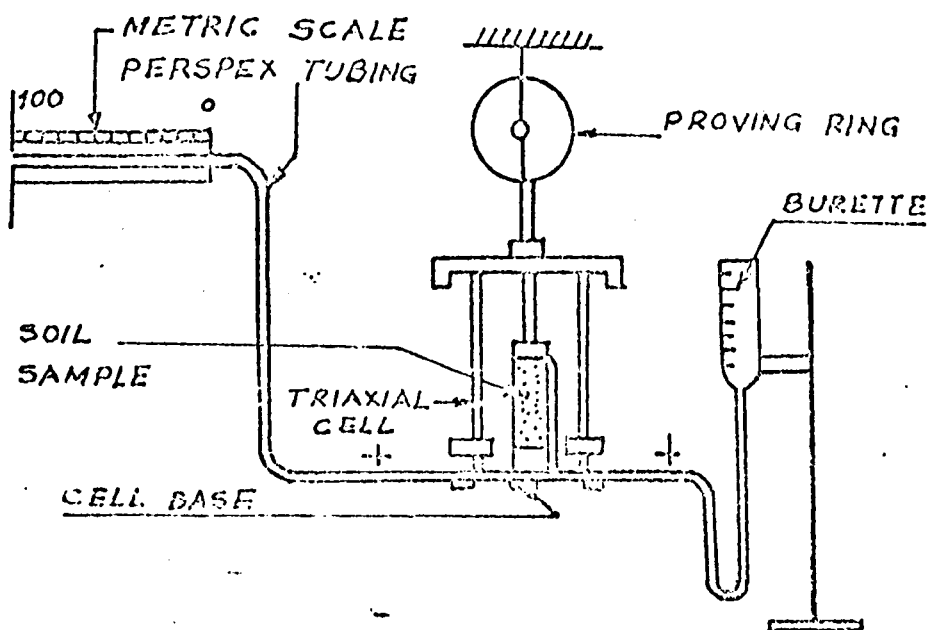


Fig. 2.13 Set-Up for Measurement of Swelling (reproduced from Katti et al,1969).

might, possibly, have accommodated a small amount of deformation. All these factors lead to an underestimation of measured values.

The triaxial equipment is useful for measurement of the swell properties especially when attempting to separate and measure the vertical and the lateral swell pressures. As the lateral swell pressure had not been chosen for study in the present investigation, the use of triaxial equipment was not considered appropriate here for swell pressure measurement, but it was used here for isotropic swell potential.

2.2.11 Finn et al (1958)

Finn et al (1958) were probably the first persons to realise the significance of volumetric swell pressure (called isotropic swell pressure in this study) in view of its similarity to an extreme in-situ case of swelling. They measured the volumetric swell pressure with the help of an apparatus designed for the purpose. Finn et al seem not to have calculated the volumetric strain, when measuring volumetric swell pressure in their apparatus. Such an analysis appears to be of paramount importance especially in view of Seed et al's (1962)^a finding that even a volume change of the sample in the order of 1% greatly underestimates the measured values. In the present study, the apparatus used for the measurement of the volumetric swell pressure (isotropic) is similar to the one used by Finn et al, with suitable modifications to improve the design. In view of this fact, it is felt appropriate to present the full details

of Finn et al's (1958) apparatus here.

The apparatus designed by Finn et al is shown in Fig. 2.14. It consists of a pressure container, a base plate, a top plate, and a rubber membrane shaped like a top hat. The pressure container has a pressure gauge for recording the pressures, an air vent valve and a pipe plug. The hole where the pipe plug fits may be used to connect the chamber to an air supply. The bottom is open and is pressed down on the bottom plate with the flange of the rubber membrane in between, as shown in the figure. The base plate is about 8 inches (203 mm) square. It contains a porous stone, $3\frac{1}{2}$ inches (89 mm) in diameter, which is set down into the plate flush with the surface. Two channels through the base plate lead to the porous stone, to supply free water to the sample. A Y-piece made from $\frac{5}{8}$ inch (16 mm) plastic tubing is connected to these channels. There are four studs in the base plate for clamping down the pressure chamber, providing a pressure tight connection. The rubber membrane was fabricated from 0.012 inch (0.3 mm) thick dental dam and two $\frac{1}{8}$ inch (3.2 mm) thick rubber rings. The dental dam was doubled and glued together with rubber cement. The compacted sample with the rubber membrane pulled down over the sample is placed in the pressure container. The chamber and the Y-piece are filled with water, and the pressure is read after 16 hours, which is taken as the swell pressure of the sample. The 16 hr period would appear to be too short; several of the samples tested in the present study took several weeks to reach equilibrium.

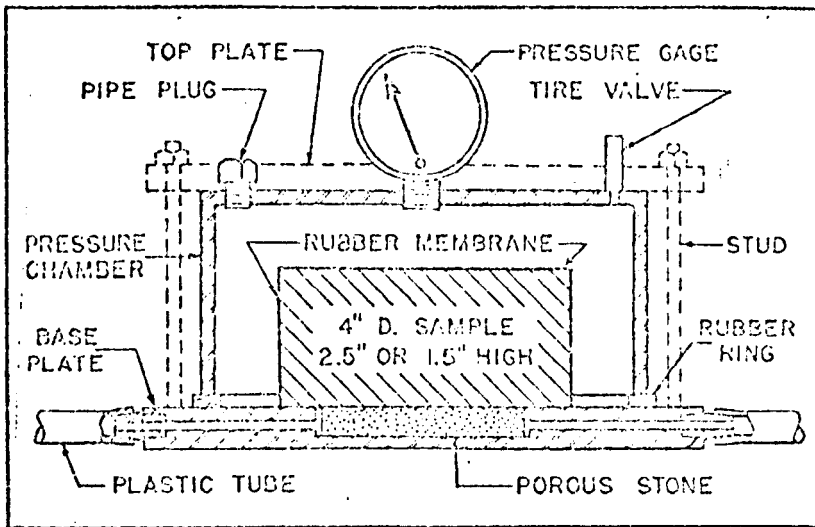


Fig. 2.14 Volumetric Swell Pressure Measuring device
 (reproduced from Finn et al, 1958).

The apparatus described above is simple and measures the volumetric swell pressure directly; but there was scope for modifications and improvements. As the apparatus for the present study was based on Finn et al's model, the critical comments on Finn et al's apparatus are deferred until the present design is described in detail in section 2.5.1

2.2.12 Agarwal and Sharma (1973)

Agarwal and Sharma (1973) proposed a refinement in the measurement of laterally confined swell pressure making use of an electrical relay system to keep the volume of the sample constant during the inundation process. They succeeded in building their relay system in such a way that when the sample swells even by " $\frac{1}{12}$ th of a division" on a dial gauge, it causes sufficient movement to close the circuit and operate or stop the loading motor; the calibration of the dial gauge was not given. Kassiff (1973) reports that although relay systems have already been successfully used in the past for this purpose by Kassiff (1961) and Holland (1968), this seems to be the first time that details of the instrumentation have been published.

The method is based on the consolidometer and uses the triaxial frame with a proving ring and is shown in Fig. 2.15. The refinements introduced into this equipment eliminate the effects of the compression of the proving ring and expansion of the frame. However, the level of the top cap will remain in the right place only if there is no tilting of the top cap during the swelling of the sample. The design would have been better if the pick-up point had

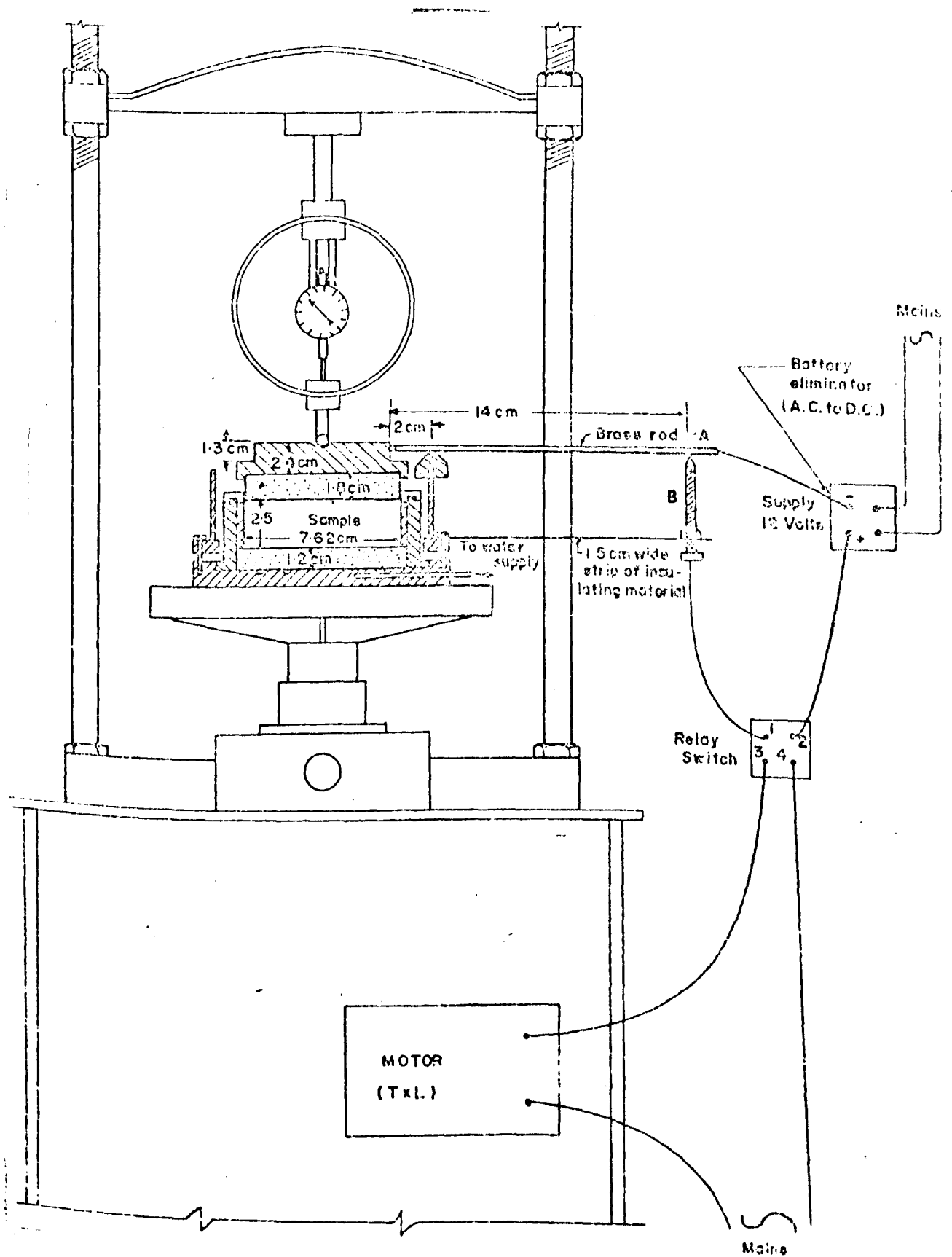


Fig.2.15 Measurement of Swell Pressure Using Electrical Relay Systems
 (reproduced from Agarwal & Sharma, 1973).

been placed in the middle (as shown in Fig. 2.16), instead of at the side. Alternatively several pick-up points might be used around the circumference. Such a modification in the design would not be difficult.

In view of the basic objective of the present study to test a large number of samples on a simple and direct apparatus, the apparatus of Agarwal and Sharma, which would take considerable time to design and construct, has not been considered. It is important to note that, even in such a sophisticated apparatus, the compression of the compressing parts (except the proving ring) still exists, and corrections need to be made for this compression, without which the measured swell pressures are slightly underestimated and will not be 'truly precise'.

2.2.13 Alpan (1957)

Alpan (1957) constructed an interesting apparatus to measure the swell pressure whilst a predetermined soil moisture tension was applied to the soil. Alpan claims that this apparatus permits duplication of field conditions, where the maximum moisture content does not necessarily reach full saturation, and it may also be used to test compacted samples having identical placement conditions for different moisture ranges. The principle involved is that if a soil sample is brought into contact with water under tension, it will take up moisture until a suction equilibrium is reached. At this stage, the soil will have a moisture content not necessarily that of saturation. By varying the water tension the soil may be made to obtain various degrees of saturation,

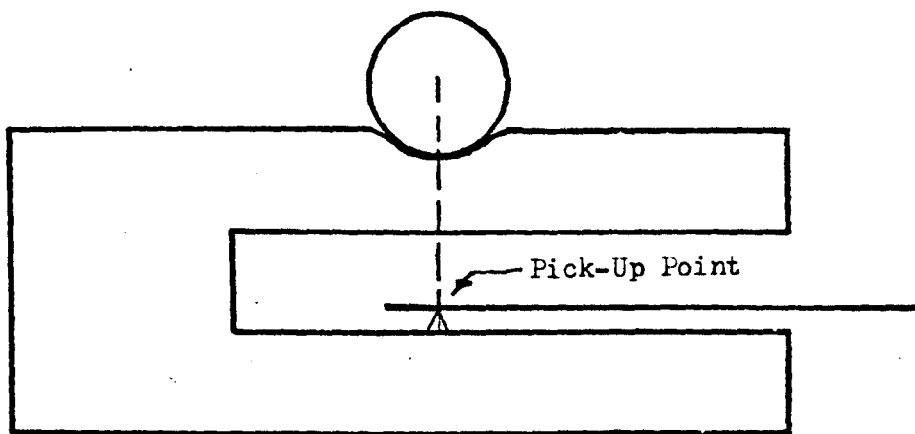


Fig. 2.16 Suggested Pick-Up Point in Agarwal and Sharma's (1973) Apparatus for Swell Pressure Measurement.

and its expansive behaviour can be studied. This procedure also permits the study of a series of samples, placed under identical conditions and brought to various degrees of saturation, whereupon full saturation is allowed.

The details of Alpan's apparatus are illustrated in Figs. 2.17 and 2.18. Although this is an important apparatus to measure swell pressures, Alpan was concerned with a different problem, regarding the effect of different moisture tensions on the swell pressure of one set of samples, whereas the present study is concerned with the swell pressure at zero water tension on a range of samples. The simpler design of Seed et al, section 2.2.8 was therefore preferred here.

2.2.14 Summary of Previous Attempts

A review of the earlier equipment for the measurement of both swell pressure and swell potential has been presented above. A brief summary of this review is given below. It should be once again emphasised at this stage that the present requirement is to choose equipment for the measurement of maximum swell amount and swell pressure for given initial conditions of the sample. In other words, the swell properties are to be measured when the sample is inundated in water until the final value of suction is either exactly zero or virtually equal to zero.

The free-swell test suggested by Holtz and Gibbs (1956) and the PVC meter designed by Lambe (1960) are suitable for identifying an expansive soil and give a preliminary idea about its potential to swell. The multiple consolidometer

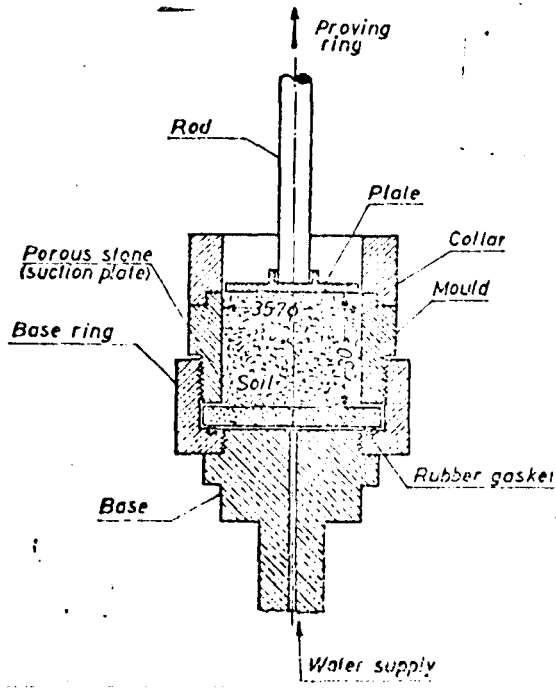


Fig. 2.17 Swell Pressure Cell (reproduced from Alpan, 1957)

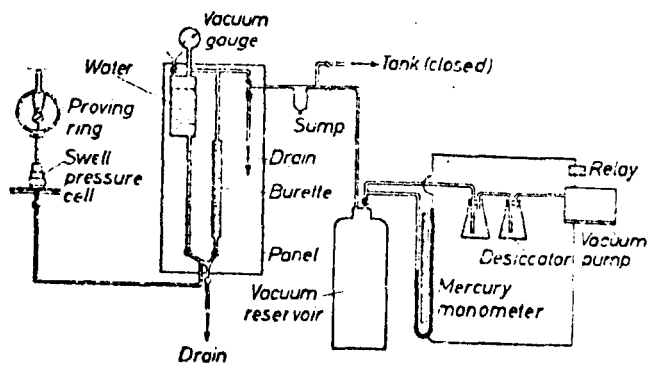


Fig. 2.18 Diagram of Swell Pressure Apparatus (reproduced from Alpan, 1957)

method suggested by Noble (1966) and a similar method suggested by Uppal and Palit (1969) to measure swell pressure require many tests to be made on each soil and are therefore unsuitable for the present study. The apparatus designed by Agarwal and Sharma (1973) using an electrical relay system to maintain a constant volume of the sample compensates for the elasticity of the frame and proving ring. However, the compression of the compressing parts still exists. Alpan's apparatus (1957), though very useful when testing samples of the same soil with different final degrees of saturation, is not suitable for the present study, where the objective is different.

Fredlund's (1969) observations showed that the use of consolidometers for measuring swell properties may lead to erroneous results unless a number of corrections for the procedural factors are made, for details see section 2.3.

The apparatus and procedure used by Seed et al (1962) for the measurement of swelling potential seems suitable for measuring laterally confined swell amount, provided the imposition of a vertical pressure of 1 psi (6.895 KN/m^2) is acceptable. Adoption of this method leads to the advantage of standardisation, so it has been used here. The detailed design of the apparatus is presented under the section 'Design of Apparatus'.

The apparatus used by Seed et al (1962)^a for measurement of laterally confined swell pressure is a simple, direct and well designed apparatus. It should be realised that when this type of apparatus is employed, there can be no measurement of pressure without permitting a slight expansion of the sample, but a well designed apparatus should restrict

this expansion. In view of this it was felt that the apparatus used by Seed et al could be taken as a model and used with slight modifications in design.

Katti et al (1969) used a modified triaxial cell to separate and measure the vertical and lateral pressures. As the lateral swell pressure study was not an objective of the present programme, it was thought that the triaxial equipment was not needed for the present study. However, a triaxial cell was used in the present study to measure the isotropic swell potential.

Finn et al's (1958) apparatus is the only apparatus found in connection with the measurement of volumetric (isotropic) swell pressure. The main drawback of Finn et al's apparatus is that no attempt seems to have been made to calculate the volumetric strain of the sample. There is scope to take Finn et al's apparatus as a model and to improve on its design in order to reduce the unwanted volumetric strain of the sample to the lowest possible value. It can be seen from the design calculations in Appendix 1 that the apparatus used in this connection has been designed to yield a volumetric expansion of 0.85% at a swell pressure of approximately 100 psi, i.e. 0.00123% per 1.0 KN/m².

An important point that has been noted from the review is that no apparatus has been found in which the volume of the sample could be kept absolutely constant during the measurement of swell pressures. This suggests that an extremely small value of strain is inevitable in such measurements and has to be accepted. However, in the present study, an attempt was made to recognise the sources of error that caused such strain and to estimate the effect of each

source in turn.

The next section reviews the points of detail which constitute many of these sources of error.

2.3 POINTS OF DETAIL

Points of detail such as side friction, sample disturbance, sample size and temperature are dealt with in the literature mainly in connection with testing soft, sensitive clays (Matlock and Dawson, 1951; Finn, 1951; Leonards and Girault, 1961; etc). Whilst some consideration of these factors is necessary, the factors that play a significant role when testing swelling clays are different from the above and ^{Such} factors are listed below.

- (i) apparatus friction,
- (ii) compressibility of apparatus,
- (iii) compressibility of filter papers,
- (iv) seating of the soil sample and porous stones.

The various apparatus described in this review for measuring swell pressure suffer from one or more of the four factors mentioned above. These are treated below in turn, and in this connection the work of Fredlund (1969) is taken as the main reference.

2.3.1 Apparatus Friction

Friction in the mechanical components of the apparatus is of interest since it affects the shape of the low pressure end of the compression and rebound curves. Fig. 2.19 (Fredlund, 1969) shows average results for the relationship between load applied to the hanger and load transmitted to the

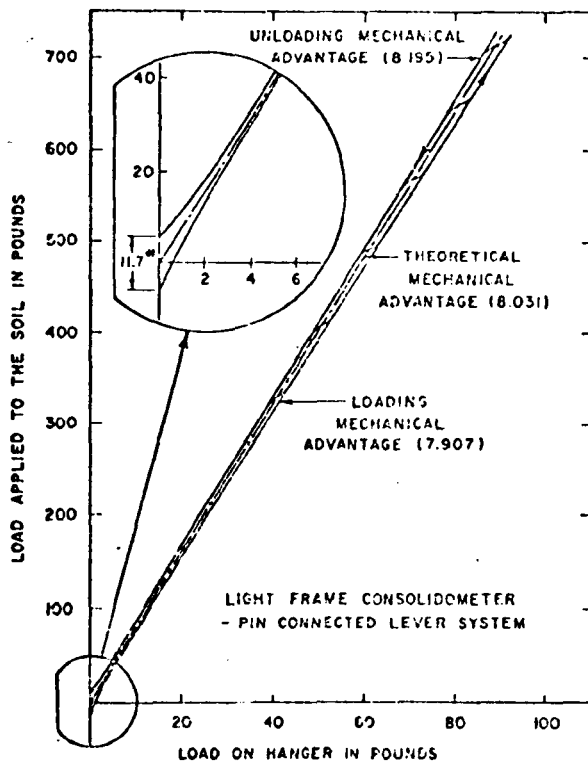


Fig. 2.19 Portion of the Load Transmitted to the Soil Sample (reproduced from Fredlund, 1969).

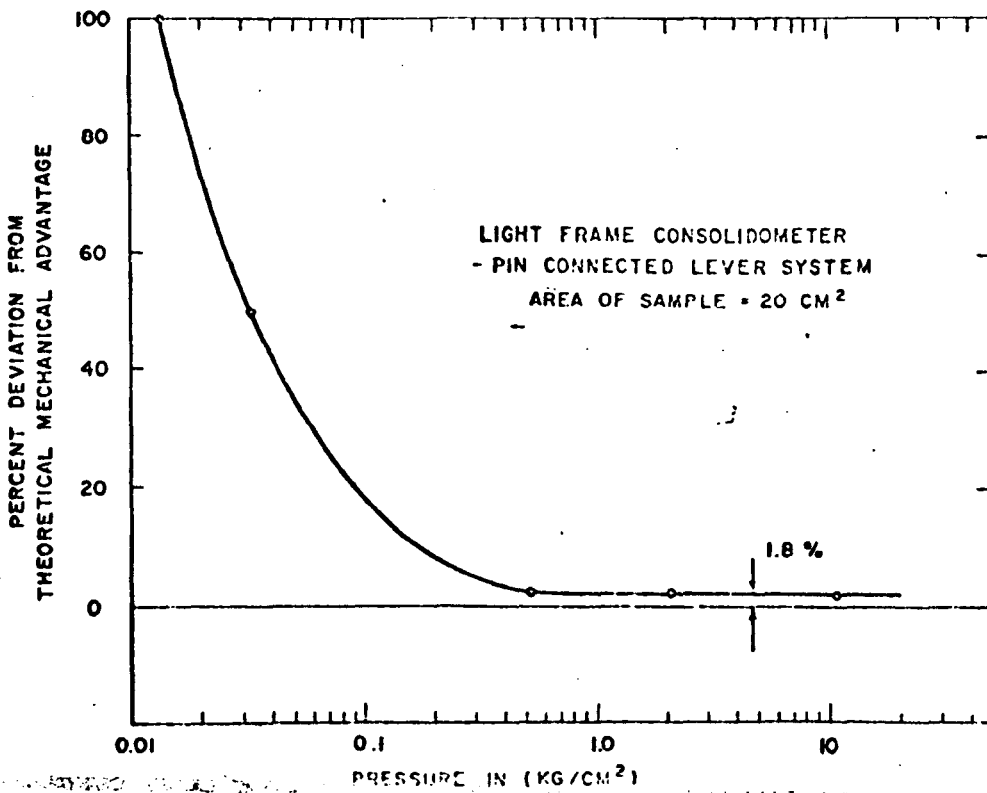


Fig. 2.20 Error in Pressure Measuring System due to Friction (reproduced from Fredlund, 1969).

sample for four light frame consolidometers. A small, highly sensitive proving ring with strain gauges was substituted for the soil sample and used to measure the load reaching the sample. The theoretical mechanical advantage is obtained by precise measurements of the lengths of the lever arms.

Throughout a loading and unloading range greater than 0.5 Kg/cm^2 (7.1 psi) the load applied to the sample is within 1.8% of the nominal value. However, at low pressures the percent error increases rapidly (Fig. 2.20). At a pressure of 0.01 Kg/cm^2 (0.142 psi) the load applied to the sample may be in error by 100%.

Similar tests on the Wykeham-Farrance bench model consolidometers showed an error of approximately 1.2% for pressure above 0.2 Kg/cm^2 (2.85 psi). There is a slight decrease in the frictional component due to the use of knife edges rather than pin-connectors on the loading mechanism.

Irregular behaviour often noticeable in the low range of loading may be largely attributable to inaccuracies in the load transmitted to the sample. Friction in the loading mechanism may be a primary factor in the flattening of the rebound curve often noticeable at low pressures. The only solution to these problems may be to resort to strain gauges or pressure transducers for swell pressure measurements, thus avoiding the unwanted friction in the loading and unloading mechanism.

2.3.2 Compressibility of Apparatus

If a portion of the deflections measured during a consolidation test is due to deflections in the apparatus rather than the soil sample, the test results will be in error unless corrections are made. Compressibility of the apparatus affects the measurement of swell pressure and the slope of the compression rebound curves. Attempts have been made to increase the stiffness of the measuring device (Seed et al, 1962^a; Kassiff et al, 1965) in order to measure more accurately the swell pressure by the constant volume procedure. Hveem (1958) states that a pressure measuring system with a stiffness of 0.04% per 0.5 psi is satisfactory. However, at 30 psi this would mean 2.4% volume change, which could cause serious errors in the measurement of swell pressure. This is equivalent to 0.0116% at 1.0 KN/m². Increasing stiffness increases the values of measured swell pressures. The compressibility of the apparatus can be measured by substituting a steel plug for the soil sample. Many earlier researchers (Means and Parcher, 1963; Hamilton and Crawford, 1959) have suggested that the compressibility of the apparatus be determined prior to running the consolidation test and that corrections be applied to the results obtained.

Fredlund tested five different types of consolidometers and presented the compressibility characteristics in terms of statistical properties. The deformations occurring for the first cycle of loading and unloading are shown in Table 2.1. The results are also plotted as log pressure versus deformation plots (Fig. 2.21) and these semi-log

Type of Equipment	No. of Observ.	Pressure Range (kg/cm ²)	DEFLECTION (INCHES)				Coeff. of Variation (Percent)
			Mean	Median	Standard Deviation	95% Confid. Limits	
Light Frame Consolidometer	25	0.0 to 0.1	0.002	0.0002	0.0001	0.0002	39.9
		0.1 to 1.0	0.0010	0.0010	0.0003	0.0006	30.3
		1.0 to 10.	0.0033	0.0033	0.0010	0.0019	28.7
		10. to 1.	0.0029	0.0030	0.0010	0.0020	34.7
		1.0 to 0.1	0.0010	0.0011	0.0004	0.0007	32.0
0.1 to 0.01	0.0034	0.0004	0.0002	0.0004	44.5		
Residual*	0.0007	0.0006	0.0005	0.0010	65.9		
Bench Model Consolidometer	6	0.0 to 0.1	0.0005	0.0004	0.0004	0.0009	88.5
		0.1 to 1.0	0.0009	0.0009	0.0003	0.0006	34.0
		1.0 to 10.	0.0030	0.0035	0.0010	0.0019	32.5
		10. to 1.	0.0024	0.0025	0.0005	0.0009	20.1
		1. to 0.1	0.0010	0.0010	0.0004	0.0007	34.6
0.1 to 0.01	0.0007	0.0005	0.0006	0.0012	87.0		
Residual	0.0007	0.0002	0.0012	0.0023	159.		
Anteus Test Lab Consolidometer	3	0.0 to 0.1	0.0003				
		0.1 to 1.0	0.0005				
		1.0 to 10.	0.0003				
		10. to 1.	0.0008				
		1. to 0.1	0.0004				
0.1 to 0.01	0.0001						
Residual	0.0004						
Large Frame Consolidometer	10	0.0 to 0.1	0.0015	0.0017	0.0009	0.0018	51.4
		0.1 to 1.0	0.0023	0.0026	0.0012	0.0024	53.8
		1.0 to 10.	0.0048	0.0052	0.0021	0.0041	43.2
		10. to 1.	0.0022	0.0021	0.0012	0.0023	51.6
		1. to 0.1	0.0029	0.0032	0.0014	0.0028	49.4
0.1 to 0.01	0.0017	0.0019	0.0010	0.0020	57.4		
Residual	0.0021	0.0012	0.0019	0.0037	87.1		
Conbel Consolidometer	2	0.0 to 0.1	0.0008				
		0.1 to 1.0	0.0023				
		1.0 to 10.	0.0028				
		10. to 100.	0.0065				
		100. to 10.	0.0050				
10. to 1.	0.0021						
1. to 0.1	0.0009						
Residual	0.0041						

*Residual is the term used for difference between starting and finishing dial readings.

Table 2.1 Compressibility of Consolidometers First Cycle of Loading and Unloading (reproduced from Fredlund, 1969).

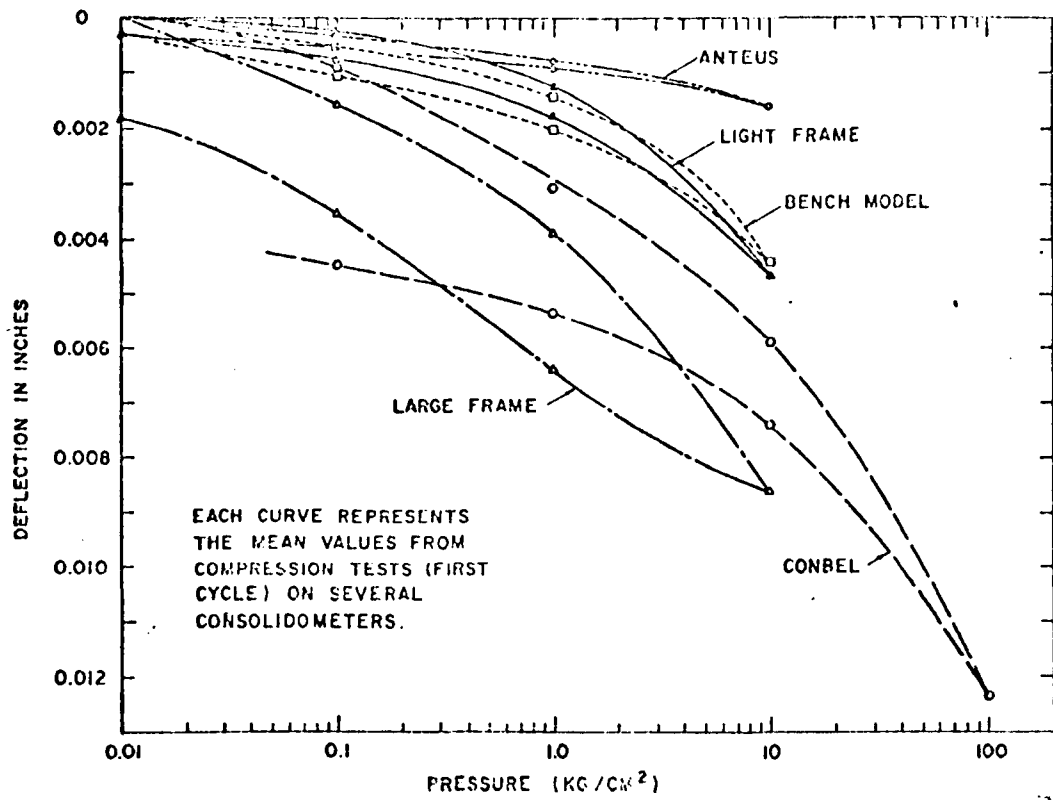


Fig. 2.21 Compressibility of Consolidometers (reproduced from Fredlund, 1969).

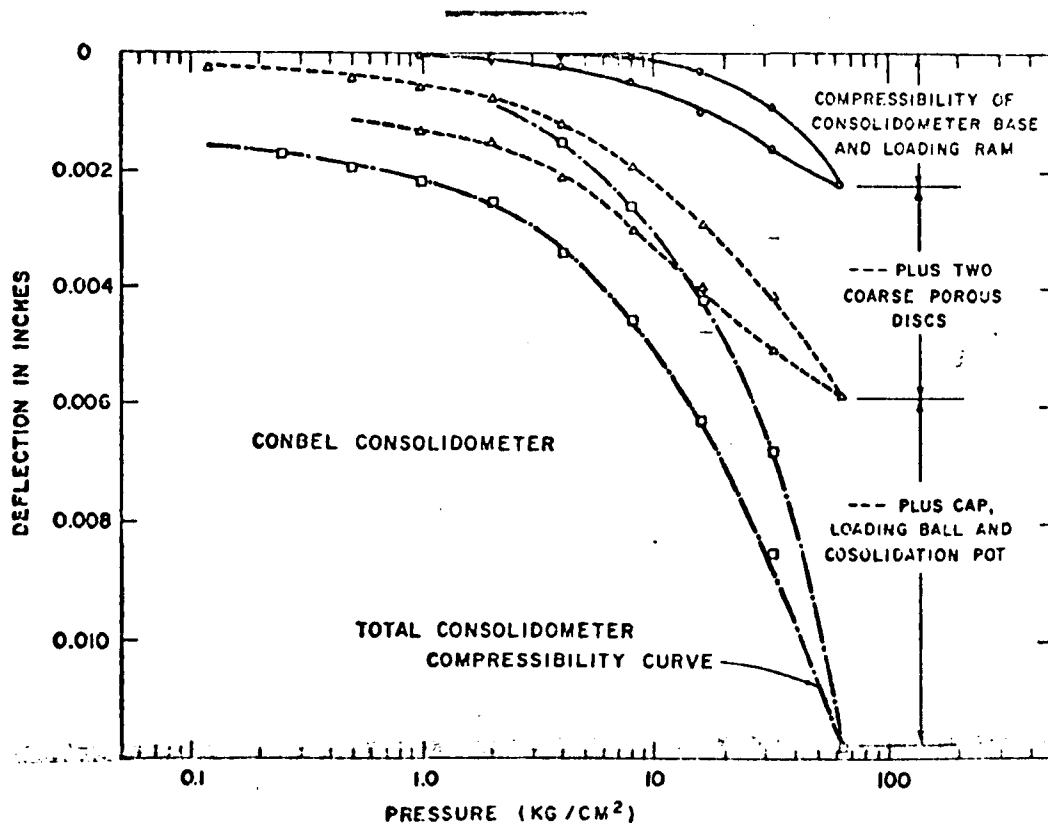


Fig. 2.22 Factors Contributing to Compressibility of Consolidometers (reproduced from Fredlund, 1969).

plots are similar to those expected from testing soil samples. The results mainly indicate that the consolidometers do not compress in an elastic manner, a greater proportion of deflection occurring at low pressures. The light frame and bench model consolidometers show similar compressibility curves with approximately 0.0045 inches (0.11 mm) occurring at 10 Kg/cm² (142 psi). The large frame and conbel consolidometers show considerably more compression. The Anteus Test-lab consolidometer shows only 0.0016 inches (0.04 mm) at 10 Kg/cm² (142 psi). All apparatus, except the Anteus, show considerable hysteresis between loading and unloading. The larger the hysteresis the more residual deflection there is remaining when the pressure is 0.01 Kg/cm² (0.142 psi). Due to hysteresis and residual effects, Fredlund suggested that there should be one compressibility correction curve for loading and another for the unloading of the sample.

Calculations of deflection based on the elastic moduli of the materials involved show that many times as much deflection occurs when loading as would be expected theoretically. For example, at 10 Kg/cm² (142.2 psi) on the light frame consolidometers the average ratio of the actual deflection to the theoretical deflection was 4.0. In the light of this observation, Fredlund took special efforts to observe the basis of measured deflections. Fig. 2.22 shows the components giving rise to the deflections occurring during loading and unloading of the Conbel consolidometer. At 30 Kg/cm² (426.7 psi), approximately 13% of the deflection occurred in the loading ram and the

base of the loading frame of the apparatus. Forty-eight percent occurred in the porous stones, which also are the major contributors to the hysteresis effects and residual deformation. The remaining 39% of deformation occurred in the consolidation pot, loading cap and the seating of the ball on the loading cap. Due to the large deformations in the porous stones, the properties were further investigated by Fredlund (see Fig. 2.23 and Table 2.2), who concluded that only thick porous stones show a deformation modulus approaching the theoretical value, and also, that factors such as roughness and warp in the stones introduce high deflections and hysteresis.

Another factor producing a variation in results is the size and smoothness of the consolidation pot. All contact areas should be machined smooth; and even after doing this, Fredlund noted that three times as much deflection occurred for a consolidation pot with a contact area of 150 cm^2 (23.25 in^2), as one with a contact area of 80 cm^2 (12.4 in^2), when loaded to 10 Kg/cm^2 (142 psi). Possibly the mating surfaces should be scraped to fit.

2.3.3 Compressibility of Filter Paper

Filter paper is often placed above and below the soil sample during a consolidation test in order to prevent the soil particles ~~away~~ from entering the small pores in the porous stones (Baracos, 1976). However, Fredlund noted that the compressibility of the filter paper is of a significant magnitude, and his experimental results are shown in Figs. 2.24 and 2.25. It can be noted that the filter paper has not only an instantaneous compression

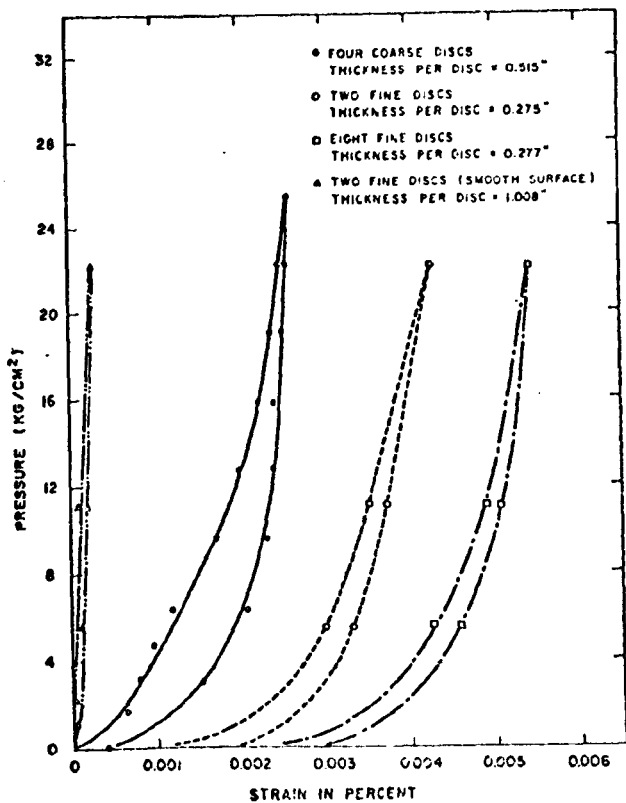


Fig. 2.23 Stress - Strain Properties of Porous Stones (reproduced from Fredlund, 1969).

Type of Porous Disc	PRESSURE RANGE		
	0 to 0.1 kg/cm ²	0.1 to 1.0 kg/cm ²	1.0 to 10 kg/cm ²
	MODULUS OF ELASTICITY IN P.S.I.		
Coarse Corundum Porous Discs			8.28 x 10 ⁴
2 - Fine, Norton Porous Discs	0.397 x 10 ⁴	0.926 x 10 ⁴	6.65 x 10 ⁴
8 - Fine, Norton Porous Discs	0.339 x 10 ⁴	0.802 x 10 ⁴	3.85 x 10 ⁴
Fine, Thick Norton Porous Discs (Anteus)	9.26 x 10 ⁴	46.3 x 10 ⁴	160 x 10 ⁴

Table 2.2 Elastic Moduli of Porous Stones (reproduced from Fredlund, 1969).

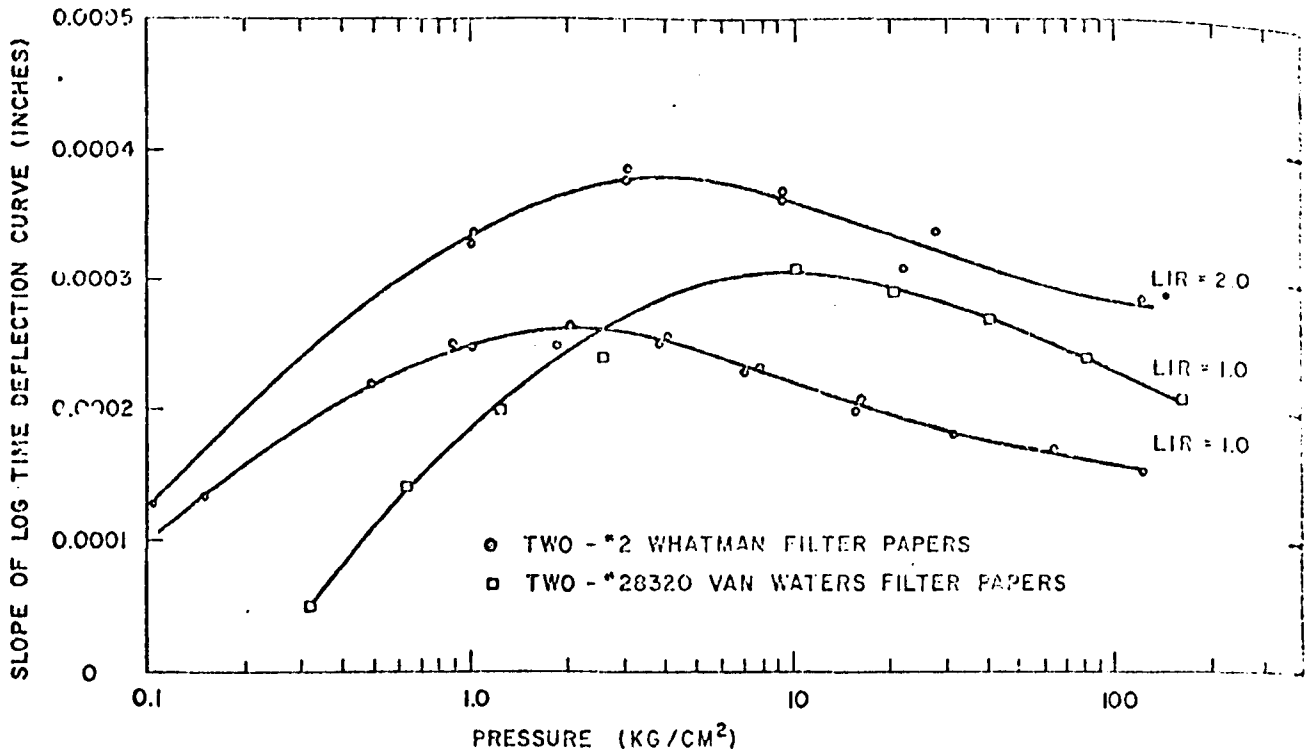


Fig. 2.24 Slope of the Time - Deflection Curves for Filter Paper (reproduced from Fredlund, 1969).

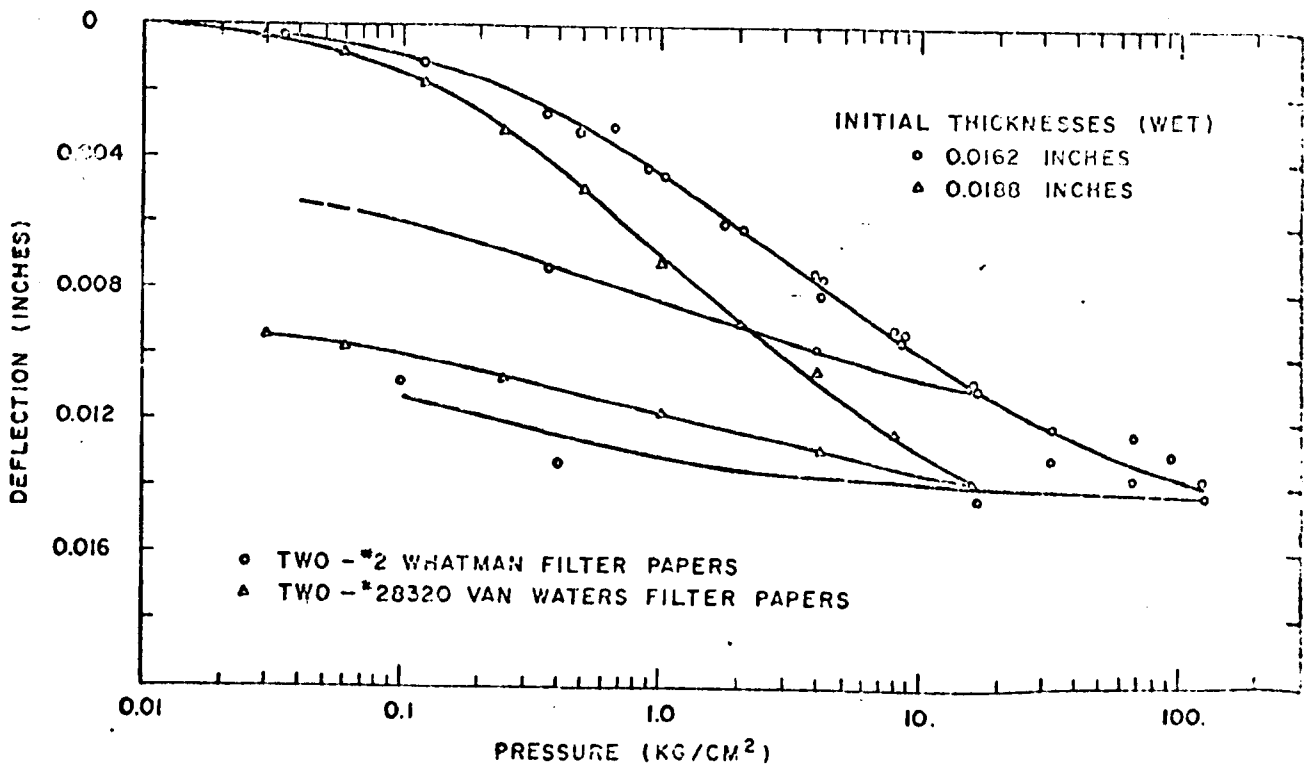


Fig. 2.25 Compressibility of Filter Paper (reproduced from Fredlund, 1969).

when the load is applied, but also compresses further with time.

Fredlund has concluded that at a pressure of 1 Kg/cm^2 (14.2 psi) the compression of the filter paper is approximately five times that of the apparatus, and approximately $2\frac{1}{2}$ times at a pressure of 10 Kg/cm^2 (142 psi).

2.3.4 Seating of the Porous Stones and the Soil Sample

Fredlund analysed the time-deflection curves of a number of consolidation tests in order to have a better understanding of the seating of the soil sample. After subtracting the compressibility of the apparatus and the theoretical correction to zero loading from the instantaneous deflection, the remaining compressibility was assumed to be due to the compressibility of air in the sample and seating of the porous stones and the soil. If no seating error occurs, a plot of accumulated deflection versus pressure should approximate a straight line in accordance with Boyle's law (Hilf, 1948; Hamilton and Crawford, 1959). It was concluded by Fredlund that it is difficult to evaluate the seating of the porous stones and the soil sample, but it is of significance primarily under low pressures. As such, it has been suggested that the modified constant volume tests give a more accurate value for swell pressure.

Some tests carried out in the present investigation to study the seating and compressibility aspects of porous stones are presented and discussed later, see Appendix 1. The results indicate that the compressibility of the porous stones is negligible, whilst the bedding errors

contribute a significant error.

2.3.5 Summary

The above discussion and data presented by Fredlund (1969) show that the compressibility of the consolidometer and of the accessories have a significant effect upon the interpretation of swell test data. Two main properties are affected; first, the measurement of swell pressure and second, the slope of the rebound curve. Corrections for both properties can be made by subtracting the deflections due to compressibility from the deflections measured during the test. Percentage errors without these corrections can be in excess of 100% for the swell pressure, and generally 10% to 50% for the swelling index (C_s) [Fredlund, 1969].

Further consideration is given to the magnitude of these errors under the section 'Design Calculations' in Appendix 1, while designing the apparatus for measurements in the present study.

2.4 DESIGN OF APPARATUS

2.4.1 Introduction

This section describes the design of the apparatus which was used in this study to measure the selected swell properties. The relevant details of design are presented in the later sections and the appropriate design calculations are reported in Appendix 1. The four apparatus designed here provide for the measurement of the following properties:

- (1) isotropic swell pressure, when the sample is held at constant volume by an equal all round pressure;
- (ii) isotropic swell potential, when the sample is able to swell freely in all directions (the set-up for this is described in Appendix 4);
- (iii) laterally confined swell pressure, when the sample is held at constant volume by lateral and vertical constraints, the vertical confining pressure being of interest;
- (iv) laterally confined swell potential, when the sample is laterally confined and allowed to swell only in the vertical direction.

The size of the sample used for testing in the first and second cases was 4 in (102 mm) in diameter and 2.5 in (64 mm) high. The diameter is that of a standard compaction mould. The height was chosen following the recommendation of Finn et al(1958). Finn et al tested both small samples in a large chamber and large samples in a small chamber, and concluded that large samples in small chambers give higher swell pressures. This can, in fact, be expected as there will be a large amount of water in a large chamber whilst using small samples, which in turn gives a higher value of the volumetric strain of the sample due to the compressibility of the water; thus reducing the measured swell pressure. However, samples larger than 2.5 in (64 mm) high may become impracticable for testing, as they take too long to reach equilibrium. The size of the samples for the third and fourth cases was 4 in (102 mm)

in diameter and 1 in (25.4 mm) high. The smaller height was chosen to provide a lower ratio of length to diameter to reduce skin friction and also to maintain agreement with the work of earlier researchers for a comparative study, if required, at a later stage.

For testing unconfined samples (2.5 in high), the samples were taken from the centre of the compaction mould in order to avoid the end effects of compaction. For testing laterally confined samples (1 in high), the samples were again taken from the centre of the mould, and in order to avoid extracting from the mould, the sample was subsequently tested within the compaction ring. It is not possible to meet these requirements with conventional compaction moulds. As such, it was found necessary to design a compaction mould to suit the present requirements. The designed mould is described below, followed by the apparatus designed in the present study. The apparatus are described in the order in which they were designed.

2.4.2 Compaction Mould

The compaction mould designed in the present study is similar in principle to the one used by Seed et al (1962), and the main dimensions are the same. The compaction mould, the accessories, and the procedure of compaction are in accordance with the standard A.A.S.H.O. compaction test. The Indian Standard specification for light compaction is exactly the same as that of the standard A.A.S.H.O. test, whilst the British Standard specification for light compaction is slightly different, viz:-

	<u>standard A.A.S.H.O</u>	<u>B.S.</u>
diameter	4.00 in (102 mm)	4.1338 in (105 mm)
height	4.6 in (117 mm)	4.5472 in (116 mm)
blows per layer	25	27

A line diagram of the special compaction mould designed in the present study is shown in Fig. 2.26. It consists of a base plate, a mould divided into three pieces, and a collar. The 4.6 inch (117 mm) high mould is made up of three pieces such that the central piece yields a sample of 1.0 inch (25.4 mm) high in one version (Fig. 2.26) and a sample of 2.5 inch (64 mm) high in the other version (not shown). In the second version the top and bottom pieces are each 1.0 inch (25.4 mm) high. The base plate 7.5 inch (191 mm) in diameter has 4 Nos. of $\frac{3}{8}$ inch (9.5 mm) diameter tie rods that are tapped in on a circle of 6.5 inch (165 mm) diameter. Four pins on a circle of 5.25 inch (133 mm) diameter are provided to ensure no movement of the mould during the compaction process. These pins are $\frac{5}{8}$ inch (15.9 mm) in overall length with $\frac{3}{8}$ inch (9.5 mm) length tapped in the base plate. A collar of 2.5 inch (64 mm) high is used as the top part of the mould and is provided with 4 Nos. of lugs. The lugs 1.25 inch (32 mm) in length have $\frac{3}{8}$ inch (9.5 mm) in diameter holes.

The tolerances for construction are shown in Fig. 2.26.

2.4.3 Isotropic Swell Pressure

The apparatus designed for the measurement of isotropic swell pressure is an improved version of Finnet al's (1958) apparatus described earlier. In this apparatus the sample is free to swell in all directions but, subject to experimental error, volume change is prevented. The line

**MODIFIED AASHO
COMPACTION MOULD**

MATERIALS : BRASS EXCEPT
DOWELS

NOTES :

- ① JOINTS MUST BE TIGHT ON INNER RIM TO KEEP SOIL OUT OF JOINT
- ② CLEARANCES ON OUTER RIM $\frac{1}{32}$ "
- ③ BRAZING
- ④ DOWELS , 4 Nos., OVERALL HEIGHT $\frac{5}{8}$ " WITH $\frac{1}{4}$ " PROJECTING OUT OF BASE PLATE (STEEL)
- ⑤ TIE RODS, 4 Nos., $\frac{3}{8}$ " ϕ (BRASS)

FIG. 2.26

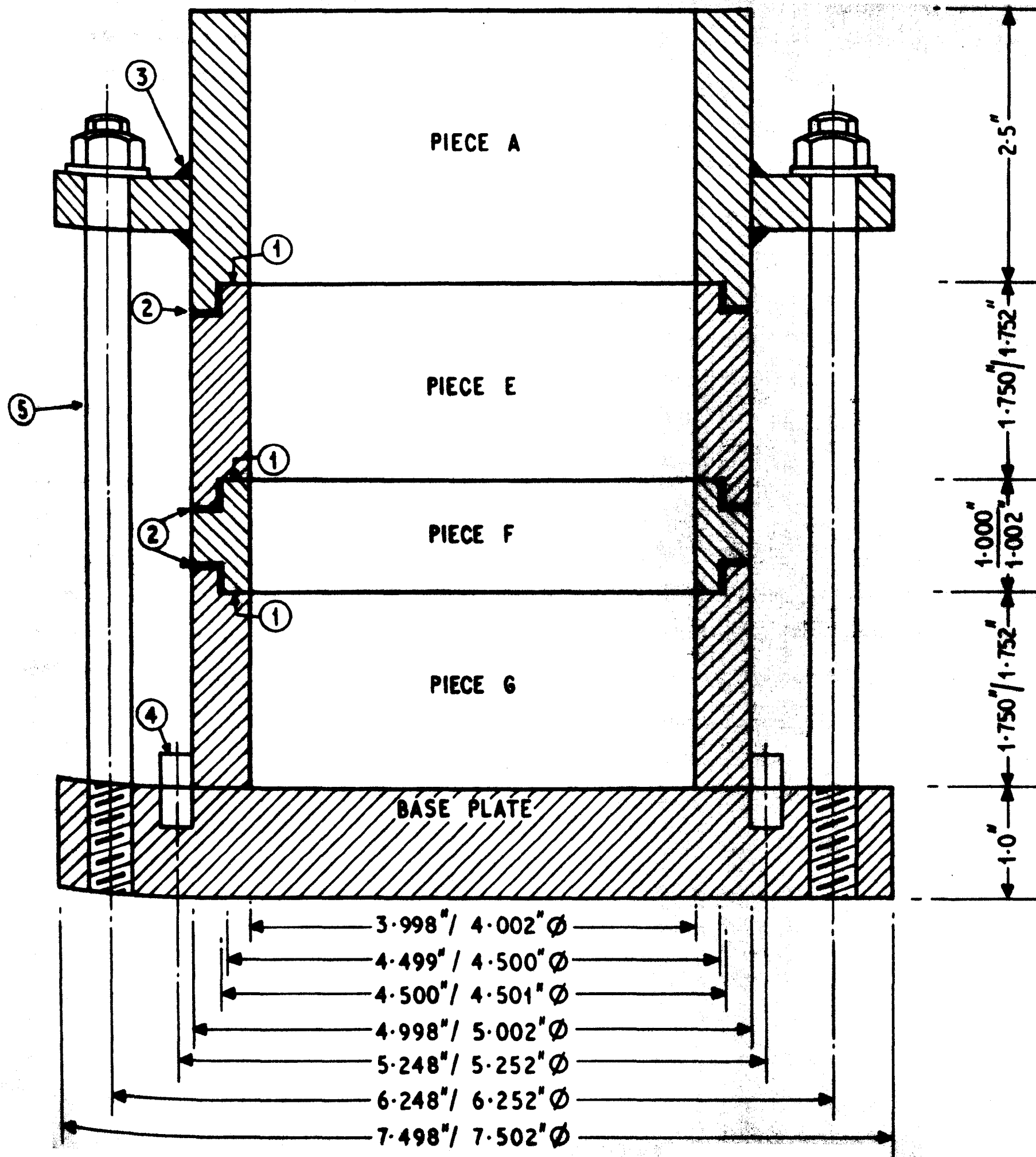


diagram of the apparatus is shown in Fig. 2.27.

The apparatus acts as a pressure chamber. Swelling of the sample is restricted by confining water which completely fills the space between the sample and the chamber. The soil sample is placed on a filter paper on a porous stone, which has been cemented to the top of a pedestal on a base plate. A rubber membrane covers the sample at the top and all around like a top hat (without brim) in order to avoid any contact between the sample and the confining water. When the sample is allowed to draw free water, it tends to swell. This tendency is suppressed by the confining water and the rigidity of the system, and as a result the sample exerts pressure which is transmitted to a pressure transducer through the surrounding water. Ideally this apparatus should maintain the change in volume of the sample equal to zero throughout the period of the test till the final value of swell pressure is recorded. As such, it is necessary to recognise the sources of error that tend to cause a volume increase, and to take suitable precautions in the design to minimise the volumetric expansion of the sample. According to the design calculations, the present apparatus is expected to yield a volumetric strain of 0.85% at a swell pressure of 100 psi (i.e. 0.00123% at 1 KN/m^2), with the percentage volume change decreasing linearly with decreasing value of swell pressure. The design calculations are in Appendix 1, and the design details of this apparatus are in section 2.5.1.

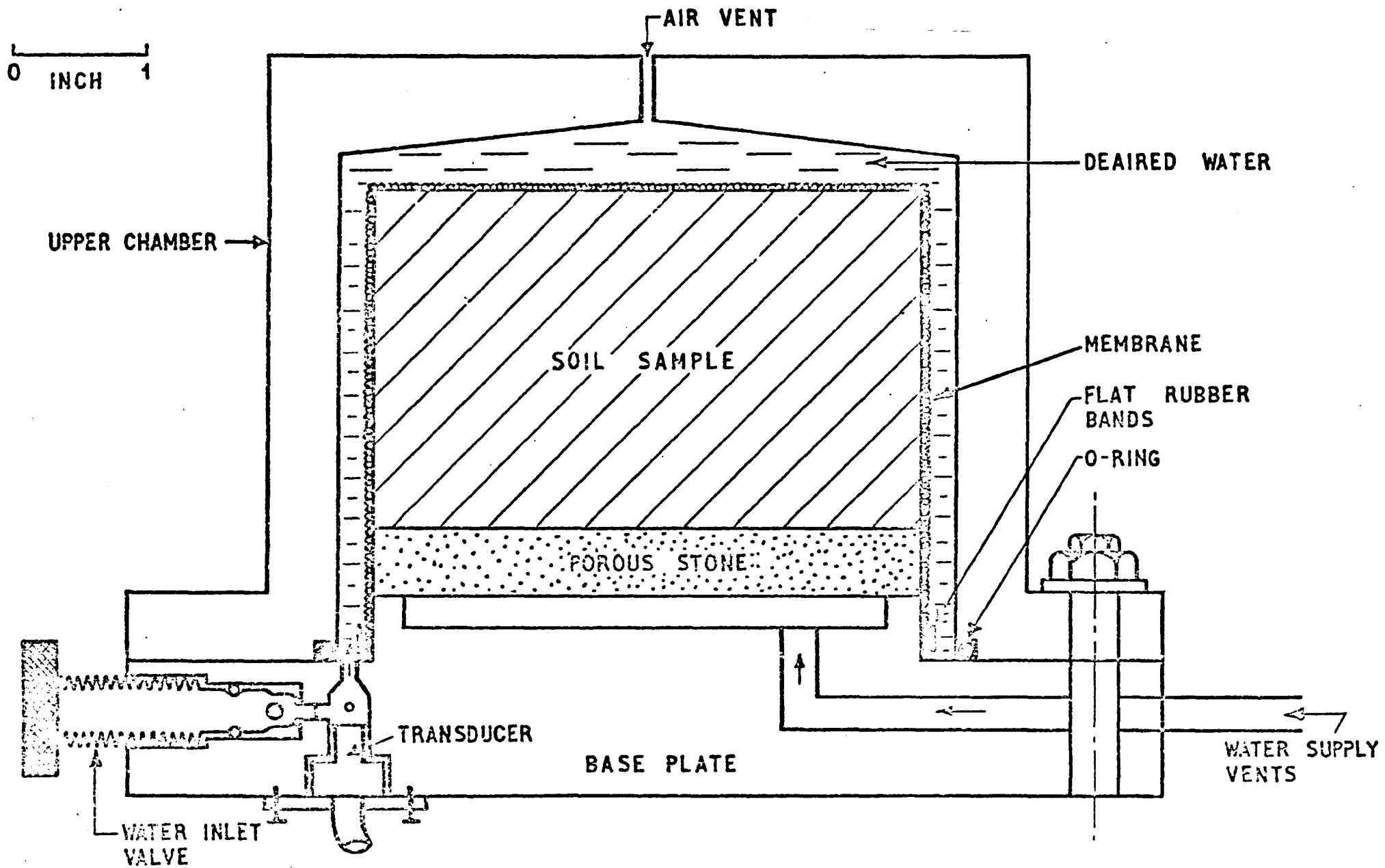


FIG.227 ISOTROPIC SWELL PRESSURE APPARATUS

2.4.4 Laterally Confined Swell Pressure

The apparatus designed to measure the laterally confined (vertical) swell pressure is shown in Fig. 2.28.. This is similar in concept to the one used by Seed et al (1962)⁸. However, suitable modifications were brought into the present design in order to make the measurement more precise.

In this apparatus the 1.0 inch (25.4 mm) high soil sample confined within the compaction ring (see section 2.4.2) is sandwiched between two porous stones in a swell pot. The top porous stone is not shown in Fig. 2.28. Filter papers are placed between the sample and the stones. The swell pot consists of a sample base with a 2.0 inch (51 mm) high rim brazed around its circumference. The sample base is brazed to the top of a screw. A main base supported on the screw moves up and down when it is rotated. Two tie rods rigidly fixed to the main base carry a 11 in x 2 in x 2 in (279 mm x 51 mm x 51 mm) clamping bar. A perforated metallic disc resting on the top porous stone is rigidly connected to the clamping bar by a stem. The swell pot is filled with water, and the sample develops swell pressure under a 'nearly no volume increase' condition.

The method of measuring the swell pressure is based on the use of strain gauges on the tie rods. However, provision is made in the apparatus to use a proving bar, in case the strain gauges become ineffective, e.g. when extremely low values of swell pressures are to be measured (Fig. 2.29).

It can be seen from the design calculations in Appendix 1 that the percentage strain of the sample is 1.6% at a

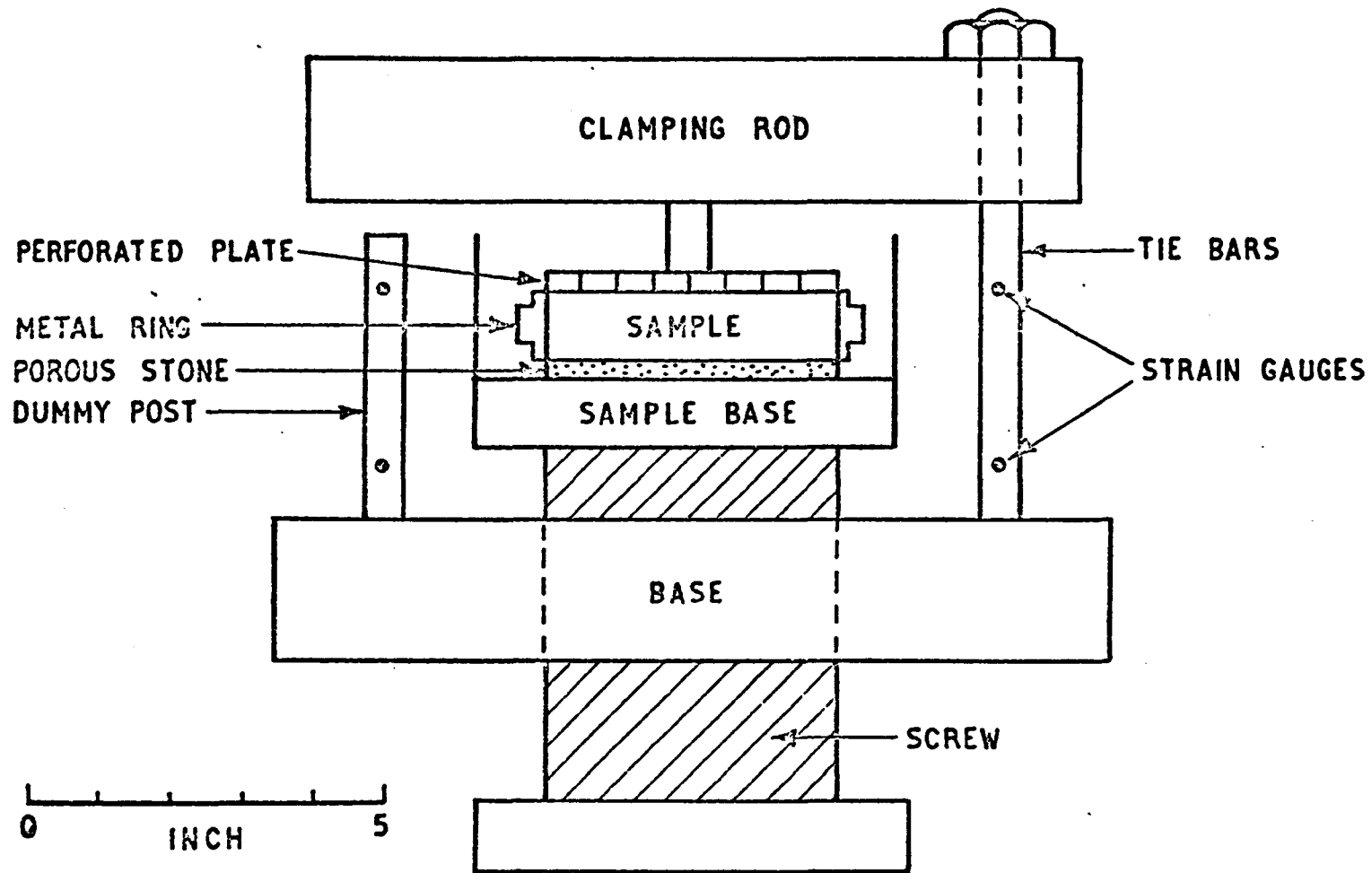


FIG. 22B LATERALLY CONFINED SWELL PRESSURE APPARATUS

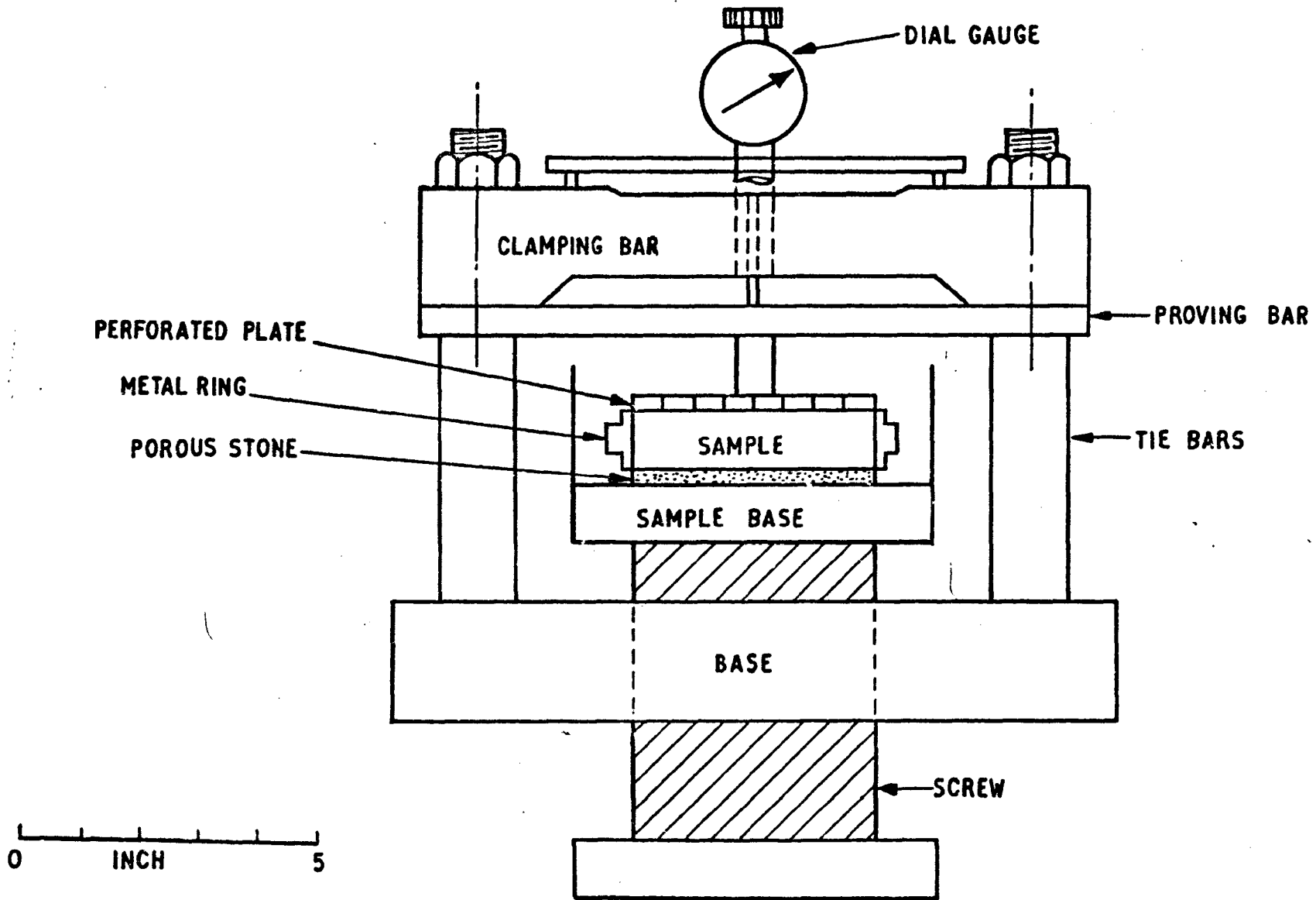


Fig.229 LATERALLY CONFINED SWELL PRESSURE APPARATUS.

swell pressure of approximately 100 psi (i.e. 0.00234% at 1.0 KN/m^2), when the measurements are made using strain gauges on tie bars. The calculated percentage strain reduces with decreasing swell pressure.

The design details of this apparatus are given in section 2.5.2.

2.4.5 Laterally Confined Swell Potential

The apparatus designed in the present study for the laterally confined swell potential enables the measurement of percentage swell in the vertical direction of a laterally confined sample under a surcharge pressure of 1 psi (6.895 KN/m^2); this corresponds to the 'swelling potential' of Seed et al (1962). The apparatus is shown in Fig. 2.30.

In this apparatus, the 1.0 in high (25.4 mm) sample confined within the compaction ring (see section 2.4.2) is placed on a porous stone. The porous stone rests on the base of a cylindrical pot. The pot is 6.0 inch (152 mm) in internal diameter and 2.0 inch (51 mm) deep, and for rigidity the base and circular walls are 0.5 inch (13 mm) thick. Grooves of 0.125 inch (3.2 mm) thick are milled on the base of the cell to conduct water to the lower porous stone. A second porous stone rests on top of the sample, with a metallic weight providing 1 psi (6.895 KN/m^2) surcharge on the top of the porous stone. Grooves of 0.125 inch (3.2 mm) thick are milled on the underside of the metallic weight. Filter papers are placed between the sample and the stones. Two 0.5 inch (13 mm) dia. posts are rigidly screwed on the cell wall. A cross bar placed across these two posts holds two dial gauges for recording the sample swell. These dial

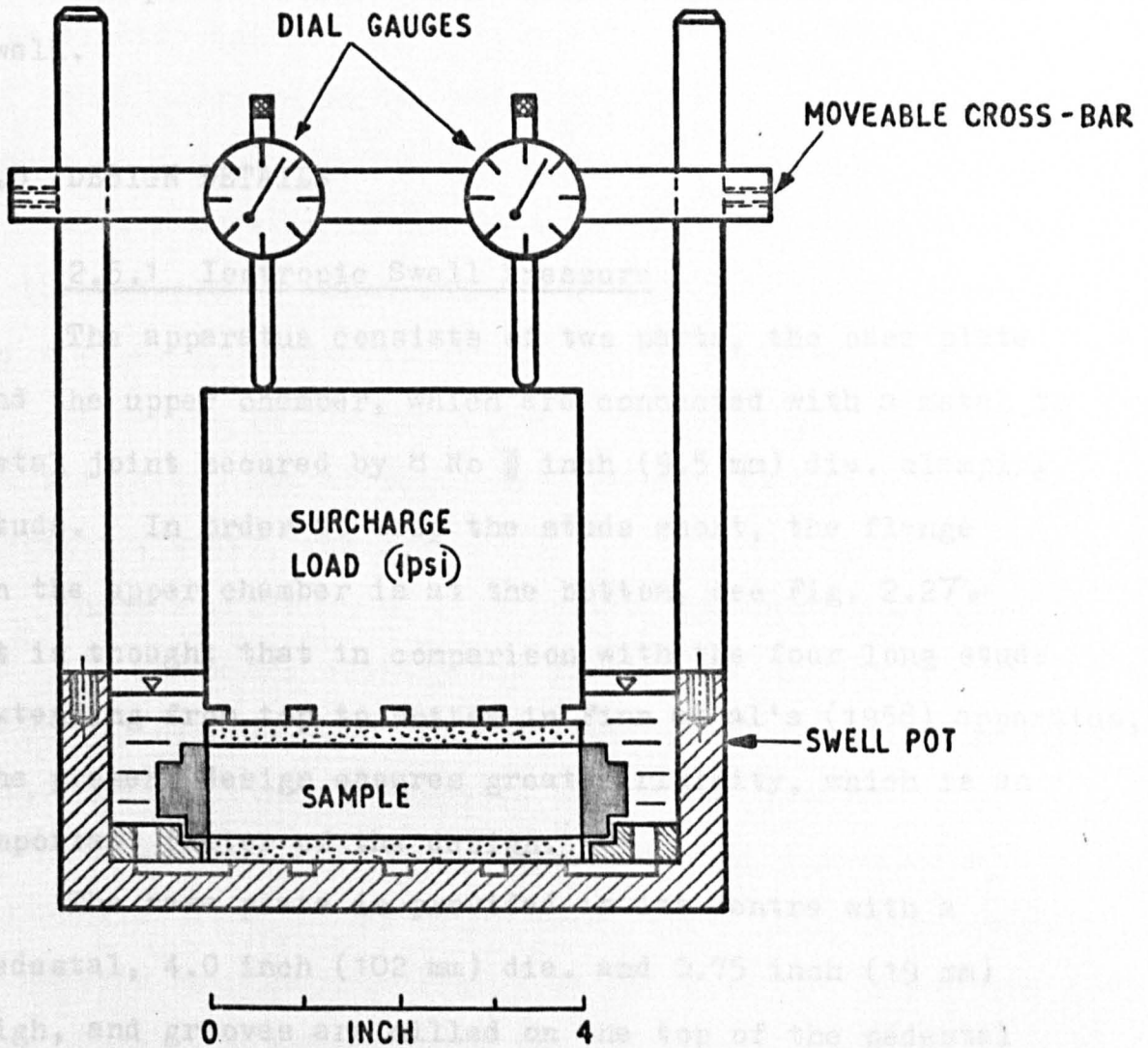


**Fig. 2.30 LATERALLY CONFINED SWELL
POTENTIAL APPARATUS**

gauges bear diametrically on the weight.

A shaped circular ring 0.25 inch (64 mm) high placed inside the pot serves to locate the bottom porous stone and the sample. The circular ring is designed so that it would support the sample ring should it fall.

The pot is filled with water to cause the sample to swell.

2.5 DESIGN DETAILS

2.5.1 Isotropic Swell Pressure

The apparatus consists of two parts, the base plate and the upper chamber, which are connected with a metal to metal joint secured by 8 No $\frac{3}{8}$ inch (9.5 mm) dia. clamping studs. In order to keep the studs short, the flange on the upper chamber is at the bottom, see Fig. 2.27. It is thought that in comparison with the four long studs extending from top to bottom in Finn et al's (1958) apparatus, the present design ensures greater rigidity, which is an important factor of the design.

The base plate is provided in its centre with a pedestal, 4.0 inch (102 mm) dia. and 0.75 inch (19 mm) high, and grooves are milled on the top of the pedestal for water supply.

The 0.25 in (6.4 mm) thick porous stone is cemented to the pedestal in order to reduce the bedding error of the stone. The inside of the top of the chamber is sloped to prevent any air bubbles sticking to the lower part of the wall during the de-airing process, see Fig. 2.27. Both

of the above details are improvements on Finnet al's design.

An air vent valve is provided at the centre of the top of the chamber and is similar to the vent valves used on Wykeham-Farrance triaxial cells.

A specially fabricated rubber membrane (Fig. 2.31) covers the sample at the top and the sides. The membrane fits tightly against the sample, but offers a negligible all round pressure on the sample, 0.003 psi at 1% volumetric strain (i.e. 0.02 KN/m² at 1% volumetric strain).

Flat rubber bands are used to seal the rubber membrane to the pedestal. Flat bands are chosen in order to prevent any air being trapped at the bottom of the band.

An O-ring is placed at the junction of the top chamber and the base plate to seal the chamber from any possible leakage of water, see Fig. 2.27.

There are 2 Nos. of 0.25 in (6.4 mm) vents through the base plate and joining the grooves on the top of the pedestal, see Fig. 2.27. One vent serves to supply free water and the other is used to de-air the grooves.

The complex part of the system is the proper design and construction of the water inlet valve and the pressure transducer chamber (see Fig. 2.27 and 2.32 to 35) in the base plate. Realising that the efficiency of these components is an important factor in keeping the volumetric strain of the sample within the design limits, special efforts were taken in their design. Proper dimensioning for these components is necessary. The design of these components is explained below.

The water inlet hole meets the water inlet chamber almost at right angles (see base plate plan, Fig. 2.32),

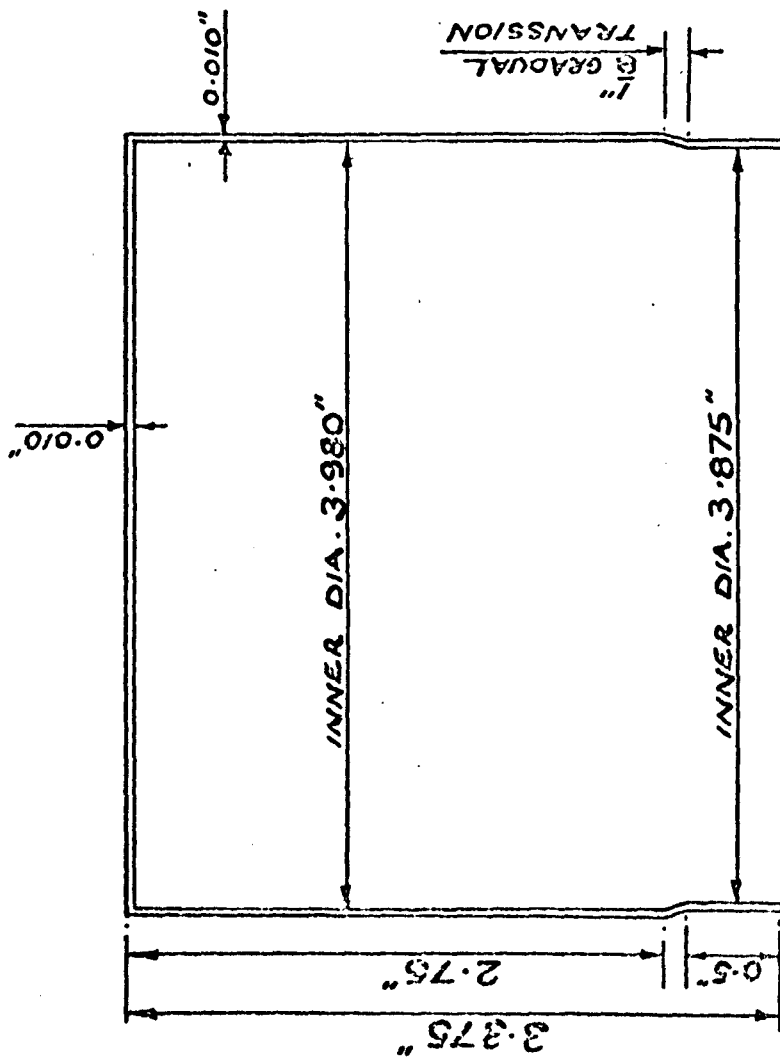
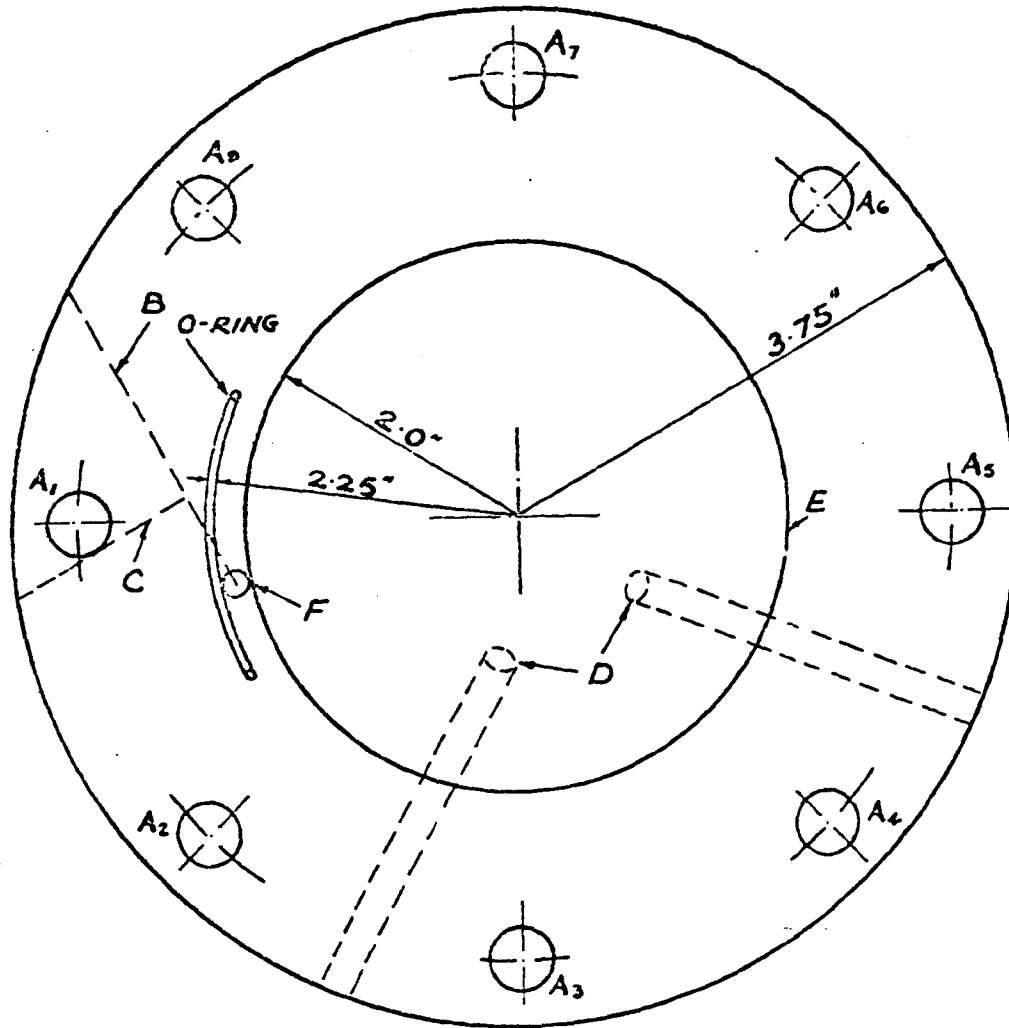


Fig. 2.31 Cross - Section of Rubber Membrane used in Isotropic Swell Pressure Apparatus.



- A → $\frac{3}{8}$ in diameter Studs (8Nos) on Base Plate to Clamp Upper Chamber. Pitch of Studs is 6.5 inch.
- B → Centre Line of Water Inlet Chamber ; C → Centre Line of Water Inlet Hole. [Water Inlet Chamber (2.50" overall length) to be drilled in Base Plate as per dimensions given in Fig.2.33. The Chamber should provide a tight fit to the Water Inlet Valve, the valve is shown in Fig.2.32. Water Inlet Hole to be drilled to meet the Water Inlet Chamber as per requirements in Fig. 2.33.]
- D → Water Supply Vents, 0.25 inch in diameter.
- E → 4" in diameter and $\frac{3}{4}$ " high Pedestal on Base Plate.

Fig. 2.32 Plan of Base Plate, Isotropic Swell Pressure Apparatus.

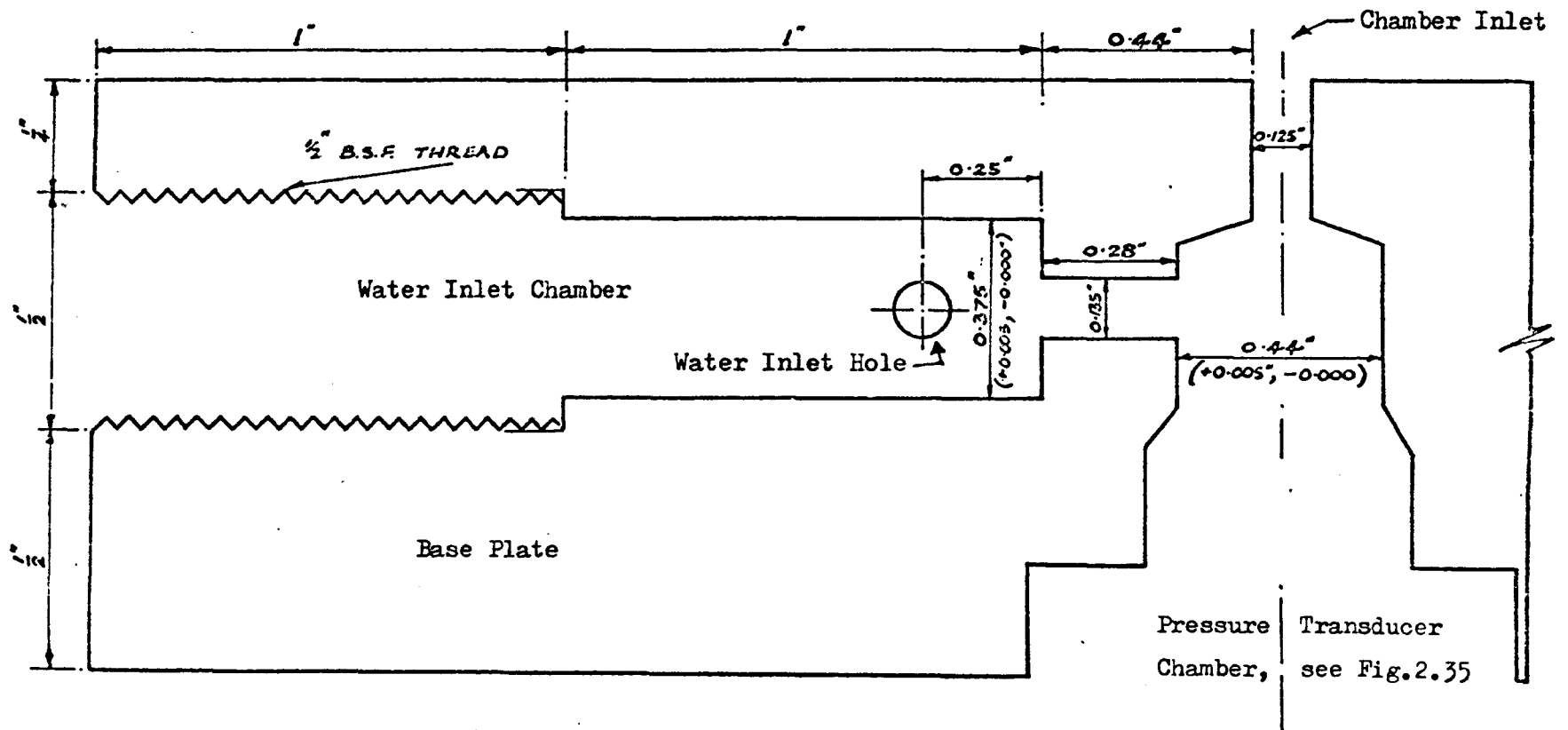


Fig. 2.33 Cross-Section of Water Inlet Chamber.

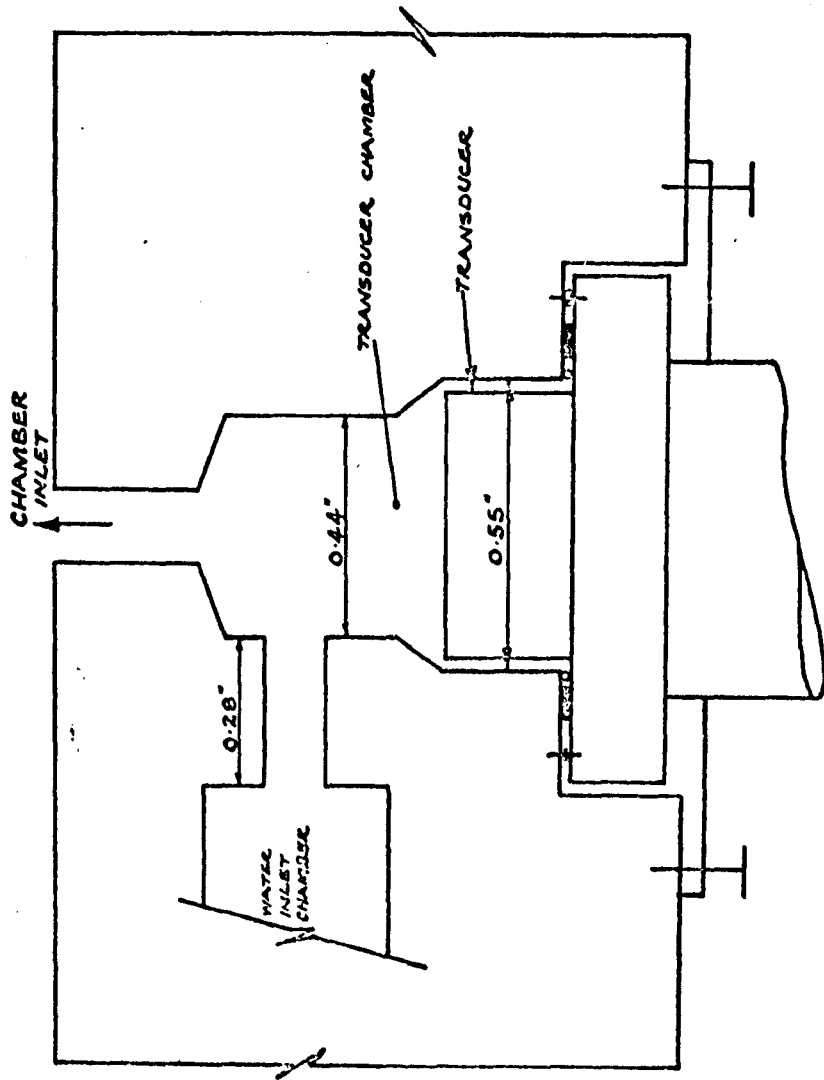


Fig. 2.35 Position of Pressure Transducer.

and the water inlet chamber is connected to the pressure chamber inlet through the pressure transducer chamber (see Fig. 2.33). The water inlet valve is a screw, which in the fully tightened position (as shown in Fig. 2.27) closes the water inlet hole. It has two 'O'-ring seals, a back seal and a forward seal. The seal provided at the back serves to prevent any low pressure water entering the threads of the screw. When closed, the forward seal prevents water from entering or leaving the pressure chamber. The length and position of the water inlet valve is governed by the following requirements:

- (a) The pressure transducer chamber is placed directly below the pressure chamber inlet, see Fig. 2.35.
- (b) Enough metal is left between the pressure transducer chamber and water inlet chamber to provide solidity for the bearing surface of the forward seal, see Fig. 2.35.
- (c) When the water inlet valve is open, the forward seal should withdraw behind the water inlet hole, see Fig. 2.27.
- (d) The start of the thread is positioned so that the back seal continues to seal when the water inlet valve is open, see Fig. 2.27.
- (e) The length of the thread must provide a positive bearing in the fully open position.
- (f) The threads require lead-ins for their construction.

The dimensions of the water inlet valve are fixed in accordance with these requirements (see Figs. 2.33 and 2.34), and it is then found necessary to drill the water inlet chamber angularly on the base plate, Fig. 2.32.

The pressure transducer chamber leads at the top to the pressure chamber inlet and extends at the bottom to accommodate a pressure transducer. The water inlet chamber meets the pressure transducer chamber tangentially (Fig. 2.35) in order to create a forced vortex to assist in the removal of air bubbles from the pressure transducer chamber when filling the apparatus with water.

A pressure transducer was chosen as a means of measuring the swell pressure with the minimum of deflection. The transducer used, is made by Bell & Howell, Model 4-312 with pressure range of 0-100 PSIA and is diagrammatically shown in Fig. 2.36.

2.5.2 Laterally Confined Swell Pressure

The apparatus consists of a main cylindrical base 12 inch (305 mm) in diameter and 2 inch (51 mm) thick. Two holes made at a pitch of 9 inch (229 mm) on this base hold two tie rods of 0.5 inch (13 mm) dia. and 8 inch (203 mm) long, and another two holes at the same pitch hold two dummy tie rods. These four rods are used when the strain gauges are used in the apparatus. However, two more holes are drilled on this base at a pitch of 9 inch (229 mm) to hold two numbers of 1.25 inch (32 mm) dia. tie rods. These 1.25 inch (32 mm) dia. tie rods are used when the measurements are made using a proving bar. The plan of the main base and the dimension of the tie rods are shown in Figs. 2.37 and

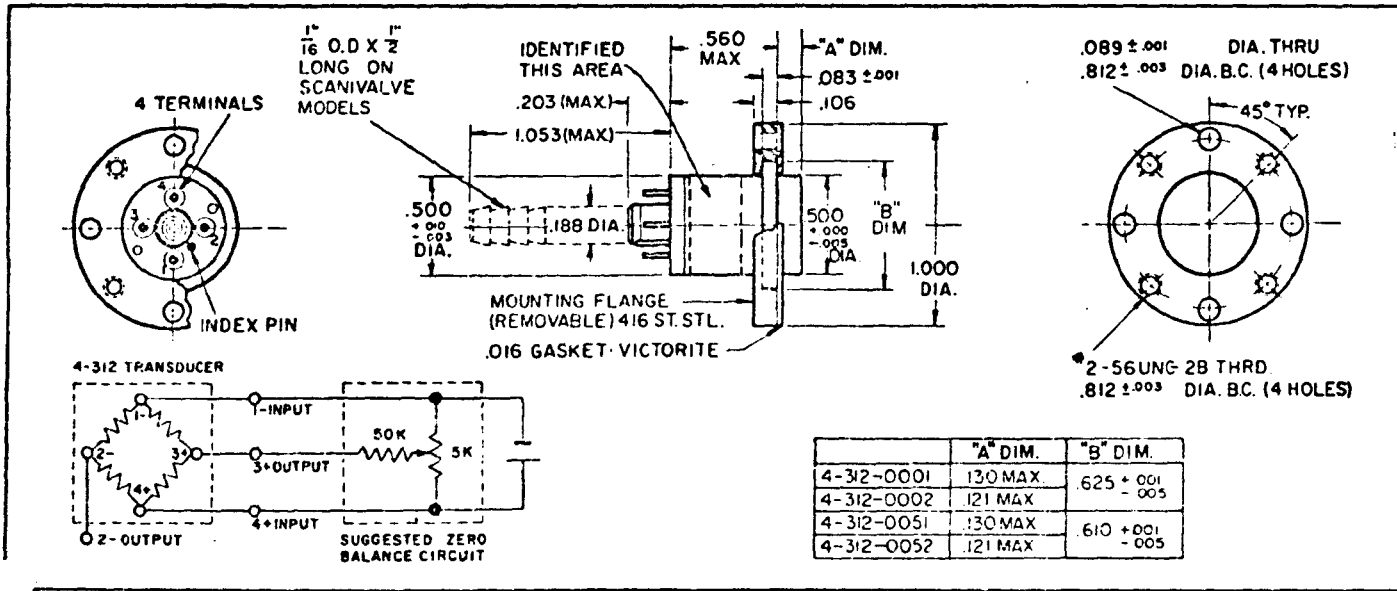


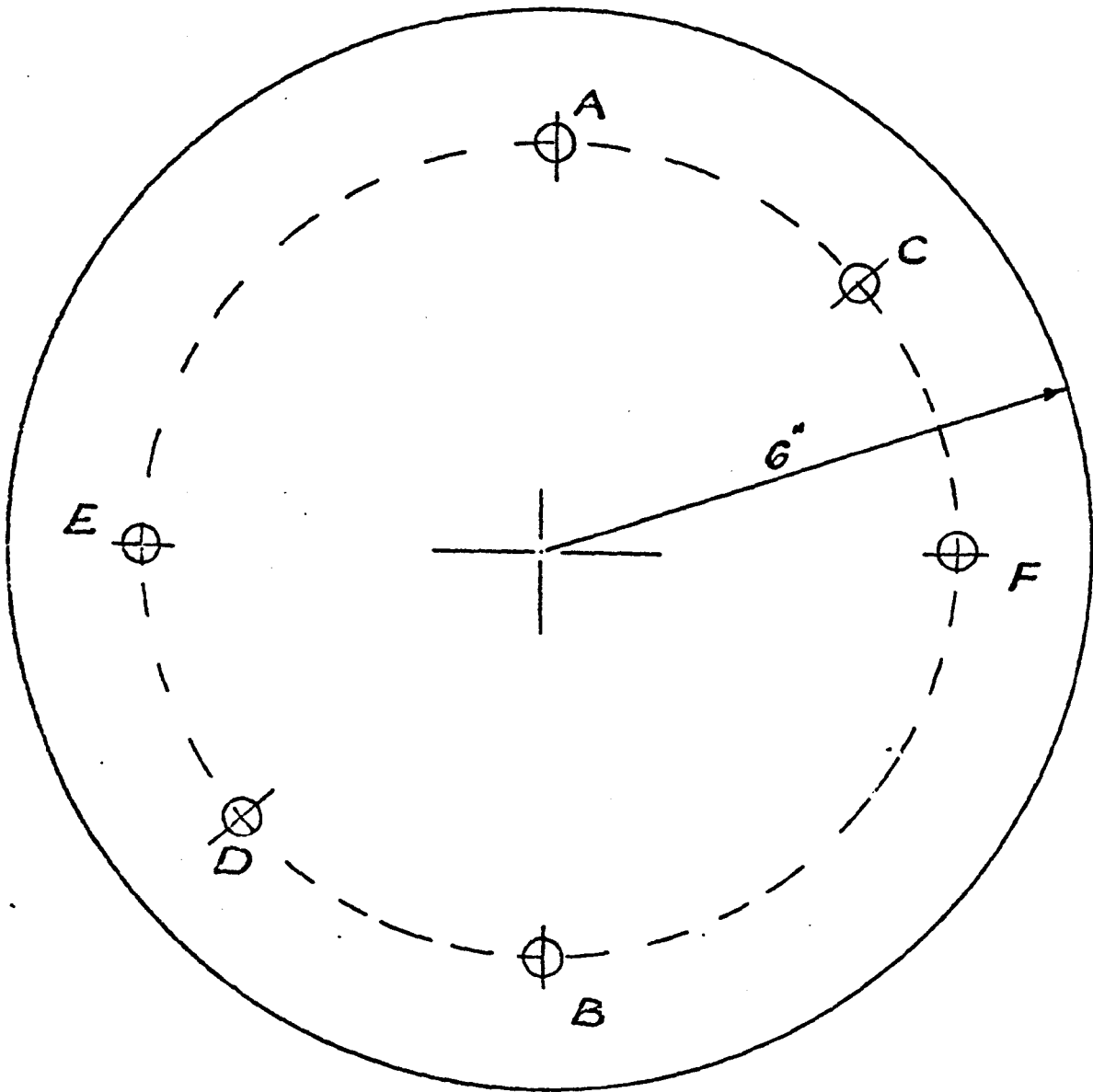
Fig.2.36 Pressure Transducer Details.

2.38 respectively.

A screw 4 inch (102 mm) dia. and 5 inch (127 mm) long is provided at the centre of the main base; and the screw has a hand-wheel at its bottom to facilitate its rotation. To eliminate backlash the threads are made to fit tightly. Theoretically a backlash eliminator would be preferable, but the simpler design did seem satisfactory. The screw carries a sample base, 6 inch (152 mm) in dia. and 1 inch (25.4 mm) thick, at its top. This sample base carries a rim 2 inch (51 mm) high, brazed all around its circumference. The sample base and the screw are constructed as a single unit to avoid bedding errors. Triangular threads are provided on the screw in order to achieve greater rigidity in the system. A porous stone 4 inch (102 mm) in dia. and 0.25 inch (6.4 mm) thick is cemented at the centre of the sample base in the swell pot.

The central piece of the compaction mould carrying a 4 inch (102 mm) dia. and 1 inch (25.4 mm) high sample is placed on the porous stone, with a second porous stone on the top of the sample. A 4 inch (102 mm) dia. and 0.25 inch (6.4 mm) thick perforated plate is placed on the top of the porous stone, and has a 0.5 inch (13 mm) dia and 1 inch (25.4 mm) long stem brazed on top at its centre. The other end of the stem butts against a 11 in x 2 in x 2 in (279 mm x 51 mm x 51 mm) clamping bar.

The two 0.5 inch (13 mm) dia. and 8 inch (203 mm) long tie rods coming from the main base pass through two $\frac{3}{8}$ inch (16 mm) holes made at the two ends of the clamping bar. The clamping bar is held rigidly by using two $\frac{3}{8}$ inch (16 mm) dia. nuts on each of the two tie rods. Two strain



- A and B — Position of two tie rods (0.5" dia, 8" long) at a Pitch of 9".
- C and D — Position of two tie rods (Dummy Posts of length 5") at a Pitch of 9".
- E and F — Position of two tie rods (1.25" dia, 8" long) at a Pitch of 9".

Fig. 2.37 Plan of Main Base in Laterally Confined Swell Pressure Apparatus.

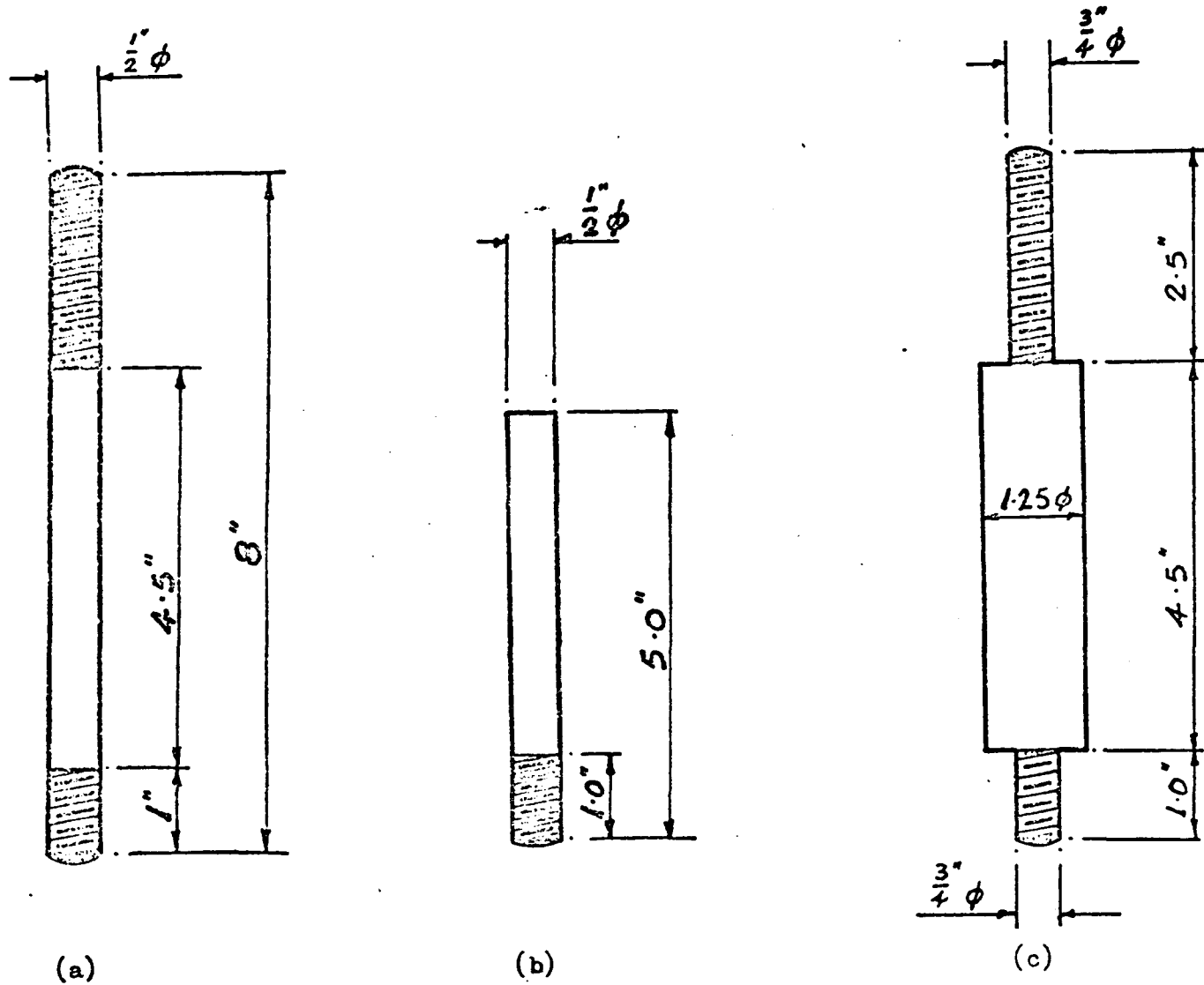


Fig. 2.38 Details of Tie Bars, (a) and (b) to be used in Strain Gauge System, (c) to be used in Proving Bar System.

gauges (1×10^{-6} inch) are fixed on each of these two tie rods to measure the extension of tie rods during swell pressure development of the sample. Two dummy tie rods, fitted with strain gauges, are provided for temperature compensation.

Should it become necessary to use a proving bar as the method of measuring swell pressure, in place of strain gauges; the four tie rods are replaced by two tie rods of 1.25 inch (32 mm) diameter. The proving bar and a clamping bar on its top are fixed by bolting them onto the top of the tie rods. A dial gauge is fixed to record the deflection of the proving bar and in this case the vertical stem butts against the proving bar (see Fig. 2.29)

Noting that, the smaller the volumetric expansion of the sample, the more reliable is the measurement of swell pressure, it can be seen from the design calculations (see Appendix 1) that using strain gauges is more advisable. Appendix 1 shows that the deflection of the proving bar at 100 psi (689.5 KN/m^2) swell pressure is 0.014 in (0.36 mm) compared with a deflection of tie bars equal to 0.00084 in (0.02 mm) in the strain gauge system.

2.5.3 Summary of The Design of Apparatus

In the present study, Finn et al's (1958) apparatus and Seed et al's (1962)^A apparatus were used as models to design isotropic swell pressure apparatus and laterally confined swell pressure apparatus respectively. Swell pressure measurements are subject to a systematic underestimate. In the isotropic swell pressure apparatus, these errors are due to:

- a) bedding errors,
- b) compressibility of the membrane,
- c) compressibility of the filter paper,
- d) compressibility of the O-ring,
- e) compressibility of the water,
- f) expansion of the chamber,
- g) deflection of transducer (negligible).

In the laterally confined swell pressure apparatus, the errors are due to:

- a) bedding errors,
- b) extension of the tie bars,
- c) compressibility of the filter papers.

It was assumed that preloading of the laterally confined swell pressure apparatus would eliminate the error due to compressibility of the filter paper. It was recognised that the effect of the extension of tie bars could be eliminated by using a servomechanism to compensate for the extension. However, the experimental work on which the estimations of bedding error were based showed them to be both substantial and somewhat erratic, in that different tests gave different results. They were also non-linear. It was concluded that it would be extremely difficult to pre-programme a servomechanism to compensate for bedding errors in a reliable manner and that in practical terms some error is unavoidable.

In the present apparatus, the design calculations in Appendix 1 suggested that the swell pressure samples expanded by approximately 1.0 to 1.5% volumetric strain. The observations cited in section A1.2.8 suggested that

this value might be an overestimation, whilst the values of probable expansion shown later in Tables 5.1, 5.4, and 5.5 of chapter 5 suggested that this value might be an underestimate. Small values of volumetric expansion are known to be associated with much larger errors of swell pressure measurement, and in section A1.2.10 it was suggested that the results here are underestimated by 15% or more.

The design of apparatus to measure swell potential in accordance with Seed et al's (1962) definition was straightforward, and no serious problems were encountered in its subsequent use. The problem of measuring isotropic swell potential is discussed in Appendix 4, in which it was concluded that a full-scale investigation would be required before it would be possible to measure isotropic swell potential with any degree of accuracy.

The next chapter discusses the programme of testing that was undertaken in the present study.

CHAPTER 3

MATERIALS, METHODS AND RESULTS

3.1 INTRODUCTION

An outline of the soils investigated and the test procedures used in the course of this research are presented in this Chapter. This Chapter also reports the results obtained in the programme of tests and presents a discussion of those of the observations which bear on the reliability of the results. A further analysis of the results will be presented later in Chapter 5.

The soils tested in this programme include three series of artificial mixtures, providing in total 18 artificial soils, and one series of 10 natural soils. Each of the series of artificial mixtures studied in this programme was composed of two components, clay and sand or bentonite and illite. For each series, the mixtures ranged from 100% of one component to 100% of the other.

As a preliminary to the other tests, the specific gravities of all 28 samples were measured as reported in Appendix 2. Cation exchange capacity was also measured for two of the natural soils, see Appendix 3. Atterberg limit tests, standard A.A.S.H.O. Compaction tests, laterally confined swell pressure tests, and laterally confined swell potential tests, were done on all the soils considered in this study. In addition, 16 isotropic swell pressure tests were carried out on the illite-sand series (of artificial samples) and on the natural samples. A preliminary series

of isotropic swell amount tests is reported in Appendix 4. The details of the main tests and the results are reported in the following sections.

3.2 MATERIALS

3.2.1 Soils for Artificial Mixtures

Two artificial soils, bentonite and illite, and a local sand were used in preparing three artificial mixtures in the present study. The details of these soils are reported below.

The bentonite used is Fullbent 570, produced and supplied by the Fuller's Earth Union Ltd. in England. According to the suppliers, this material is composed of sodium montmorillonite and contains a preponderance of particles of less than 2μ size, see Fig. 3.1. The material was supplied in 25 kg bags, but it was observed that some of the properties varied slightly from bag to bag. With this in view, material from a single set of bags was used for the compaction and swell tests in a given series of mixture. Thus, Batch 1 of the material containing a mixture of 3 bags was used for the bentonite-sand series; and Batch 2 containing a mixture of another three bags, was used for the bentonite-illite series. For the compaction and swell tests, two sets of 100% bentonite samples, made from the appropriate batches, were used for the bentonite-sand and bentonite-illite series respectively. Tables 3.4 and 3.5 show the results[†] obtained for these two sets of samples respectively. For the Atterberg limit and specific gravity

[†] see after page 82.

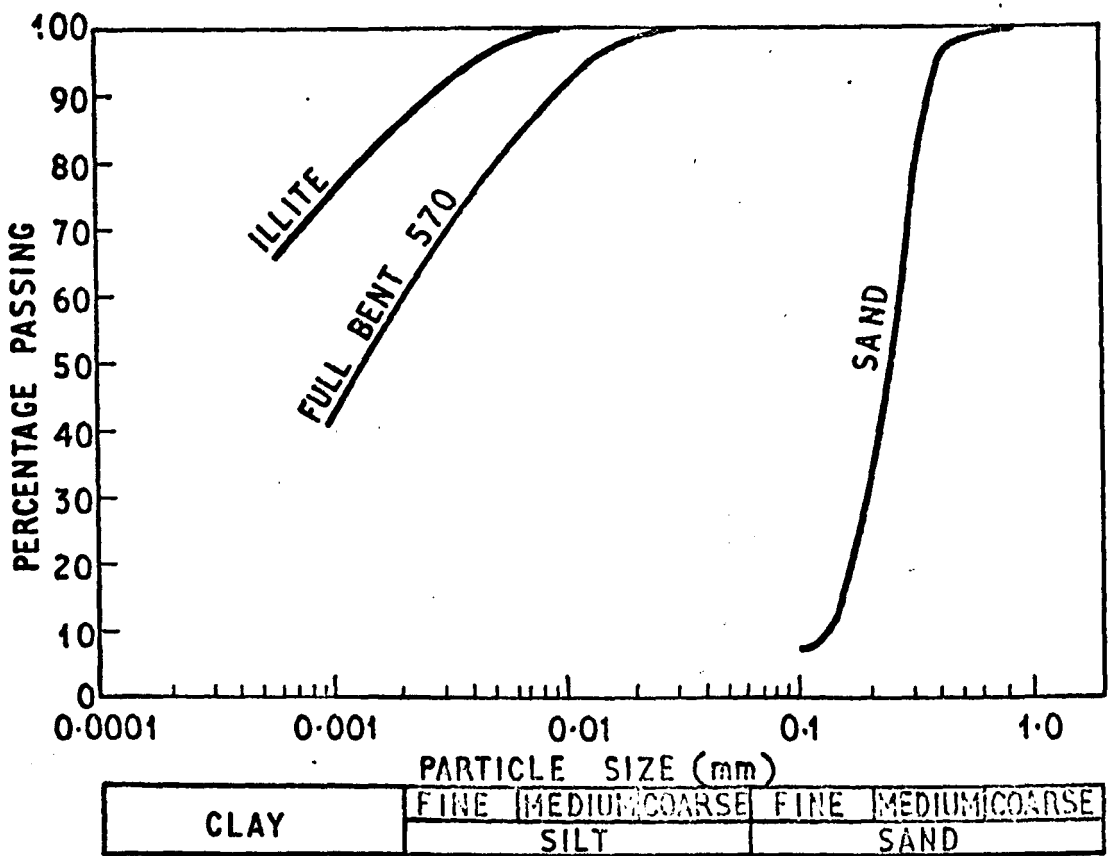


Fig. 3.1 Particle Size Distribution Curves, Illite; Bentonite (from manufacturer); Lochaline Sand (from M.A.Osman).

tests, equal proportions of Batches 1 and 2 were mixed together, and this composite material was used for both the bentonite-sand and the bentonite-illite series. The properties of the bentonite are:

$$LL = 192\% ; \quad PL = 55\% ;$$

$$PI = 137\% ; \quad G_s = 2.490.$$

The illite used in this study is Hybond Blue Illite, supplied by the Fayle's Blue Company in England. The material was supplied in 20 kg bags and seemed to be fairly uniform from bag to bag. A test made by the present writer showed approximately 88% of the particles to be finer than 2μ size (Fig. 3.1). X-ray diffraction showed some kaolinite as well as illite. The properties of this material are:

$$LL = 71\% ; \quad PL = 32\% ;$$

$$PI = 39\% ; \quad G_s = 2.71$$

The sand used in preparing the clay-sand mixtures was obtained from the Lochaline area in Scotland. According to M.A. Osman (per. comm.) the material is closely graded fine to medium size, Fig. 3.1. The sand particles were observed to be rounded with a few of them being sub-angular. Some properties of the sand are:

$$G_s = 2.65 ; \quad d_{10} = 0.15 \text{ mm} ;$$

$$U = 1.7.$$

There is some doubt about the accuracy of the particle size analysis of bentonite quoted in Fig. 3.1, because these results relate to a different sample than that used

here. It was therefore decided to treat the bentonite as 100% clay when calculating the proportions of the bentonite-sand mixtures. The illite was treated in the same way. This was appropriate because the smallest sand particles are much larger than any silt particles which the bentonite or illite might contain.

3.2.2 Artificial Mixtures

The three artificial mixtures studied were:

- (i) Illite-sand
- (ii) Bentonite-sand
- (iii) Bentonite-Illite

The proportions by weight of clay in the illite-sand mixture were 100%, 82%, 64%, 50%, 32%, 14% and 0%.

In both bentonite-sand and bentonite-illite mixtures, the proportions by weight of bentonite were 100%, 83.3%, 66.7%, 50.0%, 33.3%, 16.7% and 0.0%

For each of these mixtures, a stock of 5-6 kg was prepared and used for all the tests, except as noted.

3.2.3 Natural Soils

Ten soil samples were obtained for this study from the plough layer from a farm called Wootton Broadmead near Bedford, England, Map Reference TL 0242. The samples were selected and 'collected' by Messrs. C.M. Darlow and J. Darlow, who have farmed there for 45 years approximately. The samples were labelled from 350-1 to 350-10 and were accompanied by a 6 inch-plan showing the approximate positions from which they had been taken. It was reported that the heavier of these

soils crack widely during summer, up to 20 mm at the surface.

All the ten samples were disturbed when brought into the laboratory. These ten soils had been chosen to differ widely in clay content (9 to 87%), but they appear to have similar mineralogy, see results in section 3.4.3. The Unified Classification system for these soils is shown in Fig. 3.2, from which it is seen that all the soils fall near the A-line.

According to King (1969), these soils were mapped in a single mapping unit containing mainly Rowsham Series and Denchworth Series of the Rowsham Association and Milton Series of the Milton Association. Although these are of different Associations, it was stated that areas of Milton Series occur within the Rowsham Association. Moreover, an occurrence of Milton Association is mapped within 2 km. to the South of the sampling site. A brief description of Rowsham, Denchworth, and Milton Series is reported below following King (1969).

The Rowsham Series is most widespread and is formed in a layer of clayey drift containing some stones and appreciable amounts of sand, often with a narrow gravelly seam immediately overlying the Jurassic clay at depths of between 18 and 36 in (460 and 920 mm). A dark brown clay loam or sandy clay loam surface horizon overlies an olive or greyish brown clay loam to clay subsoil with distinct fine ochreous mottling. Below, a discontinuous seam of gravelly sandy clay loam overlies grey plastic clay faintly mottled with olive and brownish yellow, often

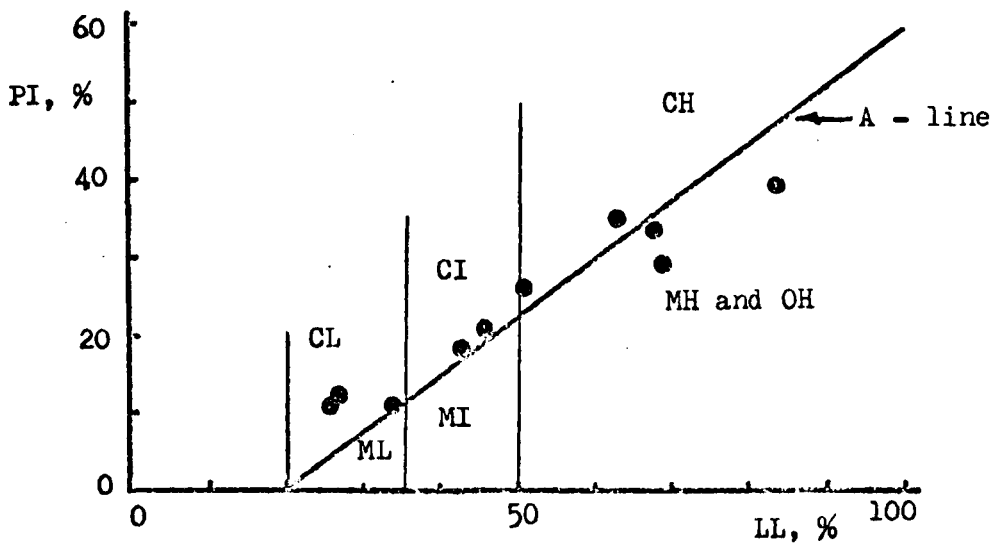


Fig. 3.2 Casagrande's Classification Chart,
Natural Soils.

with some small secondary calcium carbonate concretions. Intimately associated with the Rowsham series in a complex mosaic are soils of the Denchworth series in which the superficial drift layer, if present, is predominantly clayey. The surface soil is a dark greyish brown clay loam or clay, with rusty mottling along root channels under old grass. Between 9 and 18 in (230 and 460 mm) there is a very tenacious, grey and yellow-brown, prominently mottled, clay subsoil with coarse blocky or prismatic structure merging at greater depths into darker grey clay with faint to distinct olive-yellow mottling and some secondary calcium carbonate concretions. These heavy soils are imperfectly or poorly drained and crack severely in periods of drought. The parent material for the Milton Series is gravelly and loamy drifts, which is the same as that for the Rowsham Series. However, the Milton Series is found on gravelly terrace deposits, with no gravel occurring within 36 in (920 mm) of the surface. The Milton Series has a dark greyish brown, more or less stony, sandy clay loam or clay loam plough layer.

C.M. Darlow reported that a thin gravelly seam was present at site No. 3, which is a characteristic feature of the Rowsham soil Series. Sample 350-6 had been obtained from a "slight rise similar to a terrace" and was therefore at first thought to belong to Milton Series, which are mainly found on gravelly and loamy drifts. The clay contents of the surface soils for the Milton, Rowsham and Denchworth Series are quoted by King (1969) as 19%, 33% and 75% respectively. However, as stated earlier, the ten

soils chosen for the present study widely vary in their clay content (9% to 87%) and it was assumed as a first approximation that the selected soils belong to one of the three series mentioned above. Although this assumption is approximately correct, a detailed analysis of the particle size distribution results is presented later in Chapter 5.

The coarse organic matter and the stones were removed from all the soils before they were subjected to the laboratory tests in the present study. The coarse organic matter was mainly grass with some roots and stalks and varied from 0.04% to 0.2%. The stones detected were mainly flint with sandstone, chalk and some rounded quartz pebbles. The stone content in the soils varied from 0.07 to 3.5% by weight.

3.3. METHODS

3.3.1 Limit Tests

The Atterberg limit tests, viz; liquid limit and plastic limit were determined in accordance with BS 1377: 1975 Test No 2 (A). For the illite-sand series, the tests were duplicated by a second person.

3.3.2 Allophane Test

Clay crystals are often coated with amorphous alumina-silicate material, which is often loosely called allophane. This is highly reactive in its ability to combine with anions, cations and organic matter. Thus, despite the small amount, when present, it can play a significant role in modifying the properties of the soil.

A quick test was used to determine whether allophane was present in the natural soils of this study! This test is usually called the 'Sodium Fluoride Test For Amorphous Alumina-Silicates! The allophane was detected by treating the soil with sodium fluoride solution. The F-ions complex 'mobile' or reactive aluminium, displacing its hydroxy groups, so that the pH of the suspension rises. The details of the test are as follows:

An approximately 1N solution of NaF was made up by preparing a saturated solution and drawing off 50 ml of the supernatant. 1 gm of air dry soil was placed in a 100 ml beaker. The pH electrode was placed in readiness above the soil and the 50 ml NaF solution was added. The pH reading was taken immediately. Further pH readings were taken at $\frac{1}{2}$ minute intervals, with stirring at the time of measurement. As the rate of change slowed down, the intervals were increased to 1 minute. The pH was plotted against time for 10 minutes.

As a first indication of allophane content, the pH after 10 minutes was considered, the following interpretation being made: The allophane content was negligible if $\text{pH} < 9.0$, low if pH is 9.0 to 9.8, medium if pH was 9.8 to 10.5, and high if $\text{pH} > 10.5$. The rate of fall of pH also gave an indication of the amount of Allophane present.

The writer thanks Dr H.Fullerton for providing the details of the test.

3.3.3 Particle Size Distribution Tests

The particle size distribution tests for the ten natural soils and for the illite were carried out using the hydrometer technique in conjunction with sieving in accordance with BS 1377 : 1975 Test No 7 (D).

This method covers the quantitative determination of particle size distribution in a soil from the coarse sand size downwards. Test 7(D) was used in preference to Test 7(B) because, in all the natural soils tested in this investigation, more than 10% of the material passed the 63 μm BS test sieve.

3.3.4 Organic Matter

The percentage by mass of organic matter present in the natural soils used in the investigation was determined in accordance with BS 1377:1975 Test No 8.

3.3.5 pH Value

The pH values of the natural soils were determined by the standard electrometric method described in BS 1377:1975 Test No 11 (A).

3.3.6 X-Ray Diffraction Tests

X-ray diffraction was used for a qualitative identification of the clay minerals in the natural soils used in this programme.

In order to prepare samples for x-ray diffraction, about 10 gm of soil were ground in an agate pestle and mortar, and mixed in water. This suspended soil was spread on a glass microscope slide of size 2 in x 1 in and allowed to dry under an electric lamp for 12 to 24 hours. Care was taken to spread a thin layer in all cases.

Copper K α radiation was used in the x-ray machine. The settings of the instrument are shown in Table 3.1. The results from the x-ray machine were in the form of a

Table 3.I Control Settings for Tests on X-Ray
Diffraction Machine

Control	Setting
Power	40 Kv × 20mA
Slit	1.0 × 0.2mm
Time Constant	4
Counts per Second	200
Chart Speed	300mm/hr
Scan Speed	$\frac{1}{2}^{\circ}$ /min
Suppression	Zero

graph showing the intensity of reflected radiation against diffraction angles, 2θ values. Fig. 3.3 is a small scale reproduction of one of these graphs. For the Cu K α radiation, the wave length λ is 1.541 \AA , hence

$$d = \frac{n \lambda}{2 \sin\theta} = \frac{0.7705}{\sin\theta}$$

for the first order reflection ($n=1$). Using this formula the 2θ values were converted into d-spacings (\AA). These d-spacings were used in identifying the various minerals. Supplementary tests were performed (e.g. by heating or by adsorption of ethylene glycol), wherever it was found necessary. The criteria used in identifying the clay minerals are summarised below.

Peaks with d-spacings of 7.1 to 7.2 \AA suggest Kaolinite or chlorite; 10 \AA peaks suggest illite or halloysite; 12.5 \AA peaks suggest montmorillonite; and 14 \AA peaks suggest chlorite, vermiculite, montmorillonite or a mixed layer clay.

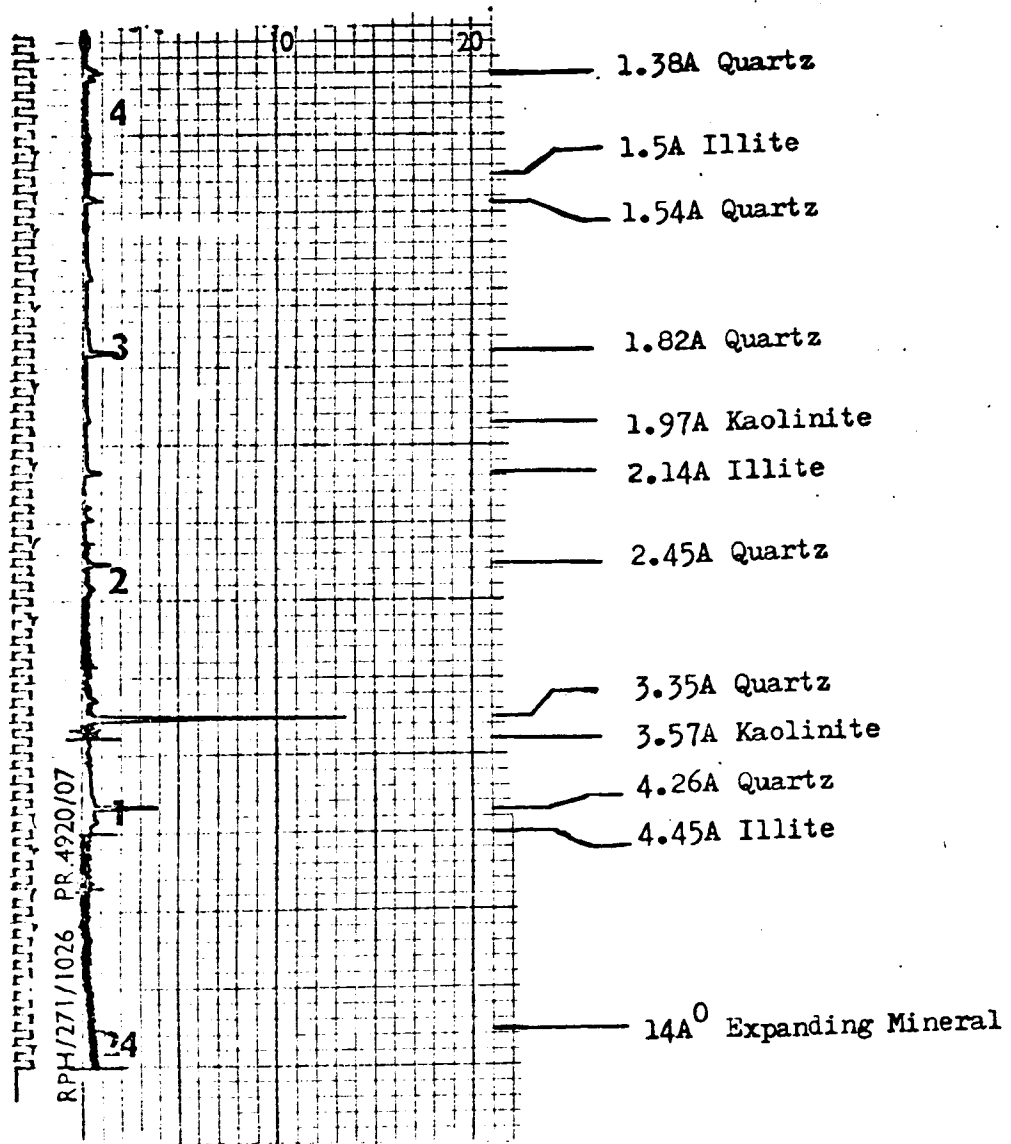
After heating to 110° C the 10 \AA peak shifts towards the 7.2 \AA range for halloysite.

Heating to $300\text{--}400^\circ \text{ C}$ shifts the 12.5 \AA peak to a spacing around 10 \AA for montmorillonite.

Heating to 600° C destroys the structure of halloysite completely, whereas for illite the 10 \AA peak remains stable at this temperature. This temperature also causes the 7.2 \AA peak to disappear for both kaolinites and chlorites.

Heating to 700° C causes the 14 \AA peak to intensify for

Fig. 3.3 X-Ray Diffraction Pattern (Small Scale Version),
Soil No. 350-1.



chlorite, otherwise the 14 \AA° peak may be montmorillonite, vermiculite or a mixed layer clay.

Ethylene glycol treatment shifts the 14 \AA° peak to a spacing of 17 \AA° for montmorillonite; and for a mixed layer clay containing montmorillonite the 14 \AA° peak will be shifted to some lesser and variable spacing. For vermiculite, the ethylene glycol treatment shifts the 14 \AA° peak to a spacing of 16.3 \AA° .

It can be seen from the above description that whilst it is comparatively easy to identify Kaolinite, illite and halloysite; it is difficult in normal practice to resolve the 14 \AA° peak for a precise identification of the mineral involved. However, a 14 \AA° peak does indicate a mineral with an expanding lattice of a swelling nature.

In addition to the general procedure discussed above, the subsidiary peaks and their relative intensities were also considered to assist in the clay mineral identification. This data for some important minerals was compiled from Brown (1961) and are shown in Table 3.2.

3.3.7 Compaction Tests

The compaction tests reported in this study were performed in accordance with the standard A.A.S.H.O (DSIR, 1972) test requirements, and were carried out in the special compaction mould designed in this programme, see section 2.4.2, Fig. 2.26 . For the natural soils, samples were passed through a 20 mm BS sieve, but in the case of the artificial soils the compaction tests were made on the material as it had been mixed. In all cases, different samples were mixed at the different moisture contents, with

Table 3.2 Diagnostic X-Ray Diffraction Peaks

Quartz

2θ	$d(A^\circ)$	I	hkl
26.6	3.35	I00	I0I
20.85	4.26	35	I00
36.55	2.458	I2	IIO
39.48	2.282	I2	I02
50.2I	I.8I7	I7	II2
60.03	I.54I	I5	2II
68.23	I.375	II	203

Calcite

2θ	$d(A^\circ)$	I	hkl
23.04	3.86	I2	I02
29.42	3.04	I00	I04
35.99	2.495	I4	IIO
39.43	2.285	I8	II3
43.I8	2.095	I8	202
47.53	I.9I3	I7	I08
48.55	I.875	I7	II6

Kaolinite

2θ	$d(A^\circ)$	I	hkl
I2.36	7.I6	I0	00I
24.92	3.575	I0	002
38.50	2.338	9	202
39.38	2.288	8	I3I
36.05	2.49I	8	200
62.36	I.489	8	200
37.8I	2.379	6	20I
45.60	I.989	6	203
55.27	I.662	7	204

Illite

2θ	$d(A^\circ)$	I
8.9	9.9	Very Strong
I8.I0	4.9	Medium
I9.95	4.45	Very Strong
22.97	3.87	Medium
26.60	3.35	Very Strong
35.00	2.56	Very Strong
37.6	2.39	Medium
42.2	2.I4	Medium
62.0	I.497	Strong

Metahalloysite

2θ	$d(A^\circ)$	I
II.95	7.4I	6
20.03	4.432	I0
24.7I	3.603	4
35.02	2.562	4
62.59	I.484	5
54.63	I.680	2

Gypsum

2θ	$d(A^\circ)$	I	hkl
II.70	7.56	I00	020
29.I9	3.059	57	I4T
20.80	4.27	5I	I2T
33.45	2.679	28	022
3I.20	2.867	27	002
23.47	3.79	2I	03I

two or three falling below the plastic limit and two or three above the plastic limit. These samples were well mixed and kept in air tight polythene bags for 7 to 14 days in order to attain moisture equilibrium. All the soil samples for one compaction test were tested on the same day, and the actual moisture was determined by taking a representative sample from top, bottom and middle of the compacted sample. The sample was compacted in 3 layers, with 25 blows per layer using a rammer of 5.5 lbs (2.5 kg) falling through 12 inches (300 mm).

3.3.8 Sample Preparation For Swell Tests

In order to obtain samples for the swell potential and swell pressure tests, air dry (and sieved) samples were brought close to the optimum moisture content. After allowing two weeks for them to attain moisture equilibrium, the samples were tested for their moisture content. The moisture content was then corrected by air drying or wetting, depending on whether the moisture content is above or below the optimum moisture content. This trial and error approach was continued until the moisture content of the sample falls within $\pm 1\%$ of the optimum moisture content. The only exception was in the case of the earlier tests on pure bentonite clay, which were used for the bentonite-sand series, where the initial moisture content exceeded the optimum moisture content by 2.3%. The prepared samples were compacted to the A.A.S.H.O specification in the special compaction moulds, see section 2.4.2. The height of the central

compaction ring was 1.0 in (25.4 mm) for the laterally confined tests and 2.5 in (63.5 mm) for the isotropic tests. After compaction, the upper and lower parts of the compaction mould were removed, and the sample was trimmed level with the edges of the central compaction ring. A certain amount of difficulty was experienced in trimming the compacted natural soils. In many cases, a few repetitions of the compaction test were necessary before finally obtaining a satisfactory sample for the swell tests. The artificial soils were relatively easy to trim.

The laterally confined samples were left in the compaction rings for the swell tests, whereas the samples for the isotropic tests were extruded using a hydraulic jack.

3.3.9 Swell Potential Tests

The swell potential tests were carried out in accordance with the definition of Seed et al (1962) by measuring swell on a laterally confined sample under 1 psi (6.895 KN/m^2) surcharge load. The equipment designed for this purpose in the present study was shown in Fig. 2.30 .

The 1.0 in (25.4 mm) high soil sample alongwith the surrounding compaction ring was placed on the base of the swell pot, sandwiched between two dry porous stones. Filter papers were placed both at top and bottom between the sample and the stone. The weight providing the 1 psi surcharge was placed on the top porous stone. The cross

bar carrying the dial gauges was brought down until both the dial gauges were firmly in contact with the weight. A time of about 15 minutes was allowed for the sample to settle and the initial readings of both the dial gauges were noted. Next, the swell pot was filled with distilled water until the top porous stone was submerged. This initiated the process of swelling. The dial gauges were read at close intervals in the beginning and after about 100 minutes, readings were taken every 24 hours. The readings were continued until the soil attained its maximum swell becoming steady with time. At this stage, the swell potential test was taken as completed.

After the completion of the swell potential test, the water in the swell pot was removed by syphoning.

Then the sample inside its compaction ring was taken out and a representative composite sub-sample was taken from top, middle and bottom of the sample to determine the final water content.

The average of the change in dial gauge readings was taken as the net change in height of the sample. The ratio of the net change in height to the original height, expressed as a percentage was designated as the swell potential (S_c).

3.3.10 Laterally Confined Swell Pressure Tests

The apparatus designed and fabricated to measure laterally confined swell pressure is shown in Fig. 2.28 and was detailed in section 2.4.4 . Plate 3.1 shows

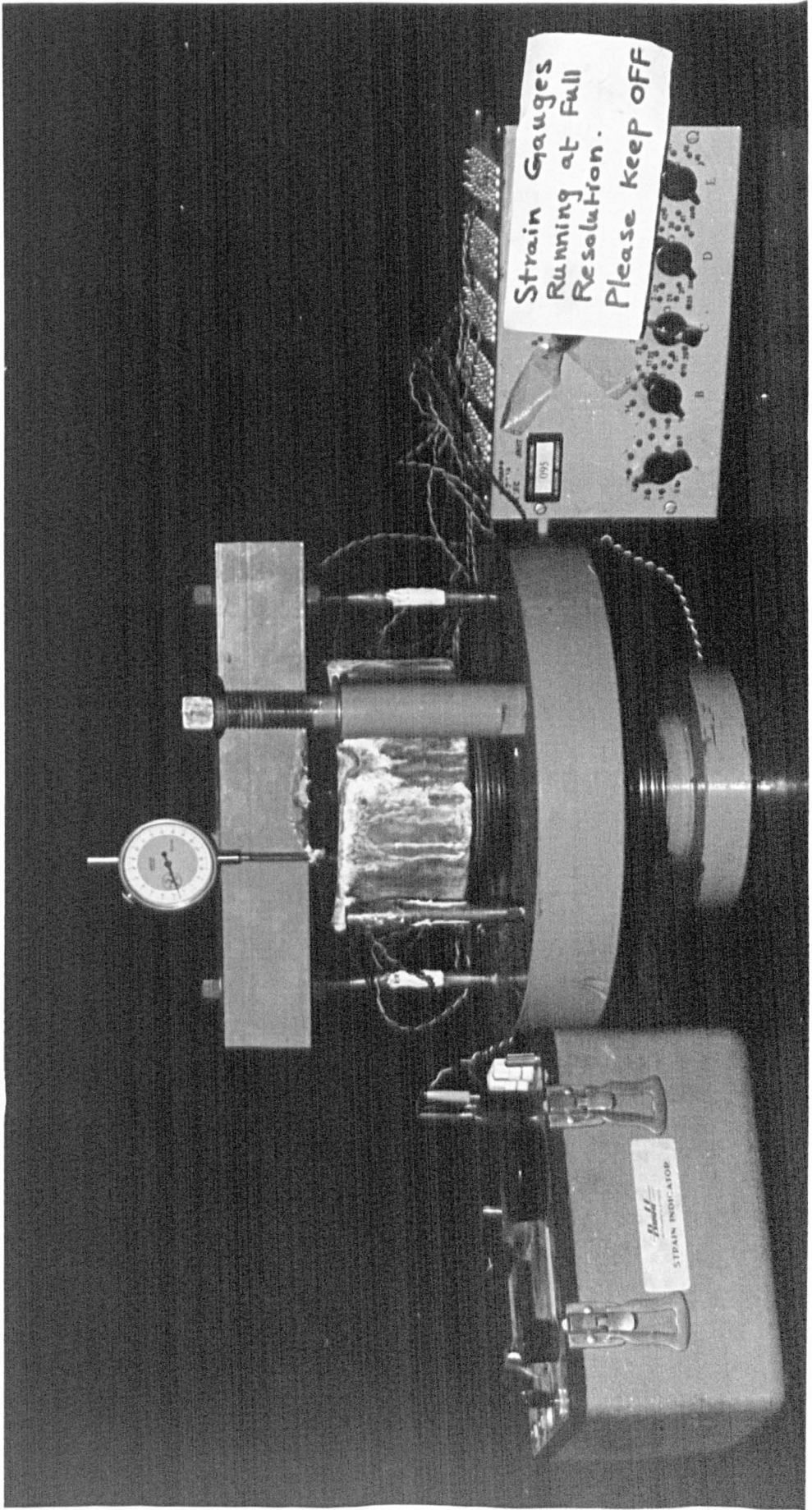


PLATE 3.1

the general arrangement of this apparatus. The strain gauge system of measuring the pressure was used for all the tests made in this study.

The 1.0 in (25.4 mm) high soil sample with its compaction ring was placed in the swell pot on the porous stone, cemented to the base. A second porous stone was placed on the top of the sample. Filter papers were used between the stone and the sample both at top and bottom.

The cross bar was placed across the tie bars carrying the strain gauges in such a way that there was about $\frac{1}{8}$ to $\frac{1}{4}$ in (3.2 to 6.4 mm) space between the perforated plate of the cross bar and the top porous stone. After ensuring that the cross bar was perfectly horizontal, the nuts were tightened to lock the bar in place. Next, the main base was rotated about the screw until the perforated plate just touched the porous stone on top of the sample.

The screw was then tightened to apply a small compressive force on the sample, and then released. This tightening was repeated 4 - 6 times in order to reduce the bedding error due to the stones (see section A1.2.6). Finally the screw was adjusted until the perforated plate was just in contact with the porous stone, and the initial strain gauge readings were taken.

Distilled water was poured into the swell pot until the perforated plate was submerged. The strain indicator readings were taken at close intervals up to 5 or 6 hours and thereafter every 24 hours. The test was taken to be completed after the swell pressure had risen to a maximum.

At the end of the test, water was removed from the pot first, and then the load was released. The soil sample was taken out and a representative sub-sample was used to determine the final moisture content.

For each tie bar, the average of the two sets of strain gauge readings was used to calculate the load using the relevant calibration chart (Fig. 3.4). The sum of the loads carried by the two tie bars was taken as the total load. The total load was divided by the cross-sectional area of the soil sample to obtain the swell pressure (P_c).

3.3.11 Isotropic Swell Pressure Tests

The apparatus designed and fabricated to measure isotropic swell pressure was shown in Fig. 2.27 and was described in section 2.4.3. Plate 3.2 shows the general arrangement of this apparatus.

The 2.5 in (63.5 mm) high test sample, which was extruded from its compaction ring, was placed on the porous stone that had been cemented onto the base plate of the apparatus. The first of the two rubber membranes designed for the purpose (Fig. 2.31) was pulled over the sample, and after this was coated with silicon grease the second membrane was pulled over it. Care was taken to squeeze out any air present between the two membranes, and to see that they were perfectly 'glued' to each other. This double membrane was a tight fit to the sample and rubber bands were used to seal the sample from any contact with outside water in the chamber. The upper chamber was

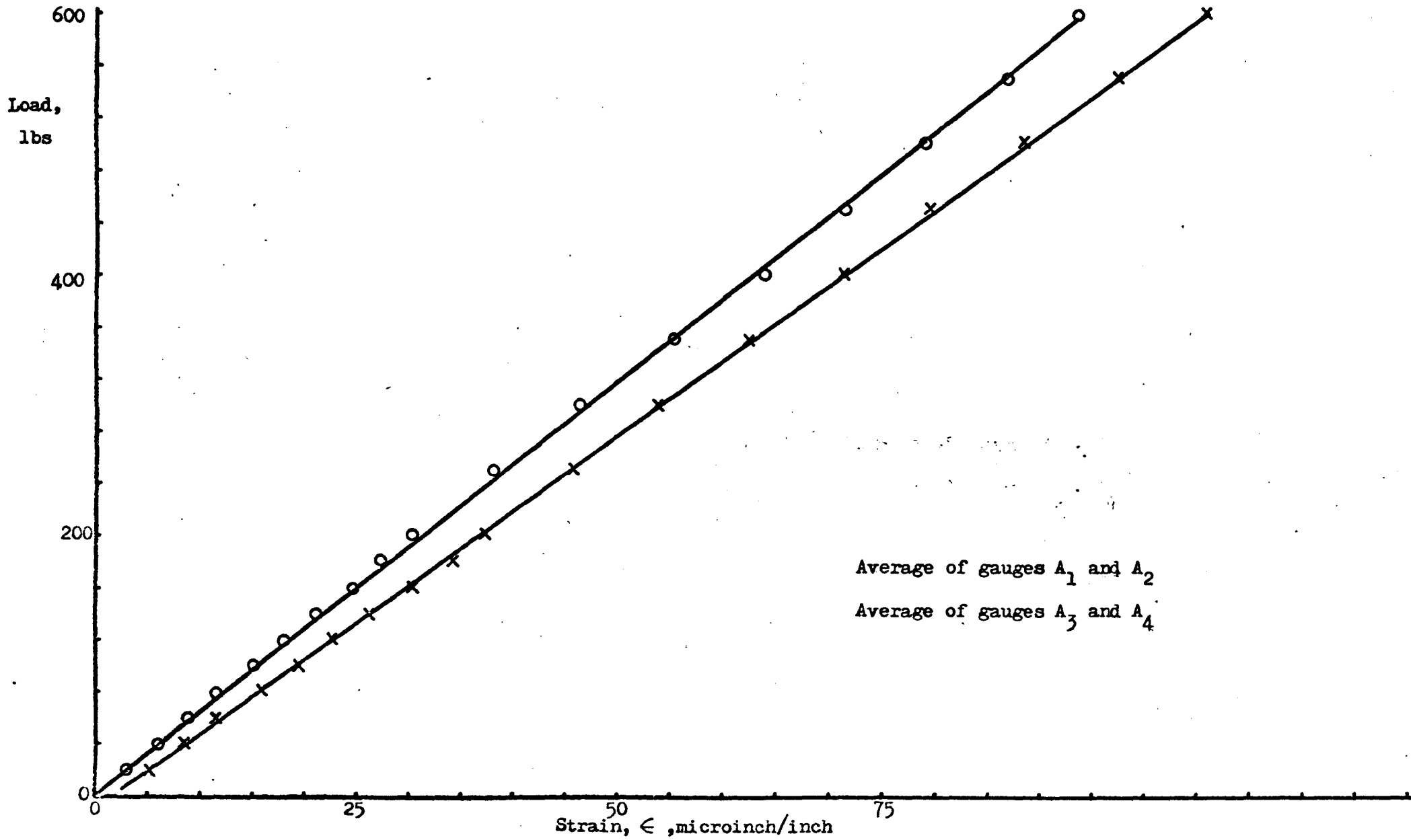


Fig.3.4 Calibration Chart For Strain Gauge System, Gauges A₁+ A₂ are on one tie rod, A₃+ A₄ on the other.

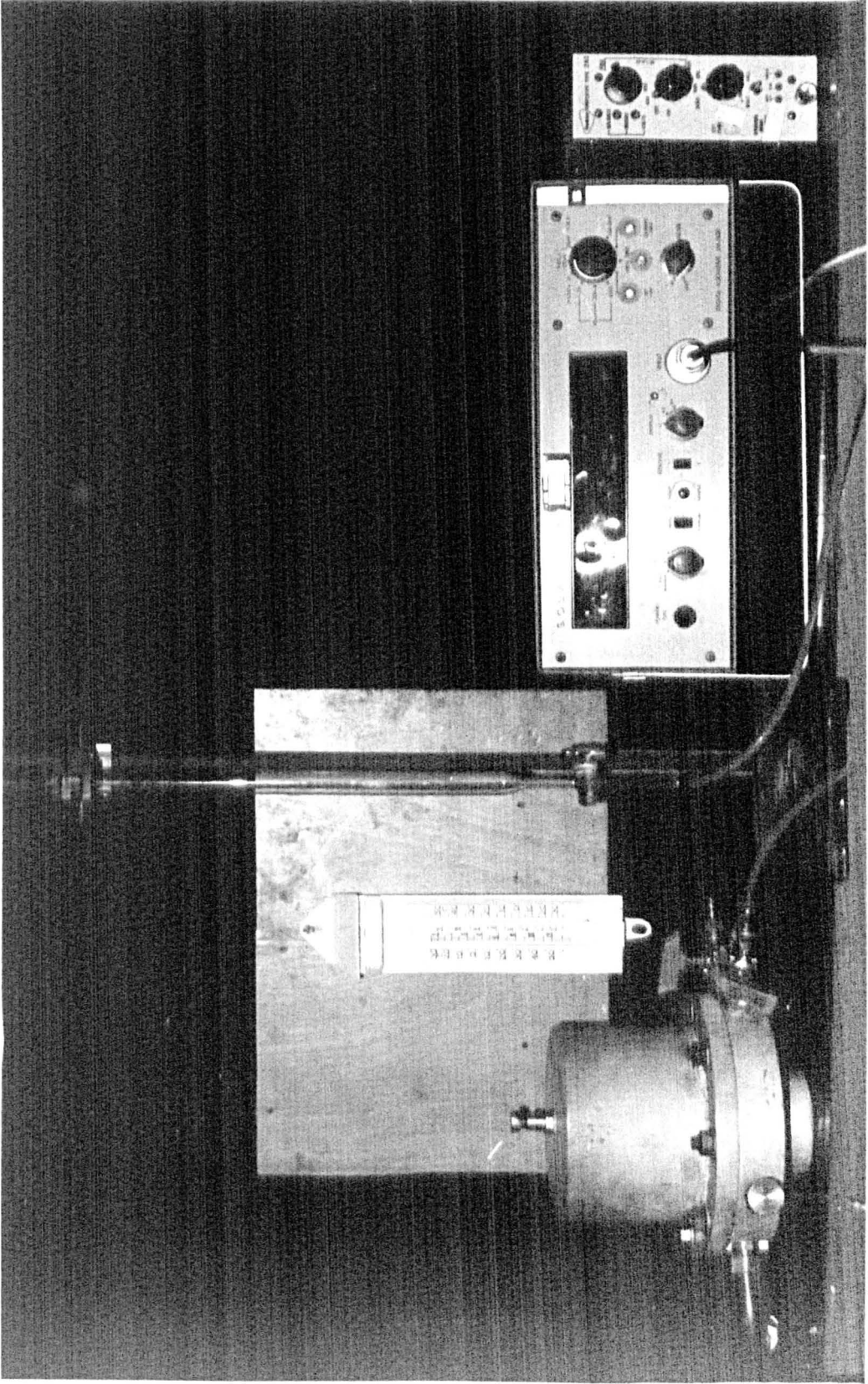


PLATE 3.2

placed in position on the base plate and the two halves of the apparatus were clamped together using the 8 studs provided on the base plate.

The burette connected to one of the water supply vents was filled with water. The other vent was used to permit the air trapped in the apparatus to escape. To achieve this, the valve between the burette and the vent was opened simultaneously with the valve on the other vent. When all the air had been driven out, and when water flowed freely through the apparatus, both the valves were closed simultaneously.

Next, the air vent valve on the top of the apparatus was opened, and the chamber was filled with water via the water inlet valve in the base of the chamber. When the chamber was full of water, the water inlet valve and the air vent valve were closed. About one hour was permitted for the apparatus and its parts to acquire temperature equilibrium. It was subsequently realised that it would have been preferable to have left the air vent valve open until equilibrium has been achieved.

The initial reading of the transducer and the room temperature were recorded, and the water vent valve between the burette and the vent was opened allowing free water to the sample. This was taken as the start of the isotropic swell pressure test.

The pressure transducer readings were recorded at close intervals in the initial stages of the test, and at 24 hour intervals thereafter, until the sample developed the maximum swell pressure. The transducer calibration

chart (Fig. 3.5) was used to convert the recorder readings to swell pressures.

At the end of the swell pressure test the apparatus was dismantled, and a representative sub-sample was used to determine the final moisture content.

3.4 RESULTS

3.4.1 Introduction

The results of all the main series of tests carried out in this investigation are presented in this section. The next two sub-sections introduce the results for the artificial mixtures and natural soils respectively. The last three sub-sections report some detailed observations which have bearing on the methods of measurement and the assessment of the results.

3.4.2 Results on Artificial Mixtures

The results of the various tests chosen in the present study for the three artificial mixtures are shown in Tables 3.3 to 3.5. The liquidity index, LI, values in Tables 3.3 to 3.5 were calculated for optimum moisture content values. V_w/V_g refer to the volumetric water content at optimum conditions. Each pair of W_i and W_f refer to the initial and final water contents for the swell property quoted on the line above.

Table 3.3 pertains to the illite-sand mixtures, Table 3.4 to bentonite-sand mixtures, and Table 3.5 to bentonite-illite mixtures. The results reported in these Tables include the Atterberg limit values, activity, moisture content and dry density at optimum compaction

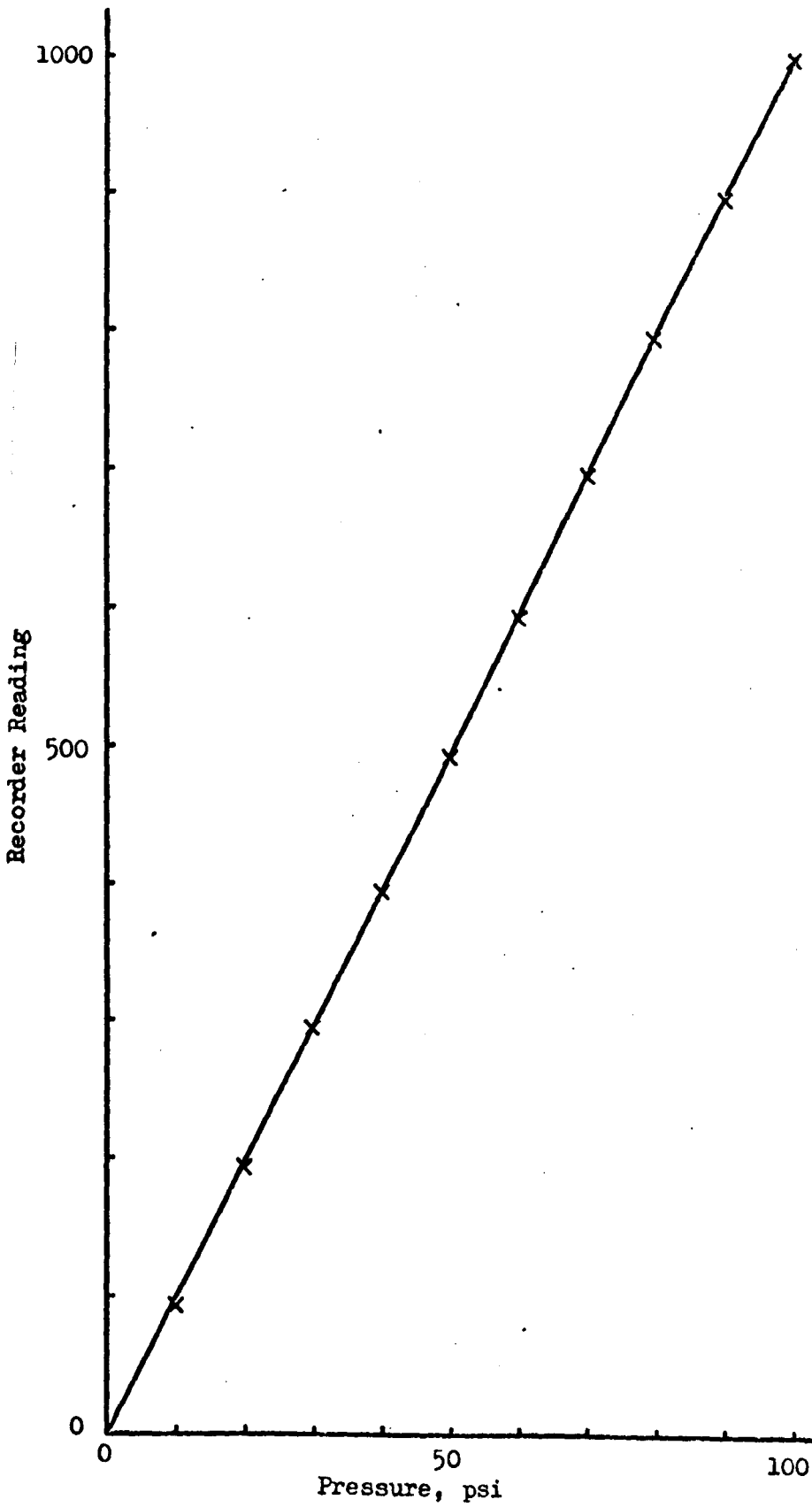


Fig. 3.5 Calibration Chart For Pressure Transducer.

Table 3.3 Properties of Illite - Sand Mixtures

Composition

Illite	%	100	82	64	50	32	14	0
Sand	%	0	18	36	50	68	86	100

Index Properties

G _s	-	2.71	2.70	2.69	2.68	2.67	2.66	2.65
LL	%	70.5	58.7	49.3	39.0	29.1	19.1	
PL	%	31.9	27.7	20.4	16.9	14.1	NP	
PI	%	38.6	31.0	28.9	22.1	15.0		
A †	-	0.44	0.43	0.52	0.50	0.54		
LI	-	-0.13	-0.1	0.03	0.05	-0.01	---	---

Compaction Prop.

OMC	%	27.0	24.6	21.2	18.0	14.0	11.8	11.4
Y _d	pcf	94	97	102	106	112	105	102
	kg/cu.m	1510	1553	1630	1697	1800	1685	1637
V _w /V _s	-	0.73	0.65	0.52	0.47	0.36	0.30	0.30
Y _d /Y _s	-	0.56	0.57	0.61	0.63	0.68	0.64	0.61

Lat. Con. Swell

P _c	psi	39.8	36.6	23.6	18.7	9.2	3.5	
	kN/sq.m	275	252	163	129	64	24	
W _i	%	27.2	24.5	21.2	18.2	14.0	11.8	
W _f	%	30.2	27.8	24.7	21.8	15.4	12.8	
S _c	%	21.8	17.5	14.4	10.8	1.8	0.5	
W _i	%	27.2	24.5	21.2	18.2	14.0	11.8	
W _f	%	43.0	36.5	30.6	24.8	15.7	14.2	

Isotropic Swell

P _i	psi	31.0	27.2	21.7	17.2	8.5	1.2	
	kN/sq.m	213	187	149	119	58	9	
W _i	%	27.2	24.1	21.2	18.2	14.0	11.6	
W _f	%	29.9	27.6	25.0	19.6	15.7	12.7	
P _i /P _c	-	0.78	0.74	0.92	0.92	0.92	0.36	

NP - Non Plastic

† Activity is calculated using clay less than 2 μ .

Table 3.4 Properties of Bentonite - Sand Mixtures

<u>Composition</u>								
Bentonite	%	100	83.3	66.7	50.0	33.3	16.7	0
Sand	%	0	16.7	33.3	50.0	66.7	83.3	100
<u>Index Properties</u>								
Gs	-	2.49	2.51	2.54	2.57	2.59	2.62	2.65
LL	%	192.0	160.0	132.0	97.8	66.0	42.6	
PL	%	55.1	39.9	32.7	26.5	12.8	NP	
PI	%	136.9	120.1	99.3	71.3	53.2		
A	-	1.37	1.45	1.48	1.43	1.61	--	--
LI	-	0.02	0.08	0.08	0.02	0.13	--	--
<u>Compaction Prop.</u>								
OMC	%	58.5	49.5	41.0	28.0	19.8	17.3	11.4
Yd	pcf	60	70	77	88	97	105	102
	kg/cu.m	955	1115	1235	1410	1555	1685	1637
Vw/Vs	-	1.45	1.23	0.98	0.72	0.56	0.45	0.30
Yd/Ys	-	0.38	0.44	0.48	0.55	0.59	0.65	0.61
<u>Lat. Con. Swell</u>								
Pc	psi	42.8	38.8	33.7	28.0	20.6	11.2	
	kN/sq.m	294	269	233	193	146	78	
Wi	%	60.8	49.3	41.7	27.7	20.1	16.9	
Wf	%	66.7	51.1	42.2	31.8	22.5	19.1	
Sc	%	79.4	74.7	65.3	51.2	39.8	22.2	
Wi	%	60.8	49.3	41.7	27.7	20.1	16.9	
Wf	%	148.2	114.5	91.5	62.8	47.8	30.8	

NP - Non Plastic

Table 3.5 Properties of Bentonite - Illite Mixtures

Composition

Bentonite	%	100	83.3	66.7	50.0	33.3	16.7	0
Illite	%	0	16.7	33.3	50.0	66.7	83.3	100

Index Properties

Gs	-	2.48	2.52	2.56	2.60	2.64	2.68	2.72
LL	%	192.0	174.5	149.8	135.2	117.5	91.2	70.5
PL	%	55.1	50.3	46.7	43.1	40.2	36.8	31.9
PI	%	136.9	124.2	103.1	92.1	77.3	54.4	38.6
A	-	1.37	1.25	1.07	0.98	0.84	0.61	0.44
LI	-	-0.03	-0.05	-0.09	-0.09	-0.11	-0.11	-0.12

Compaction Prop.

OMC	%	51.5	43.5	37.0	34.5	32.0	30.8	27.2
γ_d	pcf	61	64	70	76	80	86	94
	kg/cu.m	980	1020	1120	1225	1285	1380	1510
Vw/Vs	-	1.25	1.10	0.95	0.90	0.86	0.83	0.73
γ_d/γ_s	-	0.40	0.41	0.44	0.47	0.49	0.52	0.56

Lat. Con. Swell

Pc	psi	52.2	51.8	50.5	49.8	46.7	43.7	39.9
	kN/sq.m	360	357	348	344	322	302	275
Wi	%	50.6	42.8	37.5	35.0	32.2	30.3	27.2
Wf	%	59.3	52.8	45.4	40.5	34.9	33.2	30.2
Sc	%	87.3	85.5	74.3	61.0	52.5	36.6	21.8
Wi	%	50.6	42.8	37.5	35.0	32.2	30.3	27.2
Wf	%	137.4	134.5	111.3	90.2	79.5	60.2	43.0

conditions, and the swell potential and swell pressure values for the samples compacted at optimum conditions. Isotropic swell pressure tests were made only on the illite-sand series, and the results are reported in Table 3.3. Graphical presentation of the variation of many of these properties with composition are given in Chapter 5.

The compaction results are presented on a non-dimensional plot, details of which are given in Appendix 5. This is necessary because the specific gravities vary from mixture to mixture within each series. Fig. 3.6, 3.7 and 3.8 show the compaction results of illite-sand mixtures; bentonite-sand mixtures; and of bentonite-illite mixtures respectively. Two separate compaction tests were made on pure bentonite, one on the material used with bentonite-sand series, and the other on the material used with bentonite-illite series; both these tests yielded slightly different values with regard to the optimum moisture content, see Tables 3.4 and 3.5. As expected, the optimum conditions lay around 5% air voids content for the more clayey samples, rising to around 20% for the sandier samples. The optimum conditions predicted from these curves were used as the basis for the swell tests. Further analysis of these compaction and swell results is deferred until Chapter 5.

3.4.3 Results on Natural Soils

The results of the various tests for the natural Wootton Broadmead soils are reported in Table 3.6. In addition to the tests made on the artificial soils, Table 3.6 shows the results of particle size distribution tests,

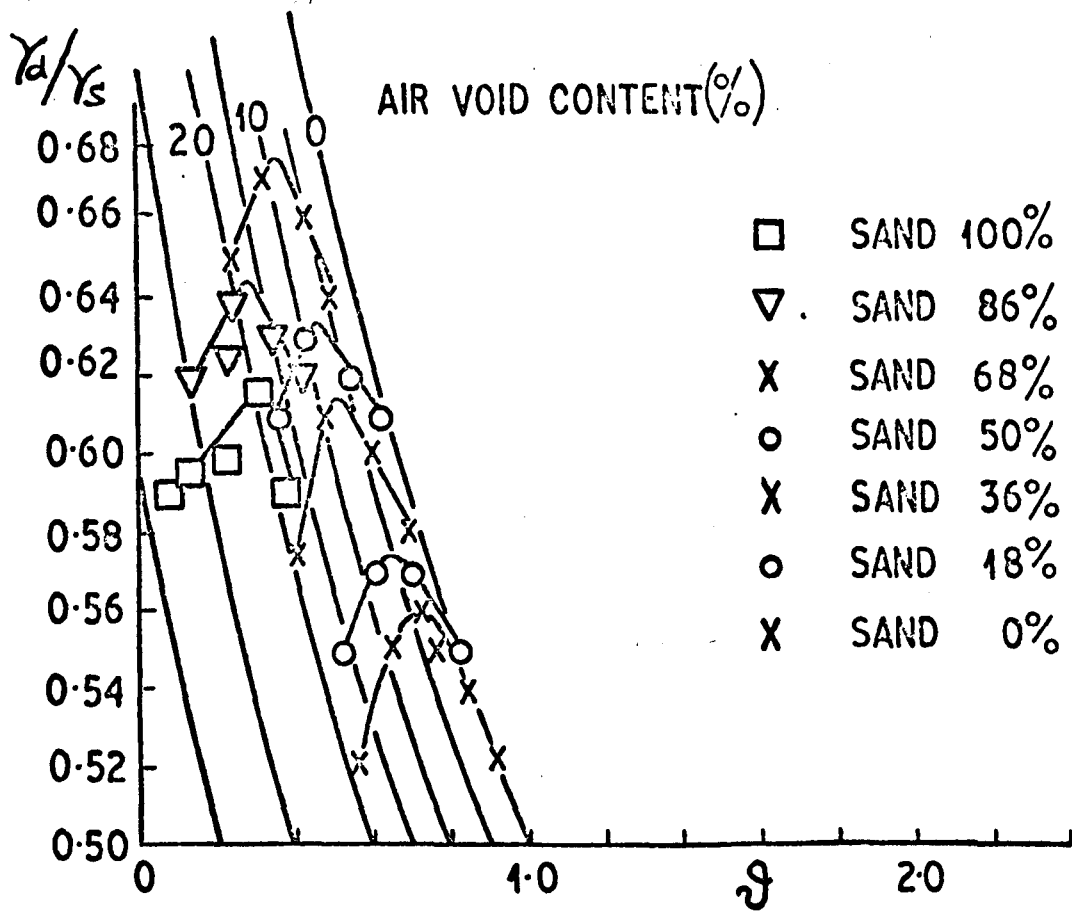


Fig. 3.6 Non - Dimensional Compaction Curves, Illite-Sand Mixtures.

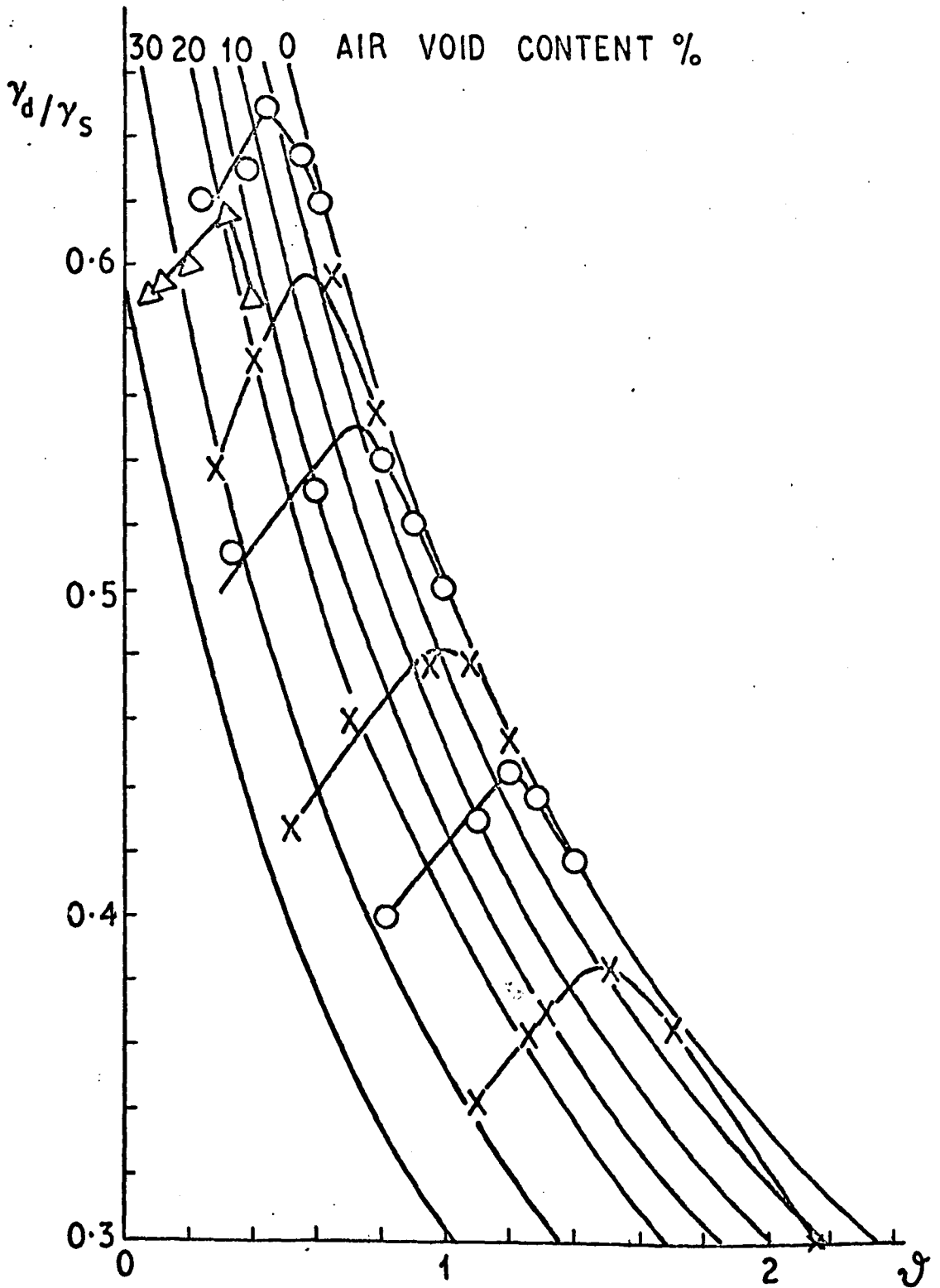


Fig. 3.7 Non - Dimensional Compaction Curves, Bentonite-Sand Mixtures.

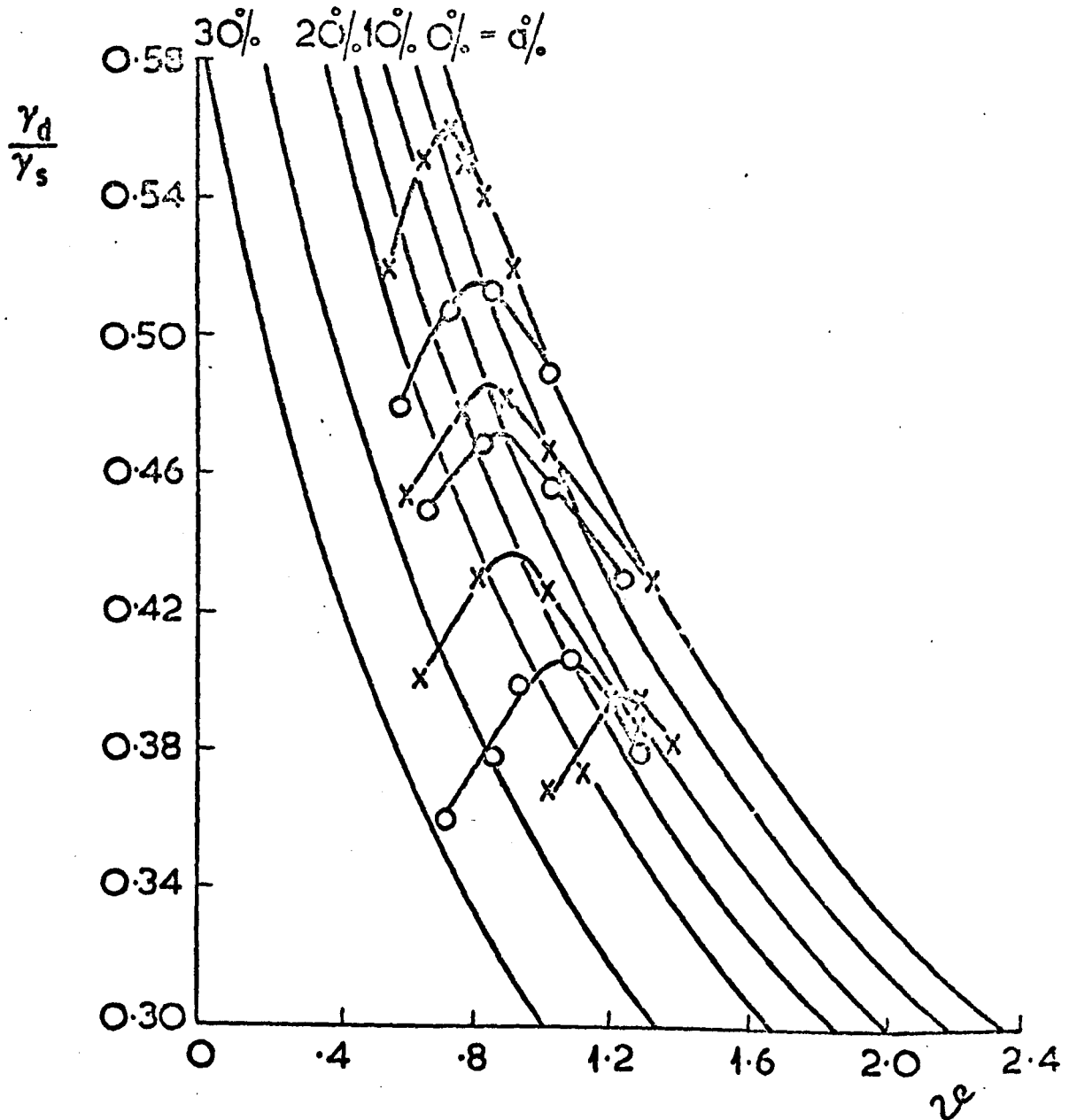


Fig. 3.8 Non - Dimensional Compaction Curves, Bentonite-Illite Mixtures.

Table 3.6 Properties of Natural Wootton Broadmead Soils

Soil No		I	2	3	4	5	6	7	8	9	10
<u>Property</u>											
<u>Grain Size</u>											
Clay	%	42.0	21.0	25.0	48.0	62.0	9.0	40.0	87.0	32.0	10.0
Silt	%	28.0	34.0	28.0	32.0	28.0	33.0	5.0	9.0	58.0	63.0
Sand	%	29.0	44.0	46.0	19.0	9.0	55.0	45.0	4.0	9.0	26.0
Gravel	%	1.0	2.0	1.0	1.0	1.0	3.0	10.0	0.0	1.0	1.0
<u>Index Properties</u>											
Gs	-	2.68	2.67	2.67	2.65	2.52	2.76	2.56	2.48	2.47	2.50
LL	%	50.9	27.0	43.2	63.1	67.8	26.4	34.1	84.3	68.6	45.7
PL	%	24.5	14.5	25.0	28.2	34.4	15.0	23.0	45.0	40.0	24.7
PI	%	26.4	12.5	18.2	34.9	33.4	11.4	11.1	39.3	28.6	21.0
A	-	0.63	0.60	0.73	0.73	0.54	1.27	0.28	0.45	0.89	2.10
LI †	-	0.02	+0.04	0.22	0.03	0.27	0.19	0.36	0.15	0.40	0.20
<u>Chemical Prop.</u>											
Organic Matter	%	3.60	1.80	4.33	3.80	4.20	1.70	4.60	7.10	6.70	3.50
pH	-	7.53	4.14	4.37	3.93	5.59	5.52	4.67	3.87	5.17	4.67
CEC	meq/100gm						2.3		30.2		
Allophane	-	Nil	Nil	Nil	Nil	Nil	Nil	Nil	Nil	Nil	Nil
<u>Compaction Prop.</u>											
OMC	%	24.0	15.0	21.0	27.0	25.5	12.8	19.0	39.5	28.5	20.5
	pcf	98	118	101	90	91	119	105	79	87	102
γ _d	kg/cu.m	1570	1890	1618	1442	1463	1913	1688	1257	1397	1626
V _w /V _s	-	0.64	0.40	0.56	0.72	0.64	0.35	0.49	0.97	0.70	0.51
γ _d /γ _s	-	0.59	0.71	0.61	0.54	0.58	0.69	0.66	0.51	0.57	0.65
<u>Lat. Con. Swell</u>											
P _c	psi	8.20	0.00	3.50	8.30	13.1	0.96	6.40	21.0	2.55	0.00
	kN/sq.m	57	0	24	40	90	7	44	145	18	0
W _i	%	23.1	16.2	21.7	26.9	26.2	12.6	18.4	39.4	28.3	20.3
W _f	%	25.8		22.9	29.3	28.9	13.8	20.2	41.8	29.8	
S _c	%	3.70	0.00	2.10	4.80	5.40	0.15	2.60	6.73	1.82	0.00
W _i	%	23.1	16.2	21.7	26.9	26.2	12.6	18.4	39.4	28.3	20.3
W _f	%	29.4		25.1	33.2	35.6	15.8	23.7	53.2	31.5	23.1
<u>Isotropic Swell</u>											
P _i	psi	6.50	0.00	3.00	7.25	8.50	1.00	5.50	13.0	1.50	0.00
	kN/sq.m	45	0	21	35	59	7	38	90	10	0
W _i	%	23.4	15.6	20.8	26.9	25.1	12.2	18.9	38.3	28.3	20.0
W _f	%	24.6		22.4	27.8	27.7	13.2	19.9	40.7	29.5	
P _i /P _c	-	0.79	---	0.86	0.87	0.65	1.00	0.86	0.62	0.59	---
Clay Minerals		IKx	K	KIC	KIC	IKx	KC	KIC	?	KI	K

I - Illite; K - Kaolinite; x - Trace of Montmorillonite or Vermiculite or Mixed layer clay; C - Calcite.

† The LI value for all soils is negative except for soil No 2.

pH tests and organic matter tests which were made on the natural soils. The clay minerals identified by X-Ray diffraction are also reported in Table 3.6. The sample No. 350-8 proved troublesome in that no illite or montmorillonite clay could be detected by X-Ray diffraction, whilst it showed the highest swell properties amongst the ten soils considered here. Lashley and Lindsay (1978) observed during a detailed study on this soil that the greater part of the clay content was less than one micron. However, they went to considerable trouble to get satisfactory dispersion. They used X-Ray diffraction supplemented by electron microscopy and concluded rather tentatively that Kaolinite and Saponite, possibly a mineral in the montmorillonite grouping, were present in the soil.

The details with regard to the presentation of test results are as follows:

For clarity of presentation, four of the ten natural soils were chosen which had wide variations in clay content. These soils are 350-1, 3, 5 and 8. The non-dimensional compaction curves for these four soils are shown in Fig. 3.9. The compaction curves for the remaining soils are similar without any extraordinary features, except for soil No. 350-9 which is also shown in Fig. 3.9. The flat shape of this curve posed slight difficulty in deciding the precise optimum moisture content. In the present study the point where the dry density starts falling was taken as the optimum moisture content. However, the peculiarity observed in the shape of this curve is thought unimportant in the present context. The variations in the optimum conditions of curves in Fig. 3.9 reflect the

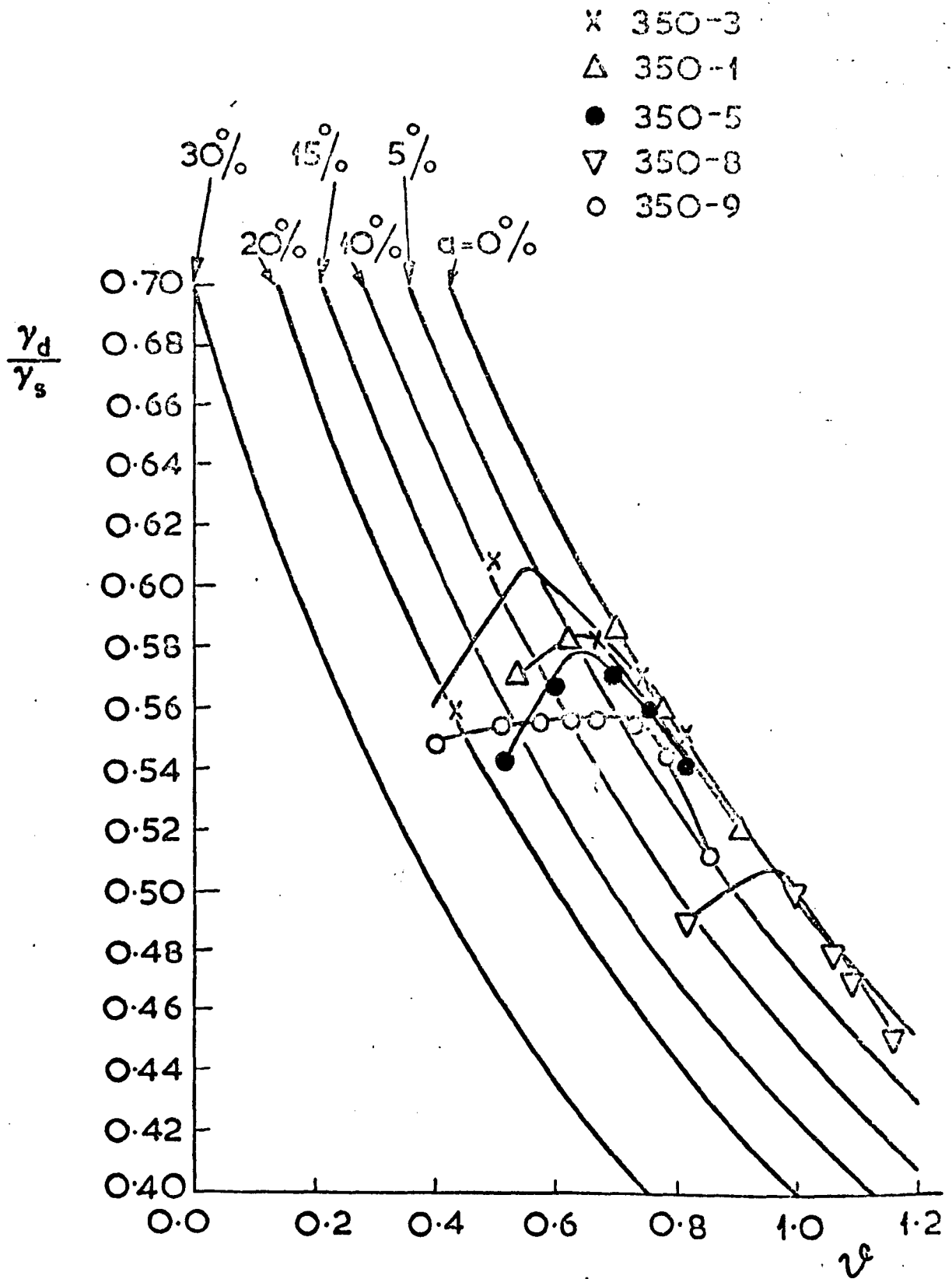


Fig. 3.9 Non - Dimensional Compaction Curves,
Natural Soils.

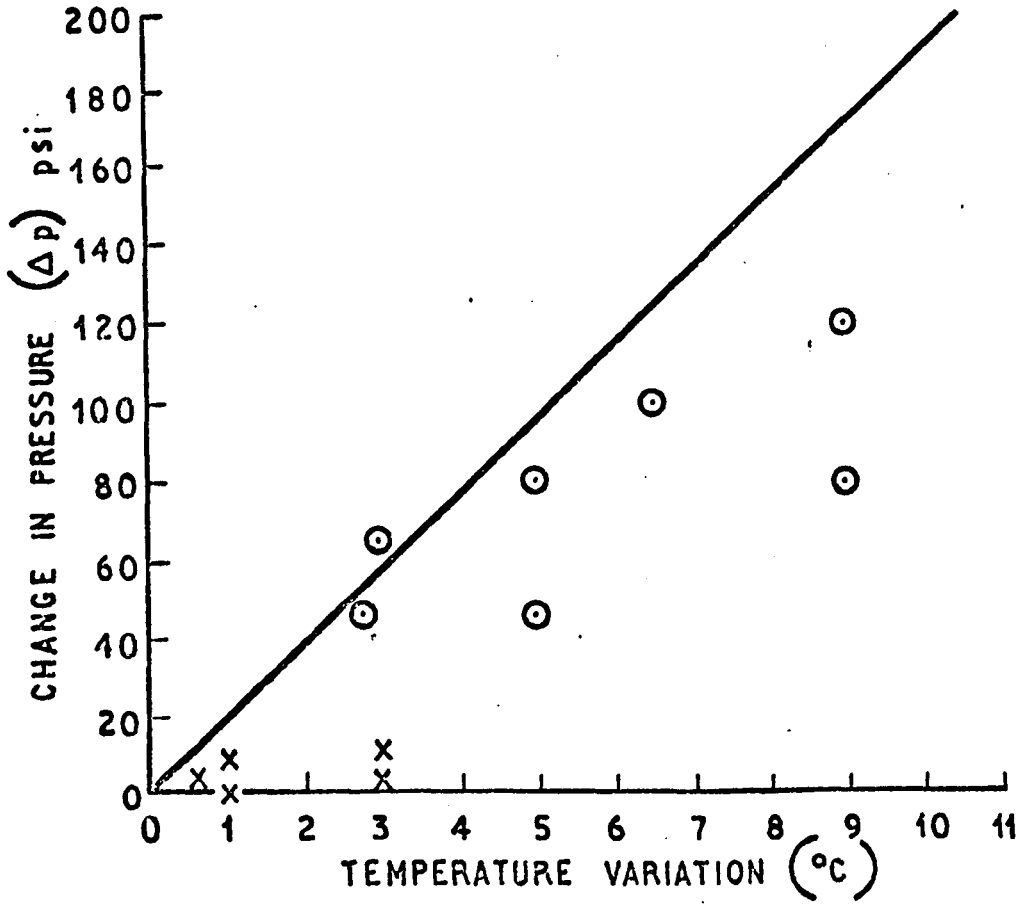
variations in texture of the soils. Except for sample 350-8 the air voids content at optimum conditions is in the order of about 3% to 5%.

The complete set of results shown in Table 3.6 for the ten natural soils is further discussed in Chapter 5.

3.4.4 Effect of Temperature on Swell Pressure

In order to estimate the effect of variations of temperature in this programme, the isotropic swell pressure test apparatus was used. A dummy mild steel sample with a single membrane was placed inside the apparatus, surrounded by water. A pressure of 100 psi was applied via the water inlet valve, and then the water inlet valve was closed sealing the high pressure water inside. The temperature of the laboratory was measured by placing a thermometer near the apparatus. As time passed the pressure in the apparatus was found to fluctuate in response to fluctuations in temperature of the laboratory. The observations were first taken in a large laboratory, in which there is no temperature control, and then repeated in a small laboratory, which has partial temperature control. The results are shown in Fig. 3.10, from which it can be seen that the fluctuations of pressure were relatively less in the small laboratory. The variations shown in Fig. 3.10 are the variations from the initial condition regardless of sign. The line in Fig. 3.10 was calculated on the assumption that the temperature would effect the pressure chamber and the water but not the sample. A cubical coefficient of expansion of 0.000033 for steel and 0.000053

⊙ LARGE RESEARCH LAB.
X SMALL RESEARCH LAB.



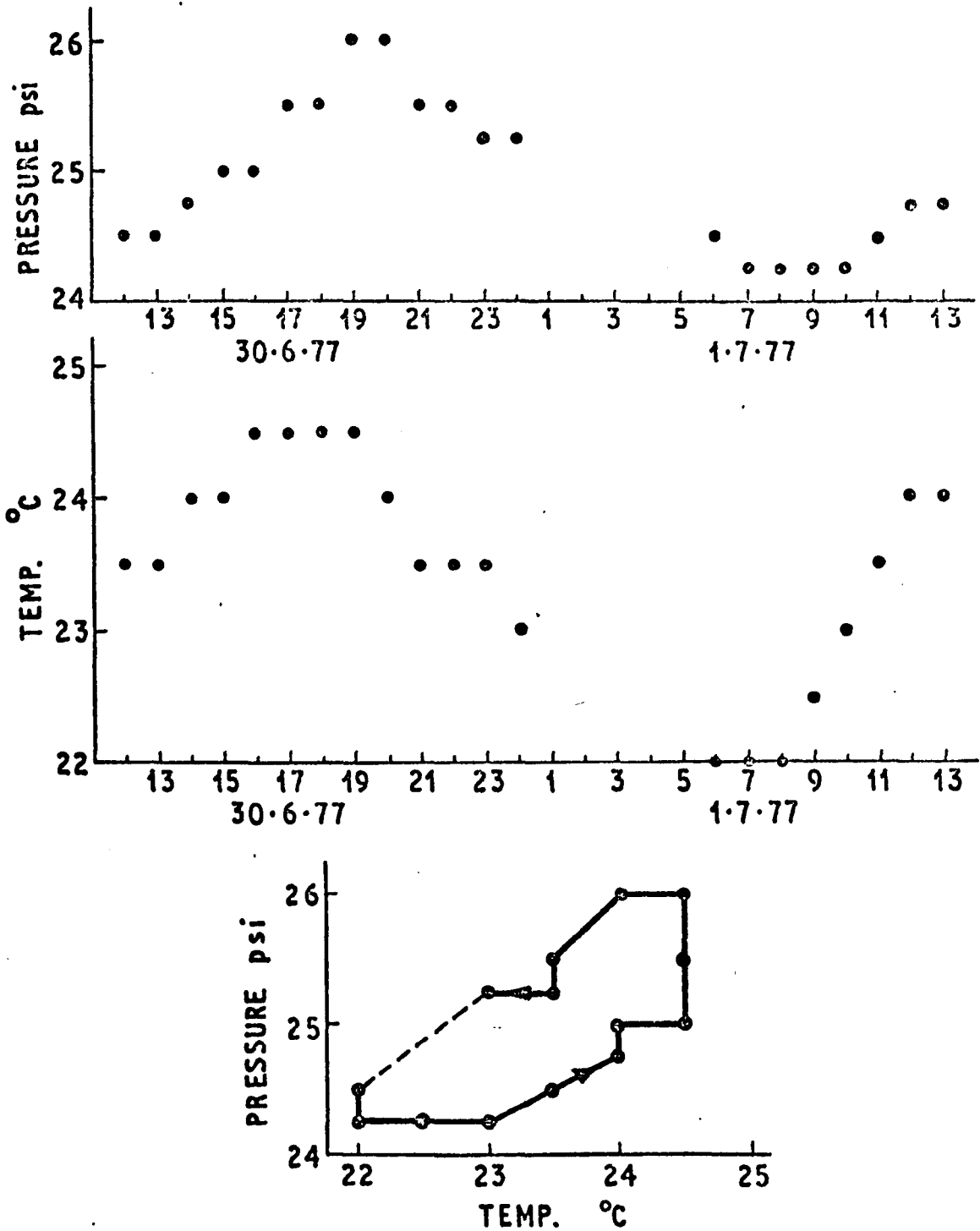
EFFECT OF TEMPERATURE ON SWELL PRESSURE

Fig.3.10

for water (5 to 10°C) were used in these calculations. On the whole and in the small laboratory in particular the observed pressure fluctuations are less than the corresponding calculated pressure fluctuations, and it can be concluded that the temperature variations do not penetrate the apparatus fully. In the small laboratory the largest recorded variations in these tests were $\pm 3^{\circ}\text{C}$ and ± 10 psi, but there appears to be a definite possibility of larger pressure fluctuations.

A further set of observations was made to study the time lag between the temperature and pressure fluctuations. These observations were made during the course of the isotropic swell pressure test on the 100% bentonite sample, the bentonite material coming from Batch 1 of the present study. Frequent readings of both temperature and pressure were taken over a period of 24 hours, and the results are shown in Fig. 3.11, as pressure against time, temperature against time, and pressure against temperature. The separation of the rising and falling branches of the cycle of pressure against temperature indicate that there is a time lag; the maximum and minimum pressures occur some two to three hours later than the maximum and minimum temperatures.

In the laterally confined swell pressure apparatus, it may be difficult to achieve an accurate temperature compensation in spite of the provision of dummy strain gauges. It can, however, be calculated that variation of $\pm 3^{\circ}\text{C}$ in temperature would result in variation of ± 30 psi on the assumption that the compensation is wholly ineffective and only the slender tie bars are affected by temperature change.



ISOTROPIC SWELL PRESSURE APPARATUS

Fig. 3.11 Time Lag Between Temperature and Pressure Fluctuations.

These observations do reveal that for accurate swell pressure measurements, the measuring devices should be used in a temperature controlled laboratory. It was hoped in the earlier stages of the present study that such a room would be available, but in the event the best available room was the small laboratory with partial temperature control. However, it was noted in practice that the scatter of points on the pressure versus time plots were not too far from the mean curve (eg. See Fig. 3.23)[†]. The error was of the order of ± 2 psi regardless of the pressure developed.

The suggestion of using a temperature controlled laboratory for swell pressure measurements is also of importance in view of the fact that changes in temperature may alter the properties of the test sample itself (Seed et al, 1962)^a. This aspect was not studied in this present investigation.

3.4.5 Variation of Swell Properties With Time

Although a detailed analysis of the variation of swell properties with time is outside the scope of the present investigation, the graphs of the observed swell properties against time reflect the reliability of the swell tests and the degree of dependability of the maximum values obtained for analysis in the present study.

The swell potential versus time plots for the artificial mixtures are presented in Figs. 3.12 to 3.14. Figs. 3.15 and 3.16 report the laterally confined swell pressure against time for illite-sand and bentonite-sand mixtures respectively. Fig. 3.17 reports the isotropic swell pressure

[†] see after page 90.

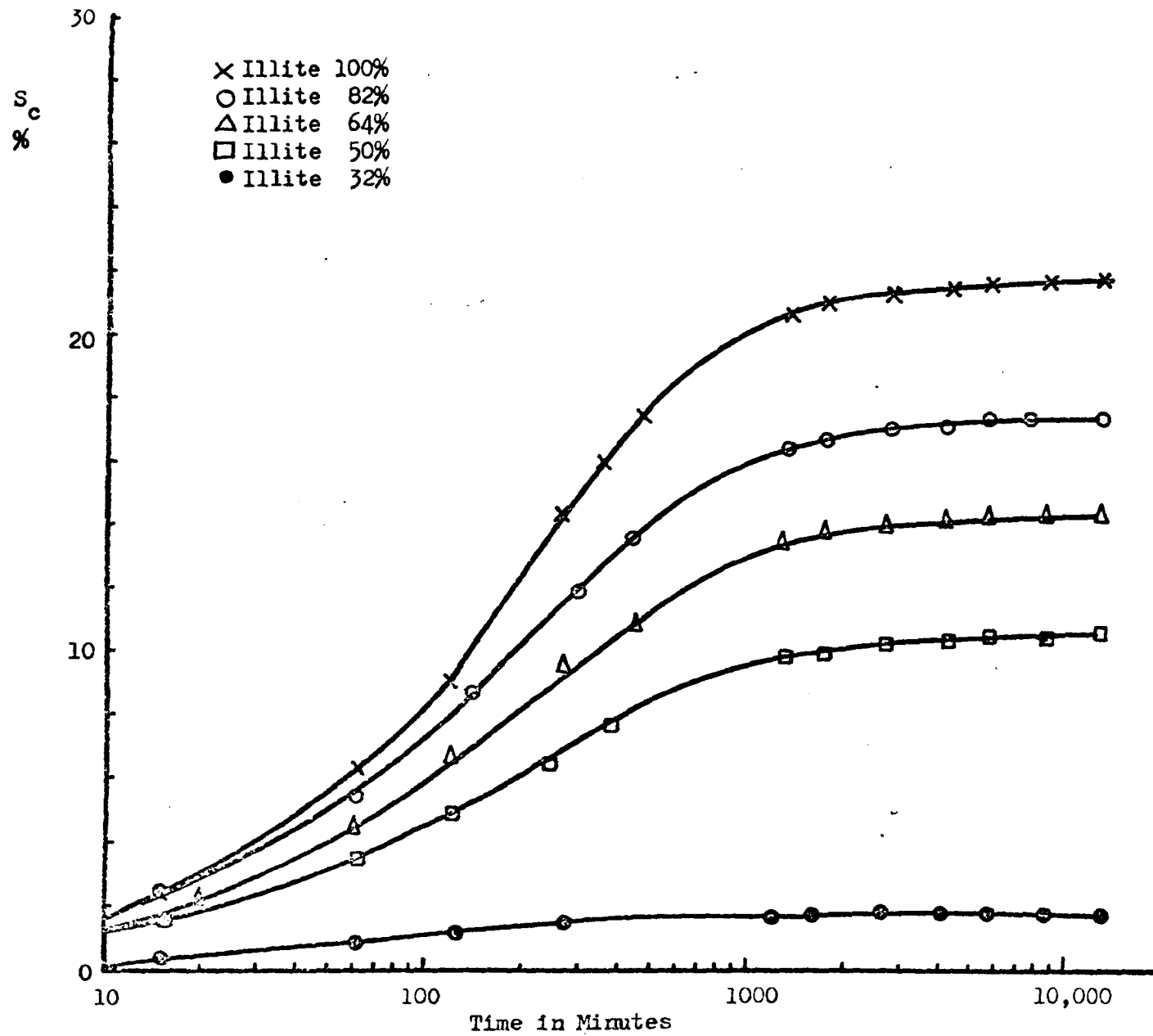


Fig. 3.12 Laterally Confined Swell Potential versus Time, Illite-Sand Mixtures.

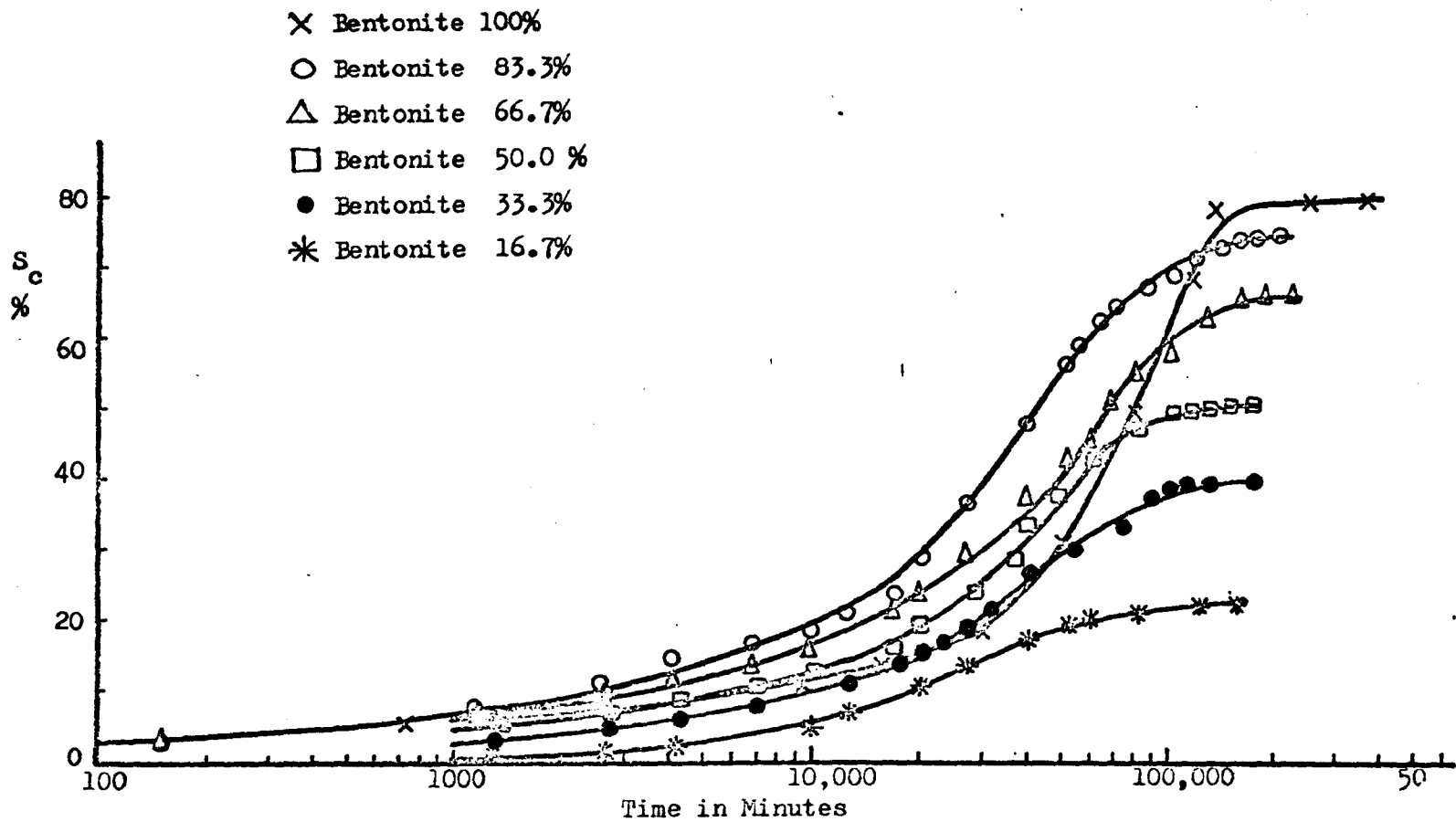


Fig.3.13 Laterally Confined Swell Potential versus Time, Bentonite-Sand Mixtures.

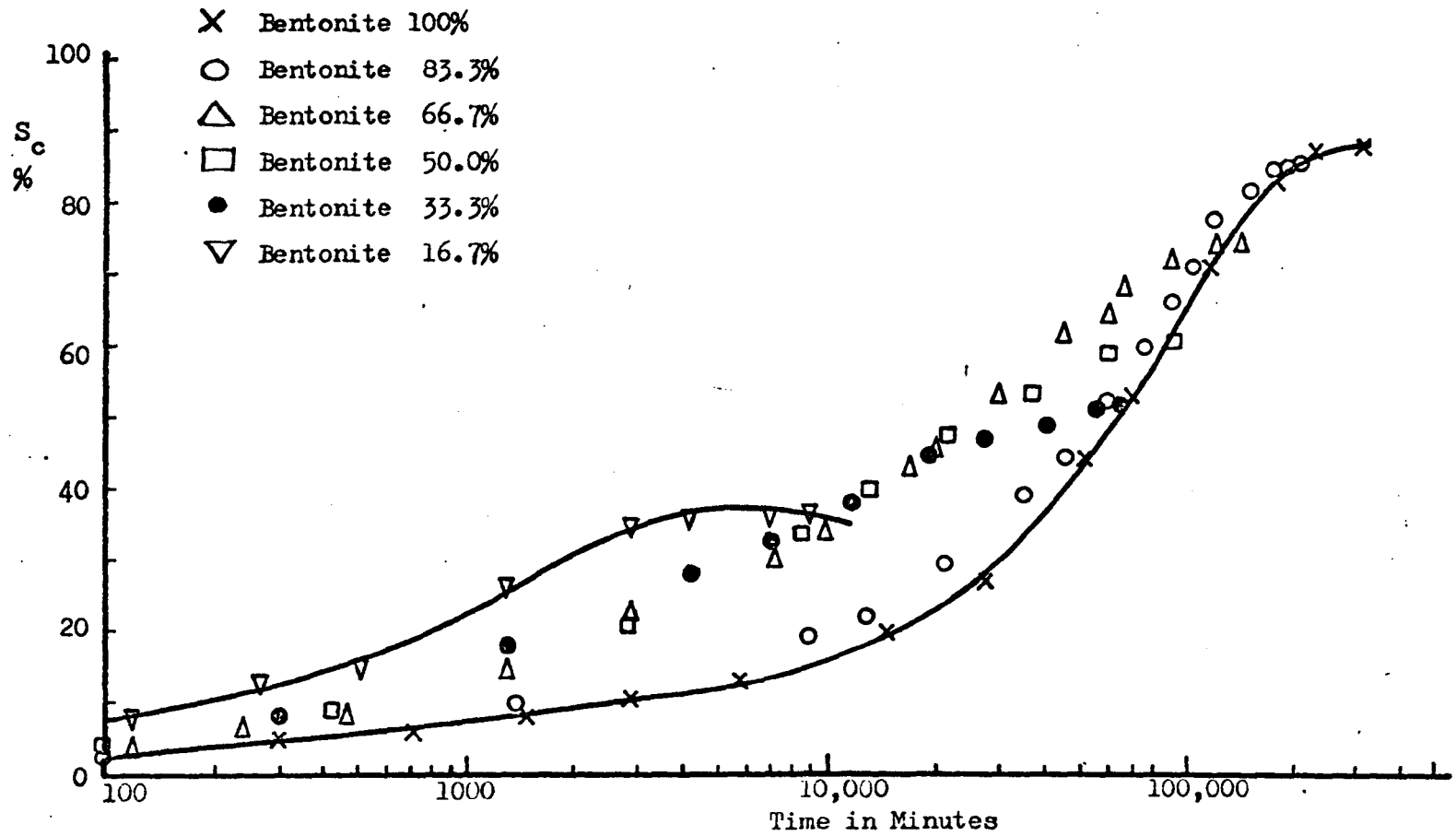


Fig. 3.14 Laterally Confined Swell Potential versus Time, Bentonite-Illite Mixtures.

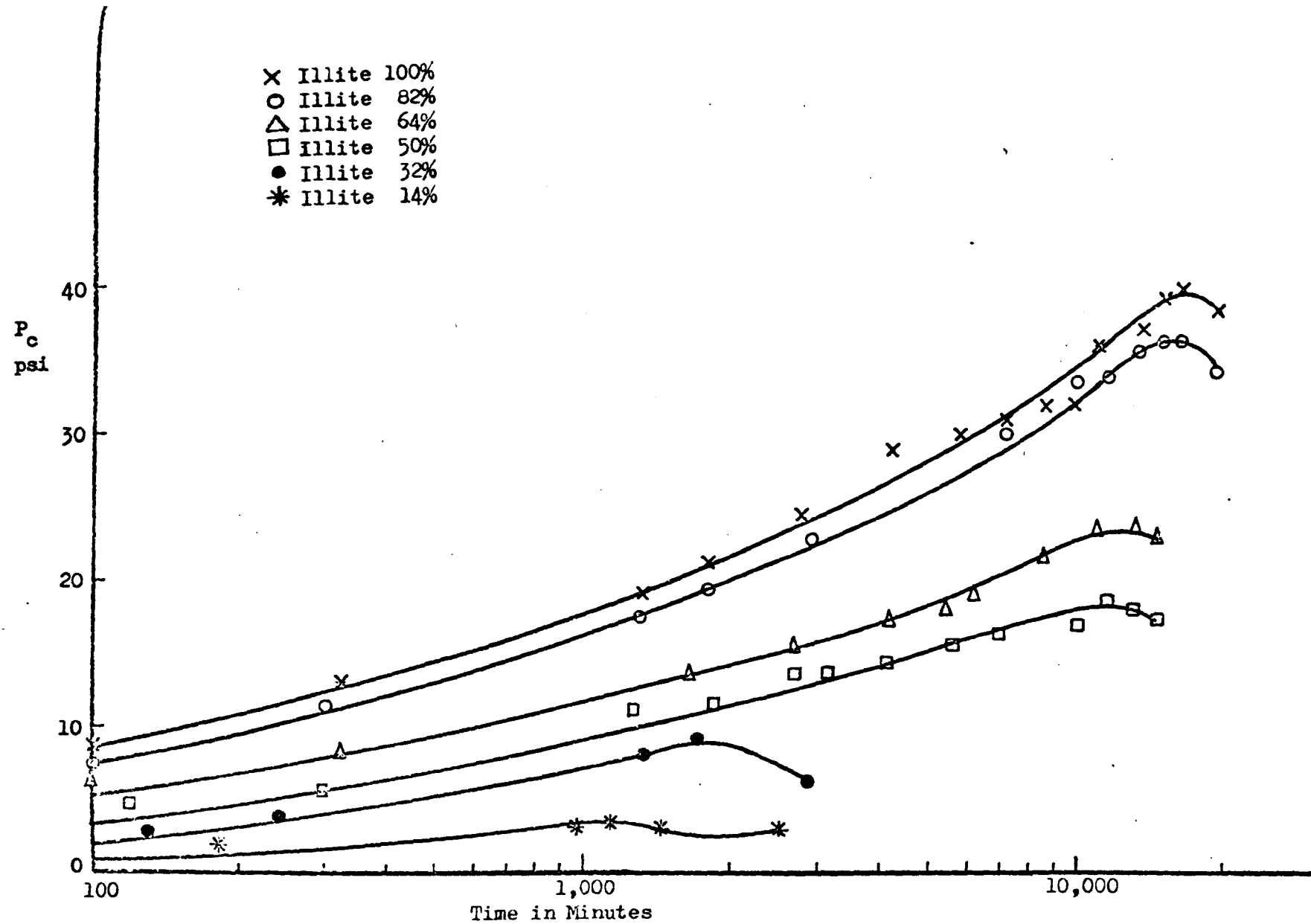


Fig.3.15 Laterally Confined Swell Pressure versus Time, Illite-Sand Mixtures.

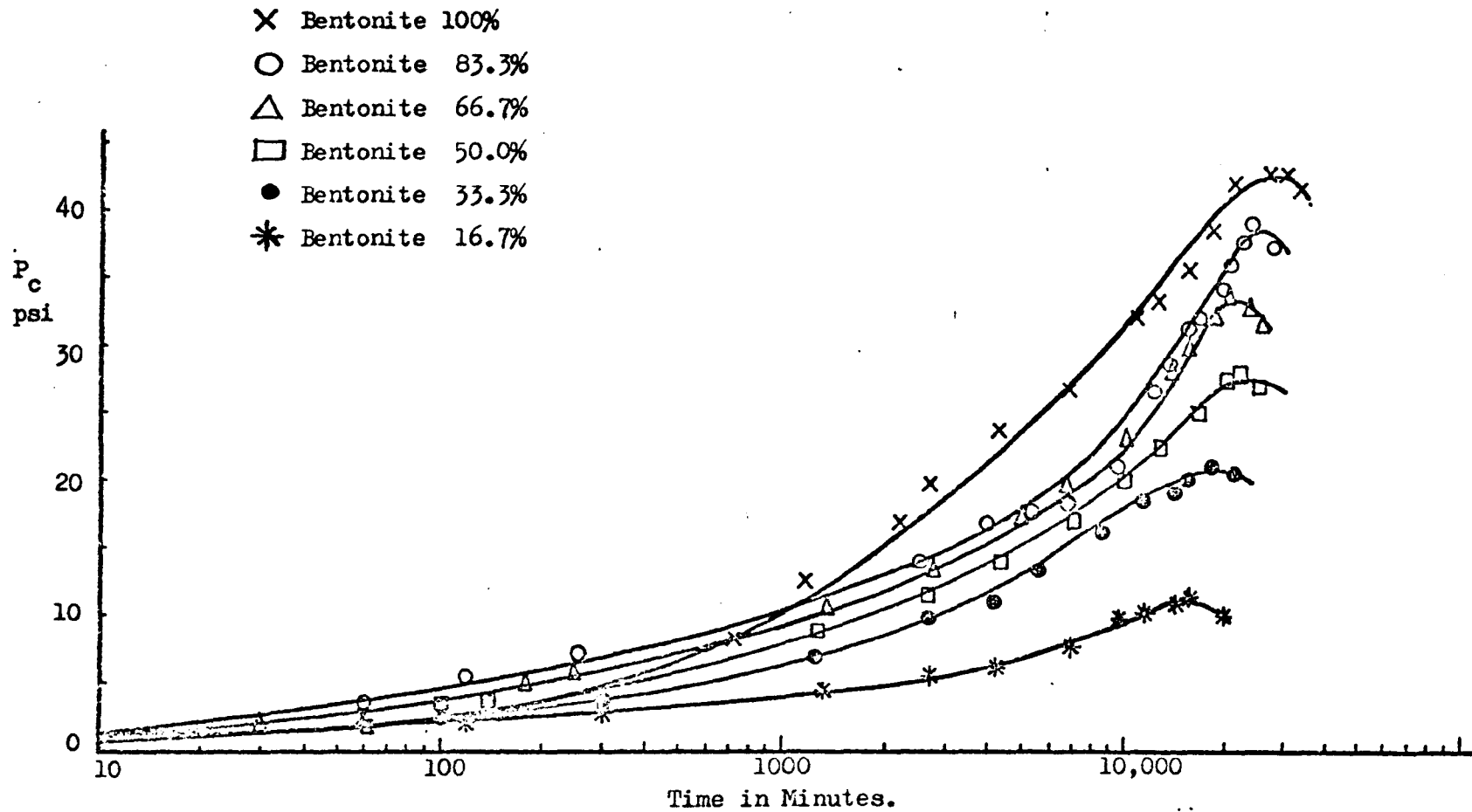


Fig.3.16 Laterally Confined Swell Pressure versus Time, Bentonite-Sand Mixtures.

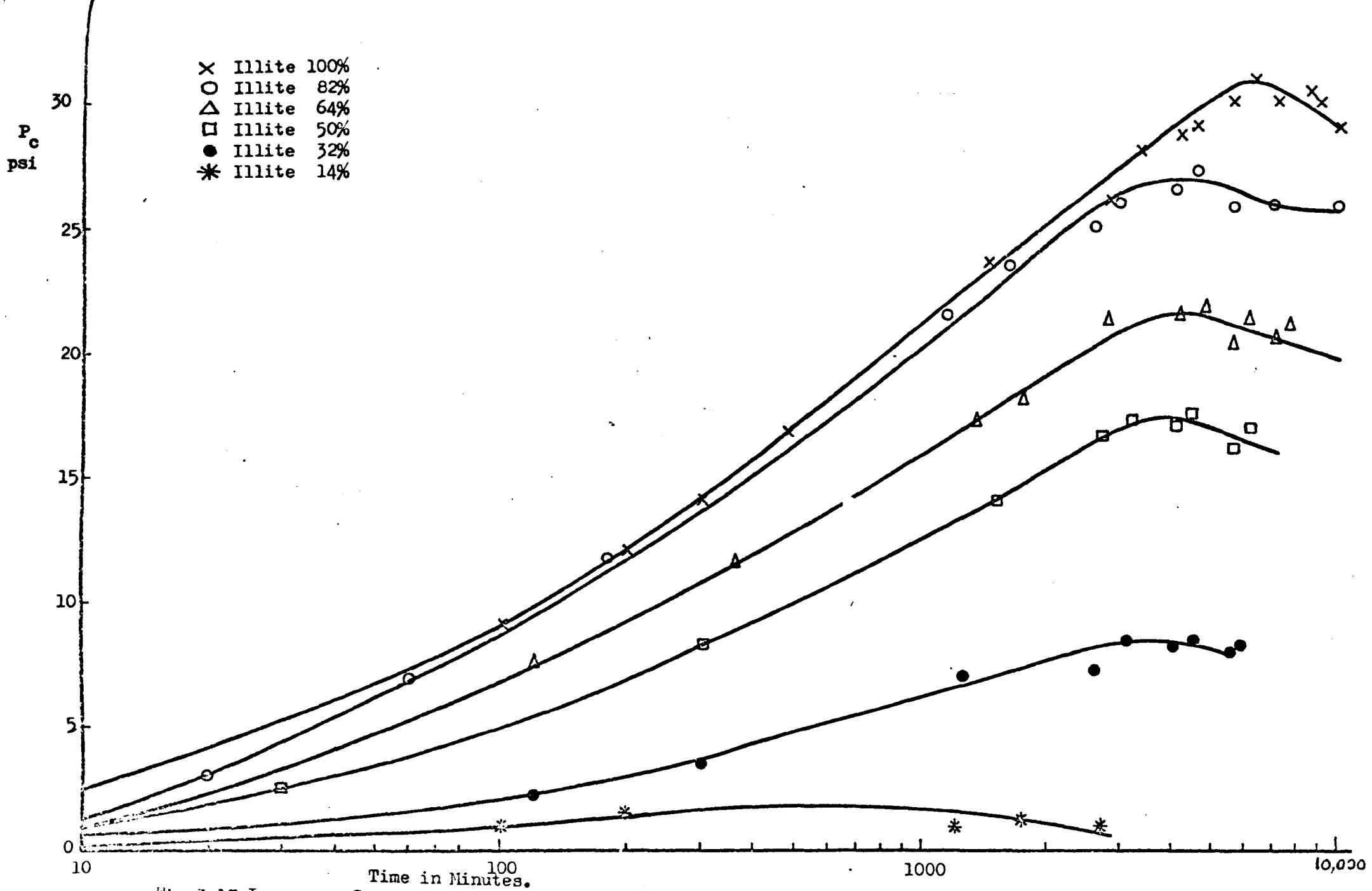


Fig.3.17 Isotropic Swell Pressure versus Time, Illite-Sand Mixtures.

versus time for illite-sand mixtures. It is seen from all these plots (Figs. 3.12 to 3.17) that they behaved in the conventional and expected manner, the swell property rising smoothly to reach a maximum value. Hence, these tests are thought to be satisfactory. The laterally confined swell pressure tests on bentonite-illite mixtures were not entirely satisfactory and are discussed in Appendix 7.

Figs. 3.18 to 3.20 report the laterally confined swell potential, laterally confined swell pressure and isotropic swell pressure against time for four of the ten natural soils, viz; 350-1, 3, 5 and 8. The graphs of swell properties against time for the remaining six soils are similar except that samples 2 and 10 were non-swelling. It can be seen from Figs. 3.18 to 3.20 that even for natural soils the swell properties rise smoothly to reach a maximum value, as observed in the artificial mixtures. Hence the various swell tests on natural soils are thought to be satisfactory and reliable.

3.4.5.1 Swell Potential Versus Time

The following trends, which are typical of all the swell potential versus time curves, can be seen from the results of the present study.

(i) The swell potential versus time relationship for a given soil appears to be a typical S-shaped curve, somewhat similar to that of consolidation.

(ii) The total time required to develop the maximum swell potential is essentially a function of the type (mineralogy) and the amount of the clay fraction, e.g.

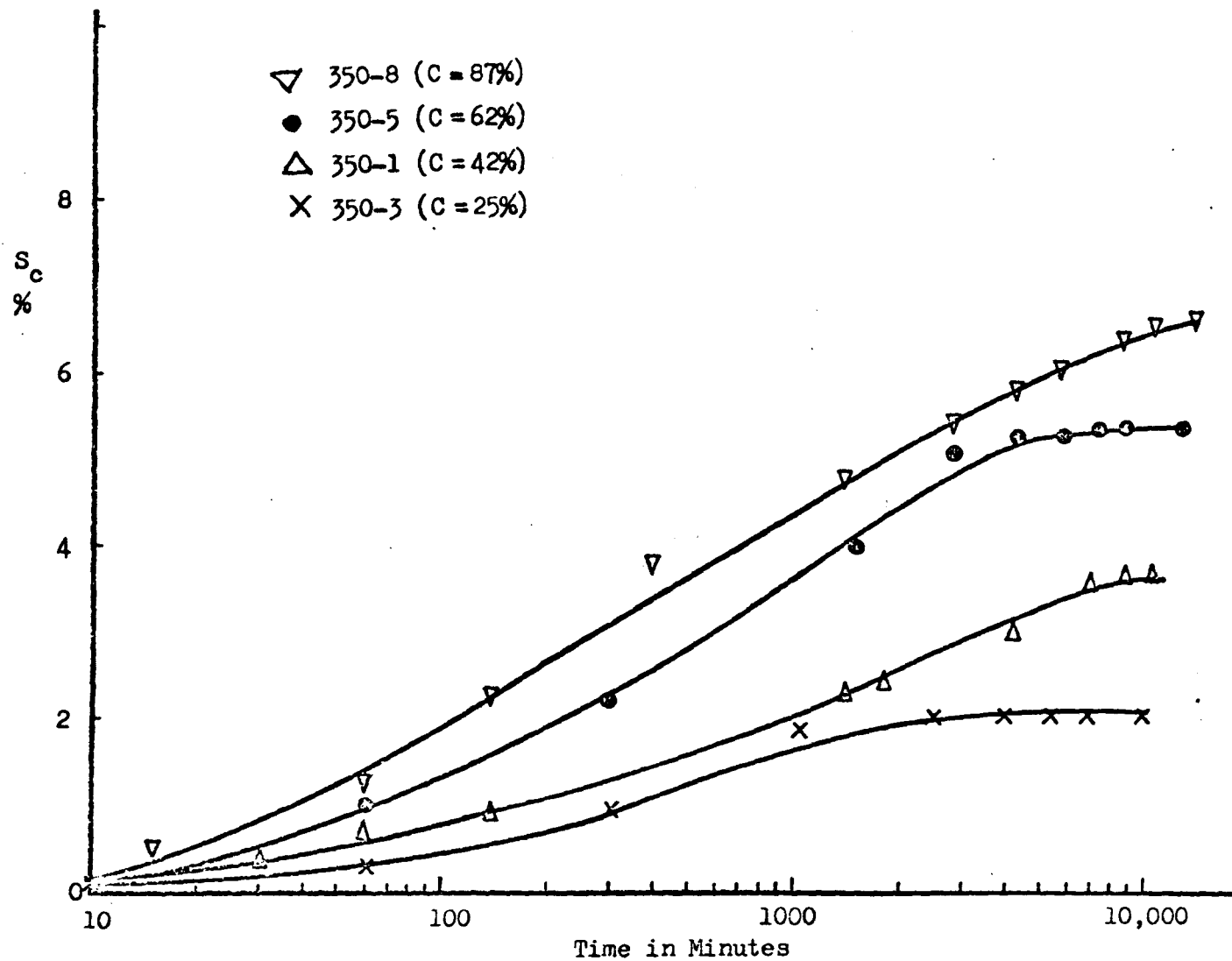


Fig.3.18 Laterally Confined Swell Potential versus Time, Natural Soils.

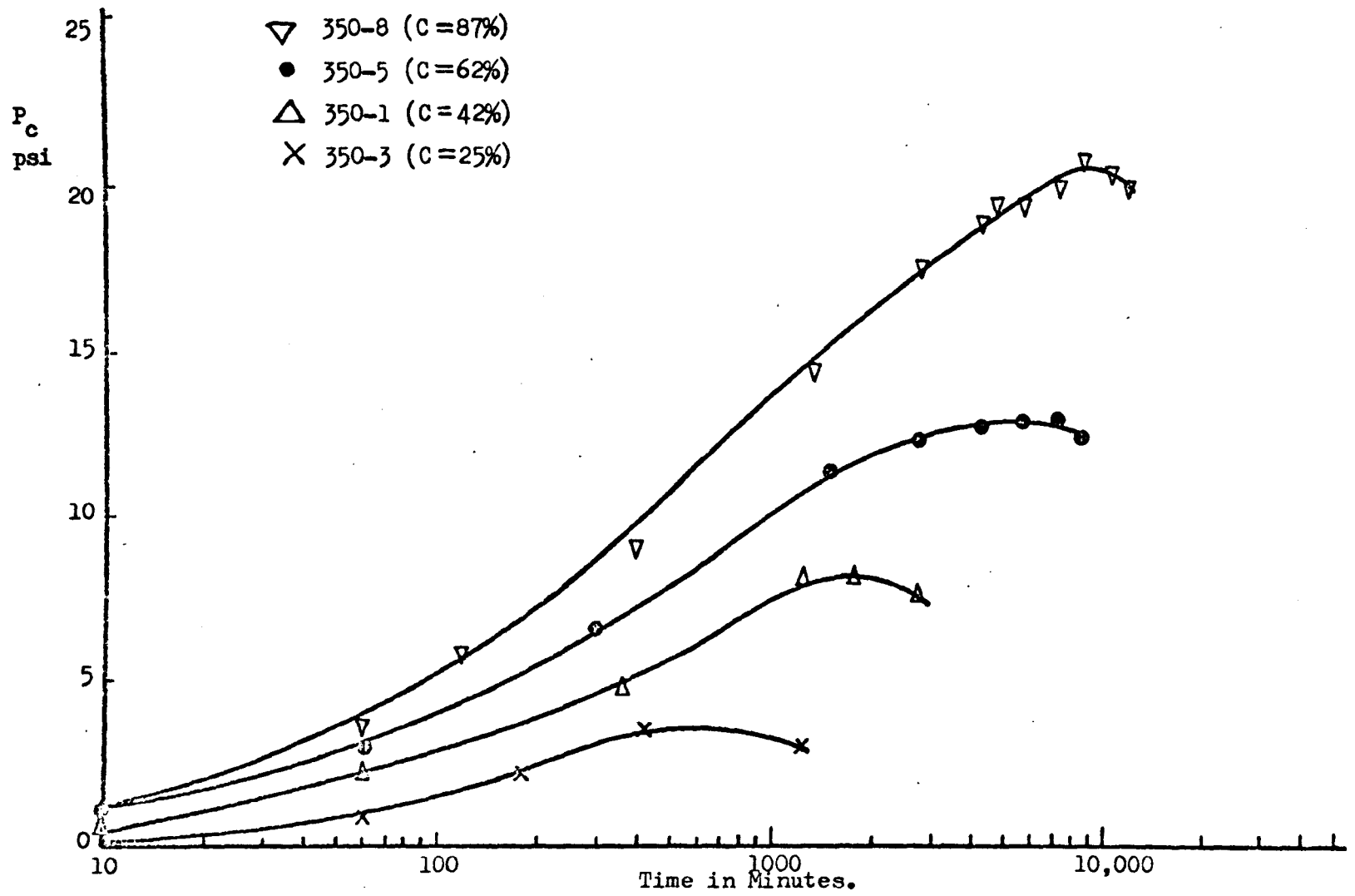


Fig.3.19 Laterally Confined Swell Pressure versus Time, Natural Soils.

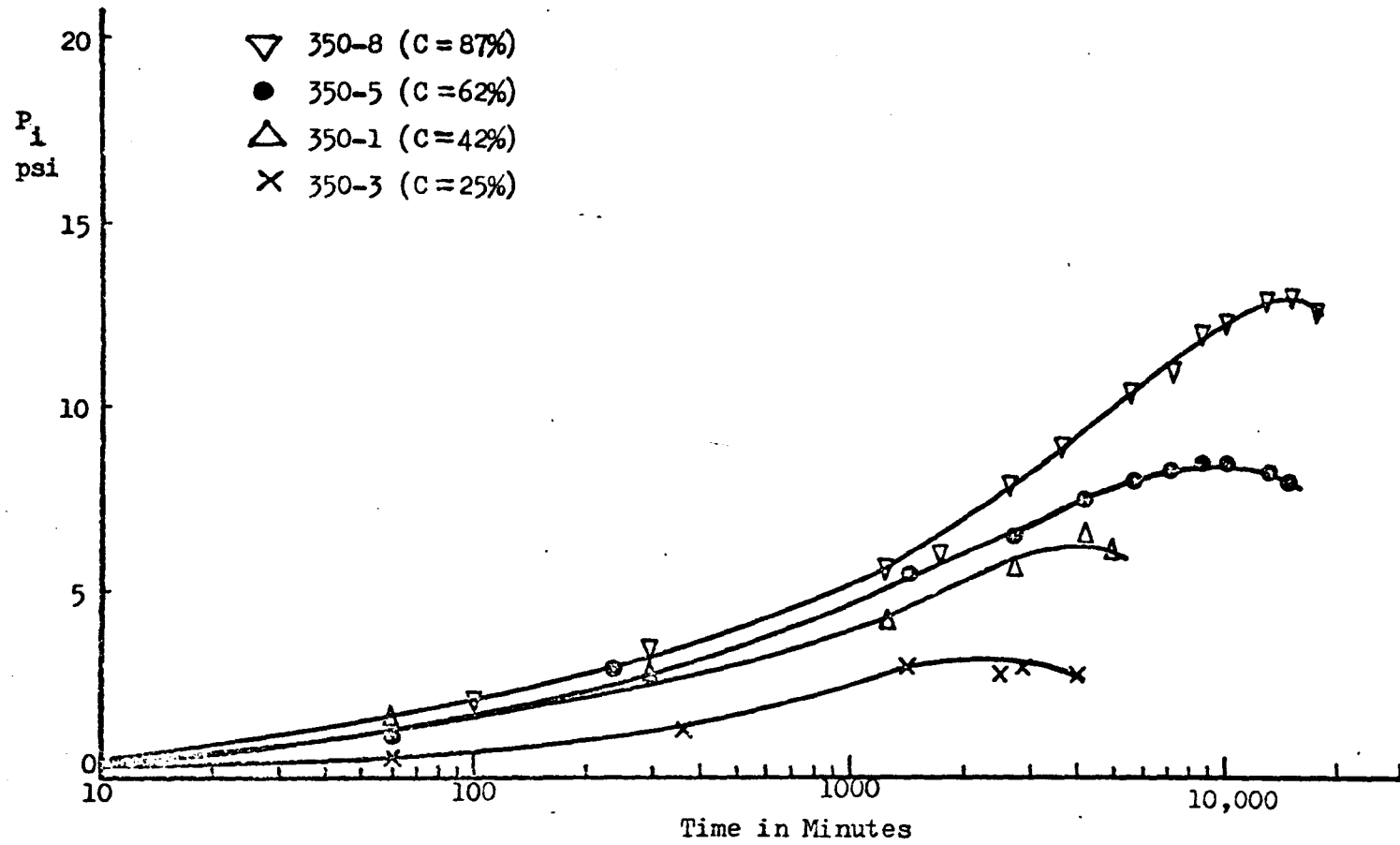


Fig.3.20 Isotropic Swell Pressure versus Time, Natural Soils.

see Figs. 3.12 and 3.13. The dependence of all the properties on the clay fraction is discussed in Chapter 5.

(iii) Graphs of swell potential versus time on natural scales for pure illite and pure bentonite (see Figs. 3.21 and 3.22) reveal that in illite, the rate of swell potential is fast in the beginning, slowing down with further increase of time, however, in bentonite the swell potential develops fairly steadily throughout the period of testing, the average rate being low from the beginning to the end of the test. This difference between illite and bentonite is thought to be due to the difference in permeabilities of the compacted samples.

3.4.5.2 Swell Pressure Versus Time

It can be seen from the graphs of swell pressure versus time reported in the present study that all the trends mentioned in the above section for swell potential, apply to the swell pressure variation with time also. Whilst the trends are similar, the only difference is in the magnitude of time, which is relatively smaller for the development of maximum swell pressure than for the development of maximum swell potential.

3.4.6 Maximum and Ultimate Swell Pressures

It can be seen from the swell pressure against time plots (e.g. Fig. 3.15) in this study that the swell pressure drops after it has reached a maximum value. Similar drops in swell pressure are evident in results reported by Alpan (1957) and Agarwal and Sharma (1973), although these investigators neither explain nor even

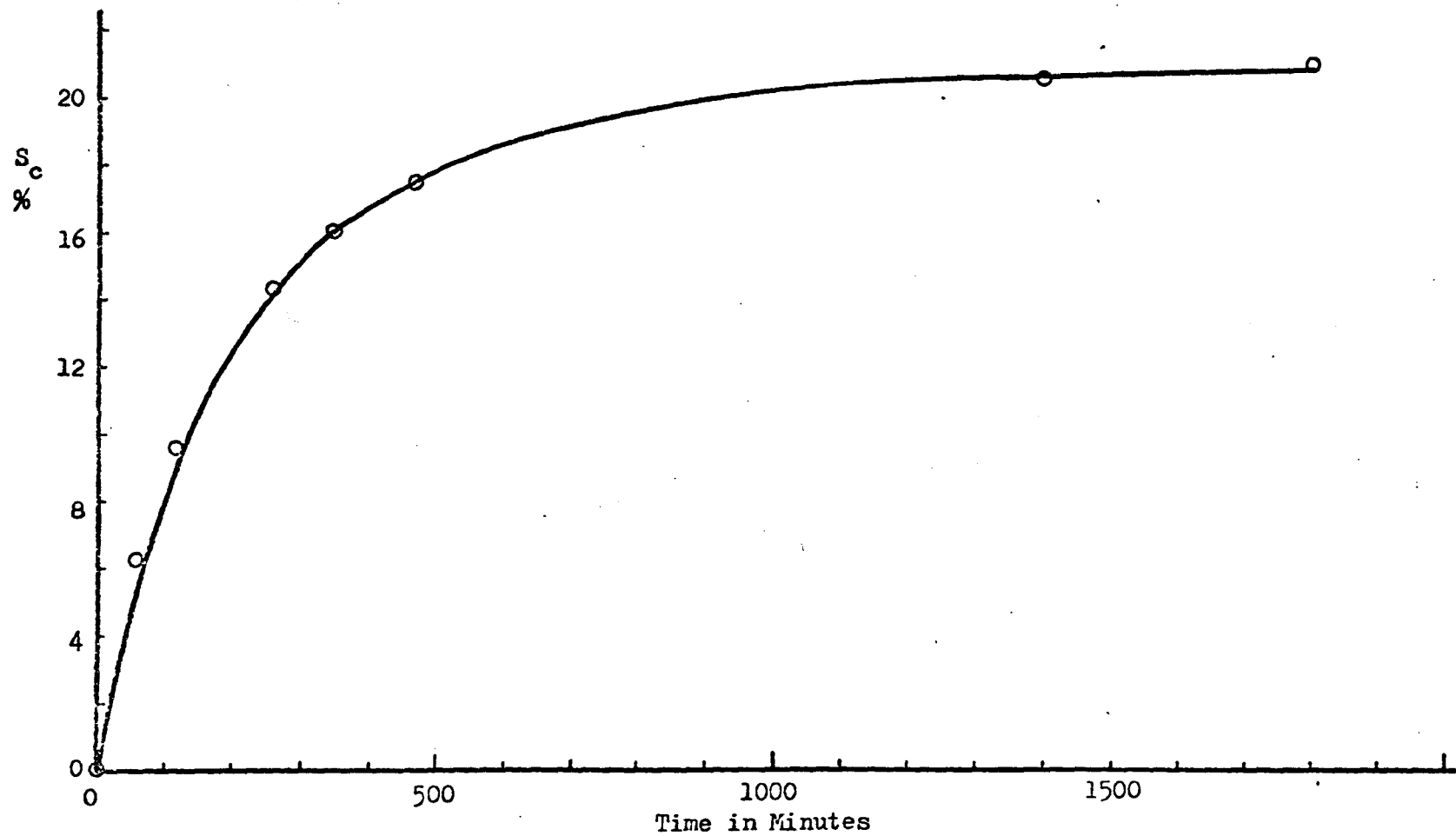


Fig.3.21 Laterally Confined Swell Potential versus Time on Natural Scales,
Illite 100%.

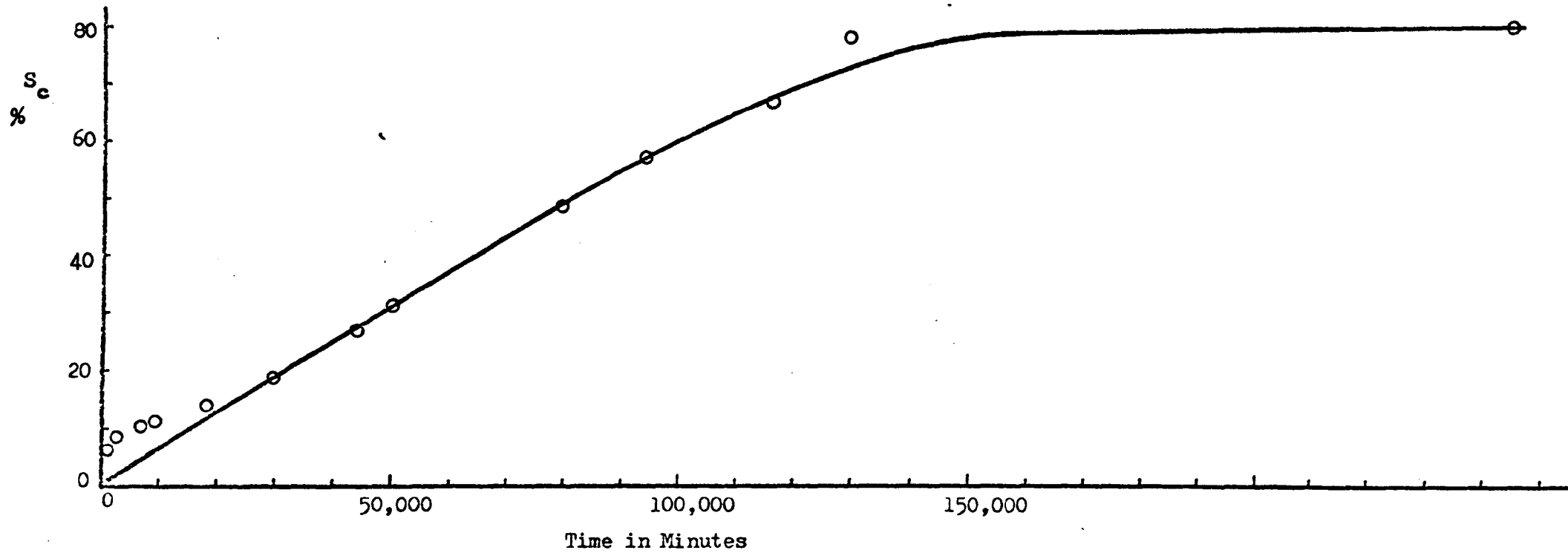


Fig.3.22 Laterally Confined Swell Potential versus Time on Natural Scales,
Bentonite 100%.

appear to notice this phenomena.

Although the design and research interests are in obtaining the maximum swell pressure, in an attempt to study the swell pressure after the drop from the maximum, a single test was conducted on a pure bentonite sample in the isotropic swell pressure apparatus. The test was run for a total time of about 100,000 minutes (3 months). The swell pressure is plotted against time in Fig. 3.23, from which it can be seen that the swell pressure, after dropping from a maximum reaches a constant value equal to 80% of the maximum value. Thus it appears that there are two swell pressures, viz;

- (i) maximum swell pressure,
- and (ii) ultimate swell pressure.

This aspect could not be studied for all the samples tested in the present study in view of the long time required for swell pressure tests.

At least three possible explanations can be given for the drop from the maximum swell pressure. They are:

- (1) there may be a plastic yield of the sample as clay is extruded from heavily stressed positions into voids,
- (2) there may be some internal swelling of the sample, in which the sample expands into voids which had originally contained air, and
- (3) there may be a change in the ionic concentration in the pore water within the sample.

Although there is no direct evidence for any of these three explanations, and all are purely hypothetical at this

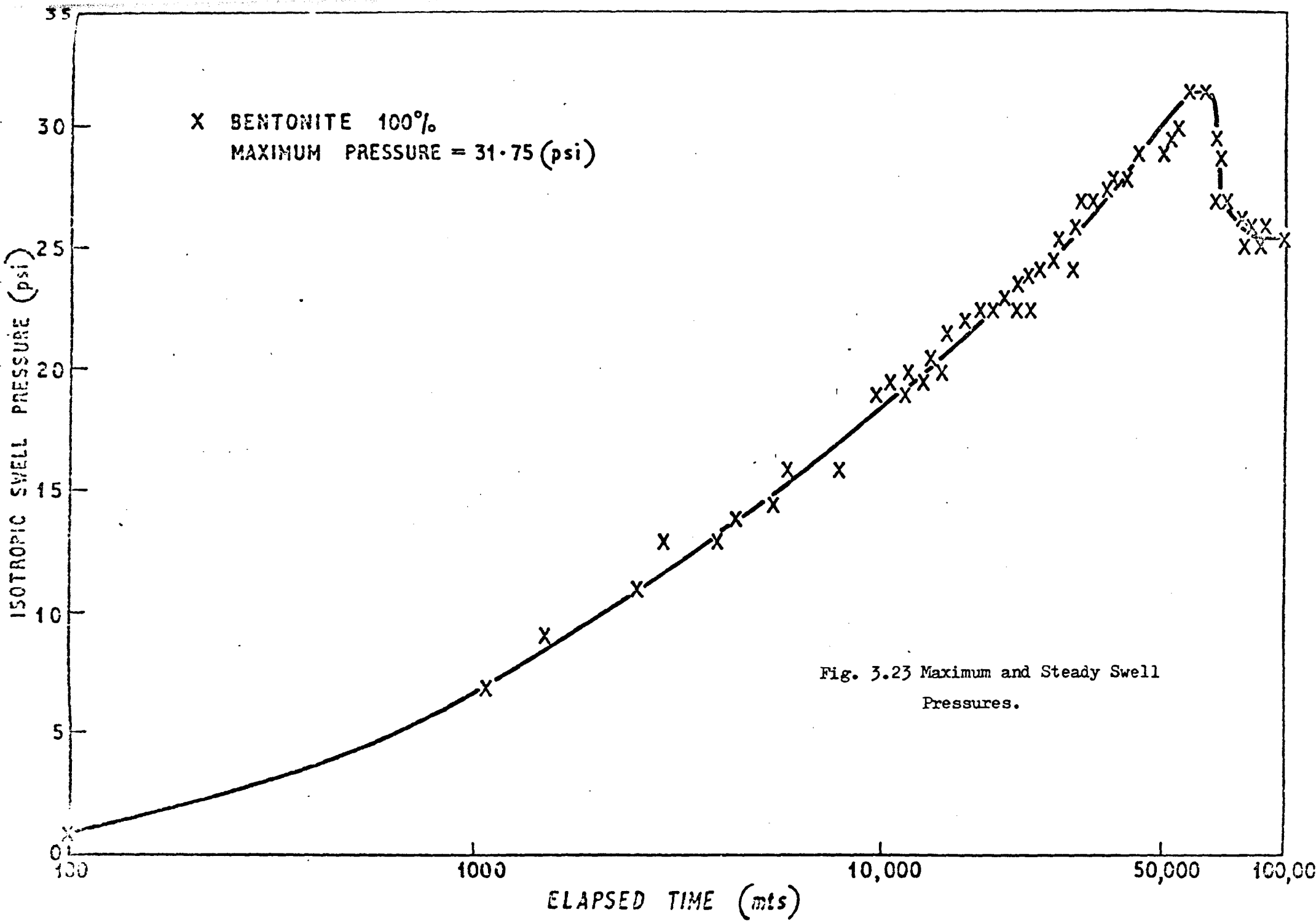


Fig. 3.23 Maximum and Steady Swell Pressures.

stage, it is thought probable that the first of the above three explanations might be the dominant one in causing the drop of the swell pressure.

3.5 SUMMARY AND CONCLUSIONS

The details regarding the type of soils and the main tests undertaken in the present study are reported in this chapter. The results of the main tests made on both artificial and natural soils, and some discussions which bear on the dependability of these results are also reported. The material presented in this chapter permits the following conclusions to be drawn:

- (1) The compaction test results were broadly as would be expected with no serious anomalies or peculiar behaviour.
- (2) The swell properties developed with time much as expected, showing a reversed S-shaped curve somewhat similar to a consolidation curve, when plotted against log time and a fairly simple rise against natural time. (The laterally confined swell pressure against time for the bentonite-illite mixtures showed a somewhat erratic behaviour, see Appendix 7. However, even this seemed unimportant in its effect on the maximum values of the swell pressure needed for analysis in Chapter 5).
- (3) After the swell pressure reached a peak, it dropped from the maximum to reach a steady state. Thus, there appeared to be two swell pressures, viz; maximum swell pressure and ultimate (steady) swell pressure. However, the peak value of swell pressure is of importance in the present study and is used for analysis in Chapter 5.

(4) Laboratory measurement of swell pressure is sensitive to the temperature fluctuations in the laboratory. For precise measurements of swell pressure, particularly on low swelling soils, it is recommended that the apparatus be used in a temperature controlled room.

Further analysis of the test results presented in this Chapter are reported later in Chapter 5, after reviewing the theories for the prediction of swell properties in Chapter 4.

CHAPTER - 4

PREDICTION OF SWELL PROPERTIES

4.1. INTRODUCTION

This chapter reviews two sets of theories which attempt to predict or explain swelling of soils. They are: (1) predictions based on soil properties, and (2) simple mixing laws to explain the behaviour of swell properties. In addition, a third set of theories, elastic mixing laws were considered in the present study but were not found useful in the present context; these laws were originally proposed to predict the elastic constants of 2-phase mixtures of polymers and solids. They are reported in Appendix - 6.

From the point of view of an engineer in practice, the most popular methods of prediction are the first set mentioned above, which use the properties of soils that can be readily determined in the laboratory. These methods are reviewed in section 4.2, and use a wide variety of properties as independent variables, of which it was decided to concentrate on texture, organic matter, and Atterberg limits in the present study, since these have been the most popular choices and are the most readily available parameters.

Since many of the predictions in the first set seemed inaccurate, consideration was given to other approaches. In particular, the simple mixing laws which form the second set of theories, although empirical in nature,

did prove useful when considering the mixtures of sand and clay tested in this programme. This set of theories is presented in section 4.3.

4.2. THEORIES BASED ON SOIL PROPERTIES

4.2.1. Introduction

A number of equations or graphs have been proposed for the prediction of the swell properties, viz, swell pressure and swell potential, from engineering properties such as Atterberg limits. The more important of these are reviewed below in a chronological order.

Comparisons of the different theories reported below with the data collected in the present study are presented in Chapter 5.

4.2.2. Holtz and Gibbs (1956)

Holtz and Gibbs (1956) were the first to investigate the identification criterion for swelling soils. In order to quantify the degree of expansion, they used the value of 'free swell' (testing details of measuring 'free swell' were given in Section 2.2.2). They suggested that soils with a 'free swell' value of more than 100% exhibit considerable volume changes in the field, and soils with a 'free swell' value of less than 50% do not show any serious volume changes even under light loadings. The authors also attempted to classify the probable amount of expansion making use of simple index properties (plasticity index and shrinkage limit), and the percentage

colloid content. The authors' classification data, Table 4.1, when subjected to multiple regression analysis by the present writer, yields the following equation:

$$\text{Probable Expansion} = 1.882 C - 0.177 \text{ PI} + 0.914 \text{ SL} - 26.796 \quad (4.1)$$

where, C = colloid content (0.001 mm) (%),
 PI = plasticity index (%),
 and SL = shrinkage limit (%)

The value of the multiple correlation coefficient (R^2) is 0.9706, which is highly significant.

4.2.3. Williams (1957)

Williams suggested a simple classification based on the relationship between plasticity index of the whole sample and the percentage clay fraction ($< 2 \mu$). He classified soil into very high, high, medium and low degrees of potential expansion using the graph in Fig. 4.1.

4.2.4. Dinesh Mohan (1957)

Dinesh Mohan (1957) studied about twenty remoulded Indian Black Cotton Soils; these soils swell strongly. Taking shear strength as half the unconfined compressive strength, he suggested a straightline relationship between liquidity index and shear strength on a log-log scale. The consolidation characteristics were obtained from samples remoulded at the liquid limit and tested in an oedometer. He observed that the relationship between the Compression index ~~compressibility~~ and the liquid

Table 4.1 Data of Holtz and Gibbs (1956) for
Estimating Probable Expansion

Data From Index Tests			Probable Expansion (%)	Degree of Expansion
Colloid Content (% < 0.001 mm)	PI (%)	SL (%)		
> 27	> 32	< 10	> 30	Very High
18-37	23-45	6-12	20-30	High
12-27	12-34	8-18	10-20	Medium
< 17	< 20	> 13	< 10	Low

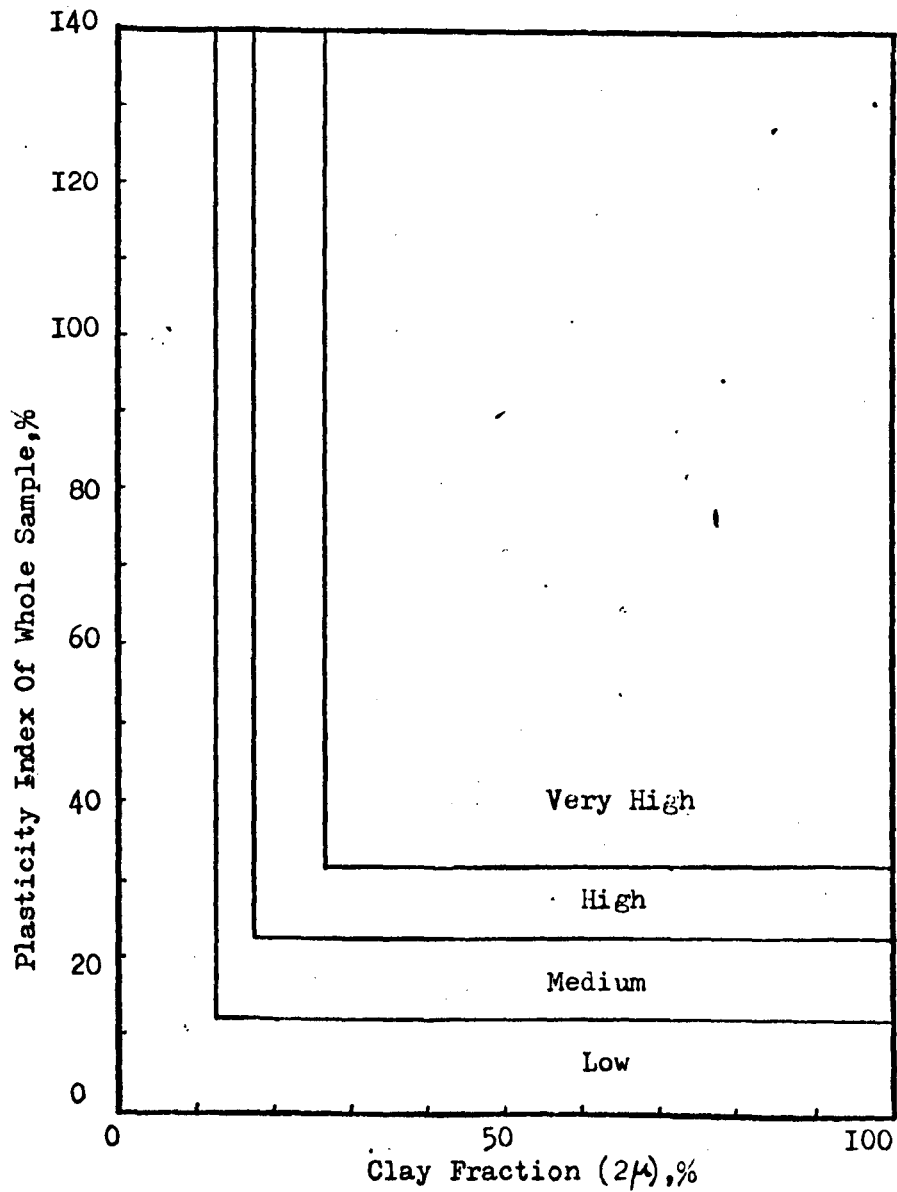


Fig. 4.I William's (1957) Chart For Identification Of Expansive Soils.

limit was close to Skempton's relationship for remoulded clays, given as (Terzaghi and Peck, 1967):

$$C_c = 0.007(LL - 10\%) \quad (4.2)$$

Terzaghi and Peck (loc. Cit.) suggested that, for undisturbed clays, the value of C_c obtained from Skempton's relation should be increased by 1.30 times; thus pointing to a difference between remoulded and undisturbed clays. A similar difference might be found for the swell properties. However, in the present context, the main importance of Dinesh Mohan's work is to suggest that there may be a correlation between the swell properties and either the liquid limit or liquidity index or both.

4.2.5. Seed et al (1962)

Seed et al (1962) used twenty three artificial soils, comprising mixtures of illite, kaolinite and bentonite, in order to develop a reliable means for predicting the potential expansion characteristics of clays from classification test data. The authors also used data from thirty eight natural soils published by the United State Bureau of Reclamation in order to verify the applicability of their approach to natural soils.

The equation obtained by these authors from their study on artificial soils, for predicting swell potential, is:

$$S_c = 3.6 \times 10^{-5} A^{2.44} C^{3.44} \quad (4.3)$$

where, S_c = swell potential (%),

A = activity,

and C = clay fraction ($< 2\mu$), (%).

The usual ratio of plasticity index and clay content for activity was modified, because the liquid limit apparatus used in the U.S.A. produces data which displaces the graph of PI versus C slightly downward and not through the origin as would be obtained with the British apparatus. The activity was taken as:

$$A = \frac{PI}{C - n} \quad (4.4)$$

where, n is the intercept on the x-axis. Substituting eqn. (4.4) in (4.3), it follows:

$$S_c = 3.6 \times 10^{-5} \quad PI^{2.44} \quad \frac{C^{3.44}}{(C - n)^{2.44}} \quad (4.5)$$

$$S_c = 3.6 \times 10^{-5} \quad PI^{2.44} \quad N \quad (4.6)$$

in which,

$$N = \frac{C^{3.44}}{(C - n)^{2.44}} \quad (4.7)$$

Noting that the possibility of a correlation between swell potential and plasticity index depends on the variability of N , the authors attempted to determine an average value of N . Both the average value of n and the range of clay content differed between the set of artificial soils and the set of natural soils studied by these authors, so that they suggested two separate equations, one for artificial soils and the other for natural soils.

These are:

$$S_c = 3.6 \times 10^{-5} (100)(PI^{2.44}) \quad (4.8)$$

for artificial clays

and,

$$S_c = 3.6 \times 10^{-5} (60)(PI^{2.44}) \quad (4.9)$$

for natural soils

The authors suggested that this method is useful to predict swell potential within an error of $\pm 33\%$.

If we assume that a British liquid limit apparatus is used, then

$$A = \frac{PI}{C} \quad (4.10)$$

Substituting Eqn. (4.10) in Eqn. (4.3) it follows:

$$S_c = 3.6 \times 10^{-5} (PI^{2.44}) (C) \quad (4.11)$$

On this basis, the difference between Eqns. (4.8) and (4.9) might be explained if it could be assumed that the clay contents of the artificially prepared soils and of the natural soils were 100 and 60 respectively. This seems to be an oversimplification.

The work of Seed et al suggests that there is a wider scope for regression analysis to obtain a multiple correlation between plasticity index, clay content and the swell potential.

4.2.6 Roderick and Jin (1963)

Roderick and Jin (1963) studied nine undisturbed soils from and around Wisconsin and obtained correlations between the results of simple physical tests and mineralogical and physico-chemical tests. Using a

least square fit, the authors give the following equations:

$$C_c = 0.0025 LL + 0.05 \quad (4.12)$$

$$C_E = 0.0025 LL - 0.06 \quad (4.13)$$

$$PL = 50.5 - 0.0712 (CEC) \times (C_a Co_3) \quad (4.14)$$

$$SL = 30.4 - 0.0409 (CEC) \times (C_a Co_3) \quad (4.15)$$

$$CEC = 35.0 - 0.589 (C_a Co_3) \quad (4.16)$$

where,

C_c = coefficient of compressibility,

C_E = coefficient of expansion,

CEC = cation exchange capacity, $\frac{meq}{100 \text{ gms}}$

and,

$C_a Co_3$ = percentage of equivalent calcium carbonate.

In the present context, this work has two implications:

(1) non-linear as well as linear regression analysis should be considered, (2) calcium carbonate or other cements might be important. Note also that Eqn. (4.12) predicts a value of C_c which is less than half that predicted by Eqn. (4.2)

4.2.7 Da Nilov (1964)

Da Nilov (1964) has devised a chart for identifying swelling and slumping soils from dry density, specific gravity of solids, and liquid limit. In this method, instead of using the shrinkage limit, the difference between liquid limit and natural water content was taken as an index in the form:

$$\frac{e_0 - e_1}{-e_1 + e_0} \quad (4.17)$$

where,

e_0 = natural void ratio,

and

e_1 = void ratio at liquid limit.

Soils with an index less than -40% are considered as swelling soils, greater than -10% as slumping soils, and the soils with intermediate values are considered as normal stable soils. The most important points that emerge from Da Nilov's paper are : (1) the initial void ratio, e_0 , should be taken into consideration (or the initial density), and (2) the swelling phenomena is volumetric.

4.2.8 Ranganatham and Satyanarayana (1965)

Ranganatham and Satyanarayana (1965) studied the swell characteristics of Black Cotton Soils obtained from Southern India. The authors observed that prediction of swell potential from empirical equations suggested by Seed et al (1962, see section 4.2.5) causes an error of 30 to 65% in predicting the measurements on soils considered in their study. In an attempt to find a more rational approach for the prediction of swell potential, the authors used shrinkage limit in place of plastic limit, as the shrinkage limit is defined as the lower end of the range of swelling states. They, therefore, define shrinkage index (SI) as the difference between liquid limit and shrinkage limit. Using a similar approach to that of Seed et al (1962), the authors arrived at the following relationships.

$$S_c = 263 \times 10^{-5} SI^{2.67} \quad (4.18)$$

for artificial clays

and

$$S_c = 41.13 \times 10^{-5} SI^{2.67} \quad (4.19)$$

for natural soils.

The authors used only six artificial clay mixtures and four natural soils in their study. It is disconcerting that the constant for artificial clays is six times greater than for natural soils, particularly as truly independent regression analyses would have yielded different values for the exponents of shrinkage index for the two different sets of data.

The approaches of Seed et al (1962) and Ranganatham and Satyanarayana (1965) when viewed in the light of the simultaneous use by Holtz and Gibbs (1956) of plasticity index, shrinkage limit, and clay content suggest that a more rewarding approach would be to measure various index and mineralogical parameters and to eliminate the insignificant parameters by regression analysis.

4.2.9 Komornik and David (1969)

Komornik and David (1969) made a statistical analysis of 200 undisturbed clays from Israel in order to correlate swell pressure with indicative parameters. The multiple correlation (with a correlation coefficient of 0.60) suggested by the authors is given below:

$$\log P = 2.132 + 0.0208(LL) + 0.00065(\gamma_d) - 0.0269 (w_0) \quad (4.20)$$

where,

P = swell pressure (Kg/cm^2),

LL = Liquid limit (%),

Y_d = dry density (Kg/m^3),

and

w_0 = natural water content (%)

The authors assumed that liquid limit is an indirect measure of the potential properties such as surface area, type and concentration of ions and type of clay; that water content is a measure of the capillary tension of adsorbed water; and that dry density is a measure of particle spacing. The authors could not find a means of formulating the effect of structure. For compacted clays, their correlation suggests that swell pressure, as might be expected, would be a function of not only the potential properties but also of the initial placement conditions. Even though the statistical approach seems to be sound in principle, the collection of data for different soils from different laboratories does not guarantee that exactly uniform procedures were used for obtaining a particular parameter, and this may be the cause of some of the unexplained variability, which resulted in the low correlation coefficient.

In the present context, the work of Komornik and David suggests that attention should be paid to the initial placement properties, viz, the dry density and the moisture content. These parameters might be kept constant uniformly for all of the soils to be tested or they might

be taken into regression analysis.

4.2.10 Livneh et al (1969)

Livneh et al (1969) suggested several correlations for clays from Israel, which were intended to aid the design engineer dealing with road and airfield pavements. The authors presented graphical correlations between index properties and other characteristics like moisture-density relationships, CBR value, swell potential and swell pressure. They did not test these correlations statistically. However, they found fairly good multiple correlation between the percent swell of the remoulded CBR samples and the plasticity index and the initial moisture content as shown in Fig. 4.2. The results show the dependence of the amount of swell on the initial conditions of the sample for a practical range of placement conditions. This correlation was recommended to determine the necessary placement conditions, allowing a minimum of 2% swell under a surcharge of 10 lbs, which is a common design practice in Israel. It should, however, be noted that very few points of the authors' test data lie in the range of 2% swell.

The second correlation deals with the swell pressure of undisturbed clay, see Fig. 4.3. The authors adopted Eqn. (4.20), assumed $G_s = 2.8$, and found that the coefficients of liquid limit and natural water content in Eqn. (4.20) are approximately:

Percent Swell in C.B.R. Mould (10 lbs. surcharge)

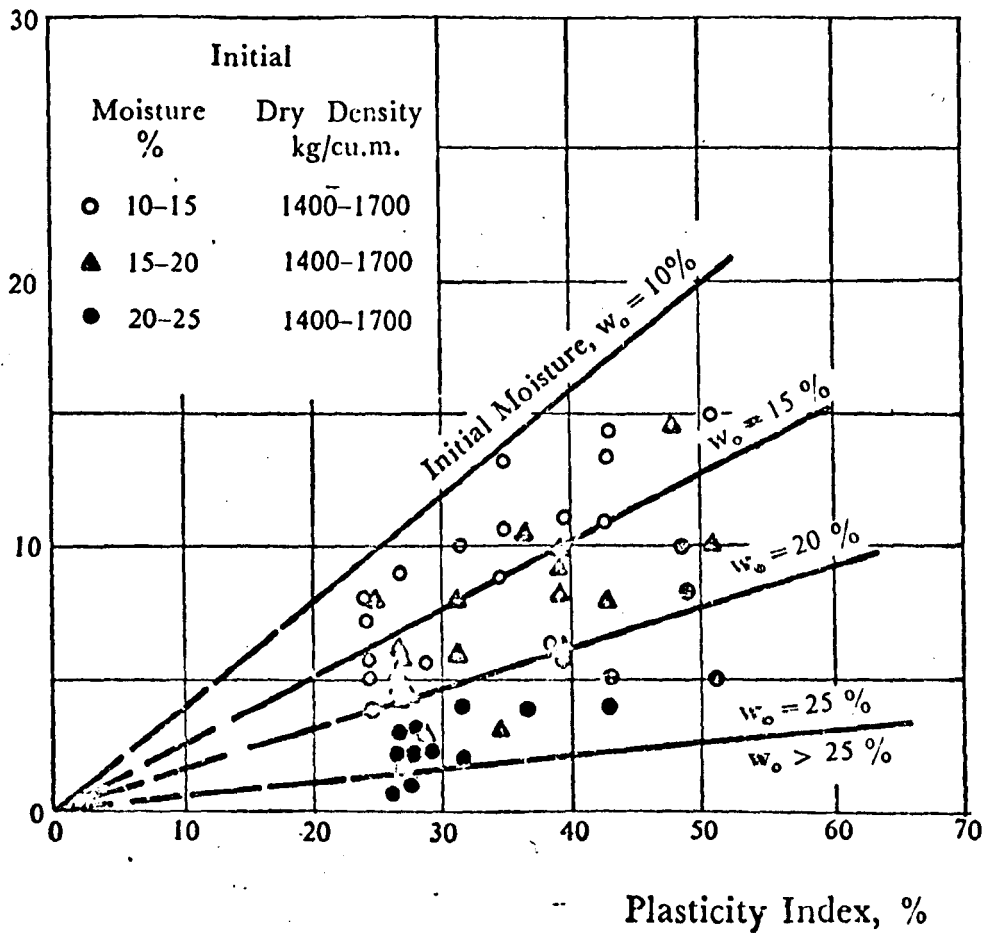


FIGURE 4.2 P.I. AGAINST PERCENT SWELL OF REMOLDED C.B.R. SAMPLES AT VARIOUS MOISTURE CONTENTS
(Reproduced From Livneh et al, 1969)

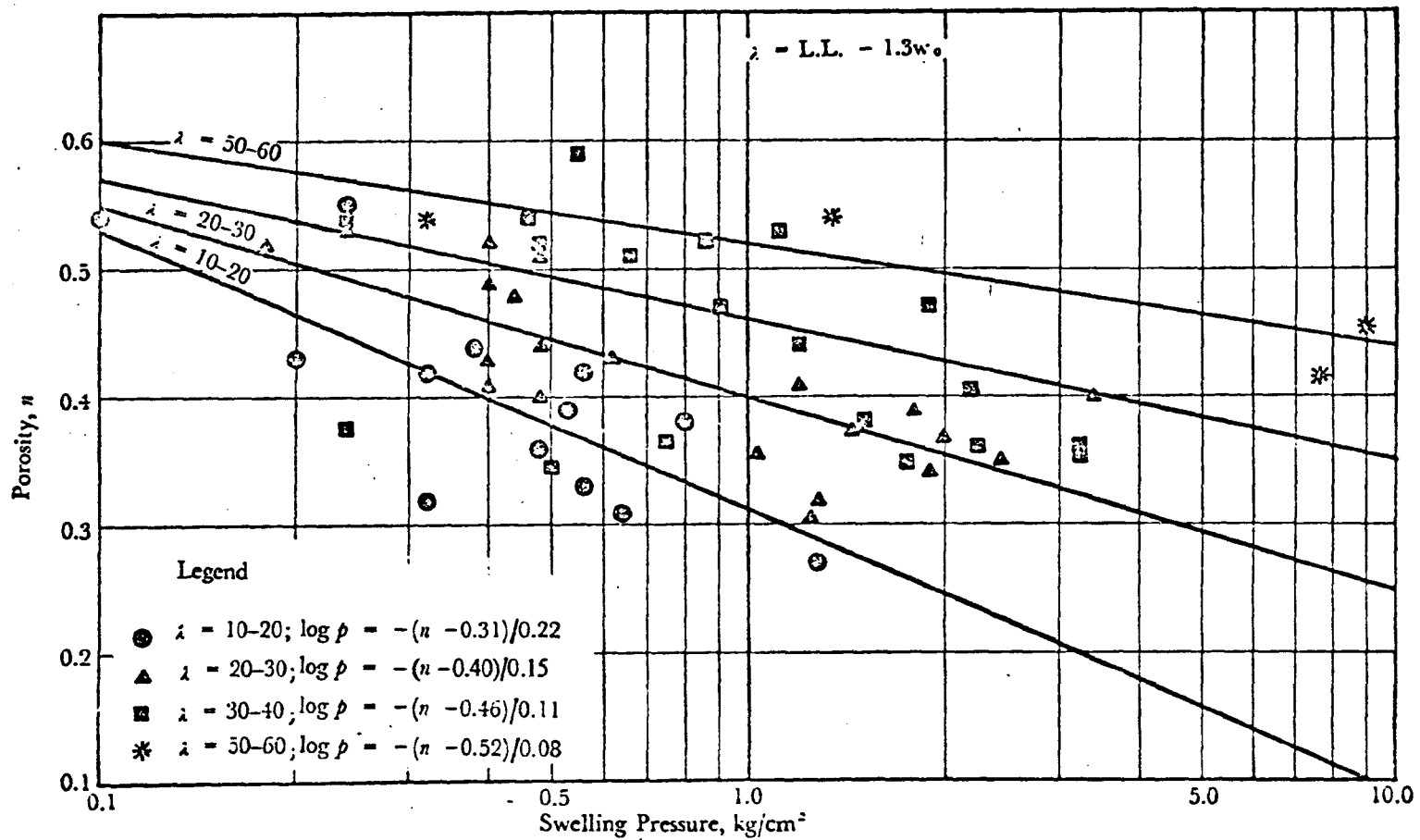


FIGURE 4.3 SWELL PRESSURE OF UNDISTURBED CLAY AGAINST POROSITY
 (Reproduced From Livneh et al, 1969)

$$0.021 (LL - 1.3 w_0) \quad (4.21)$$

They, therefore, define λ as:

$$\lambda = LL - 1.3 w_0, \quad (4.22)$$

and present their final predictions as lines for constant λ on a graph of swell pressure versus porosity. In doing so, they make further empirical changes to Eqn. 4.20 so that the constants now become in effect functions of λ , which are defined numerically, as shown in Fig. 4.3.

4.2.11. Nayak and Christinsen (1971)

Nayak and Christinsen (1971) examined the limitations of the existing methods for the prediction of swelling behaviour of compacted clays, and noted that both the purely theoretical approach (based on osmotic pressure theory of pure clay suspensions) and the purely empirical approach are inadequate to serve the purpose. They suggested a semi-empirical approach in which a model of swelling behaviour is developed leading to equations relating the swelling potential and swell pressure of compacted soil to its plasticity index, clay content, and initial moulding water content. The model was based on the concepts of the diffuse double layer, modified by introducing empirical constants to account for elastic swelling effects and other limitations (eg: in equating the osmotic pressure to the swelling pressure of a soil the effects of elastic rebound, pressure in entrapped air bubbles and the forces of attraction are neglected).

The investigators studied 18 samples of compacted artificial clay mixtures and arrived at the following equations that are claimed to be applicable to all soils.

$$P_c = 3.5817 \times 10^{-2} \text{ PI}^{1.12} \frac{C^2}{w_i^2} + 3.7912 \quad (4.23)$$

$$S_c = 2.29 \times 10^{-2} \text{ PI}^{1.45} \frac{C}{w_i} + 6.38 \quad (4.24)$$

where,

P_c = laterally confined swell pressure (lb/in²),

S_c = swell potential (%),

PI = plasticity index (%),

C = clay content (%),

w_i = initial water content (%).

4.2.12 Vijayvergiya and Ghazzaley (1973)

Vijayvergiya and Ghazzaley (1973) analysed test data from about 270 samples of undisturbed natural soils to obtain single and multiple correlations that relate swelling characteristics of soils with the routine physical and classification properties. The proposed correlations to predict swell pressure and percent swell under 0.1 tons/sq. ft. surcharge load are:

$$\log P_c = \frac{1}{12} (0.4 \text{ LL} - w_i - 0.4) \quad (4.25)$$

$$\log S_c = \frac{1}{12} (0.4 \text{ LL} - w_i + 5.5) \quad (4.26)$$

where P_c is expressed in tons/sq.ft.

Defining swell index (I_s) as the ratio of natural water content to liquid limit, the investigators established curves between I_s and LL to predict the percent swell and swell pressure under no volume change, see Fig. 4.4. The curves appear to provide a quick qualitative identification of troublesome clays. However, it should be noted that the percent swell was determined under a surcharge load of 1.5 psi against the common practice of 1 psi. The form of Vijayvergiya and Ghazzaley's expressions suggest that perhaps the logarithm of the swell properties should be considered for use in predictive equations.

4.2.13 Chen (1975)

Chen (1975) analysed the test results of 321 undisturbed samples and fitted a regression curve between plasticity index and the swell potential. The equation for the suggested curve was given as follows:

$$S_c = 0.2558 \exp (0.0838 \text{ PI}) \quad (4.27)$$

Although Chen and Seed et al (1962) use the same definition for swell potential, their predictions, Eqns.(4.27) and (4.9), differ numerically.

4.2.14 Comments

The predictions listed above differ mainly in four ways:

- (1) various definitions are used for the swell potential and swell pressure.

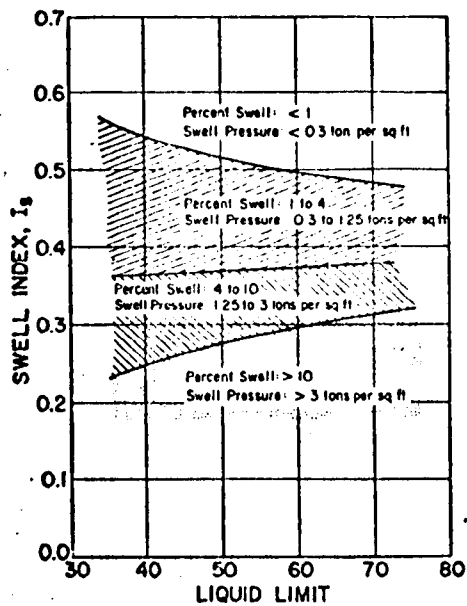


FIG.4.4 RELATIONSHIP BETWEEN WATER CONTENT AND LIQUID LIMIT FOR EXPANSIVE CLAYS

(Reproduced From Vijayvergiya and Ghazzaly, 1973)

- (2) various independent variables are used.
- (3) equations which seem to be similar differ numerically.
- (4) the initial conditions are treated differently or omitted.

Further consideration will be given to these predictions in Chapter - 5.

4.3. SIMPLE MIXING LAWS

4.3.1. Introduction

Four empirical mixing laws for mixtures of two phases are considered here, taking x as the proportion of one phase; and y as the property of interest, ie P_c , S_c etc.

These are:-

- (1) Linear relationship,
- (2) Quadratic relationship,
- (3) Smart's (1970) quadratic bounds, and
- (4) A new S-shaped relationship.

Further details are given below.

4.3.2. Linear relationship

The linear mixing law, ie $y = a + bx$ is the simplest mixing law and is based on the assumption that the swell property is linearly proportional to the amounts of sand and clay or clay and clay present in

the mixture. This relationship is similar to the law proposed by Voigt (see Appendix 6). Also, there might be an analogy between swell pressure and the pressure of a mixture of perfect gases, which also follow a linear mixing law.

4.3.3. Quadratic Mixing Law

The quadratic mixing law is the next simplest to the linear law and can be expressed in the form:

$$y = a + bx + cx^2$$

This empirical relationship is also the simplest which has interaction between the components and in some circumstances may be derived from consideration of the probability of contacts of different types. This type of quadratic relationship was suggested by Smart (1970) in the prediction of the residual angle of internal friction (ϕ_r) of sand-clay mixtures. He postulated that after a shear plane has formed, the sample can be treated as two rigid blocks one sliding over the other. It was reasoned that the area of one of the sliding surfaces contained a proportion by area of clay equal to C and a proportion by area of sand equal to (1-C). Of this area of clay, a proportion by area of C was assumed to be in contact with clay in the other surface, so that the proportion by area of clay sliding over clay was C^2 . Similarly, $(1-C)^2$ was the proportion of sand sliding over sand, and $2C(1-C)$ was sand sliding over

clay. Based on this hypothesis, Smart (1970) proposed the following equation:

$$\tan \phi_r = c^2 \tan \phi_c + 2c(1-c) \tan \phi_m + (1-c)^2 \tan \phi_s \quad (4.28)$$

where ϕ_c , ϕ_s , and ϕ_m are the friction angles for clay-clay, sand-sand, and sand-clay respectively. ϕ_c and ϕ_s may be measured by testing sand-free and clay-free samples, but the value of ϕ_m cannot be obtained directly. However, it was suggested likely that $\phi_c \leq \phi_m \leq \phi_s$.

For further consideration of Eqn. (4.28) in the next section, it is written below in the general form:

$$y = c^2 y_c + 2cs y_m + s^2 y_s \quad (4.29)$$

where c and s are the fractions of clay and sand; y_c and y_s are the properties of interest of sand-free and clay-free materials respectively. Y is the property of interest of the mixture.

4.3.4. Smart's Bounds

Smart (1970) extended the above argument to propose two bounds for the prediction of the angle of internal friction (ϕ_r) and these bounds will be considered here for a more general range of properties. If it is assumed that y_m lies between y_c and y_s , the upper and lower bounds are derived by putting $y_m = y_c$ and $y_m = y_s$ as appropriate in Eqn. (4.29), viz:-

$$y = y_c (1-S^2) + y_s S^2 \quad (4.30)$$

$$y = y_c C^2 + y_s (1-C^2) \quad (4.31)$$

Noting that the swell properties of pure sand are zero, the above equations take the following form for sand-clay mixtures:

$$\text{Upper bound: } y = y_c (1-S^2) \quad (4.32)$$

$$\text{Lower bound: } y = y_c C^2 \quad (4.33)$$

4.3.5. S-Shaped Relationship

As an alternative to the bounds mentioned above, a new S-shaped relationship can be deduced by assuming that the predominant component dominates the relationship. In other words, it is postulated that clay dominates in the region of high clay content, sand in the region of high sand content, and in between both phases contribute to the property. Assuming that,

$$y_m = C y_c + S y_s \quad (4.34)$$

where, c and s are the fractions of clay and sand per volume of solids. Substituting Eqn. (4.34) in Eqn. (4.29) it follows:

$$y = C^2 (3-2C) y_c + S^2 (3-2S) y_s \quad (4.35)$$

This is a cubic expression and as an example is fitted by Smart and Rao (in preparation) to some results of Kenny (1967) for the angle of internal friction of

illite-sand mixtures, see Fig. 4.5.

4.3.6. Summary

As will be discussed in Chapter - 5, the empirical mixing laws outlined above were found useful in explaining the swell and related properties of the artificial mixtures studied in this investigation.

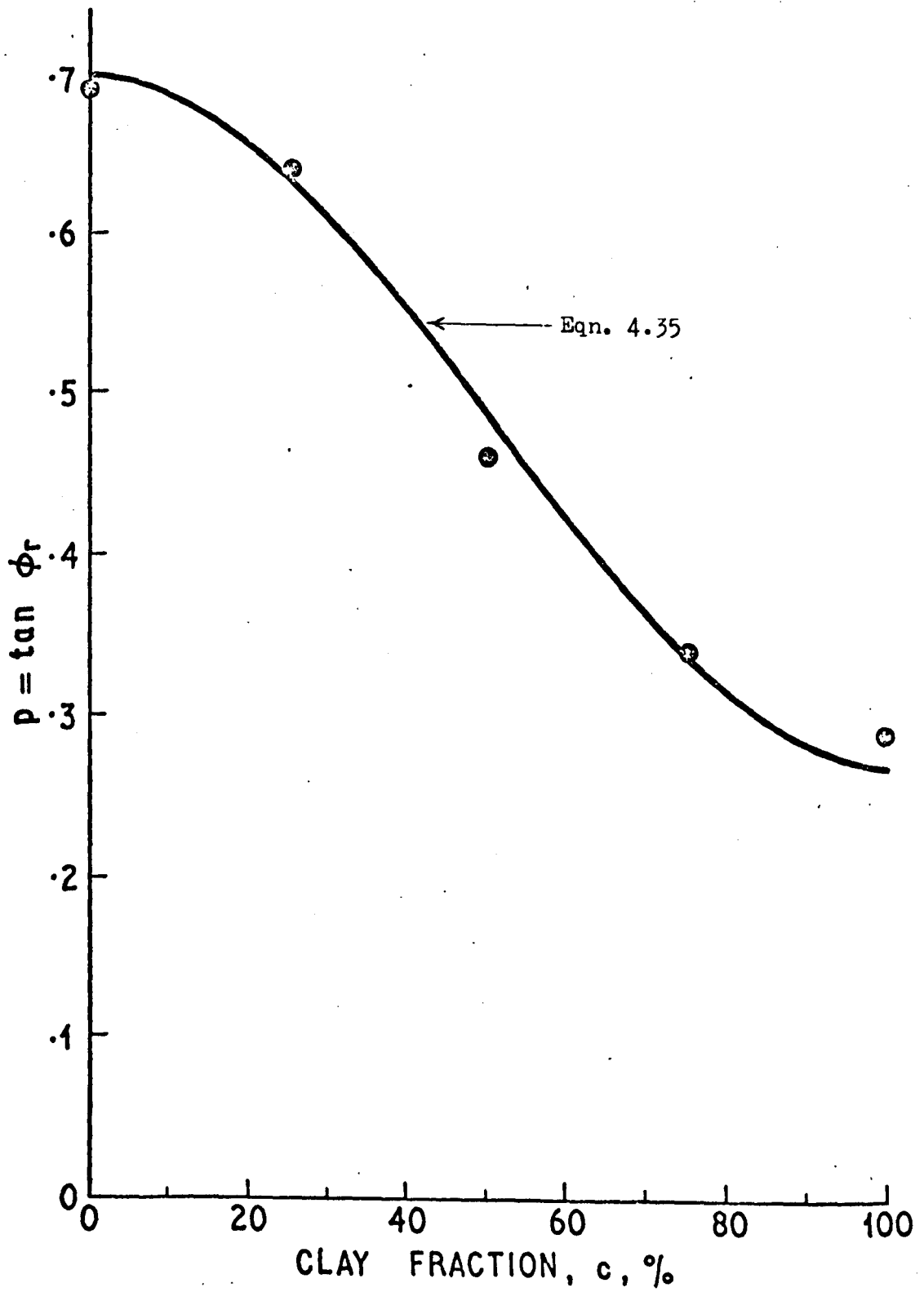


Fig. 4.5 $\tan \phi_r$ versus Clay Fraction. (Points are Kenny's Observations)

Chapter 5

DISCUSSION OF RESULTS

The test results reported in Chapter 3 are discussed in this chapter. The discussion is presented in three parts. Part-I deals with the results of tests on artificial mixtures, and Part-II with those on natural soils. The various predictive theories detailed by earlier investigators and presented in Chapter 4 are tested for their validity or otherwise in Part-III of this chapter.

Part-I: ARTIFICIAL MIXTURES

5.1 INTRODUCTION

The swelling properties of soils are controlled by (1) composition in the most general sense and including mineralogy, and (2) structure. Throughout the work reported in this thesis, an attempt has been made to standardise the effect of structure by starting all the tests from the optimum compaction conditions. The most convenient method of studying the effects of composition would be to use linear multiple regression, since this method of analysis is highly developed. However, the usefulness of linear multiple regression is curtailed unless the relationships which are being studied are either linear or can be made so by a suitable choice of variables; for example, the discussion below will suggest that the whole of the analysis will be simplified if swell amount, i.e. volume of swell per volume of solids,

is used in preference to the more usual swell potential, i.e. volume of swell per initial total volume of sample. The tests on artificial mixtures, the results of which will be discussed in Part-I of this chapter, were designed to isolate the effects of (1) clay content, in the bentonite-sand and illite-sand series, or (2) clay type, in the bentonite-illite series.

The original objective of these tests was to ascertain whether and to what extent the swell properties (and compaction properties and Atterberg limits) could be regarded as linear functions of "clay content", with a view to linear analyses of the corresponding properties of natural soils, which will be reported in Part-II. The data which will be discussed below in Part-I does suggest that linear analyses would be the most promising approach for natural soils; and the subsequent linear analyses of Part-II were successful. However, small but significant deviations from linearity are evident in much of the data reported in Part-I, and in this respect the reader is forewarned that the most important figures are: for swell pressure: 5.12, 5.23, 5.24, and 5.30; for swell amount: 5.14, 5.21 and 5.32. For this purpose, the appropriate straight line is the regression line of 'y upon x', and to avoid cluttering the diagrams it is left to the reader either to imagine this or to place a transparent straight edge over the Figures in the appropriate position.

The presentation of the discussion of Part-I is complicated by three factors: (1) almost all the data shows slight deviations from linearity; and (2) algebraic models

have been found which do represent the data accurately; and (3) consideration of these models suggests certain physical phenomena as causes of the non-linearity. The conclusions will be summarised in section 5.3.5.

In the summary, the pattern of behaviour of swell pressure will be compared to the pattern of behaviour of Kenny's (1967) observations of $\tan \phi_r$. For illite, $\tan \phi_r$ was found to be an S-shaped function of clay content, Eqn. 4.35 and Fig. 4.5; whereas for montmorillonite, $\tan \phi_r$ was represented approximately by a modification of the "bentonite-controlled" bound of the quadratic family of equations, Eqn. 4.32 and Appendix-10. In this respect, the most important Figures are the seven mentioned above, viz; 5.12, 5.21, 5.23, 5.24, 5.30 and 5.32.

Almost all the Figures of Part-I can also be analysed in a third way which might be thought to be of interest. This would be to answer the question: is it possible to predict the value of the property in question for any clay content by interpolation between measurements at 100% clay and 100% sand? For the present purposes, this is trivial and only occasional remarks are made concerning it. The appropriate straight line would be that connecting the two extreme measurements on the Figure concerned.

There is however one further question which must be considered since many of the predictions in Chapter-4 presuppose that the swell properties vary with Atterberg limits. It will be shown below that the swell properties and the Atterberg limits differ in their dependence upon clay content and thus cannot be exactly correlated.

Before discussing the compaction and swell behaviour of these mixtures, the variation of Atterberg limits with composition is considered first in the following section.

5.2 ATTERBERG LIMITS

The Atterberg limits of the three mixtures studied in this investigation are shown in Figs. 5.1 to 5.3, where the limits are plotted against sand content in clay-sand mixtures and against bentonite in bentonite-illite mixtures. In accordance with the findings of earlier investigators (e.g. Seed et al, 1964), a linear model fits the data for each mixture with reasonable accuracy except at high sand contents ($>70\%$). Dumbleton and West (1966) studied the influence of the type of coarse fraction on the plastic properties of clay soils and found that the liquid limit and plastic limit of the mixtures were proportional to the percentage of clay, only when the coarse fraction consisted of well rounded glass spheres. The majority of the sand particles in the present study were observed to be well rounded and this probably results in the linear variation between Atterberg limits and clay content in accordance with the findings of Dumbleton and West (loc. cit.). However, this behaviour is found to be valid only above about 30% clay content for clay-sand mixtures, below which the mixtures essentially showed a non-plastic behaviour. Dumbleton and West (loc. cit.) do not show any experimental points below about 30% clay content for their mixtures, so no comparison could be made in this region. The above behaviour suggests that above 30% clay content, a well rounded coarse fraction does not

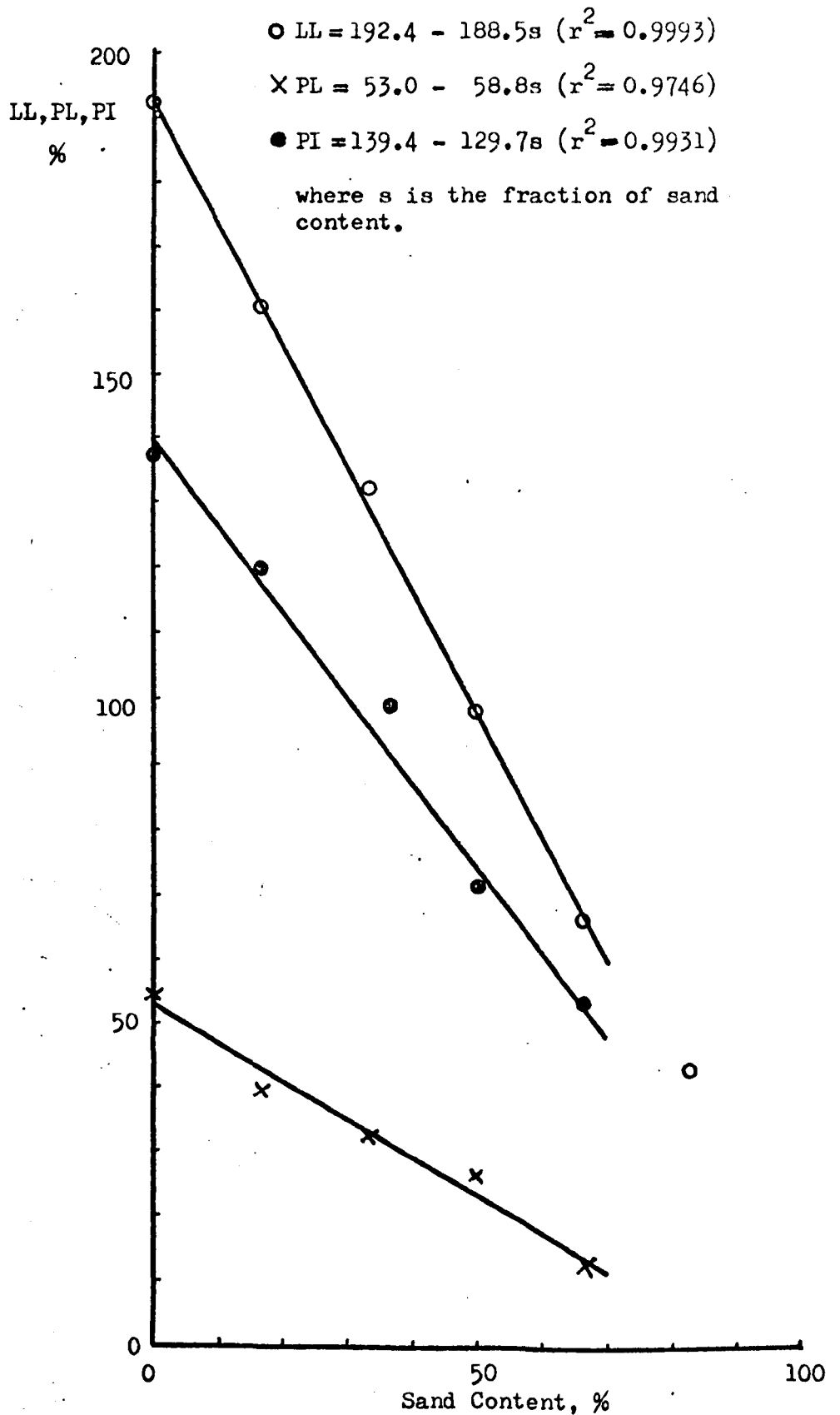


Fig.5.1 Atterberg Limits VS Sand Content, Bentonite-Sand Mixtures.

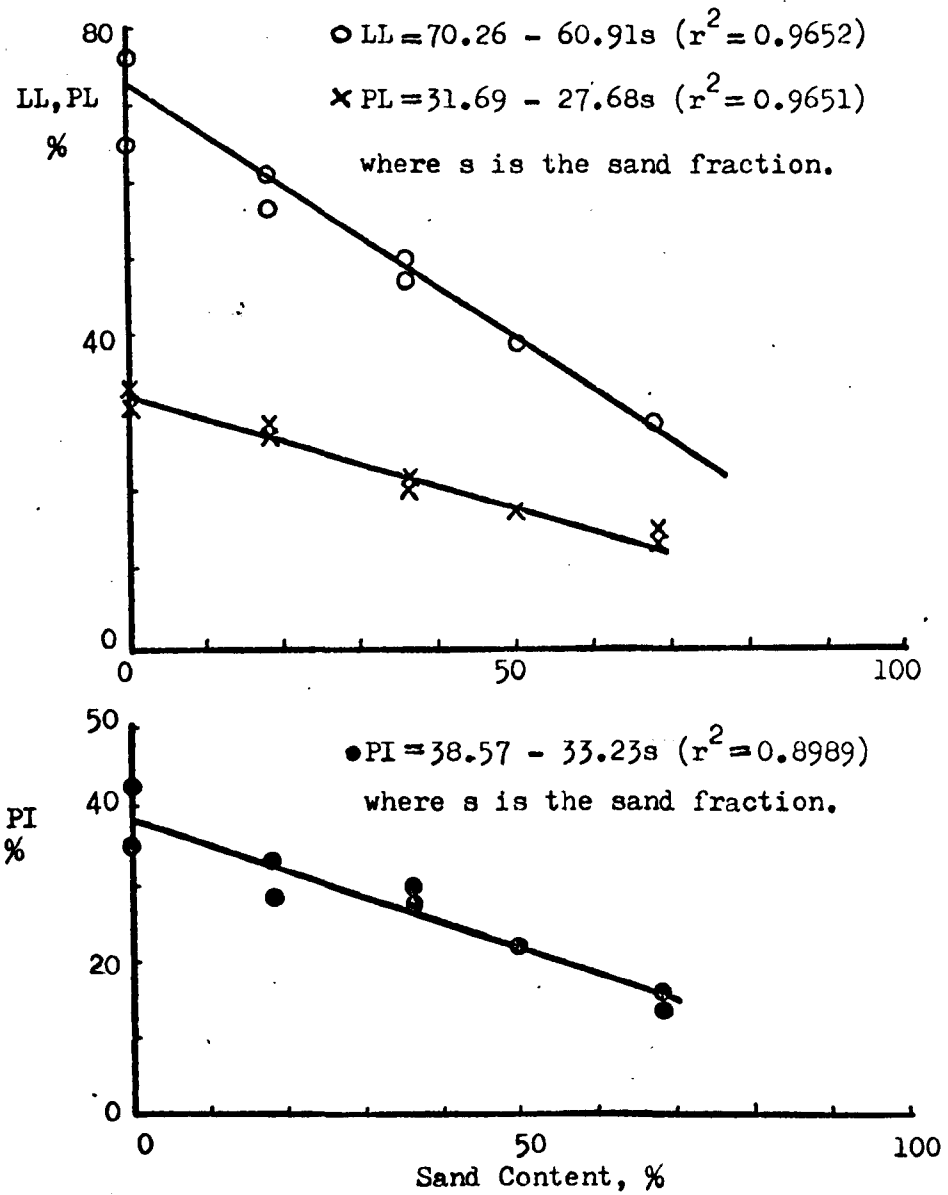


Fig. 5.2 Atterberg Limits VS Sand Content, Illite-Sand Mixtures.

$$\circ \quad LL = 72.59 + 120.74 C_b \quad (r^2 = 0.9957)$$

$$\times \quad PL = 32.40 + 22.10 C_b \quad (r^2 = 0.9951)$$

$$\bullet \quad PI = 40.20 + 98.65 C_b \quad (r^2 = 0.9937)$$

where C_b is the fraction of Bentonite in the mixtures.

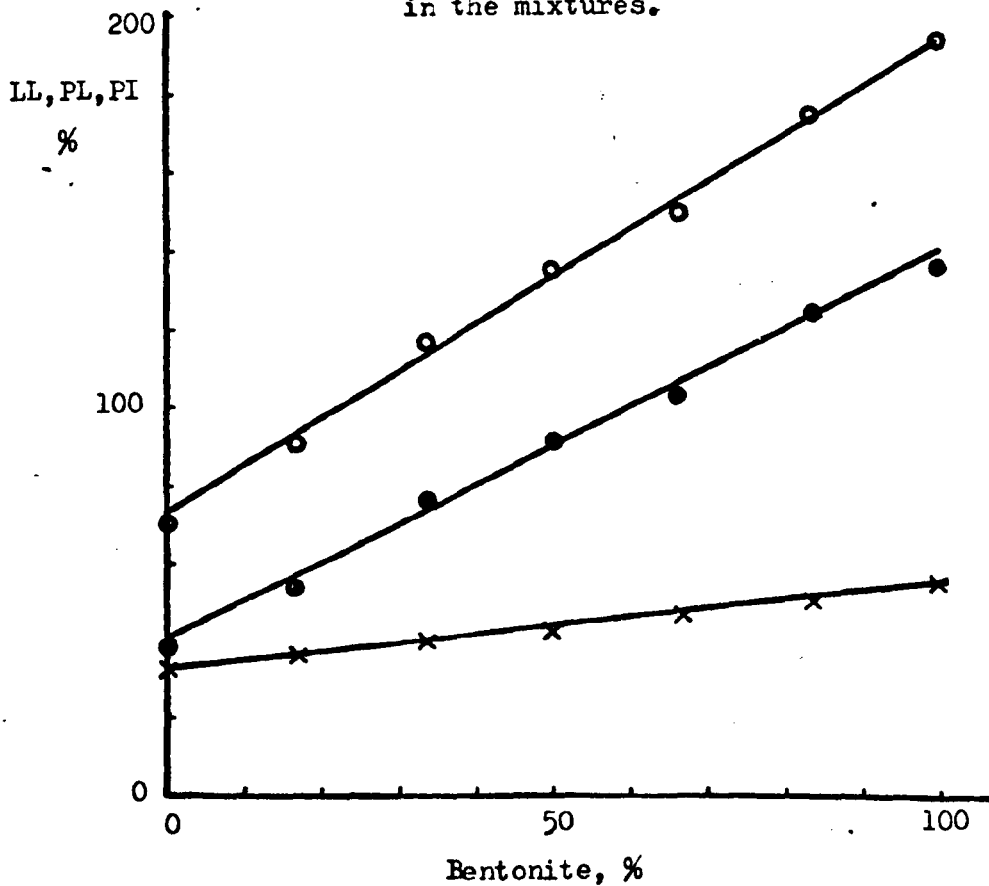


Fig.5.3 Atterberg Limits VS Bentonite Content, Bentonite-Illite Mixtures.

influence the limits of clay-sand mixtures other than as a diluent of the clay fraction, and the coarser particles themselves impose no rigidity on the mixture. However below about 30% clay content it is logical to conclude that there is a virtually continuous skeleton of granular particles, the bonding provided by the clay is negligible, and the mixtures are non-plastic. The compaction properties to be discussed below also followed different laws for high and low clay contents. The most accurate estimates of the dividing points between these two ranges were obtained for the maximum dry density results and were

bentonite - sand	83.3%	sand - 16.7%	clay
illite - sand	68.0%	sand - 32.0%	clay

Presumably different phenomena assumed importance in the high and low clay ranges.

With the above discussion in view a linear regression analysis has been made separately for each mixture, the regression being limited to about 70% sand content for clay-sand mixtures. The regression equations are reported in Figs. 5.1 to 5.3.

Novaris-Ferreria (1967) reported two distinctly separate zones of Atterberg limits for clay contents, C , greater than and less than 20.2%, respectively. He found that there were two activities, viz:-

$$A = 1.15 \text{ for } C < 20.2\%, \text{ and}$$

$$A = 0.70 \text{ for } C > 20.2\%.$$

Presumably, there was also a small transition zone around $C = 20.2\%$. However, his main conclusion was that Skempton's activity, A , of the soil will not be constant. Attention

should therefore be paid to activity here. The points in Figs. 5.4 to 5.6 show the activity plotted against composition for the three mixtures. It is apparent that activity is not constant for a given clay mineral and varies with sand content. If the linear relationships obtained from the regression analysis for plasticity index in the present study are accepted, it will be found that the variation of activity with clay content is hyperbolic, since $S = 1 - C$ and $A = PI/C$. The hyperbolic terms for activity are derived from the constant terms in the regression equations for plasticity index. These constant terms may be the results of small experimental errors in the determination of the liquid and plastic limits. The two hyperbolic curves derived in this way are drawn in Figs. 5.4 and 5.5. Whilst these curves do not resolve the question of whether the hyperbolic terms do result from errors, they do reinforce the more important conclusion that activity varies with sand content. In Fig. 5.6, the activity values of the bentonite-illite mixtures show a weakly non-linear relationship, presumably because there is a slight interaction between the clay minerals.

The plasticity index is plotted against liquid limit in Fig. 5.7 for the three mixtures. All the clays fall above and close to Casagrande's A-line. The two soils in the CI group did show moderate swelling and cannot be rejected as non-swelling soils. The one in the CL group was virtually non-swelling. (The data is tabulated in Table 3.3).

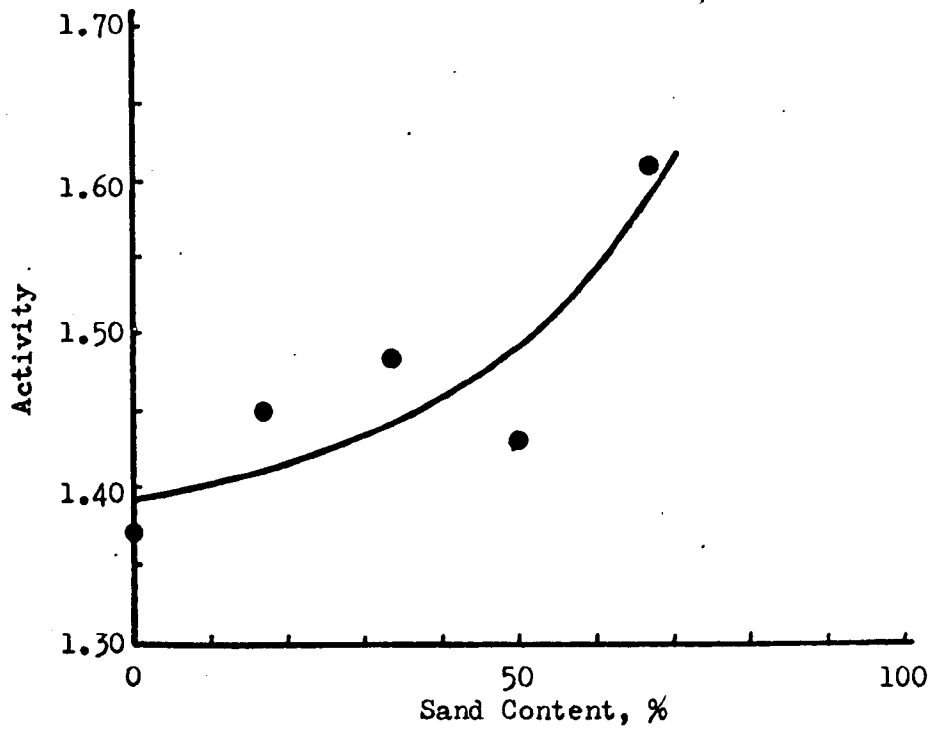


Fig.5.4 Activity VS Sand Content, Bentonite-Sand Mixtures.

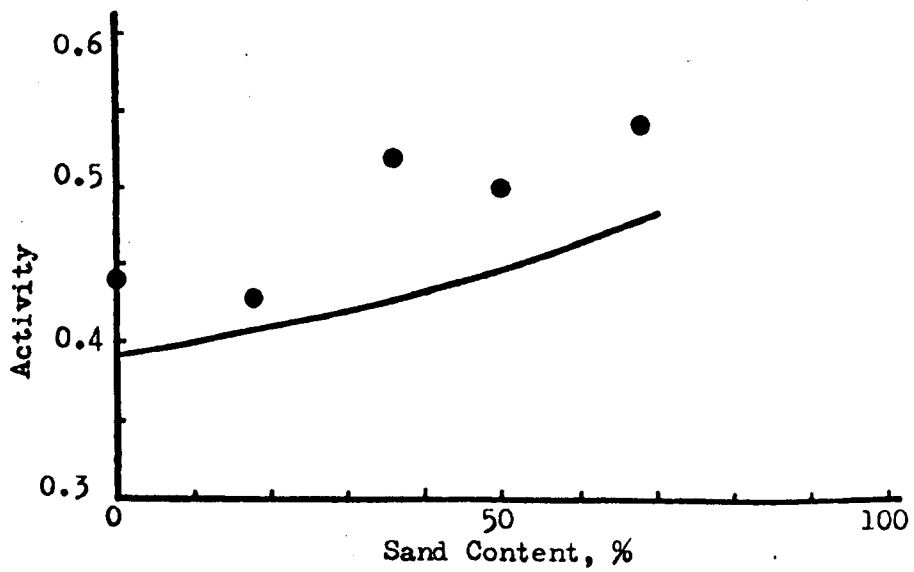


Fig.5.5 Activity VS Sand Content, Illite-Sand Mixtures.

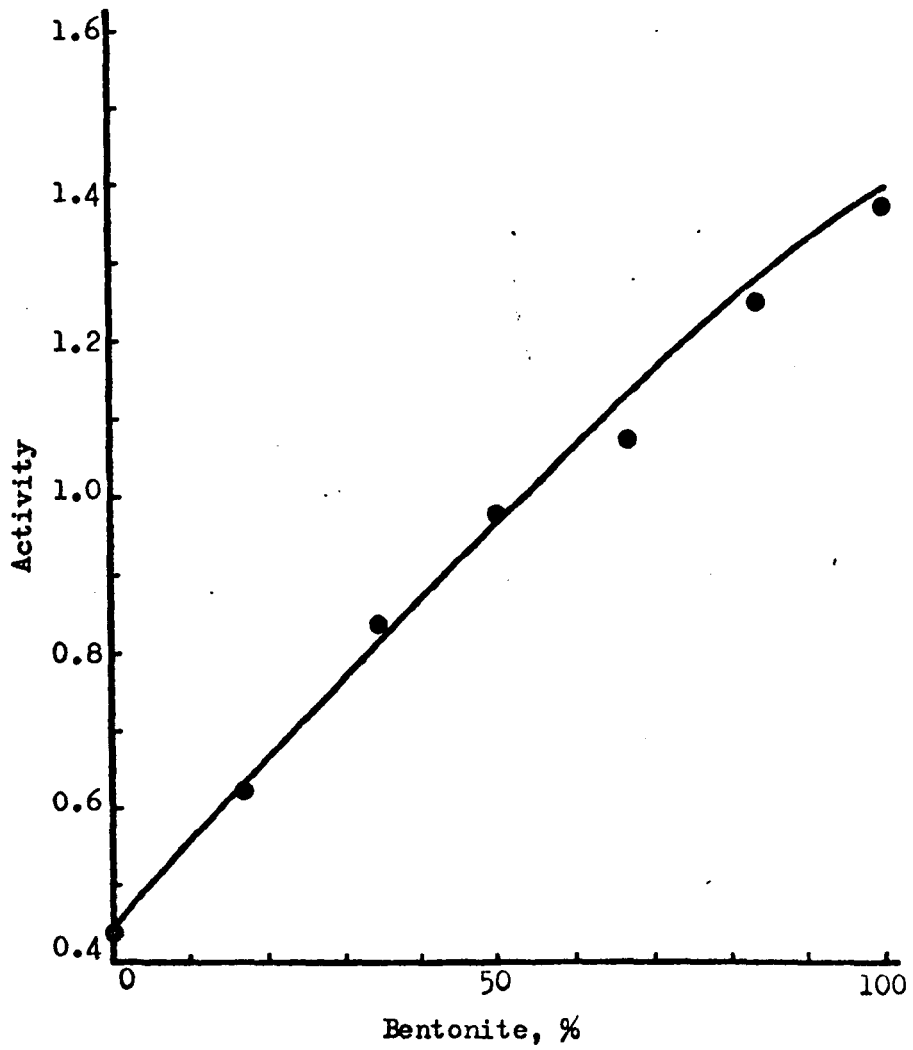


Fig.5.6 Activity VS Bentonite Content, Bentonite-Illite Mixtures.

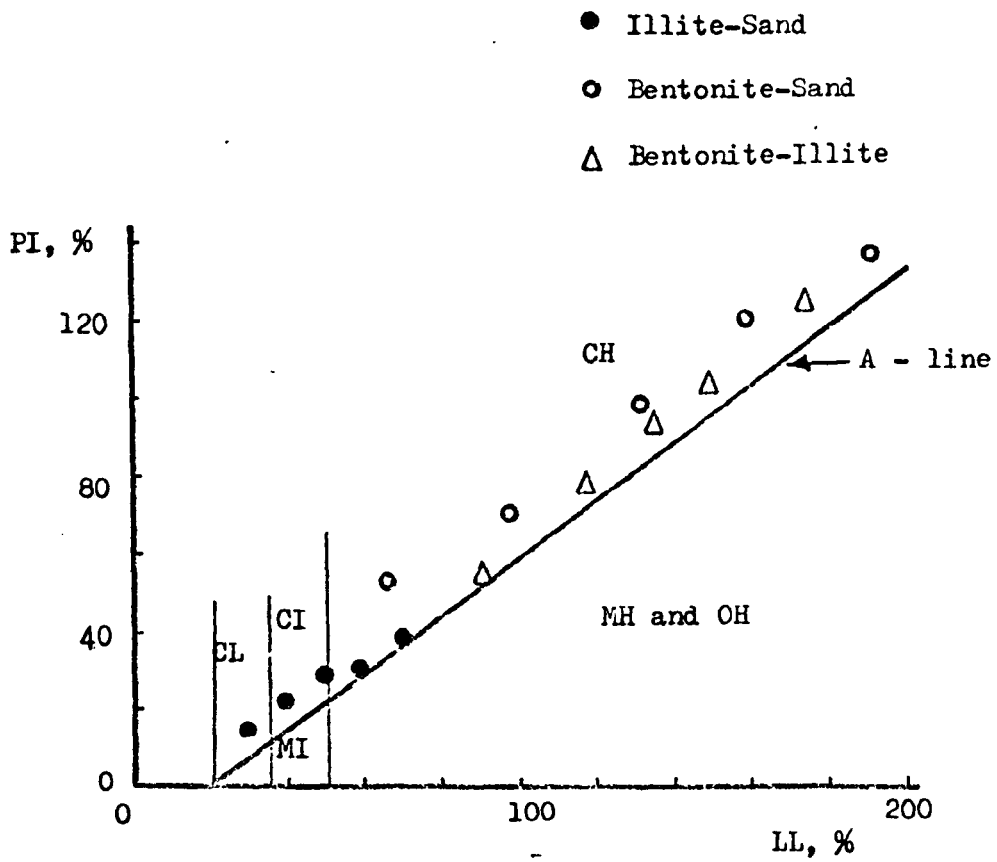


Fig.5.7 Casagrande's Classification Chart,
Artificial Mixtures.

5.3 COMPACTION AND SWELL PROPERTIES

5.3.1 Introduction

The results of compaction and swell tests on the three mixtures chosen for this study are reported in Chapter 3, see Tables 3.3 to 3.5. These results are now analysed mixture by mixture in the following sections. In the regression equations mentioned on Figs. 5.8 to 5.25, the composition in the right hand side of the equation is expressed as a fraction.

5.3.2 Bentonite - Sand Mixtures

Fig. 5.8 shows the optimum moisture content plotted against sand content by weight. The quadratic regression shown was better than a linear one presumably for empirical reasons, section 4.3.3. Fig. 5.9 shows the maximum dry density, γ_d , plotted against sand content by weight. The relationship is linear up to 83.3% sand content. Fig. 5.10 shows the initial volumetric water content, \mathcal{W}_i , (i.e. the moisture content expressed as volume of water/volume of solids) at optimum conditions before swell is permitted. This relationship is approximately linear. Fig. 5.11 shows the initial voids ratio, e_i , which is approximately linear up to 80% sand content, between 80% - 100% sand content there is extra air present in the samples. Fig. 5.10 and 5.11 are plotted against sand content by volume.

Fig. 5.12 shows the swell pressure against sand content by volume, i.e. volume of sand solids/volume of total solids, since this is the appropriate basis for non-empirical use of Eqn. 4.29, section 4.3.3.

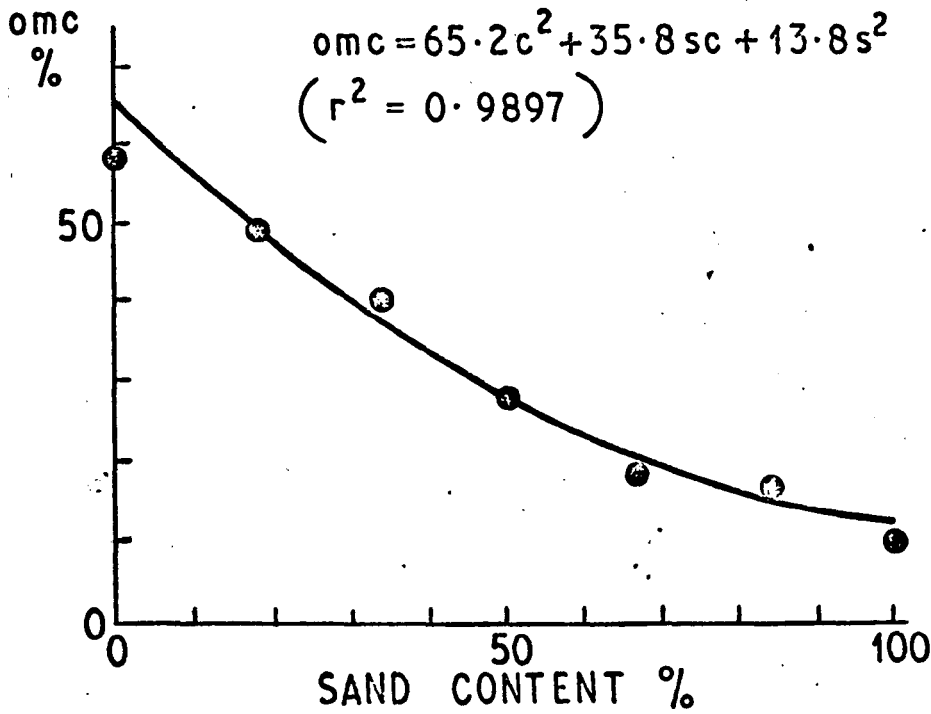


Fig.5.8 Optimum moisture content VS sand content by weight, Bentonite - Sand Mixtures.

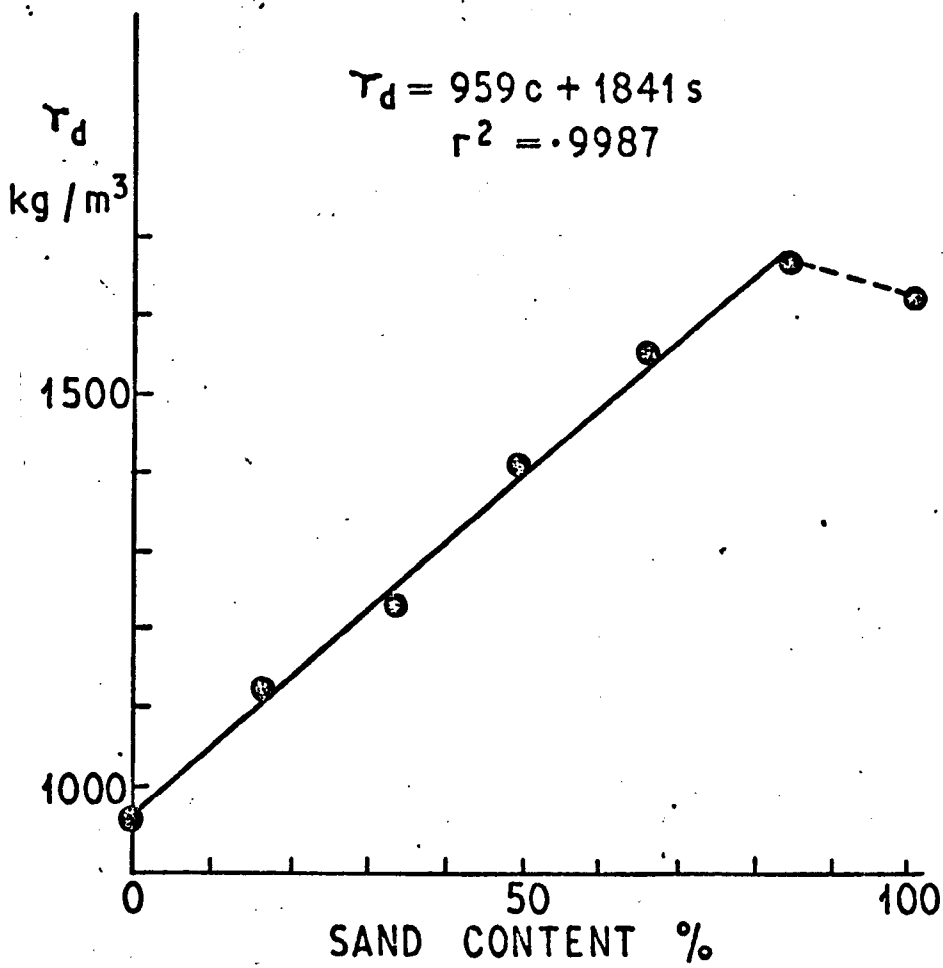


Fig. 5.9 Maximum dry density VS sand content by weight, Bentonite-Sand Mixtures.

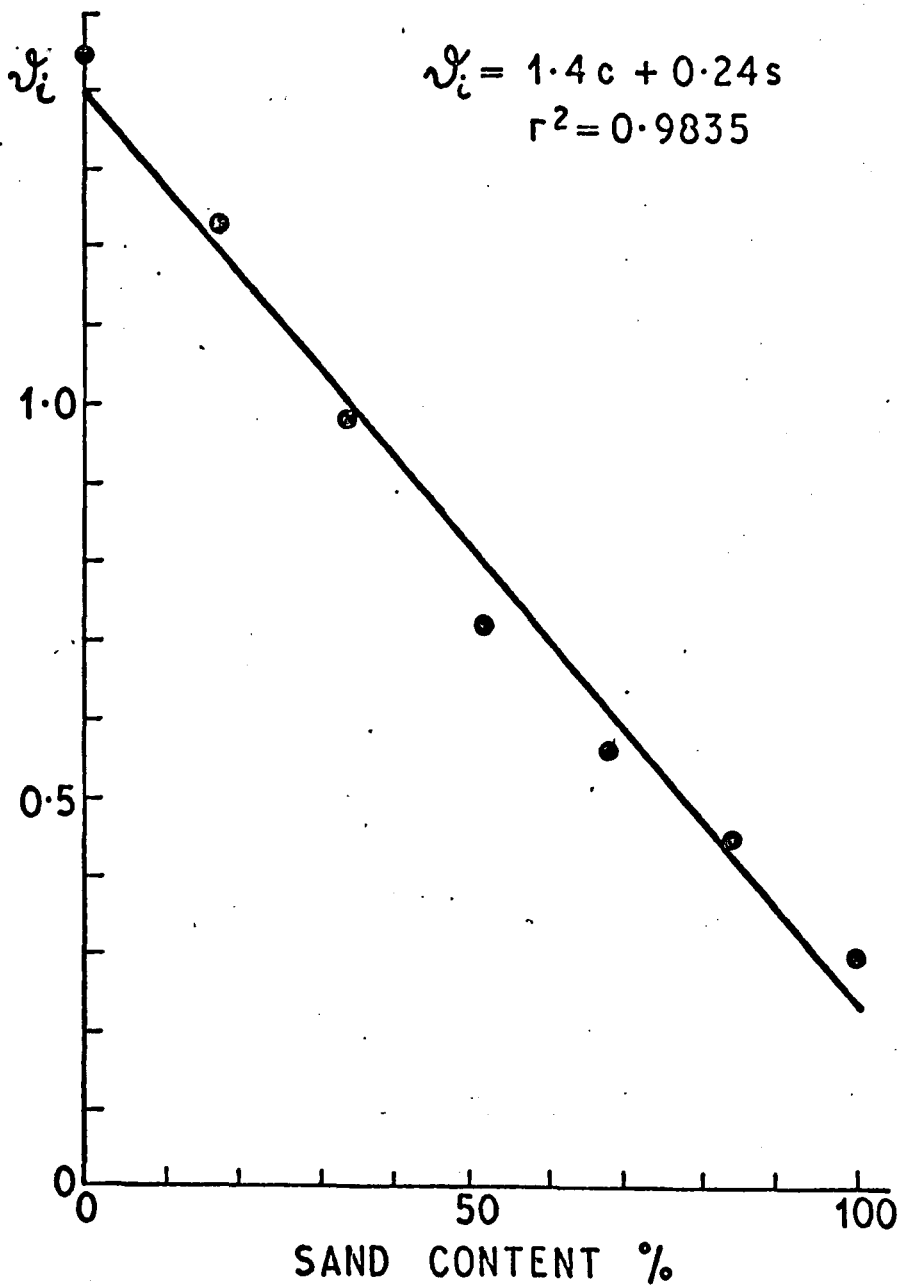


Fig.5.10 Initial volumetric water content VS sand content by volume, Bentonite - Sand Mixtures.

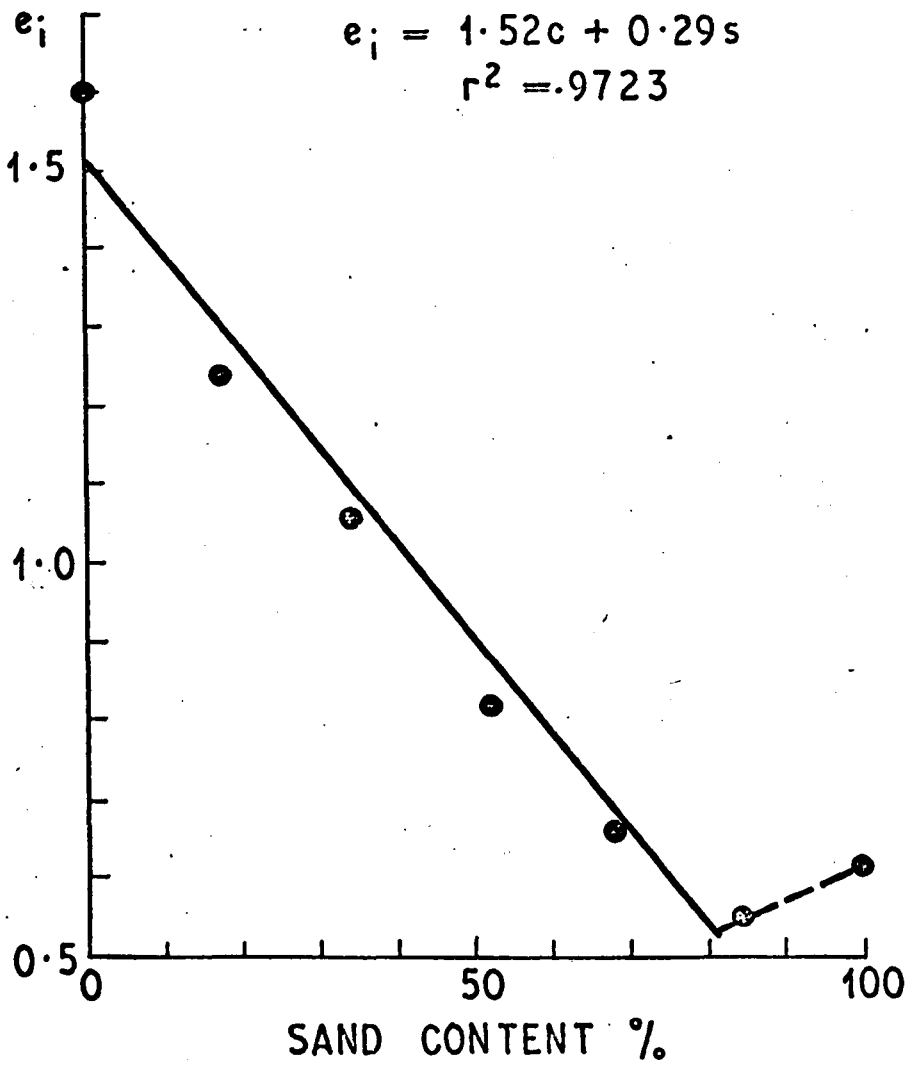


Fig.5.11 Initial voids ratio VS sand content by volume,
Bentonite - Sand Mixtures.

$$P_c = 41.6c^2 + 72.3sc + 0.3s^2$$

$$r^2 = 0.9993$$

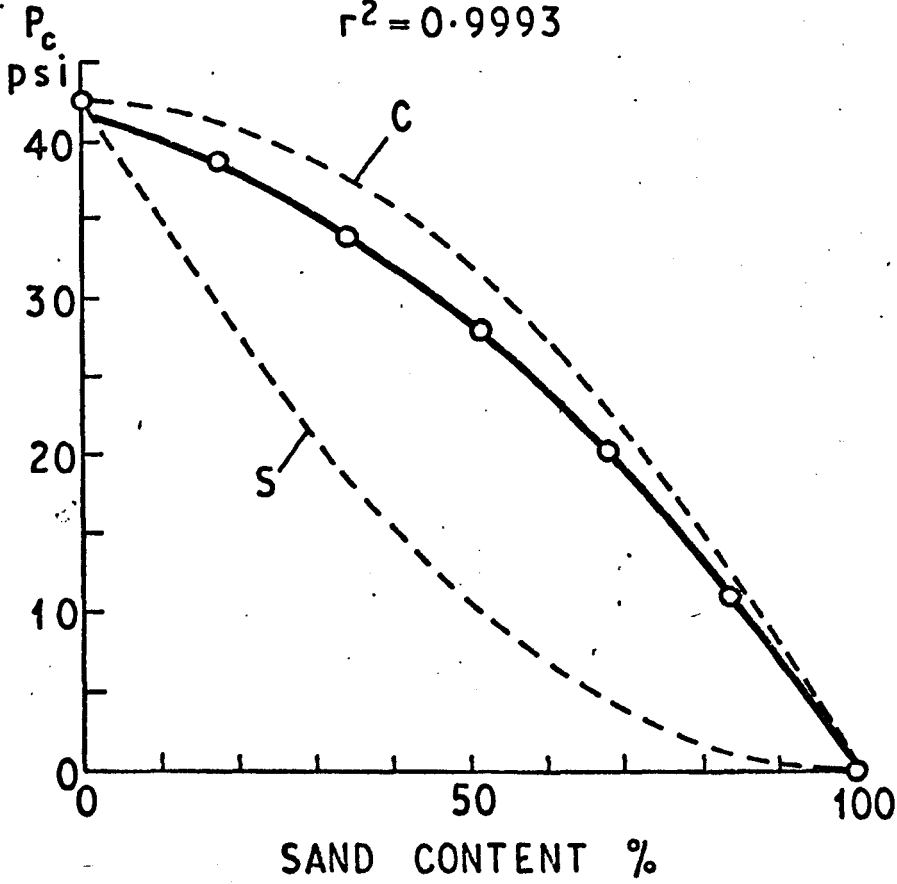


Fig.5.12 Swell Pressure VS sand content by volume,
Bentonite - Sand Mixtures.

The full line is calculated from Eqn. 4.29, the exact form being shown on the diagram. It does give a close fit to the (observed) data. The clay and sand bounds, C and S, from Eqns. 4.32 and 4.33 are also shown by broken lines. The closeness of the data to the clay bound, C, suggests that the swell pressure behaviour is dominated by the bentonite throughout the whole range. The expansions of the samples in the swell pressure tests were estimated, see Table 5.1, making use of the final water content measured after the test and assuming that the sample is fully saturated after the swell pressure test. The initial and final volumetric air void contents, i.e. volume of air/ volume of solids, α_i and α_f , are also shown in Table 5.1. These were obtained by subtracting volumetric water contents from initial void ratio. The quantities α_f , which should not be negative, and expansion, which should be zero, give some indication of the magnitudes of the errors involved in the quantities in Table 5.1, although α_f and expansion are themselves subject to error, as both α_i and α_f were calculated as the differences of two large quantities. The method of calculation is in Appendix 9. Thus the values for expansion arise from three sources: (1) errors of calculation, (2) errors of measurement, e.g. of specific gravity, (3) actual expansion of the samples. It seems from Table 5.1 that the estimate of the actual expansion, which was made in Appendix 1, was a little low, as was stated in Chapter 2.

Table 5.1 Bentonite - Sand: Laterally Confined Swell Pressure Tests

All quantities are referred to the volume of Solids, except Expansion which is referred to the original volume.

Clay %	\mathcal{D}_i %	α_i %	e_i %	P_c psi	\mathcal{D}_f %	α_f %	Expansion %
100.0	151	9	160	42.8	166	-6*	2.3
82.6	123	2	125	38.8	127	-3*	1.5
65.4	98	8	106	33.7	109	-4*	1.8
48.4	71	11	82	28.0	81	1	0.0
32.0	52	14	66	20.6	58	8	0.0
15.9	44	11	55	11.2	50	6	0.0
00.0	33	28	61	-	-	-	-

* Experimental Error.

Fig. 5.13 shows the swell potential plotted against sand content by weight. The relationship is quadratic presumably for empirical reasons. In order to explain the swell potential behaviour, all the data was reduced to a volumetric basis by reference to the volume of solids, since swell potential is volumetric expansion. This reduced data is presented in Fig. 5.14 and shows the swell amount (i.e. volume of swell/volume of solids) calculated from the swell potential test, plotted against sand content by volume. The relationship is linear throughout, and within a very small error falls to zero swell at zero clay content. Fig. 5.15 shows the water uptake, DW, i.e. the change in volumetric water content during the swell potential tests. The relationship is virtually the same as for the swell amount shown in Fig. 5.14. Fig. 5.16 shows the swell amount against water uptake. The points all lie close to the 1:1 line. Table 5.2 shows the data on a volumetric basis. The initial and final values of the volumetric air content, α_i and α_f , were obtained by subtracting volumetric water contents from void ratios, and they are therefore subject to experimental error. The values of α_i and α_f obtained suggest that as a first approximation changes of air content may be ignored. This is reasonable since the samples are submerged throughout the swell potential test. On this basis, from Figs. 5.14 and 5.15 it is possible to write:

$$\text{Water uptake, DW} = KC \quad \dots (5.1)$$

$$\text{Swell amount, } S_{cs} = DW \quad \dots (5.2)$$

$$S_c = 80c^2 + 128sc + 1.5s^2$$
$$r^2 = 0.9958$$

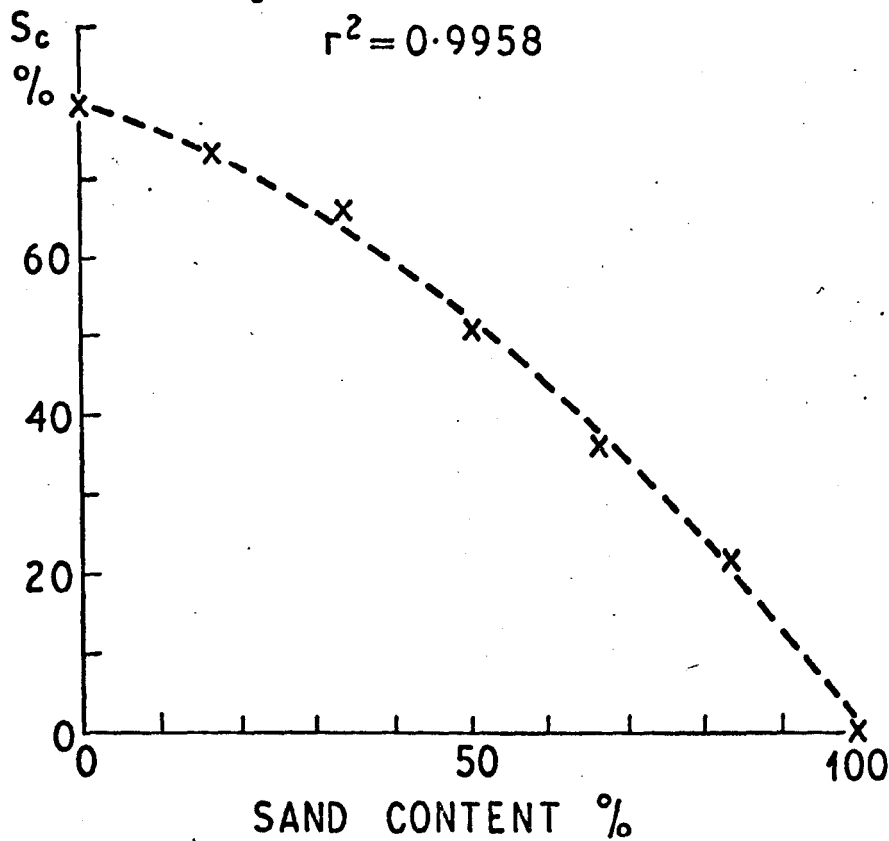


Fig.5.13 Swell Potential VS sand content by weight,
Bentonite - Sand Mixtures.

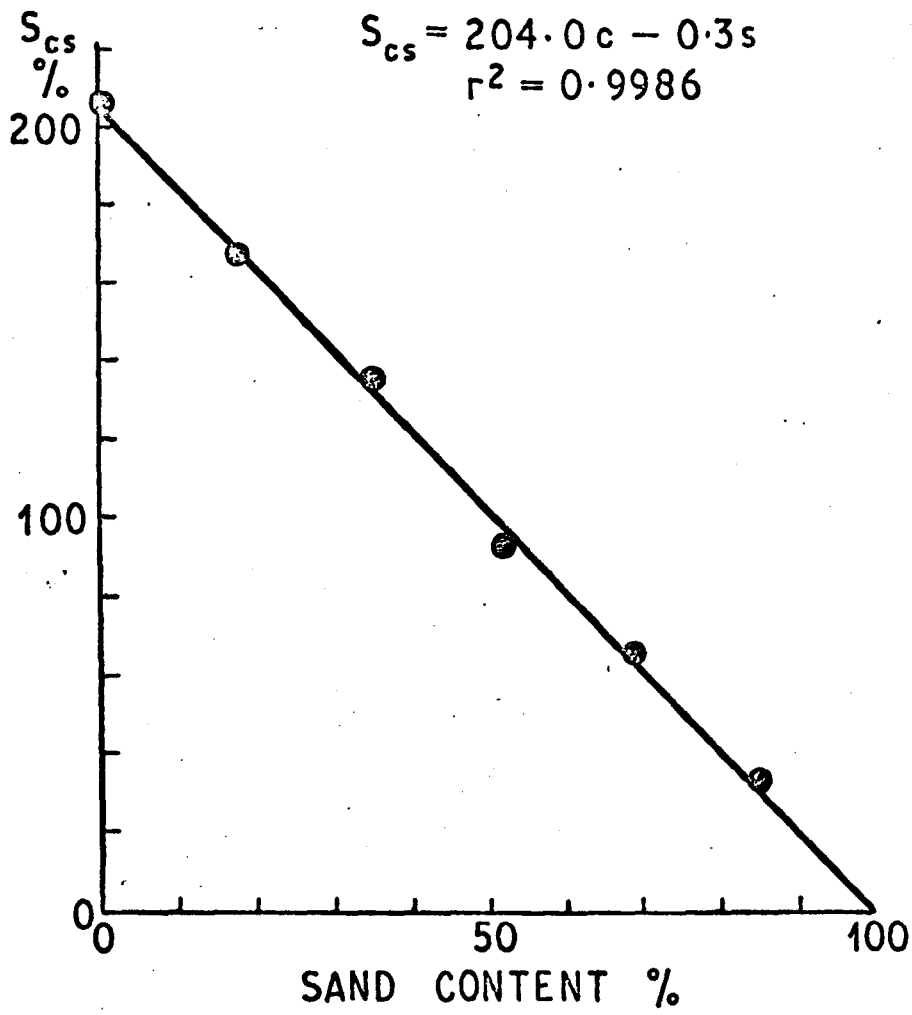


Fig.5.14 Swell amount VS sand content by volume,
Bentonite - Sand Mixtures.

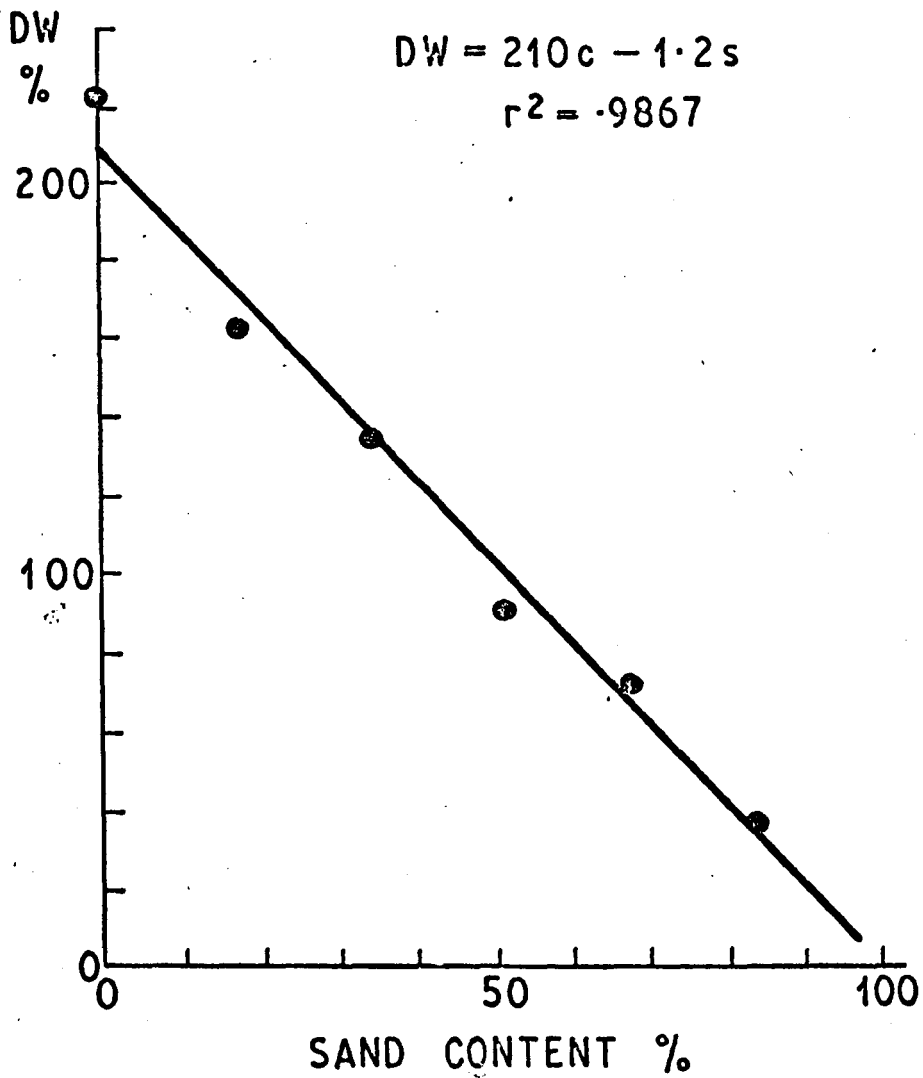


Fig.5.15 Water Uptake VS sand content by volume,
Bentonite - Sand Mixtures.

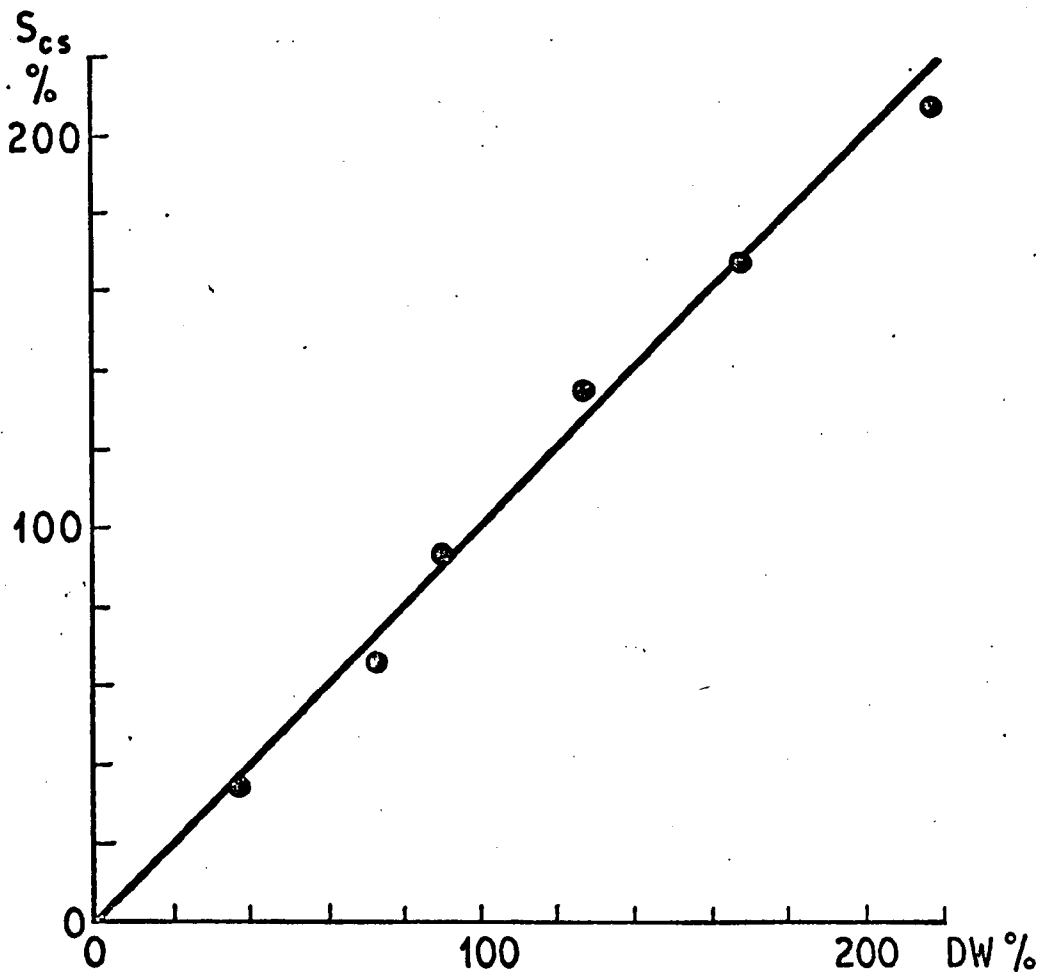


Fig.5.16 Swell amount VS water uptake, Bentonite - Sand Mixtures.

Table 5.2 Bentonite - Sand: Laterally Confined Swell Potential Tests

All quantities are referred to the volume of Solids

Clay %	\mathcal{V}_i %	α_i %	e_i %	S_{cs} %	\mathcal{V}_f %	α_f %	e_f %
100.0	151	9	160	207	369	-2*	367
82.6	123	2	125	167	290	2	292
65.4	98	8	106	134	233	7	240
48.4	71	11	82	93	162	13	175
32.0	52	14	66	66	124	8	132
15.9	44	11	55	35	81	9	90
00.0	33	28	61	-	-	-	-

* Experimental Error

where, $K = 2.10 = \text{constant}$

whence $S_{cs} = 2.10 C.$

where $C = \text{clay content expressed volumetrically.}$

5.3.3 Illite - Sand Mixtures

The specific gravities of illite and sand were approximately equal, so the proportions by weight were also taken as proportions by volume.

Figs. 5.17 to 5.20 show for illite-sand the properties presented in Figs. 5.8 to 5.11 for bentonite-sand. The maximum dry density, Fig. 5.18, followed a quadratic curve up to about 68% sand content, and it is thought that different phenomena act below and above about 68% sand content, section 5.2. This observation helps in the interpretation of Fig. 5.17. The optimum moisture content, Fig. 5.17, could be fitted in three ways of increasing accuracy.

- (1) Throughout the whole range by a quadratic curve, concave upwards, as a rough approximation.
- (2) Up to 86% sand, by a linear relationship, which was better than (1).
- (3) Up to 68% sand, close agreement was obtained with a quadratic curve, concave downwards.

Whilst the first two methods may be useful for some purposes, on the assumption that different phenomena act below and above about 68% sand content, the third method is more correct. Only the third method is illustrated in Fig. 5.17. The volumetric version of Fig. 5.17, i.e. Fig. 5.19, also shows close agreement with a quadratic curve up to 68% sand content, presumably because of a weak interaction between the components

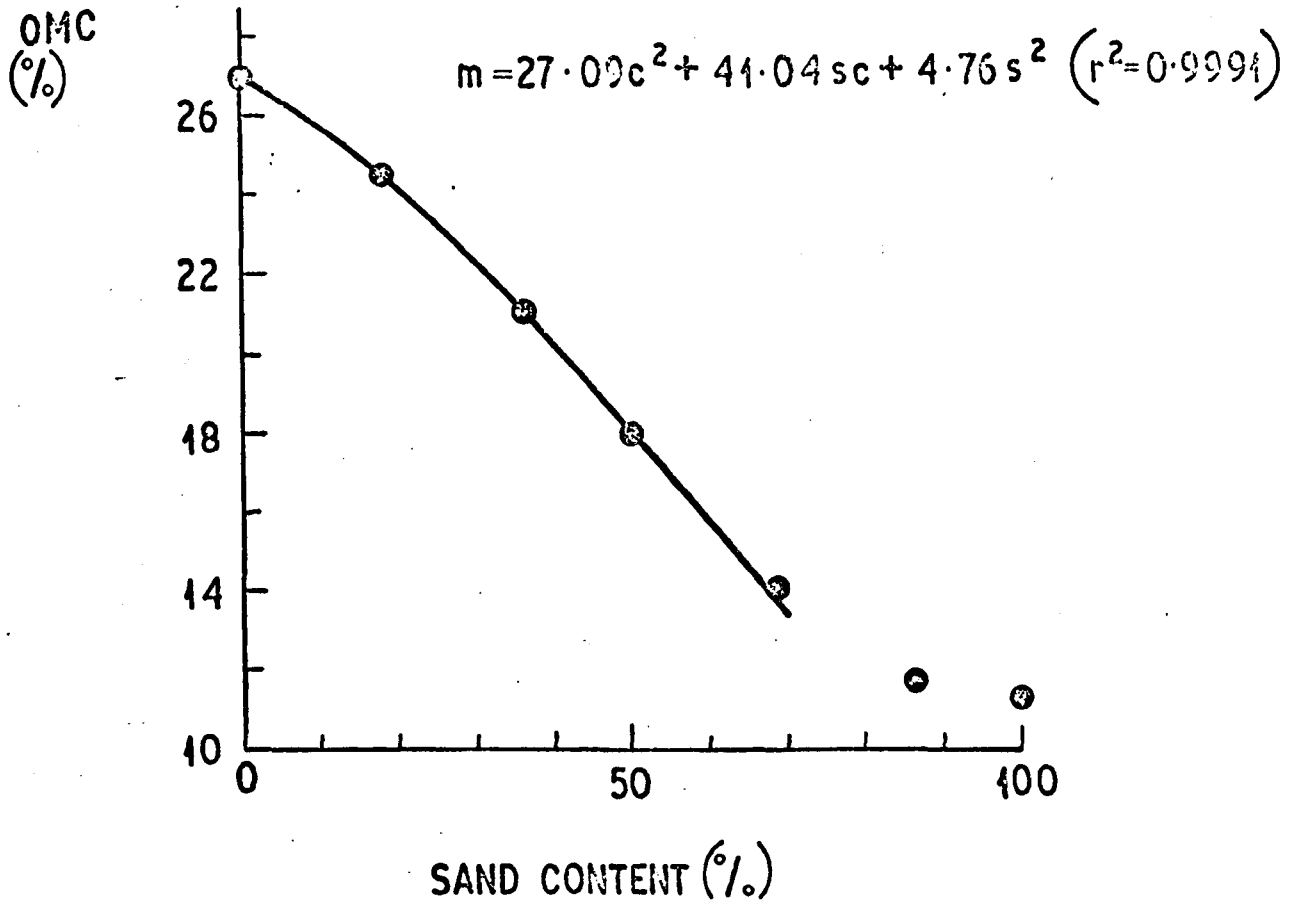


Fig.5.17 Optimum moisture content VS sand content,
Illite - Sand Mixtures.

$$\gamma_d(\max) = 15080C^2 + 32365C + 20395$$

$$(r^2 = 0.9861)$$

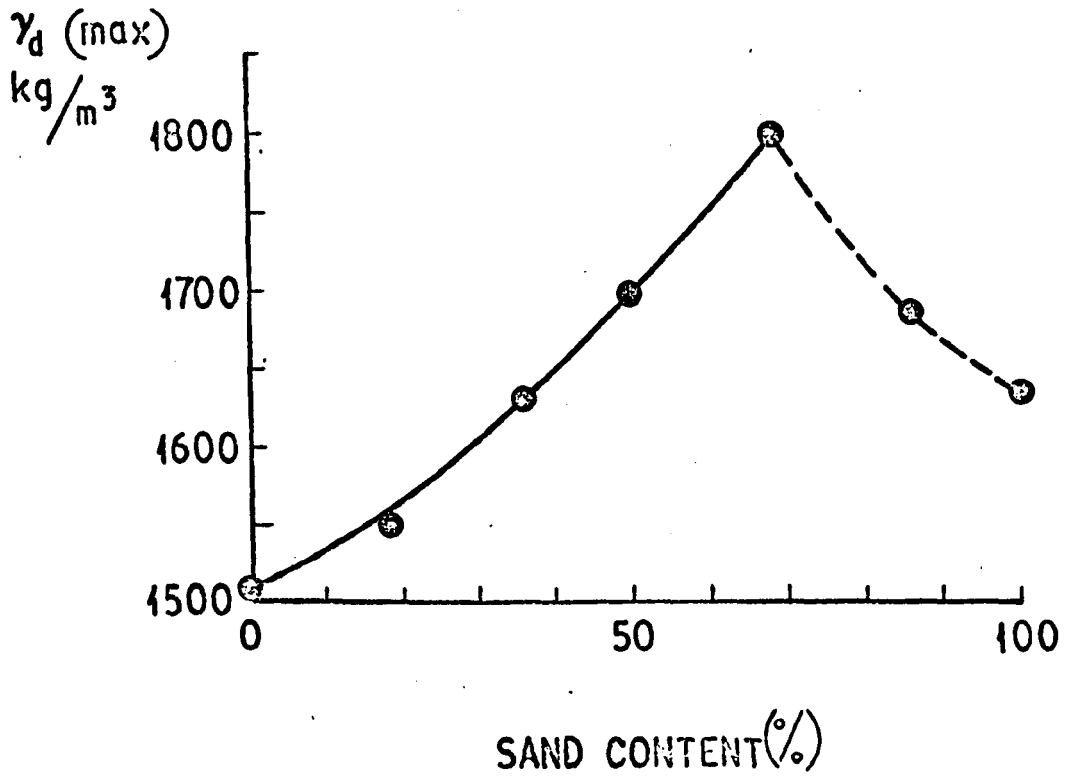


Fig.5.18 Maximum dry density VS sand content,
Illite - Sand Mixtures.

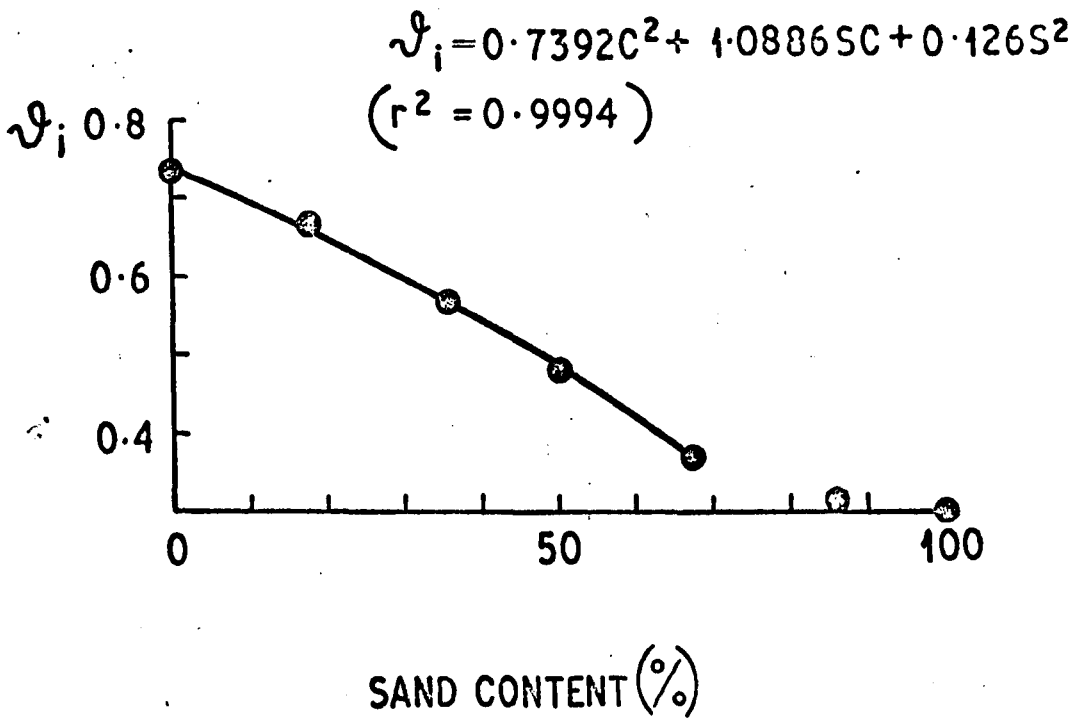


Fig.5.19 Initial volumetric water content VS sand content, Illite - Sand Mixtures.

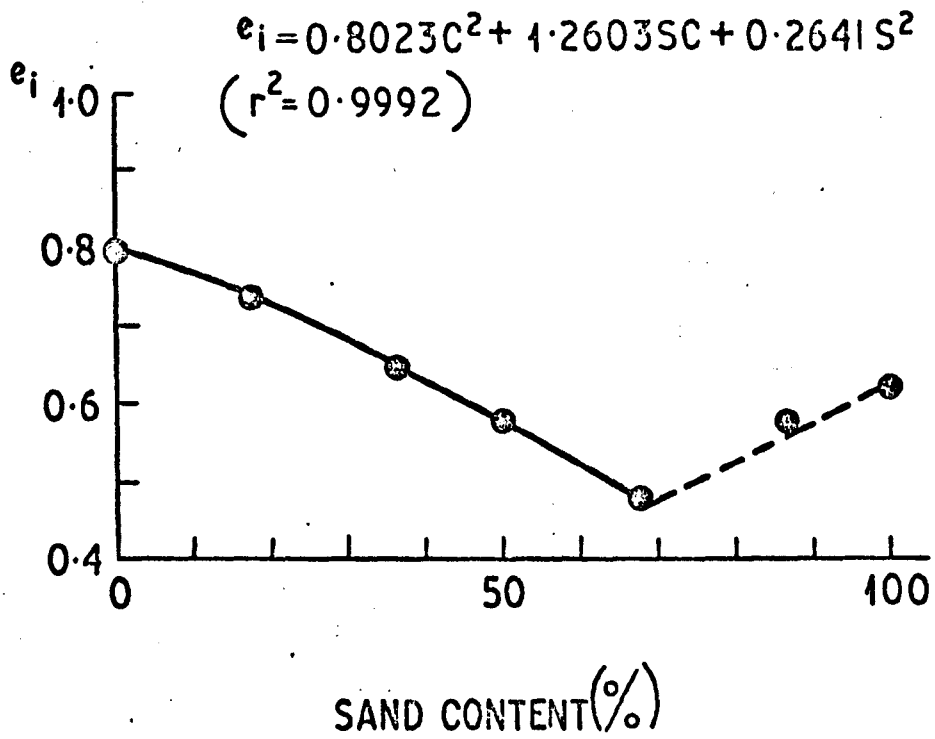


Fig. 5.20 Initial voids ratio VS sand content,
Illite - Sand Mixtures.

which was not evident in Fig. 5.10 for bentonite. Similar behaviour is shown for the initial voids ratio in Fig. 5.20.

Fig. 5.21 shows the swell amount and the water uptake as functions of the sand content for the laterally confined tests. The water uptake followed a quadratic curve up to about 68% sand content, which may be expressed as:-

$$DW = 0.4224 - 0.4179S - 0.1882S^2 \quad \dots(5.3)$$

The tangent to Eqn. 5.3 was calculated at the point of zero sand content as:-

$$Y = 0.4224 - 0.4179S \quad \dots(5.4)$$

The tangent is shown in Fig. 5.21 and falls to 0.0045 at $S = 1$. This is remarkably close to zero. It is therefore assumed that as a first approximation the water uptake is proportional to the clay content:-

$$DW = 0.42C \quad \dots(5.5)$$

but a correction of approximately $0.19S^2$ seems to be required to account for the interaction between the sand and the clay:-

$$DW = 0.42C - 0.19S^2 \quad \dots(5.6)$$

The swell amount lay close to the water uptake throughout except that there seems to have been a slight decrease in air content. The swell amount is plotted against water uptake in Fig. 5.22. Neglecting the change in air content, the swelling behaviour of illite-sand samples differed from the bentonite-sand samples (reported in the preceding section) in that a negative interaction term was required when relating the water uptake to the clay content. The data is reduced to a volumetric basis in Table 5.3. The changes in air

$$DW = 0.4224 C^2 + 0.4270 SC - 0.1837 S^2 \quad (r^2 = .9935)$$

$$S_{cs} = 0.3830 C^2 + 0.4770 SC - 0.2350 S^2 \quad (r^2 = .9921)$$

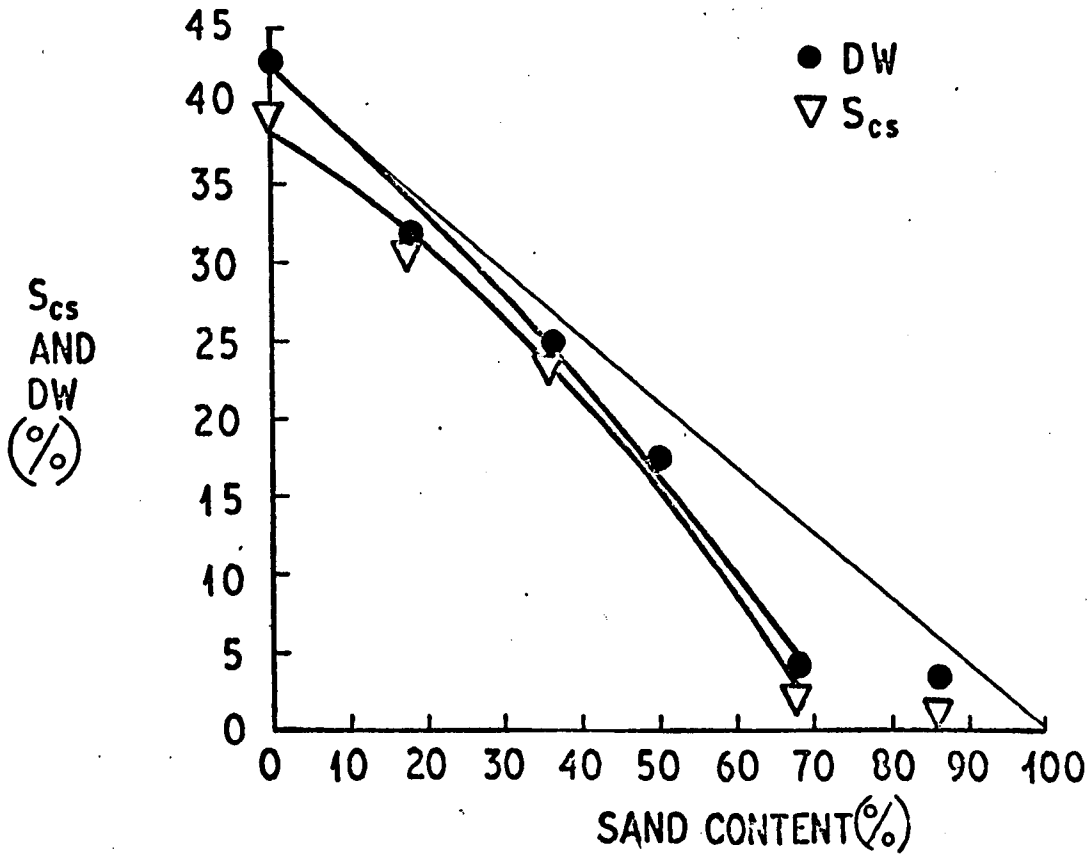


Fig.5.21 Swell amount and water uptake both VS sand content, Illite - Sand Mixtures.

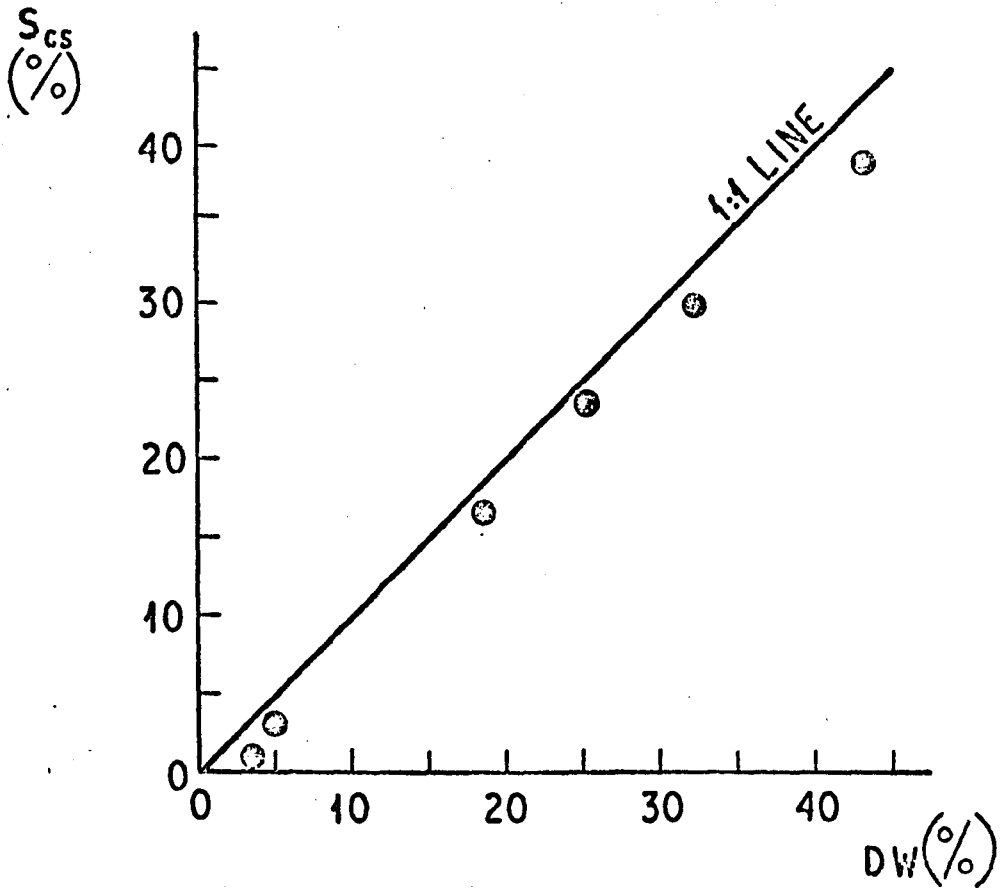


Fig.5.22. Swell amount VS water uptake,
Illite - Sand Mixtures.

Table 5.3 Illite - Sand: Laterally Confined Swell Potential Tests

All quantities are referred to the volume of Solids

Clay %	\mathcal{D}_i %	α_i %	e_i %	S_{cs} %	\mathcal{D}_f %	α_f %	e_f %
100.0	74	6	80	39	117	2	119
82.0	66	8	74	30	98	6	104
64.0	57	8	65	24	82	7	89
50.0	49	9	58	17	67	8	75
32.0	37	11	48	3	42	9	51
14.0	31	27	58	0.8	35	24	59
00.0	33	28	61	-	-	-	-

content are small and can be ignored during a swell potential test.

Figs. 5.23 and 5.24 show the laterally confined and isotropic swell pressures, both of which follow S-shaped curves according to Eqn. (4.35). This behaviour of these illite-sand samples differs from that of the bentonite-sand samples, which followed quadratic curves. The estimated volumetric expansion of the sample during swell pressure tests is shown in Tables 5.4 and 5.5, Table 5.4 referring to the laterally confined tests and 5.5 to the isotropic tests. These Tables support the comments for Table 5.1 regarding the expansion of the samples. They also show that the changes of air content are of only minor importance for illite-sand mixtures. In order to compare the isotropic to laterally confined swell pressures, their ratio is shown in Fig. 5.25. This is always less than unity presumably because the isotropic samples were free to change shape whilst kept at constant volume (within experimental error) whilst the laterally confined samples could change neither shape nor volume (within experimental error). The same result was found for natural soils, Table 3.6.

5.3.4 Bentonite - Illite Mixtures

In clay-clay mixtures such as the bentonite-illite mixtures studied here, it is reasonable to expect a linear mixing law, see section 4.3.2, ^{for any} given property of the soil over the entire range of composition. However, the main point of interest here is whether

$$P_c = 39.85 C^2 (3 - 2C)$$

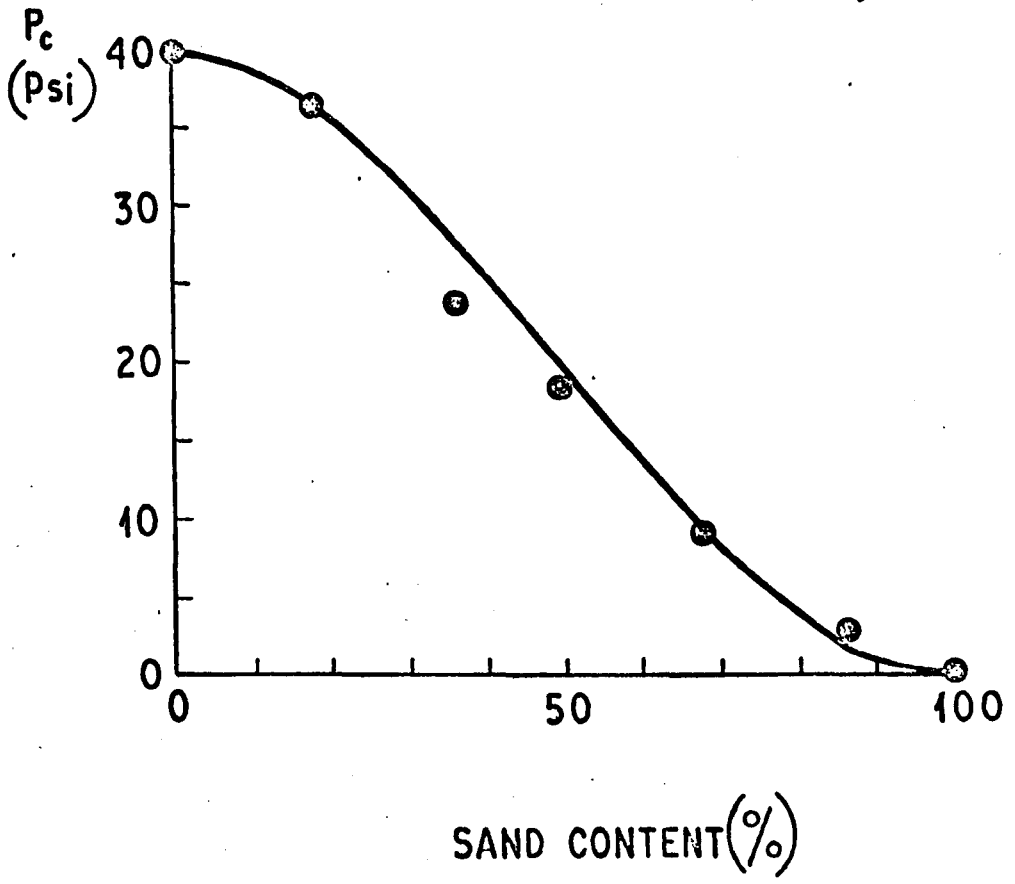


Fig. 5.23 Laterally Confined Swell Pressure VS Sand Content, Illite-Sand Mixtures.

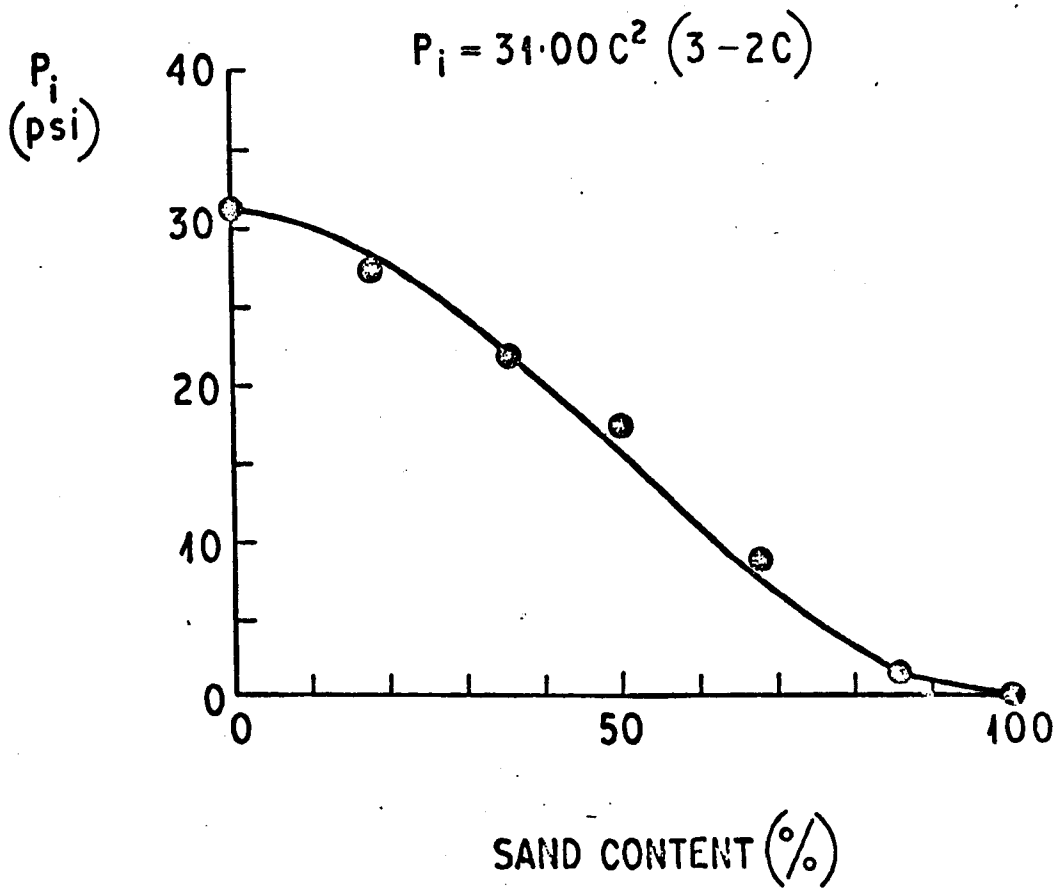


Fig.5.24 Isotropic swell pressure VS sand content,
Illite - Sand Mixtures.

Table 5.4 Illite - Sand: Isotropic Swell Pressure Tests

All quantities are referred to the volume of Solids, except Expansion which is referred to the original volume.

Clay %	\mathcal{V}_i %	α_i %	e_i %	P_i psi	\mathcal{V}_f %	α_f %	Expansion %
100.0	74	6	80	31.0	81	-1.5*	1.0
82.0	66	8	74	27.2	74	-0.7*	0.4
64.0	57	8	65	21.8	67	-2.0*	1.0
50.0	49	9	58	17.3	53	5.0	0.0
32.0	37	11	48	8.5	42	6.0	0.0
14.0	31	27	58	1.3	34	24.0	0.0
00.0	33	28	61	-	-	-	-

* Experimental Error

Table 5.5 Illite - Sand: Laterally Confined Swell Pressure Tests

All quantities are referred to the volume of Solids, except Expansion which is referred to the original volume.

Clay %	\mathcal{V}_i %	α_1 %	e_1 %	P_c psi	\mathcal{V}_f %	α_f %	Expansion %
100.0	74	6	80	39.8	82	-2*	1.4
82.0	66	8	74	36.6	75	-1*	0.9
64.0	57	8	65	23.6	66	-1*	0.9
50.0	49	9	58	18.7	58	0	0.0
32.0	37	11	48	9.2	41	7	0.0
14.0	31	27	58	3.5	34	24	0.0
00.0	33	28	61	-	-	-	-

* Experimental Error

$$\frac{P_i}{P_c} = 0.7618 + 0.2913S \quad (r^2 = 0.6650)$$

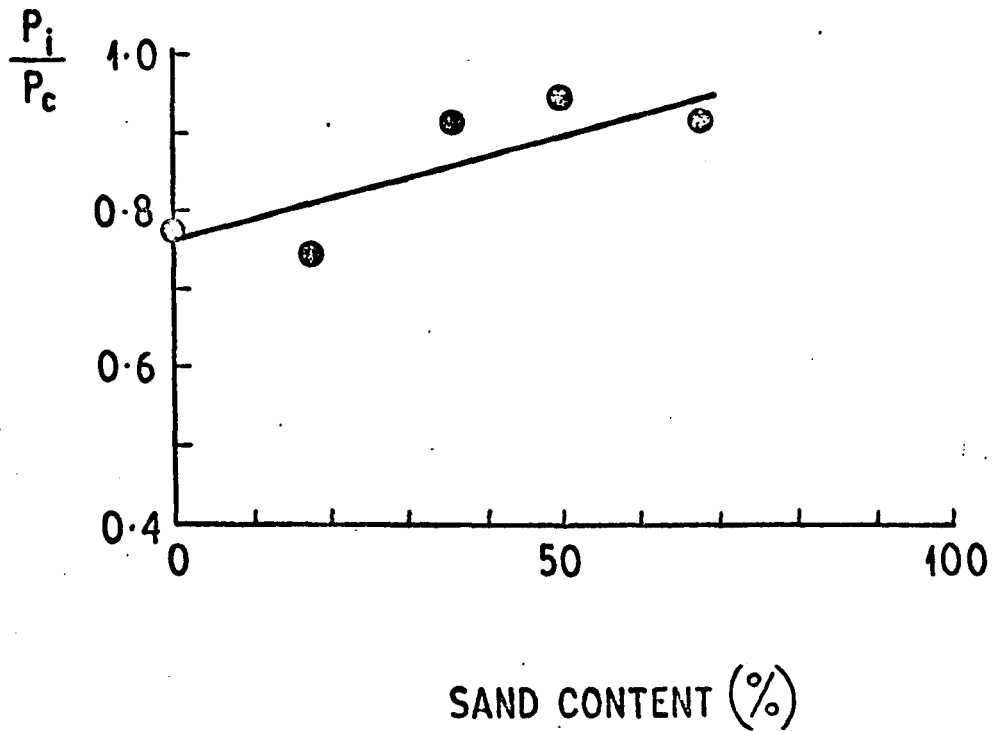


Fig. 5.25 Ratio of Isotropic to Laterally Confined Swell Pressure VS Sand Content, Illite - Sand Mixtures.

there is an interaction between the components leading to a non-linear relationship. Table 5.6 compares the linear and quadratic models for the results for the bentonite-illite mixtures. All the models in Table 5.6 are very highly significant. The most important comparison is for the initial volumetric water content, \mathcal{V}_i . Fig. 5.28 suggests that the quadratic model is the better; also r^2 is higher for the quadratic model. However, the improvement in r^2 might occur because the quadratic regression has one less degree of freedom from the linear regression. Thus, whilst it looks as if there may be a slight interaction between these two clays, it is not possible to be definite about it. The quadratic models are drawn in Figs. 5.26 to 5.31, and linear models in Fig. 5.32; these and Fig. 5.33 show the data of bentonite-illite mixtures.

5.3.5 Summary of Discussions on Artificial Mixtures

Many of the curves discussed above show two regions above and below approximately 80% sand content for bentonite and 68% sand content for illite, which is thought that in the samples in the higher ranges of sand content a continuous skeleton of granular particles is present.

The liquid limit and plastic limit of the mixtures were linearly related to the percentage clay content up to approximately 70% sand content in clay-sand mixtures, see Fig. 5.1 and 5.2; and over the full range in the clay-clay mixtures. Although other workers have found that Skempton's activity, A , is independent of the clay content and varies only with the type of clay mineral (Seed et al, 1964), it was found here that activity increases

Table 5.6 Linear and Quadratic Regression, Bentonite -
Illite Mixtures.

- Note:- 1. The term C_b in the table denotes the fraction of Bentonite in the mixture.
2. The value of correlation coefficient r^2 is mentioned in brackets after each regression equation.

Property	Linear Regression	Quadratic Regression
OMC	$25.57 - 22.14 C_b$ (.91)	$28.46 - 1.35 C_b - 20.79 C_b^2$ (.98)
γ_d	$1482 - 530 C_b$ (.99)	$1502 - 674 C_b - 144 C_b^2$ (.99)
P_c	$41.70 - 12.20 C_b$ (.91)	$39.9 - 25.19 C_b - 12.99 C_b^2$ (.996)
\mathcal{D}_i	$0.711 - 0.469 C_b$ (.92)	$0.763 - 0.097 C_b - 0.373 C_b^2$ (.97)
e_i	$0.802 - 0.739 C_b$ (.99)	$0.806 - 0.710 C_b - 0.03 C_b^2$ (.99)
S_c	$29.22 - 64.76 C_b$ (.978)	$21.53 - 106.32 C_b - 38.27 C_b^2$ (.996)
S_{cs}	$42.54 - 192.11 C_b$ (.99)	$37.60 - 227.83 C_b - 35.82 C_b^2$ (.99)
DW	$51.09 - 197.21 C_b$ (.99)	$41.73 - 262.97 C_b - 57.01 C_b^2$ (.99)

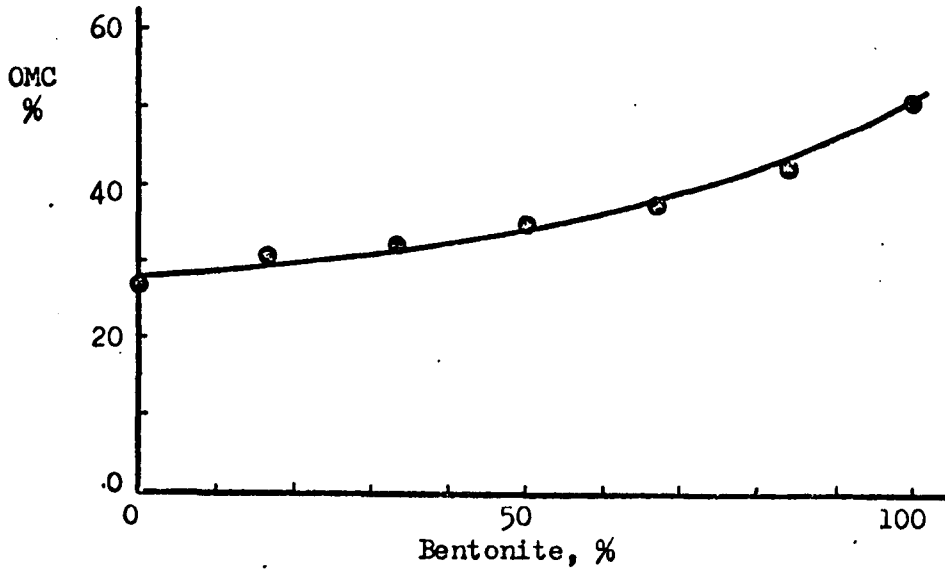


Fig. 5.26 Optimum Moisture Content VS Bentonite by Weight, Bentonite-Illite Mixtures.

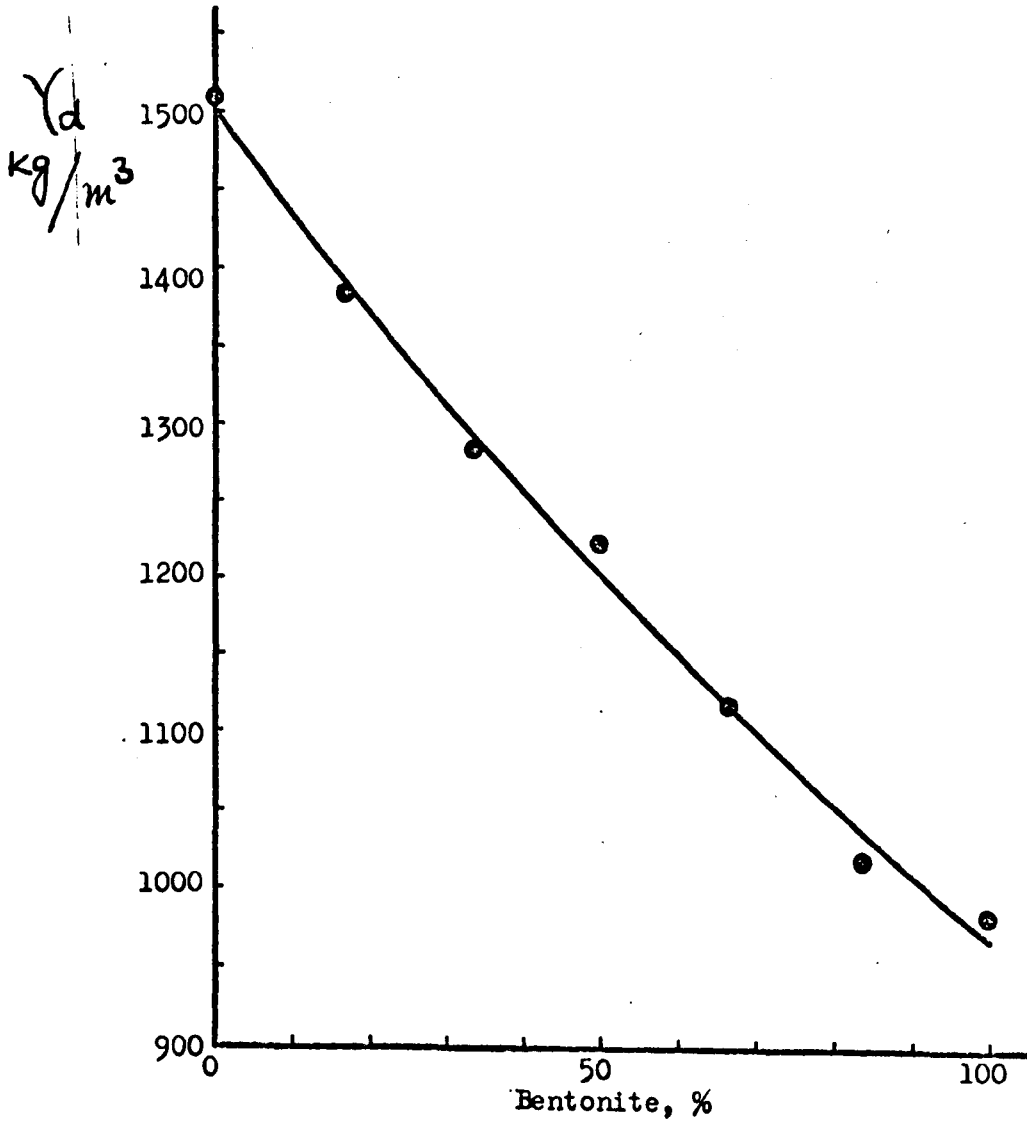


Fig. 5.27 Optimum Dry Density VS Bentonite by Weight, Bentonite-Illite Mixtures.

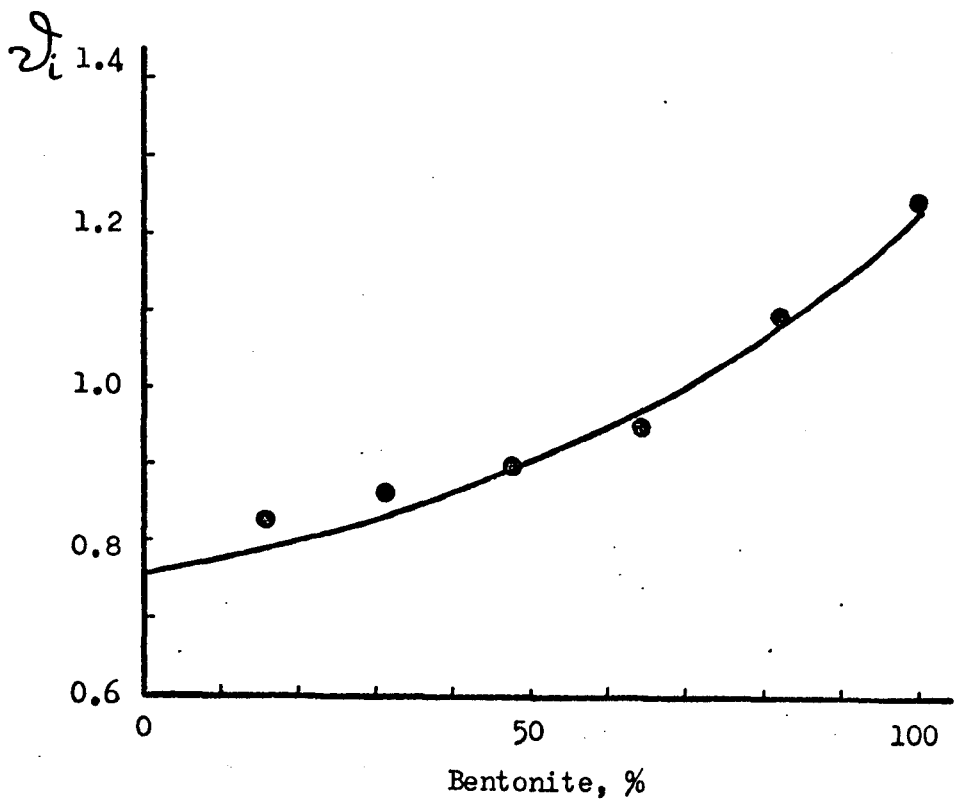


Fig. 5.28 Initial Volumetric Water Content VS Bentonite by Volume, Bentonite-Illite Mixtures.

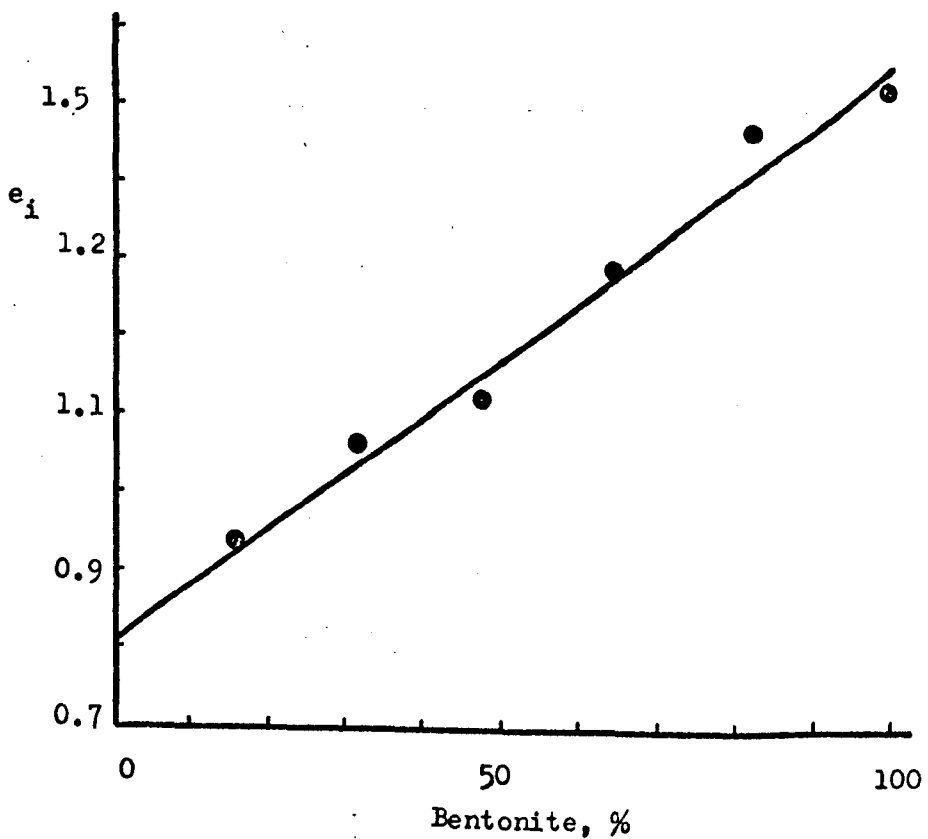


Fig. 5.29 Initial Voids Ratio VS Bentonite by Volume, Bentonite-Illite Mixtures.

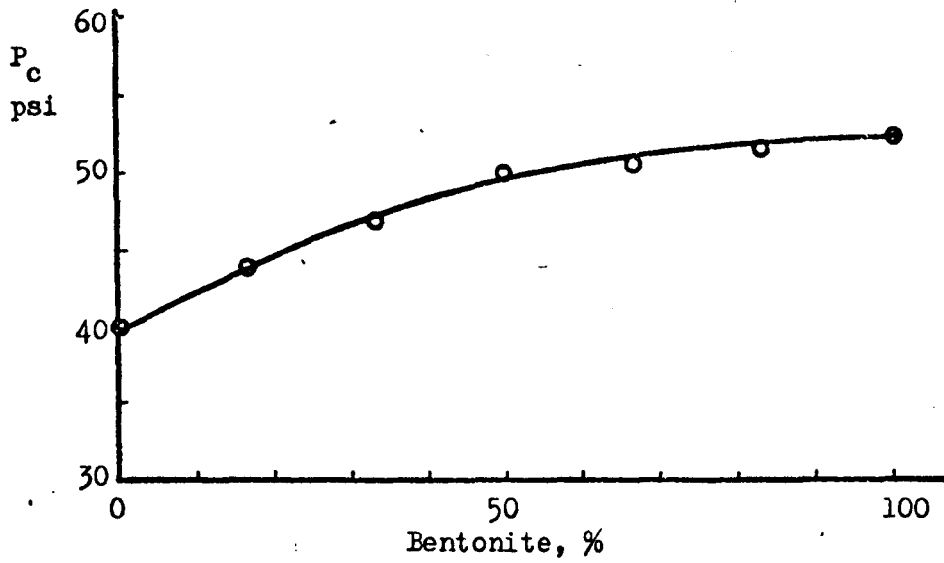


Fig.5.30 Laterally Confined Swell Pressure VS Bentonite by Weight, Bentonite-Illite Mixtures.

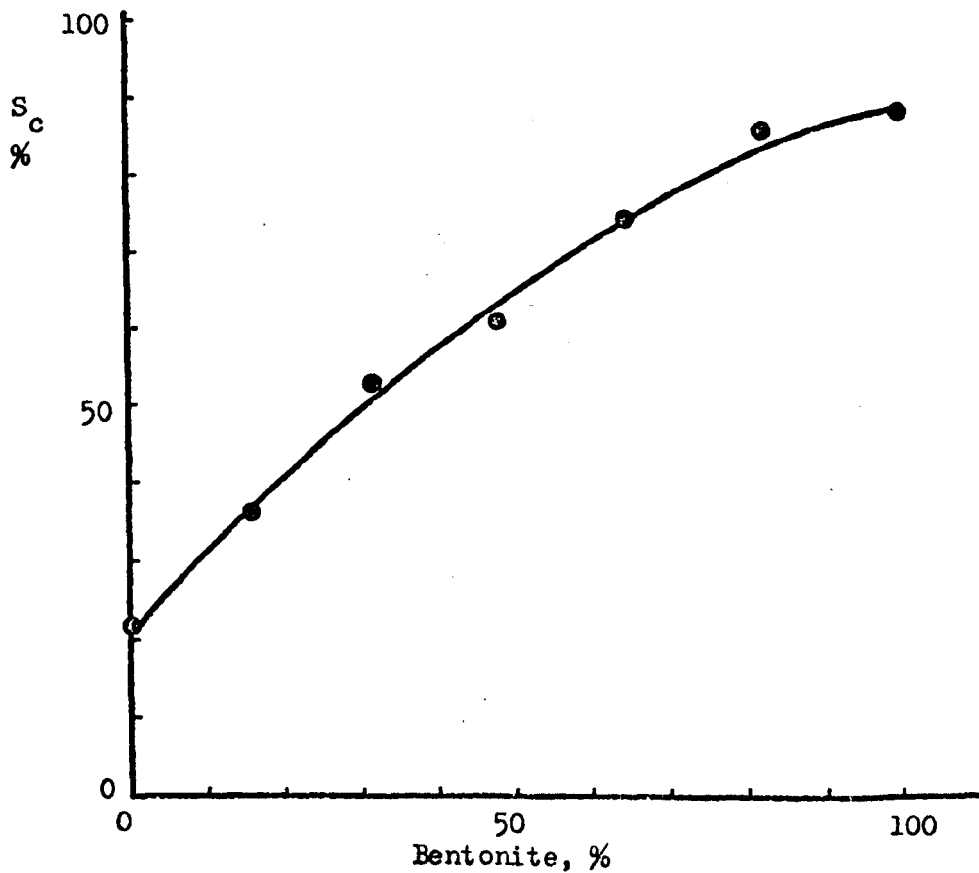


Fig.5.31 Laterally Confined Swell Potential VS Bentonite by Volume, Bentonite-Illite Mixtures.

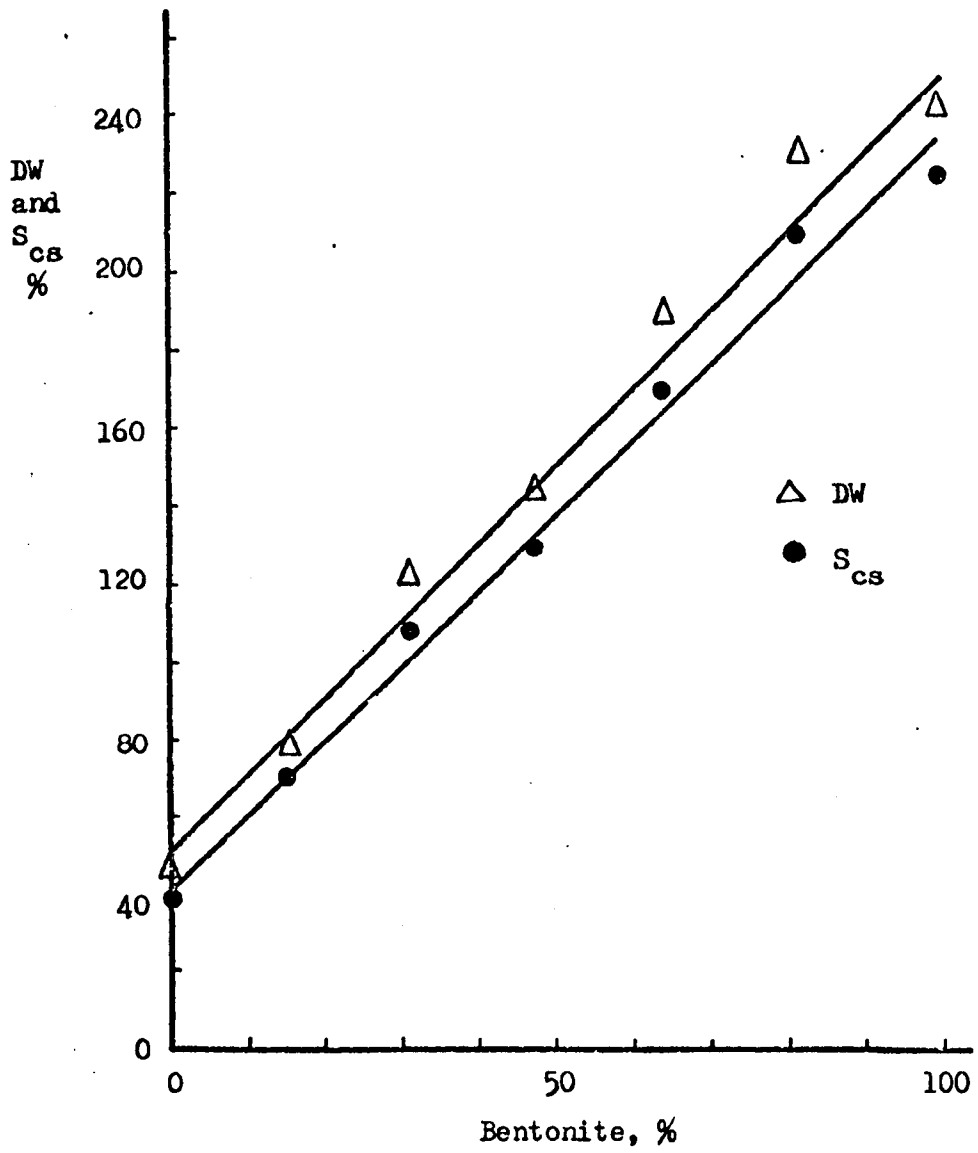


Fig. 5.32 Water Uptake and Swell Amount VS Bentonite by Volume, Bentonite-Illite Mixtures.

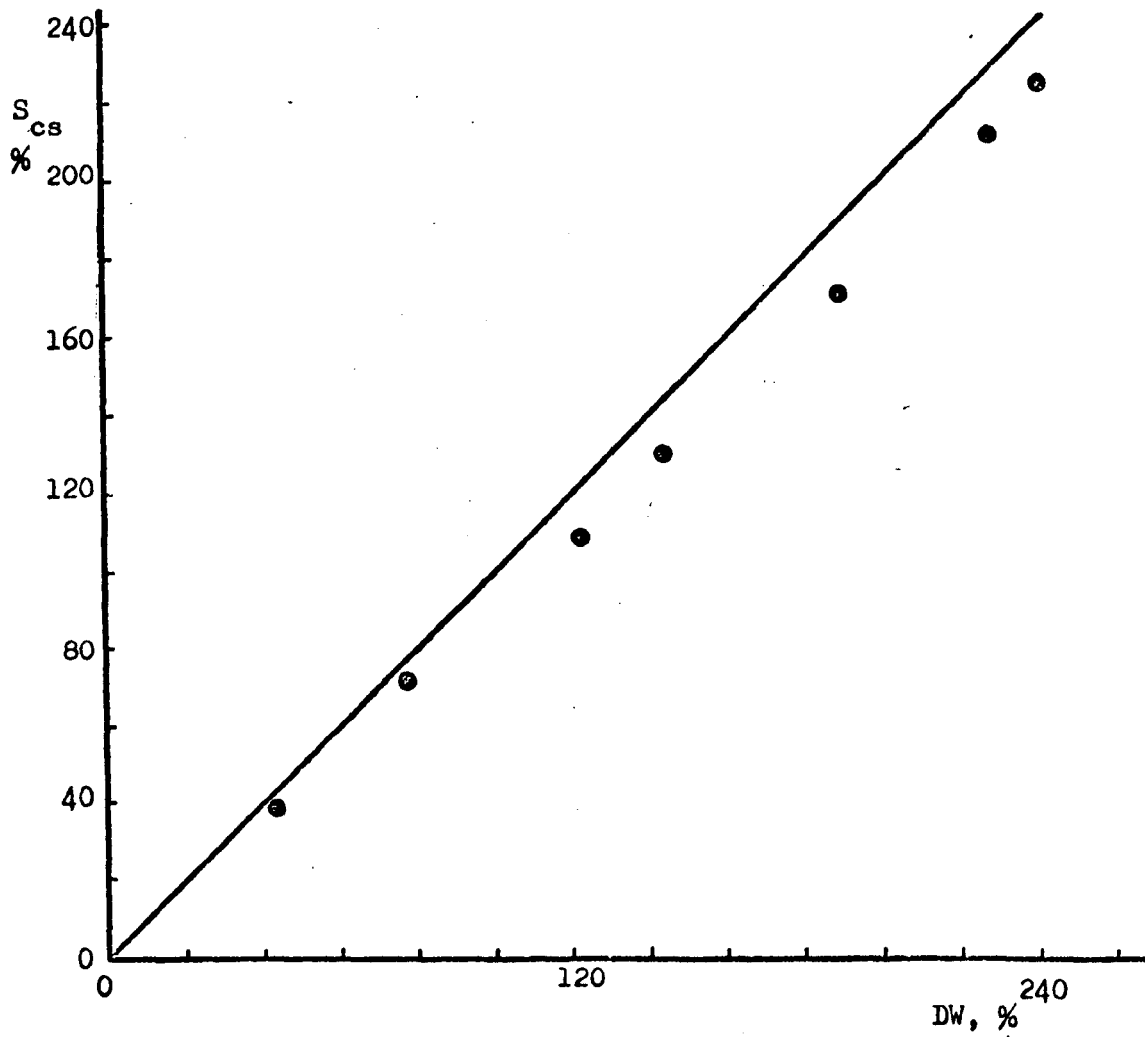


Fig. 5.33 Swell Amount VS Water Uptake, Bentonite-Illite Mixtures.

with increasing sand content. Further attention might be paid to this point in future work.

For the series of bentonite-sand mixtures, at the optimum compaction conditions, both the volumetric water content and the void ratio were approximately linear functions of the composition, expressed volumetrically. For the series of illite-sand mixtures both these properties were linear functions of composition modified by a weak interaction effect up to 68% sand. For both mixtures there was additional air present in the sandiest samples.

For both bentonite-sand and illite-sand mixtures, swell potential showed a non-linear variation with composition. However, when the swell was expressed in terms of the volume of solids, it showed a linear variation with composition in bentonite-sand mixtures and a linear variation with slight interaction effects in illite-sand mixtures. Thus, swell appears to be purely a volumetric phenomena, and swell amount is a more useful parameter than swell potential.

The swell pressure in bentonite-sand mixtures approximated a quadratic function of clay content, which lay close to the curve which would be obtained by considering the proportions of the types of contacts in a test plane, and by assuming that the bentonite dominated the behaviour, see sections 4.3.3 and 4.3.4; and Eqn. 4.32. In illite-sand mixtures the swell pressures were found to approximate a cubical S-shaped function of clay content, Eqn. 4.35. This pattern of behaviour for swell pressure is somewhat similar to the

pattern of behaviour of $\tan \phi_r$ as shown by Kenny's (1967) results, see Figs. 4.5 and A.10-1. For illite, both swell pressure and $\tan \phi_r$ follow the cubical S-shaped relationships of Eqn. 4.35 see Figs. 4.5 and 5.23. For bentonite, both properties approximate to the quadratic bound for which the bentonite controls the behaviour, see Figs. 5.12 and A.10-1, although a modification was required for $\tan \phi_r$, Appendix-10. The differences between the patterns of behaviour for illite and bentonite suggest that different physical phenomena control the behaviour of these two clay minerals. Olson and Mesri (1970) showed that in consolidation, physico-chemical forces predominate for montmorillonite (i.e. bentonite), whilst, except at low pressures, mechanical-frictional forces predominate for illite. Presumably these two sets of forces are those which control the differences between the patterns of behaviour for swell pressure.

The results discussed above suggest that some inaccuracies may arise when attempts are made to predict the swell properties from the Atterberg limits, since swell pressure, swell amount, and the Atterberg limits, all follow different algebraic functions of clay content.

As far as the original question of linear multiple regression is concerned, it is a matter of judgement whether straight lines could be substituted for the curves shown here; this would depend on the accuracy required and on the range of clay content expected. For swell amount, as a first approximation the graphs are linear, the worst error being approximately 8% at 68% sand content

for the illite-sand mixtures. For the swell pressure, the situation is more complicated because the bentonite-sand and illite-sand mixtures follow different curvilinear laws. Thus, for natural soils, it is almost inevitable that linear analysis should be considered first, although some difficulty may arise if a series of soils which contain widely differing clay minerals is to be analysed. However, for present purposes, further discussion would be of little practical importance, because linear analyses of sufficient accuracy were obtained for the natural soils discussed in Part-II below.

Part-II: NATURAL SOILS

5.4 INTRODUCTION

Part-II is concerned with the ten natural soils from Wootton Broadmead. The data was first analysed to see if the swell properties (compaction properties and Atterberg limits) could be expressed as functions of clay content alone. This showed that clay content was significant, but a more accurate method of analysis was required. Consideration of the particle size analysis suggested that samples 6,7,9 and 10 are dissimilar from the other six and by restricting attention to these six samples it was found possible to predict their properties as functions of clay content. For this reason the results for the four samples which were subsequently discarded are plotted as triangles in Figs. 5.34 to 5.40. In order to find a method of analysis which embraced all ten samples, linear

multiple regressions were made taking composition and Atterberg limits as independent variables. As in Part-I the whole body of data was analysed both for completeness and to reveal any similarities or dissimilarities in the patterns of behaviour. The most important of these patterns is the contribution of silt content to the Atterberg limits and swell properties respectively.

5.4.1 Variation of Properties with Clay Content

The natural soils in the present study were deliberately chosen to have a wide variation of clay content. They came from the same area and had a broadly similar geological and mineralogical origin. Moreover, they had been placed in a single mapping unit by King (1969), presumably on account of their similarities. Therefore it was decided, as a first step in the analysis, to see if the soil properties could be explained and predicted by clay content alone.

Figs. 5.34 to 5.40 show the various soil properties plotted against the clay content. It can be seen from these Figures that the trends of variation are broadly as expected, i.e. swell increases with clay content, etc, although there is a considerable amount of random variability. Earlier investigators (e.g. Davidson and Sheeler, 1952) show similar random variability, although the soil properties under consideration were often stated to have linear relationships with clay content. In the present study, the simple linear regression equations shown in Figs. 5.34 to 5.40 failed to reach statistical significance for all properties excepting those of swell pressure and swell potential, presumably because there are too few samples. The soils which showed large deviations from the regression line were selected

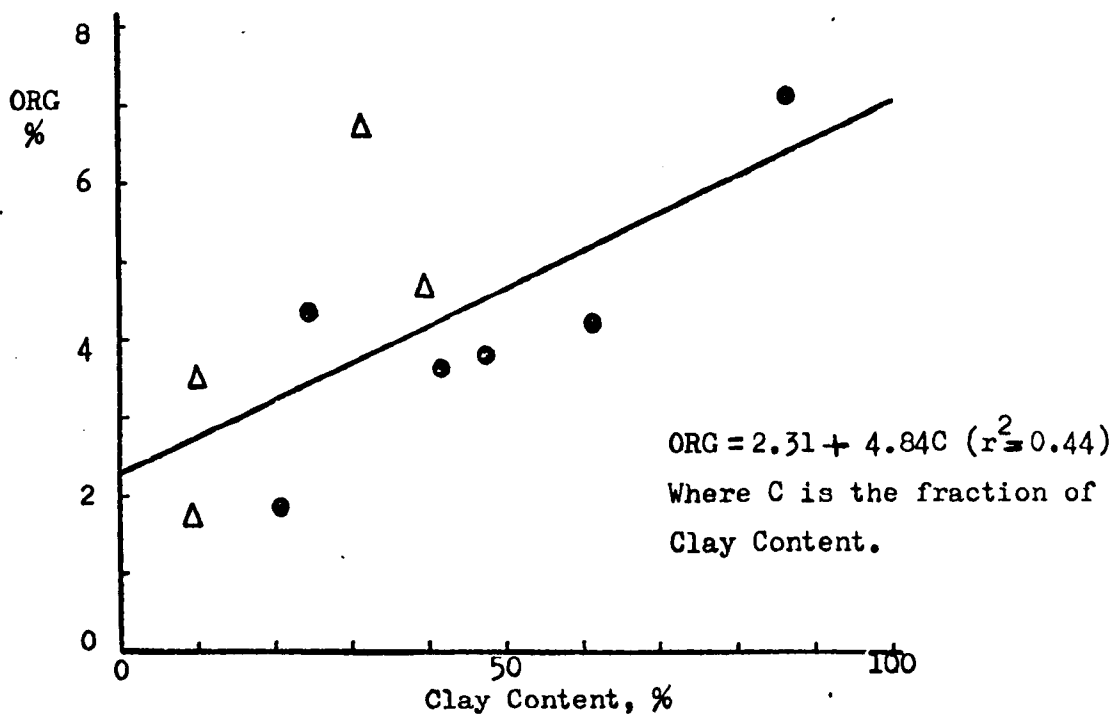


Fig. 5.34 Organic Matter VS Clay Content, All Natural Soils.

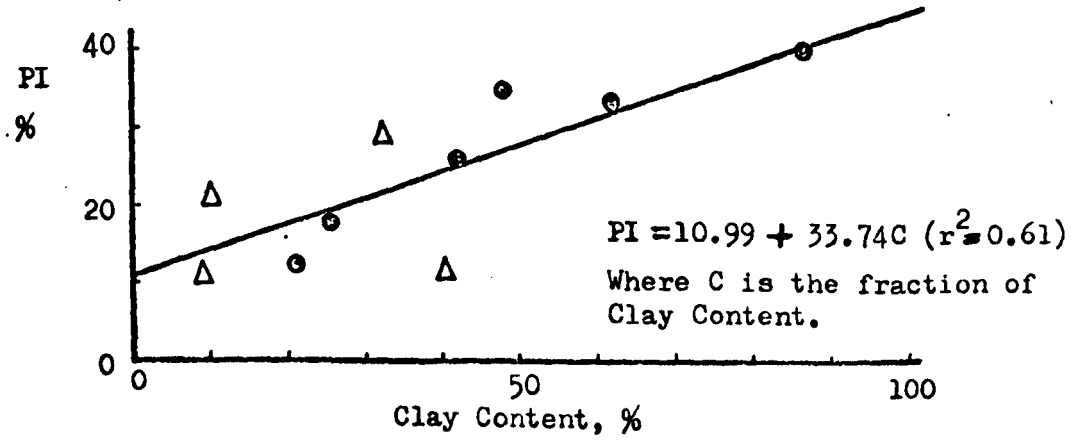
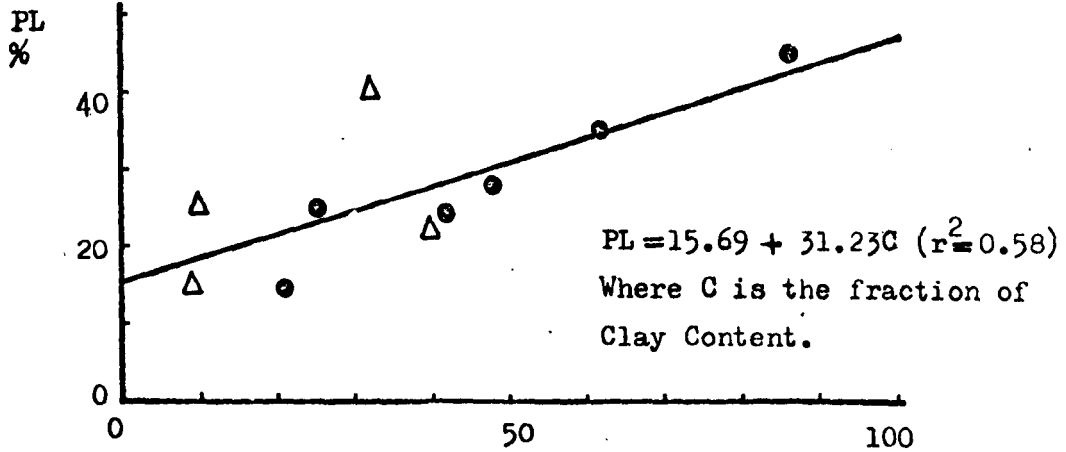
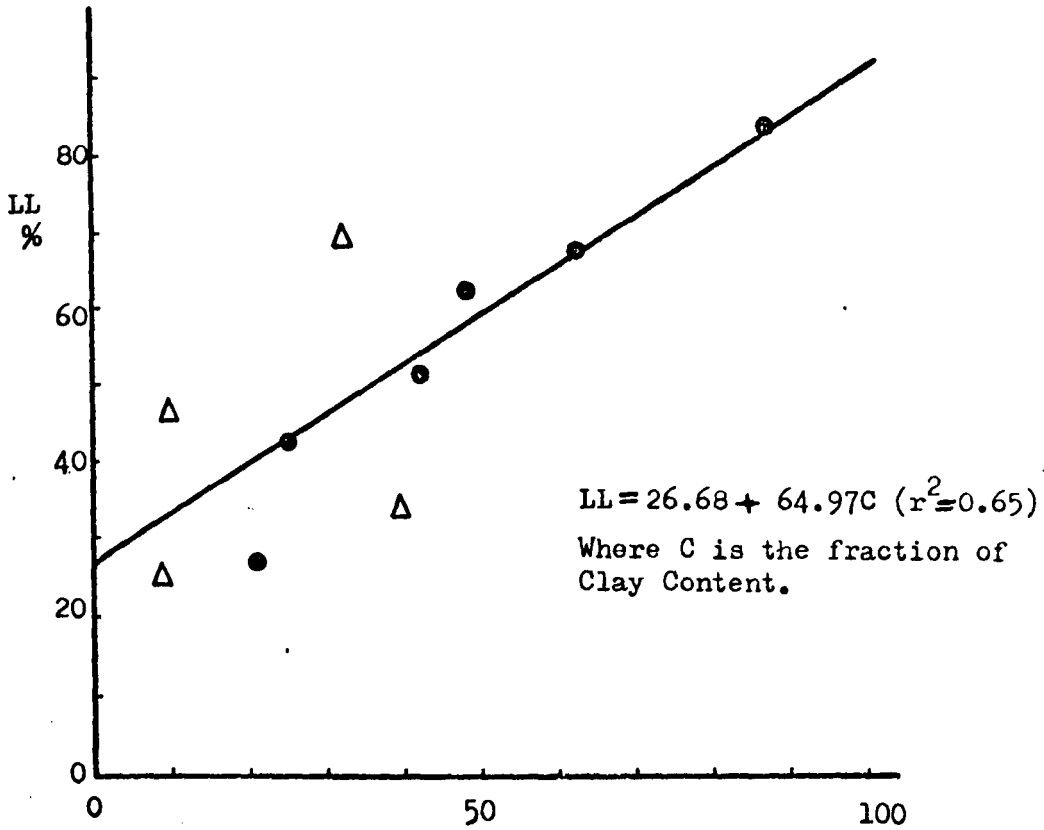


Fig. 5.35 Atterberg Limits VS Clay Content, All Natural Soils.

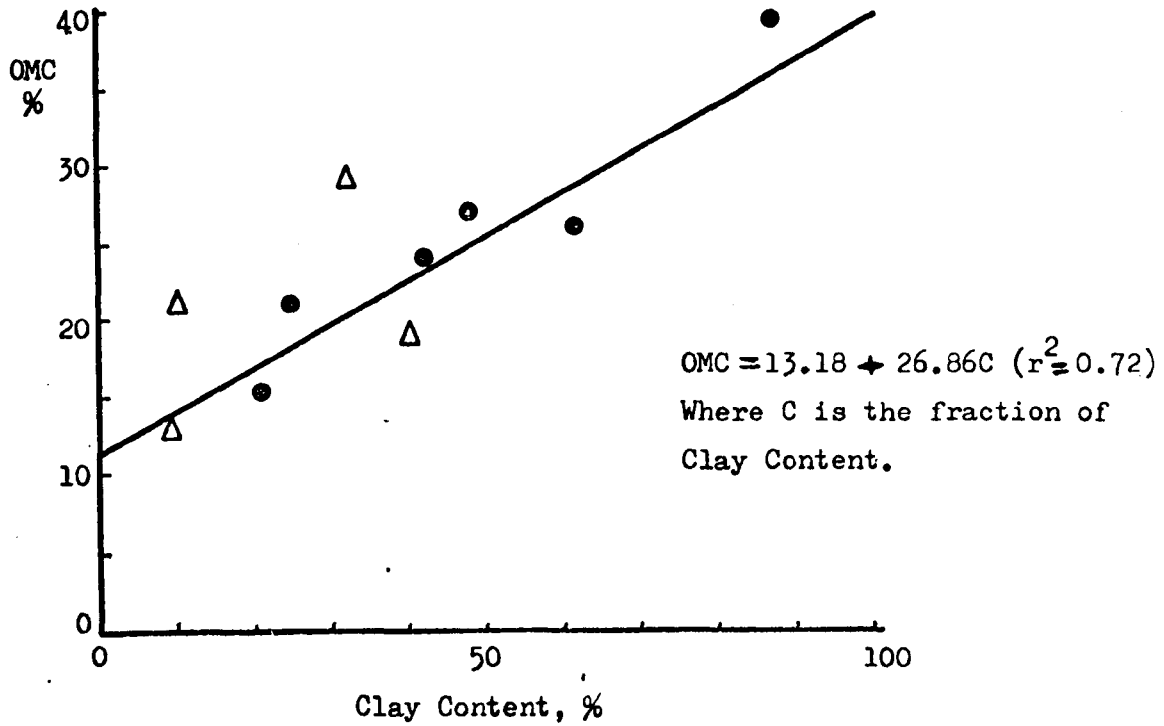


Fig. 5.36 Optimum Moisture Content VS Clay Content, All Natural Soils.

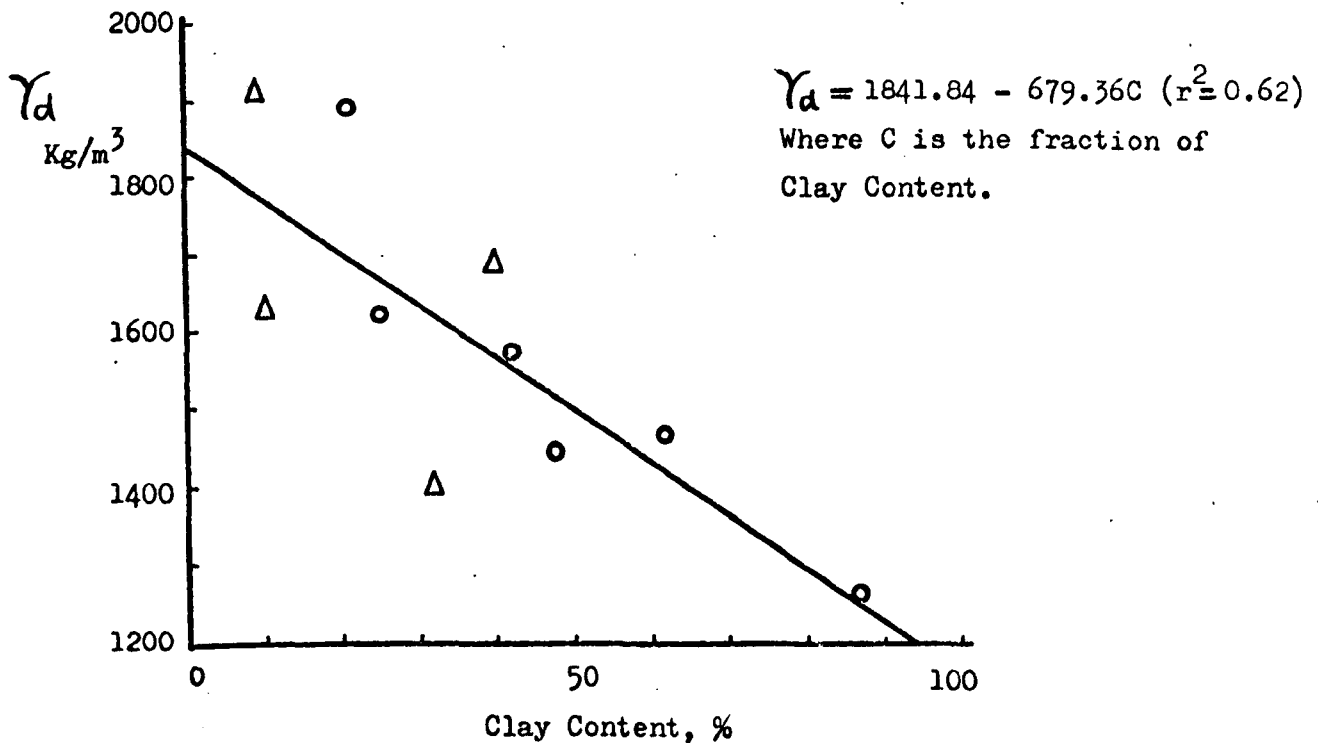


Fig. 5.37 Maximum Dry Density VS Clay Content, All Natural Soils.

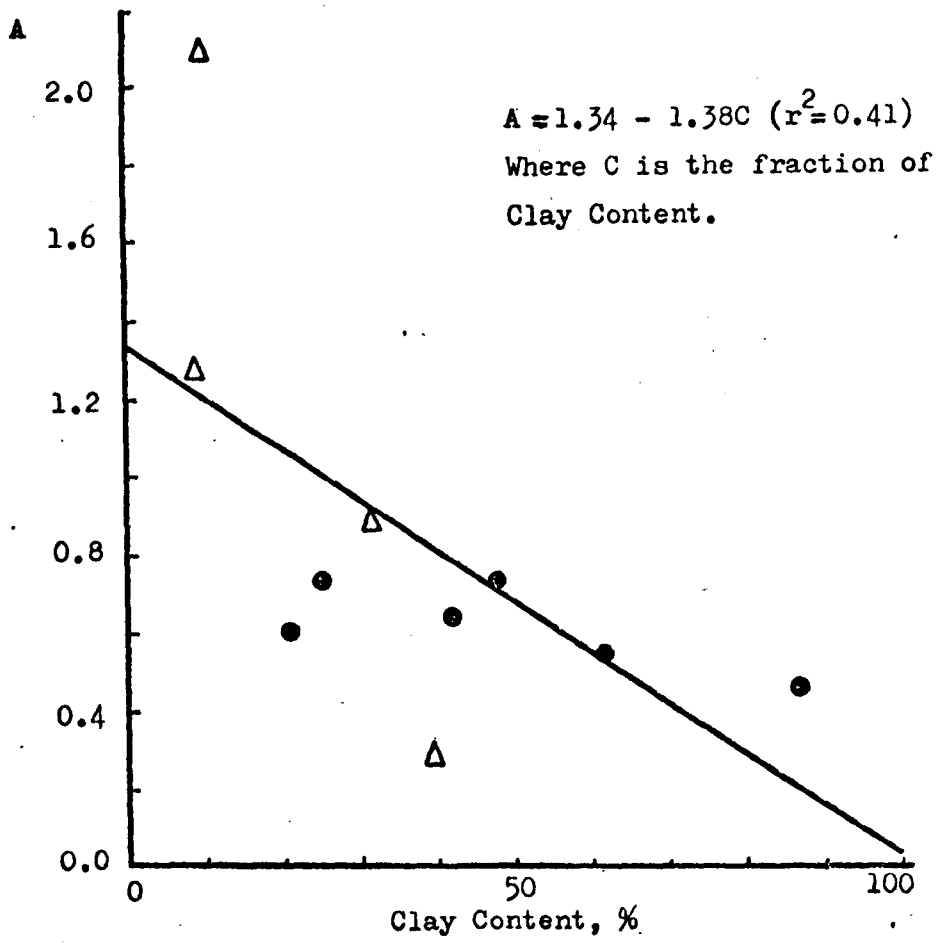


Fig.5.38 Activity VS Clay Content, All Natural Soils.

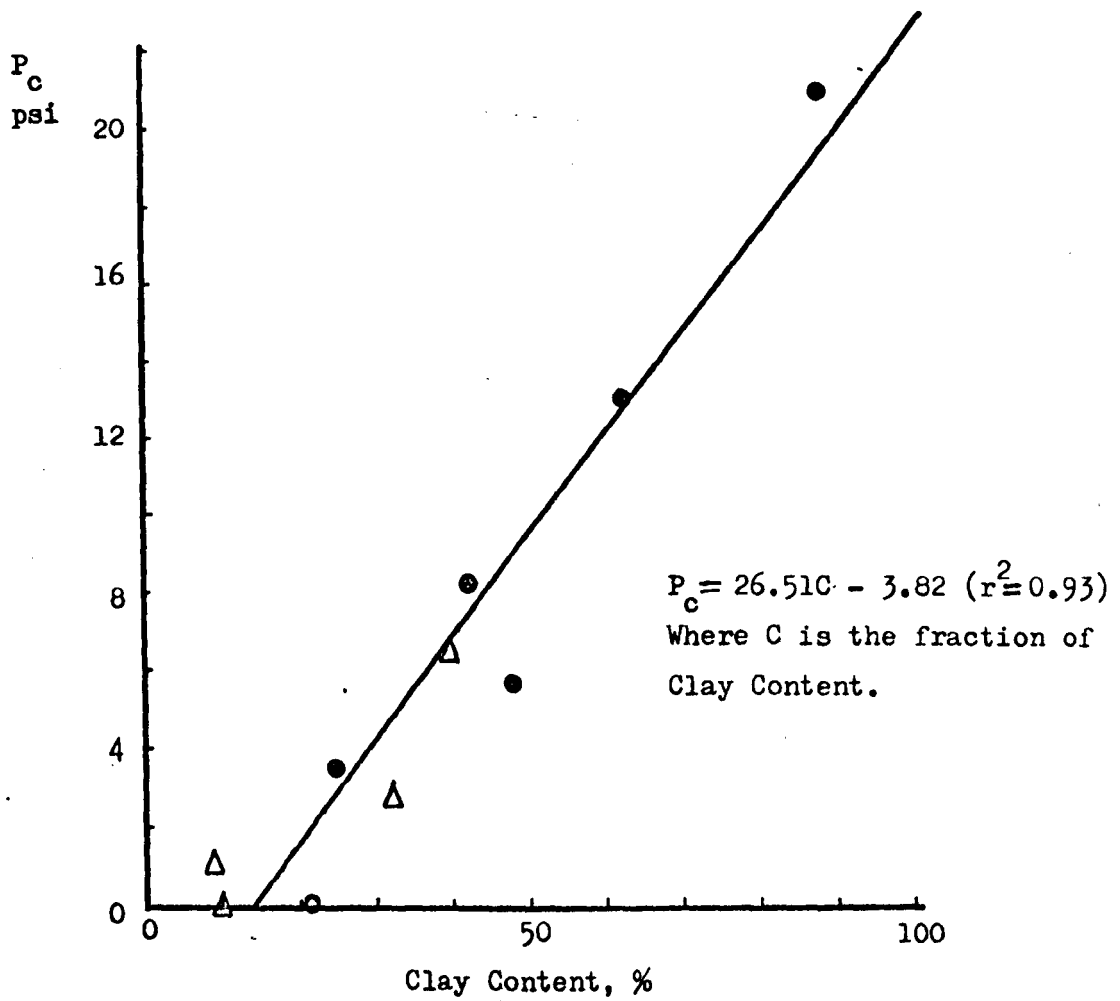


Fig. 5.39 Laterally Confined Swell Pressure VS Clay Content, All Natural Soils.

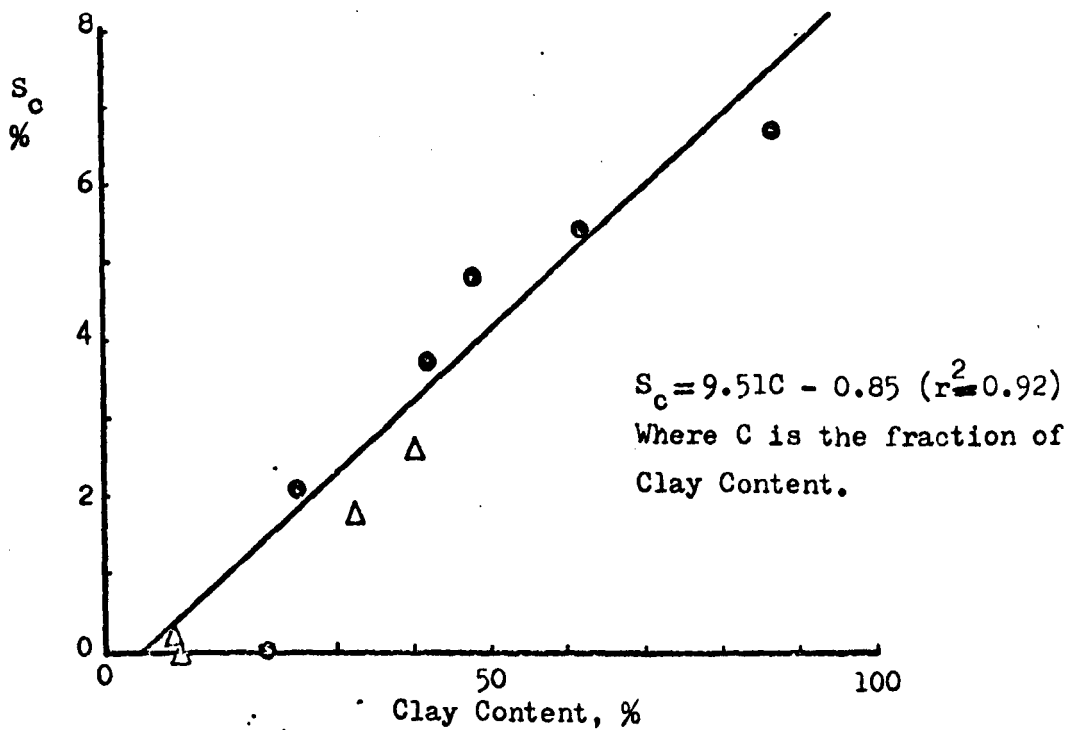


Fig. 5.40 Laterally Confined Swell Potential VS Clay Content, All Natural Soils.

visually from the graphs and are reported in Table 5.7. Samples 6, 9 and 10 featured most frequently in this Table. Further, it was noted that the particle size distribution curves of these three samples differed from those of the other samples, except perhaps sample 7; therefore further consideration was given to particle size distribution as is discussed below.

5.4.2 Analysis of Particle Size Distribution Curves

Partly as a result of King's (1969) account, it had been thought in the first place that the soils were derived from the underlying Oxford clay with varying amounts of an admixture of glacial origin. If this idea were correct, it would be possible to predict the particle size distributions of the medium textured samples from the particle size distribution of the lightest and heaviest samples; the method of calculation is explained in Appendix 8. As these results were examined more closely, the idea was progressively modified, until it was thought that four separate sources of material were involved.

Data quoted by King (1969) for the surface horizon of the Milton, Rowsham and Denchworth Series are shown in Fig. 5.41, where the observations are plotted as points. Smooth curves were drawn through the points of Milton and Denchworth; the proportions of clay, fine, medium and coarse silt, fine, medium and coarse sand were read off; and using these figures and the assumption that Rowsham Series consists of a mixture of Milton and Denchworth Series, the predicted particle size distribution of Rowsham Series was calculated using the method of Appendix 8. The

Table 5.7 Outlying Samples For Regression against
Clay Content

<u>Property</u>	<u>Soils Showing Variability</u>				
Organic Matter	2	6	.	9	.
Liquid Limit	2	.	.	9	10
Plastic Limit	.	.	7	9	10
Plasticity Index	.	.	7	.	10
Activity	2	.	7	.	10
Optimum Moisture Content	.	.	.	9	10
Optimum Dry Density	2	6	.	9	10
Swell Pressure	2
Swell Potential	2

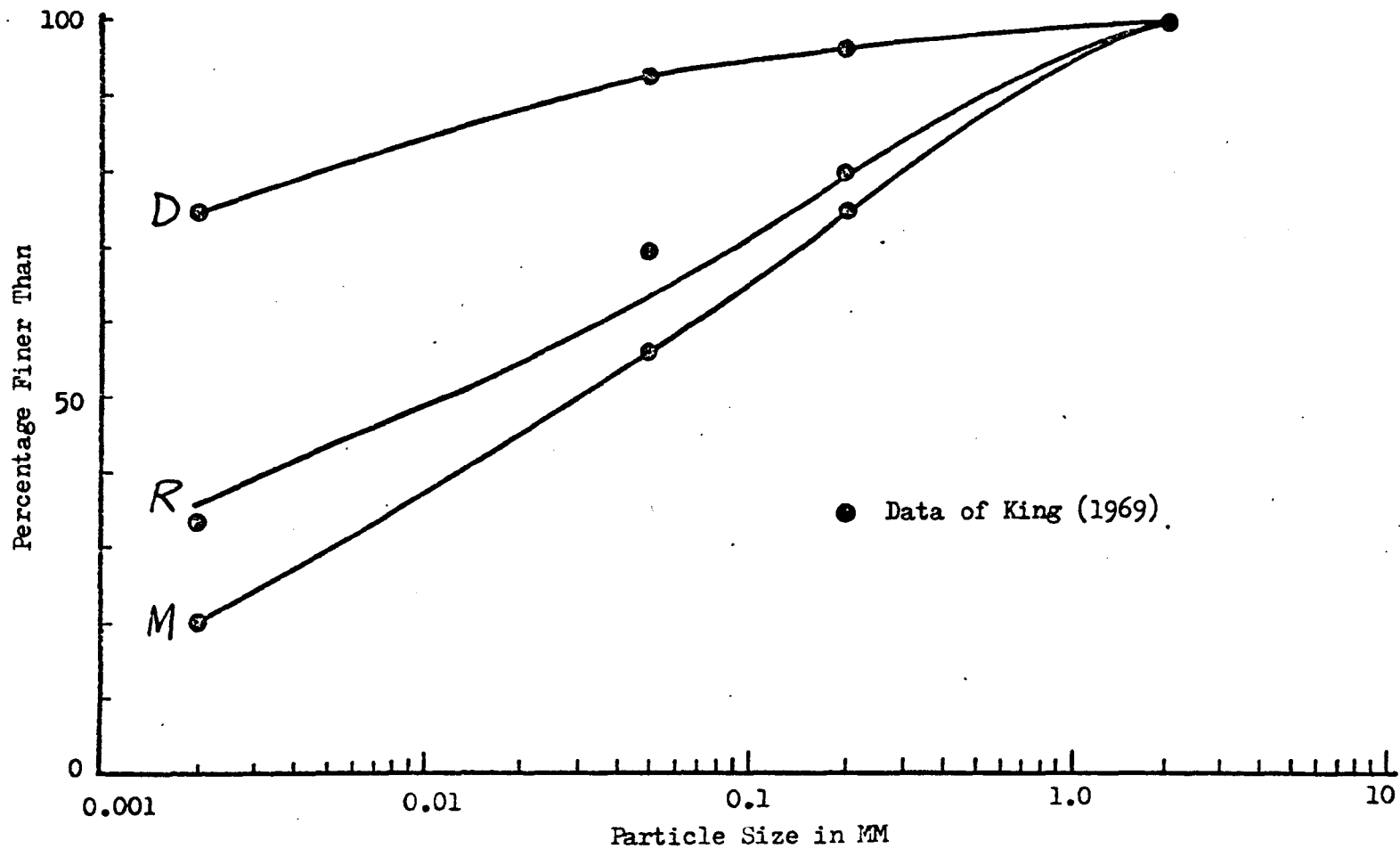


Fig. 5.41 Particle Size Distribution Curves, Milton, Rowsham and Denchworth Series.

prediction is shown by the third full line in Fig. 5.41. This line agrees quite closely with the observed particle size distribution for Rowsham Series. It was decided therefore to treat these three soils as belonging to a single family.

Samples 2, 3, 1, 4, 5 and 8 are compared with Milton, Rowsham and Denchworth in Figs. 5.42 and 5.43. For samples 2 and 3, the lines shown were calculated from Milton and Rowsham Series; for the other samples, the lines were calculated from Rowsham and Denchworth. There is fairly good agreement between the observed and predicted particle size distribution; and all those samples were thought to belong to a single family, which is more or less a simple mixture of two sources approximated by samples 2 and 8. None of the other four samples (6,7,9 and 10) could be fitted into this family.

Sample 6, 9 and 10 were compared in Fig. 5.44. The lines for 6 and 9 are smooth curves drawn through the observations, and that for 10 is calculated from 6 and 9. Although the agreement between the observed and predicted particle size distribution for sample 10 was not entirely satisfactory, as a matter of expediency, these three samples have been placed together in a second family whose sources are approximated by 6 and 9.

Samples 6, 7 and 8 are compared in Fig. 5.45 which shows the smooth curves from Fig. 5.44 and 5.43 for samples 6 and 8, together with the predicted curve of sample 7. The reobserved particle size distribution of 7 is shown by triangles and agrees fairly well with the predicted

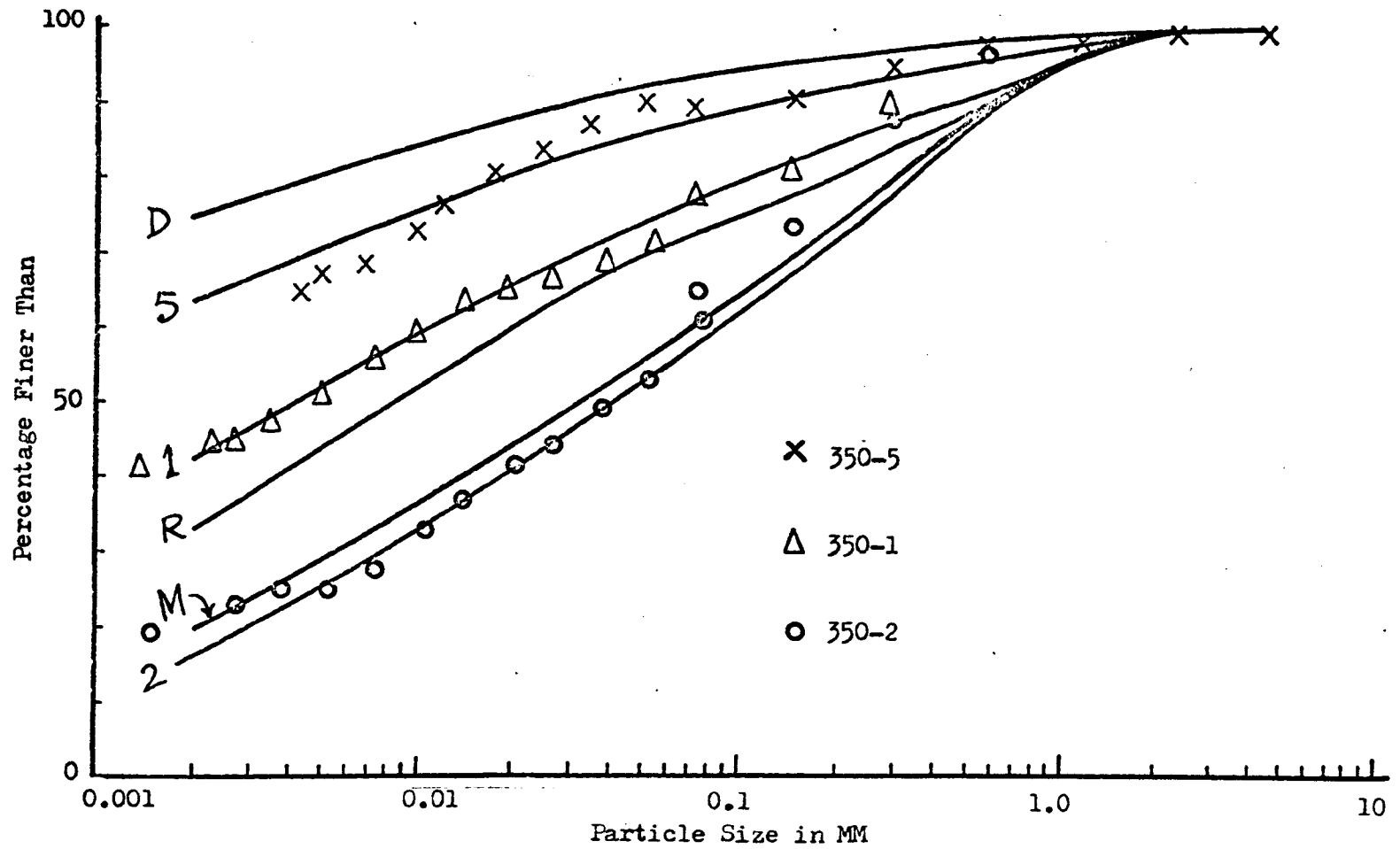


Fig.5.42 Particle Size Distribution Curves, Soils 1, 2, 5.

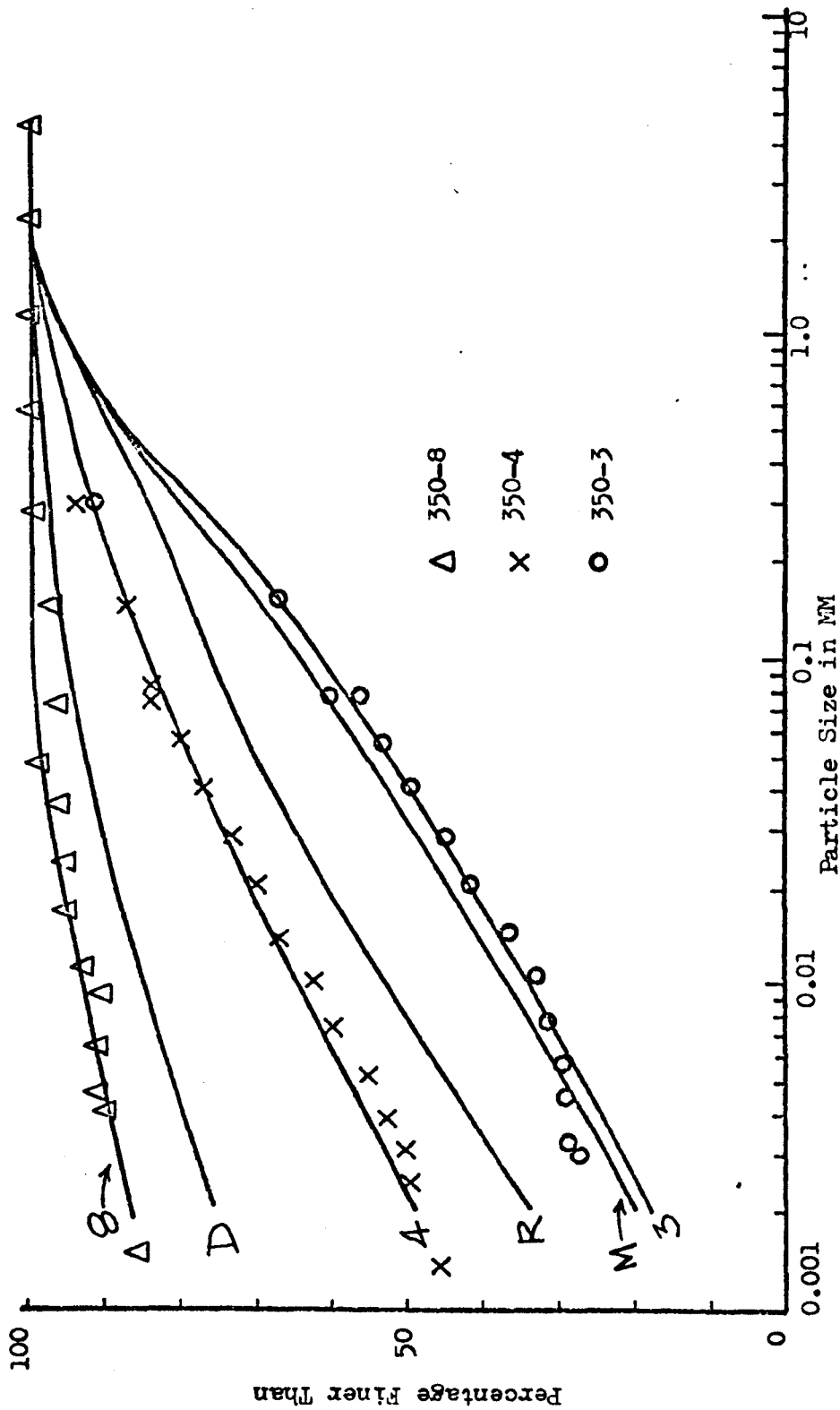


Fig. 5.43 Particle Size Distribution Curves, Soils 3, 4, 8.

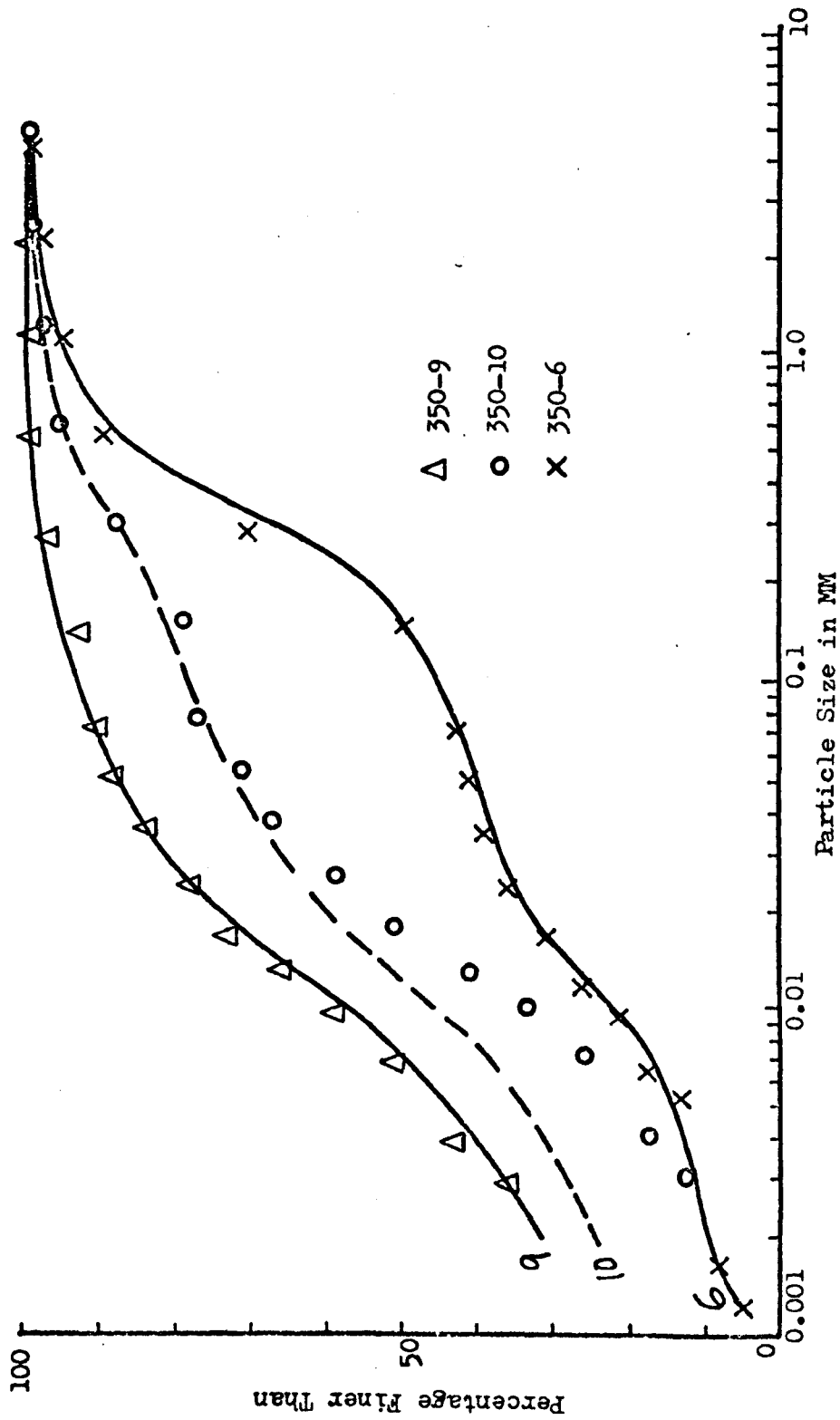


Fig. 5-44 Particle Size Distribution Curves, Soils 6, 10, 9.

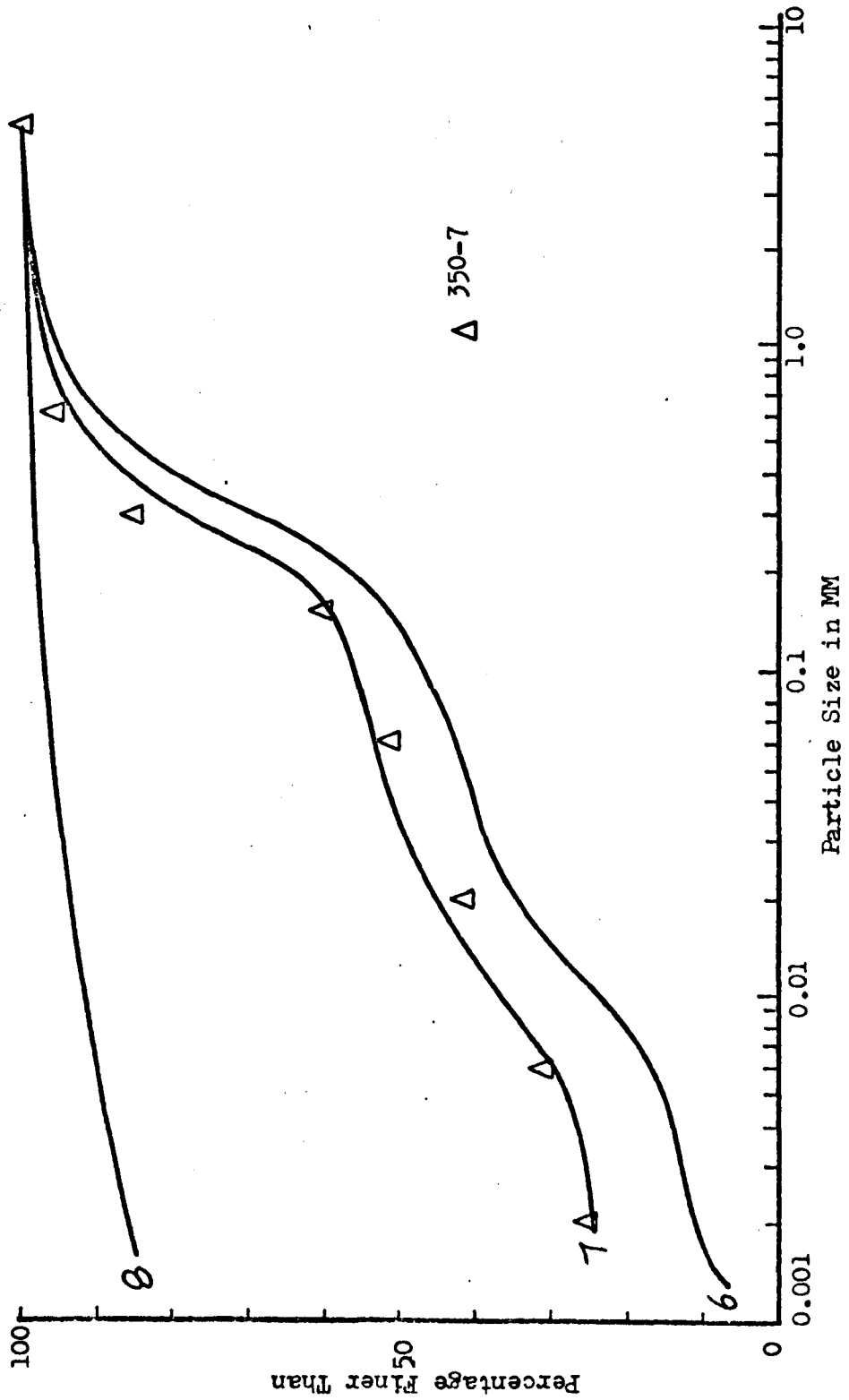


Fig. 5.45 Particle Size Distribution Curves, Soil No. 7.

curve. It was therefore assumed that these three samples formed a family whose sources were approximated by samples 6 and 8. It was partly on account of the agreement of the reobserved particle size distribution with the predicted values plotted in Fig. 5.45 that the reobserved particle size distribution was preferred to the original. There is of course some danger in making this choice, although the reason for requesting the reobservation was that the original observations were thought to be in error.

In summary, therefore, the ten samples fall into three families as follows:

1, 2, 3, 4, 5 and 8;

6, 9 and 10;

6, 7, and 8.

This helps to explain the discrepancies summarised in Table 5.7, which involves samples 2, 6, 7, 9 and 10. Of these five samples, 6, 7, 9 and 10 differed in their particle size distribution from the other six samples. It was therefore decided (a) to consider the effect of clay content on its own for samples 1, 2, 3, 4, 5 and 8; and (b) to use multiple regression to analyse the data for all ten samples in terms especially of the contents of clay, silt, organic matter and plasticity index. These analyses are reported below.

5.4.3 Effect of Clay Content For First Family of Soils

Figs. 5.46 to 5.52 show the results of simple regressions for the various properties against clay content of the first family of samples, i.e. samples 1, 2, 3, 4, 5 and 8

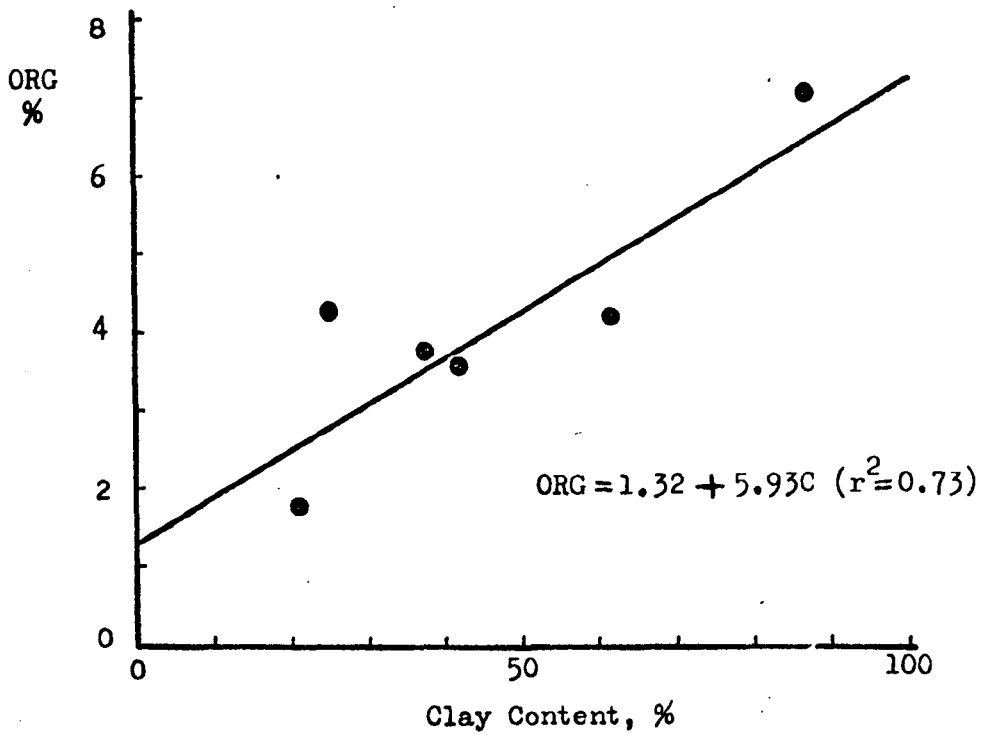
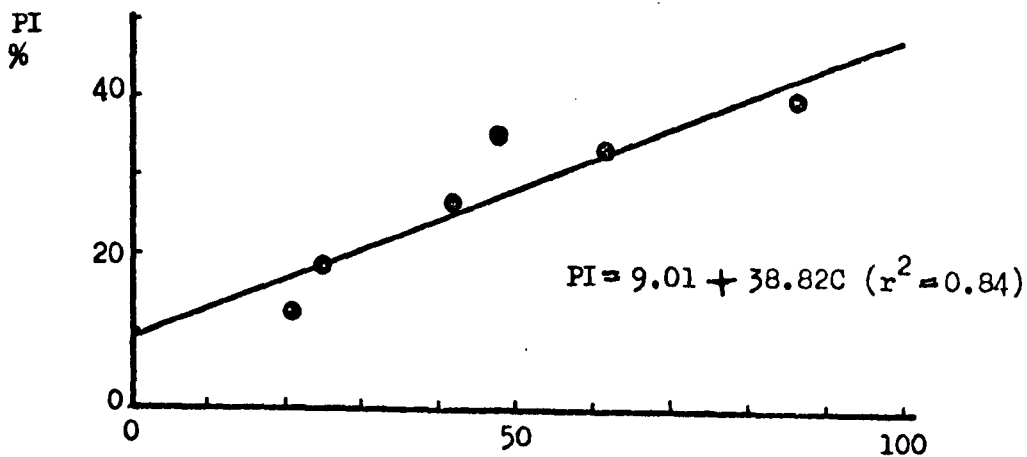
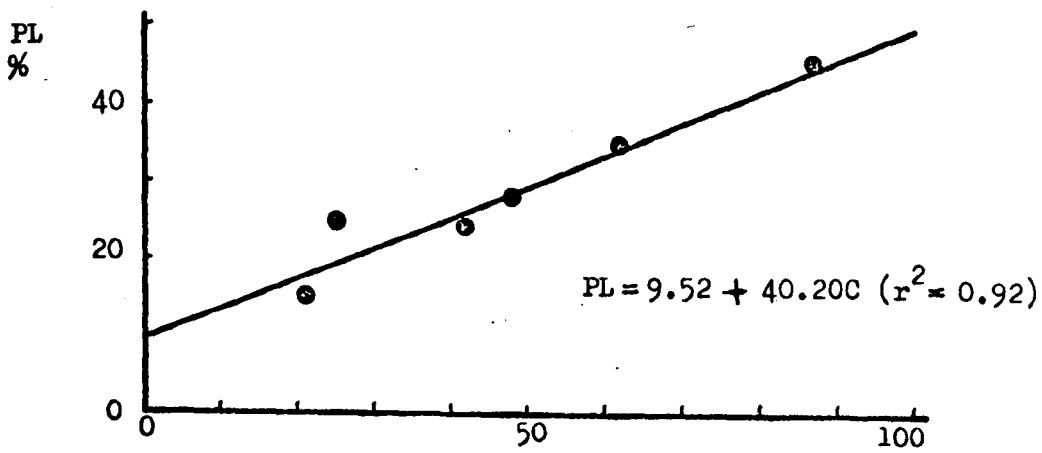
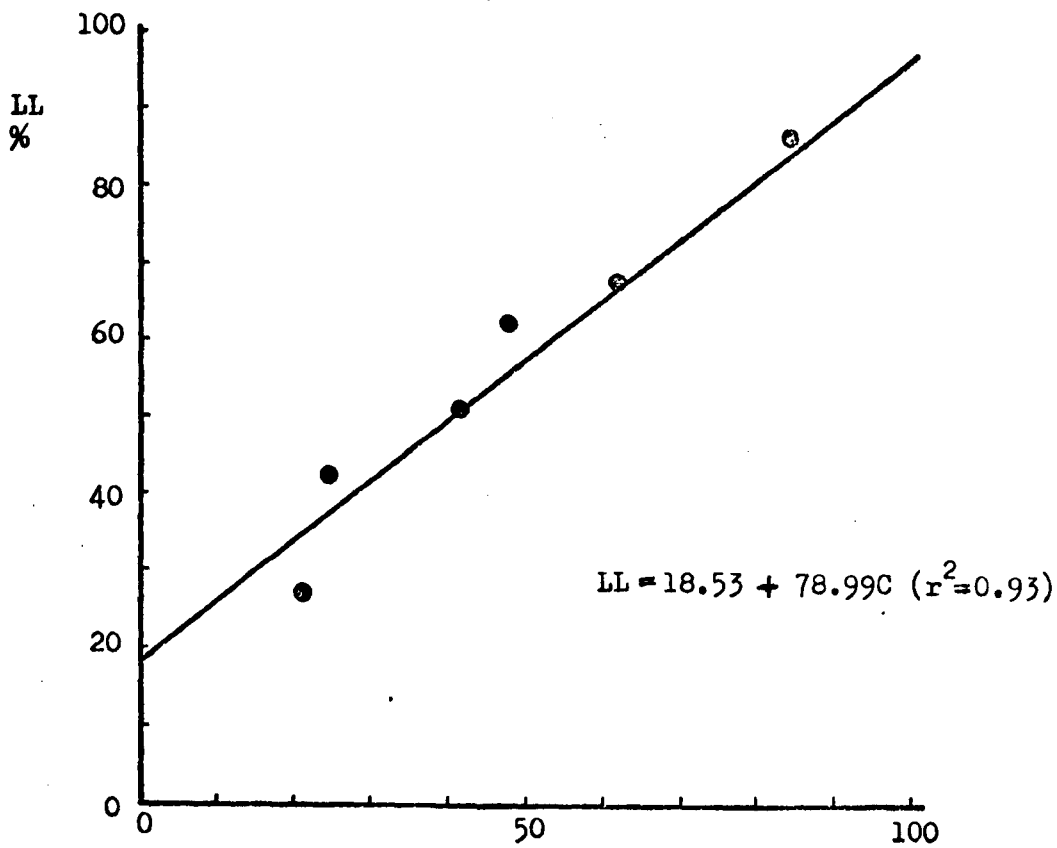


Fig.5.46 Organic Matter VS Clay Content, Six Soils of First Family.



Clay Content, %

Fig. 5.47 Atterberg Limits VS Clay Content, Six Soils of First Family.

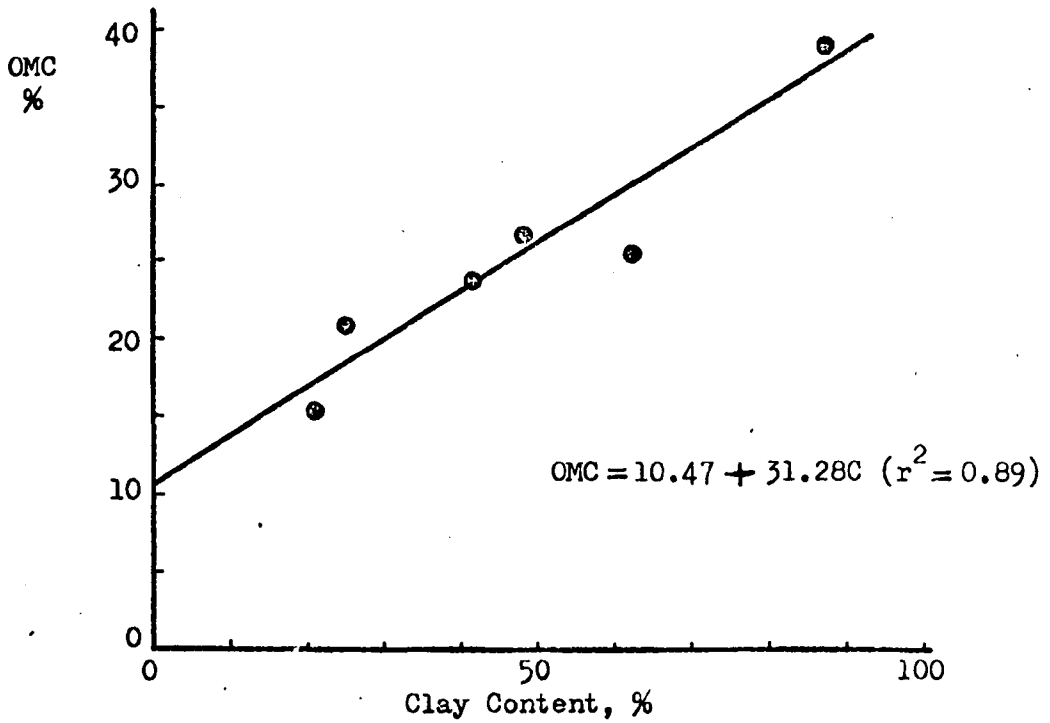


Fig.5.48 Optimum Moisture Content VS Clay Content, Six Soils of First Family.

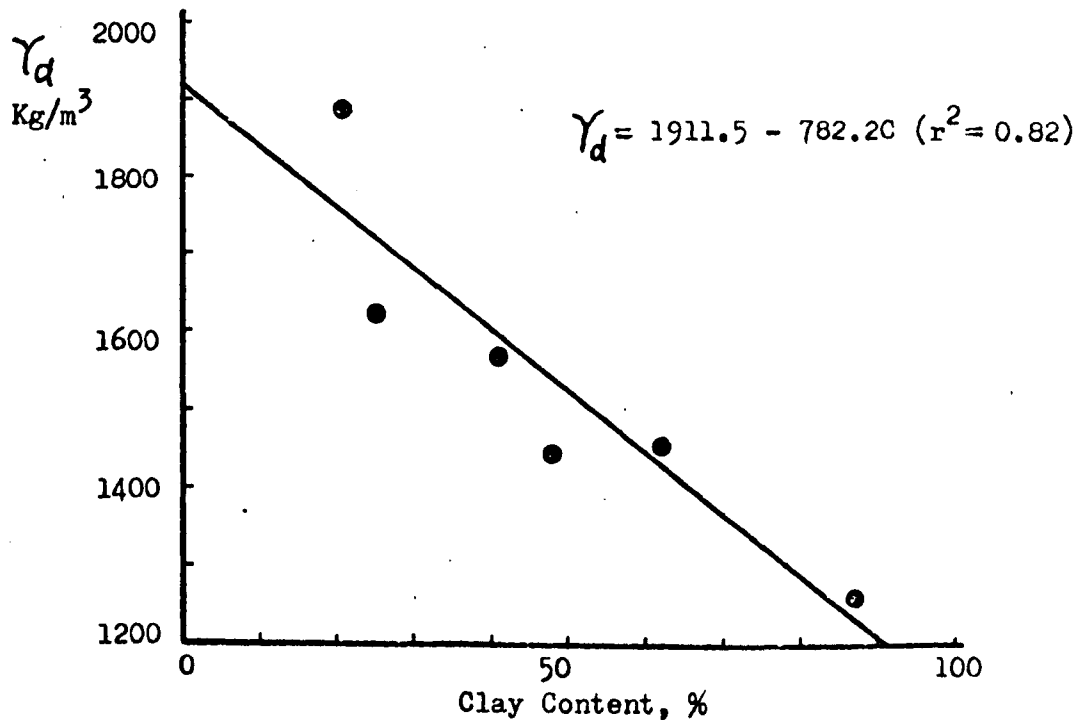


Fig.5.49 Maximum Dry Density VS Clay Content, Six Soils of First Family.

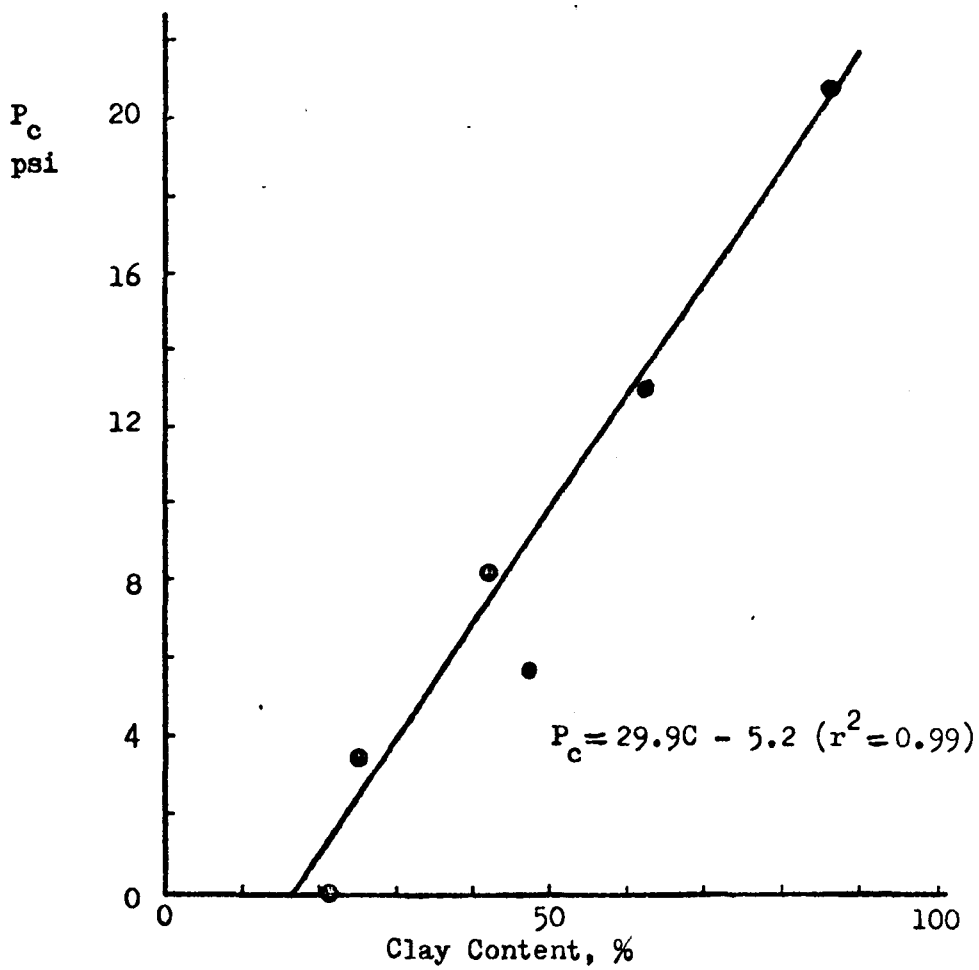


Fig.5.50 Laterally Confined Swell Pressure VS Clay Content, Six Soils of First Family.

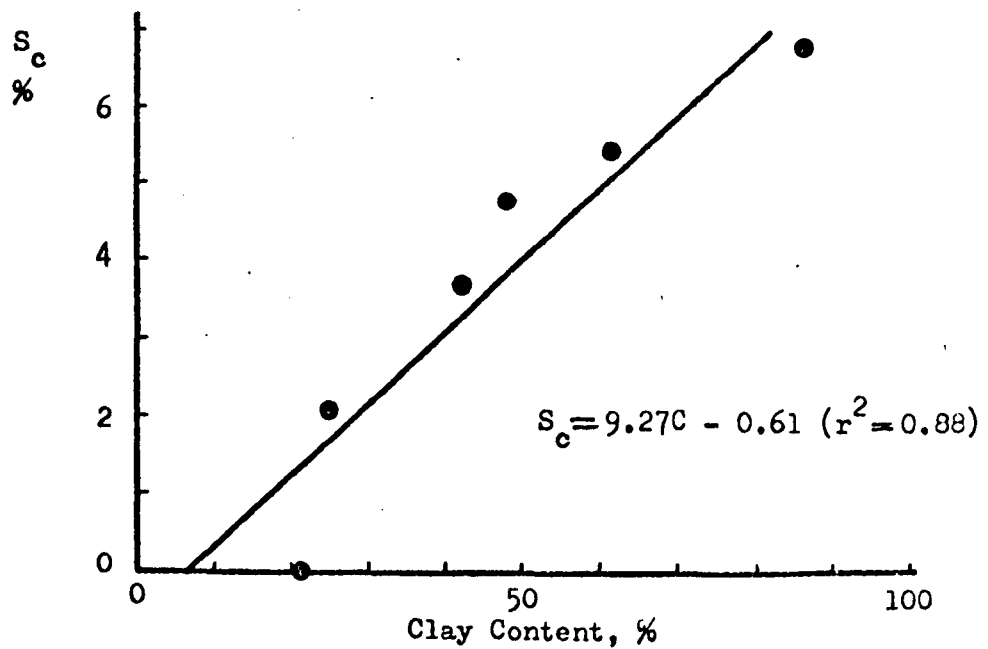


Fig.5.51 Laterally Confined Swell Potential VS Clay Content, Six Soils of First Family.

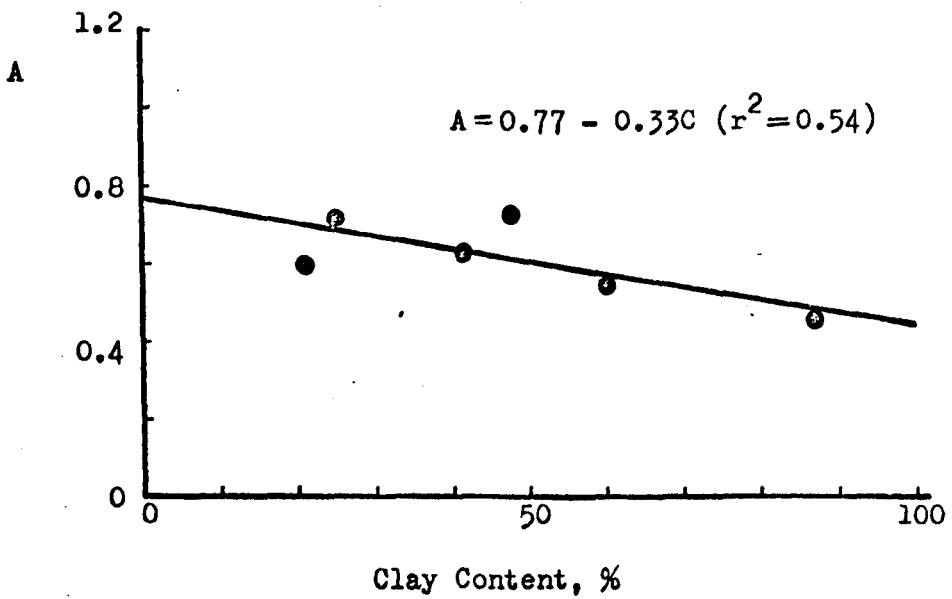


Fig.5.52 Activity VS Clay Content, Six Soils of First Family.

In the regression equations mentioned on these Figures the clay content is expressed as a fraction. Table 5.8 compares the level of significance for all nine properties considered for the two cases, the first based on all ten samples and the second on the six samples of the first family. Although there are less degrees of freedom in the second case since four samples have been dropped from the analysis, the variability is less, and the degree of significance is generally high.

On this basis, the prerequisite for an accurate prediction of the properties of a soil from its clay content alone are that all of the geological history, mineralogical composition and particle size distribution should be similar. Further, it can be seen from this example that if an accurate prediction is required from clay content alone, the criterion of similarity is a strict one and must be carefully investigated.

5.4.4 Multiple Regression Analysis For Prediction Of Soil Properties

As an alternative to the method outlined in the section above, predictions must be based on the simultaneous use of several independent variables.

In order to investigate the dependence of the compaction and swell properties, etc, on the composition of the soil, linear multiple regression analyses were made using programme O2R in the BMD package (Dixon, 1971) and checked with the regression programme in the SPSS package (Norman H. Nie et al, 1975).

Table 5.8 Level of Significance for Simple Regressions

Property	Level of Significance, %	
	Using all 10 Samples	Using 6 Samples of First Family
Organic Matter	> 5	> 5
Liquid Limit	> 5	1 *
Plastic Limit	> 5	1 *
Plasticity Index	> 5	< 5 *
Activity	> 5	> 5
Optimum Moisture Content	> 5	< 5 *
Optimum Dry Density	> 5	< 5 *
Swell Pressure	1 *	0.1 * * *
Swell Potential	1 *	< 5 *

- * Significant
- * * Highly Significant
- * * * Very Highly Significant

One of the main problems in forming multiple predictive equations in soil mechanics arises from the fact that the various 'independent' variables considered to predict a dependent variable are themselves dependent. Therefore, the following approach was used:-

As a first approximation, only composition is regarded as independent. The variables are:

- C = clay content, %
 Z = silt content, % (or s = sand content, %)
 ORG = organic matter, %

For practical reasons, these were expressed by weight with respect to weight of solids. As a second approximation, for compaction and swell properties, only one of the liquid limit, plastic limit, plasticity index or activity is included with composition.

The final results of these analyses are shown in Table 5.9, and Table 5.10 reports the predictive equations. The regression data for specific gravity is taken from Appendix 2, section A2.3. The regression programmes used place the individual variables in order of importance in accordance with the amount of variability associated with each variable. The individual variables are entered in Table 5.9 in this order. Other regressions which were made to clarify particular points are summarised in Tables 5.11 to 5.13.

The soils in the present study are surface soils, so it is reasonable to expect that organic matter would increase with clay content. Organic matter also depends on management. Arable use of the soil is expected to deplete the organic

Table 5.9 Multiple Regression Analysis, Natural Soils.

Dependent Variable	Independent Variables	R ²	Degrees of Freedom	F	Significance, %
ORG	C, Z	.53	2 7	4.0	> 5
G _s	ORG, Z, C	.76	3 6	6.4	5
	ORG, Z	.71	2 7	8.5	2.5 *
LL	C, Z, ORG	.97	3 6	60.6	0.1 * * *
PL	ORG, C, Z	.98	3 6	102.3	0.1 * * *
PI	C, Z, ORG	.92	3 6	23.9	0.1 * * *
A	Z, ORG, C	.61	3 6	3.2	2.5 *
OMC	C, ORG, Z	.95	3 6	41.1.	0.1 * * *
	PI, ORG	.96	2 7	74.8	0.1 * * *
Y _d	ORG, C, Z	.94	3 6	30.1	0.1 * * *
	PI, ORG	.98	2 7	199.0	0.1 * * *
P _c	C, Z, ORG	.96	3 6	43.8	0.1 * * *
	C, Z, PI	.96	3 6	50.1	0.1 * * *
S _c	C, Z, ORG	.91	3 6	24.7	0.1 * * *
	C, Z, PI	.93	3 6	28.0	0.1 * * *
S _{cs}	C, Z, ORG	.93	3 6	27.9	0.1 * * *
	C, Z, PI	.95	3 6	37.4	0.1 * * *
P _i	C, Z, ORG	.92	3 6	23.9	0.1 * * *
	C, Z, PI	.93	3 6	24.9	0.1 * * *

Table 5.10 Predictive Equations from Multiple Regression Analysis.

$$\text{ORG} = -0.0187 + 0.0667C - 0.0514Z$$

$$G_B = 2.9240 - 0.0330(\text{ORG}) - 0.00373Z - 0.00181C$$

$$G_B = 2.8650 - 0.0472(\text{ORG}) - 0.00216Z$$

$$\text{LL} = -9.1310 + 0.8111C + 0.6065Z + 2.5166(\text{ORG})$$

$$\text{PL} = -2.1210 + 3.2367(\text{ORG}) + 0.2525C + 0.2083Z$$

$$\text{PI} = -7.0110 + 0.5586C + 0.3982Z - 0.7202(\text{ORG})$$

$$A = 0.1834 + 0.0262Z - 0.0817(\text{ORG}) + 0.00241C$$

$$\text{OMC} = 3.899 + 0.2335C + 1.797(\text{ORG}) + 0.104Z$$

$$\text{OMC} = 4.329 + 0.4308\text{PI} + 2.1171(\text{ORG})$$

$$Y_d = 2205.83 - 51.085(\text{ORG}) - 6.596C - 5.02Z$$

$$Y_d = 2114.39 - 12.248\text{PI} - 57.587(\text{ORG})$$

$$P_c = 0.7043 + 0.2073C - 0.0975Z + 0.3668(\text{ORG})$$

$$P_c = 1.139 + 0.1676C - 0.0945Z + 0.1791\text{PI}$$

$$S_c = -0.0379 + 0.0834C - 0.01695Z + 0.062(\text{ORG})$$

$$S_c = 0.605 - 0.002985C + 0.193\text{PI} - 0.0735Z$$

$$S_{cs} = 0.2319 + 0.1450C - 0.0464Z + 0.270(\text{ORG})$$

$$S_{cs} = 1.7468 + 0.052C - 0.111Z + 0.2172\text{PI}$$

$$P_i = 2.18 + 0.123C - 0.082Z + 0.189(\text{ORG})$$

$$P_i = 2.92 + 0.081C - 0.111Z + 0.107\text{PI}$$

Table 5.11 Comparison of Regressions Using Silt and Sand
respectively.

Property	F values	
	C, ORG, Z	C, ORG, S
G	6.44	6.81
LL	60.56	56.02
PL	102.27	100.99
PI	23.87	22.18
A	3.16	2.99
OMC	41.11	38.80
γ_d	30.13	29.34
P_c	43.79	39.18
S_c	24.66	20.26
S_{cs}	27.90	27.18

Table 5.12 (A). Comparison of Regressions Using Clay, Plasticity Index, Liquid Limit and Plastic Limit respectively.

Property	F Values			
	ORG, C, Z	ORG, Z, PI	ORG, Z, LL	ORG, Z, PL
OMC	41.1	68.6	52.2	23.6
γ_d	30.1	118.9	62.2	20.7
P_c	43.8	27.2	32.6	33.0
S_c	24.7	30.9	26.3	14.4
S_{cs}	27.9	52.8	41.2	19.3

Table 5.12 (B). Comparison of Regression Using Clay, Plasticity Index, Liquid Limit and Plastic Limit respectively.

Property	Simple Regression Coefficients			
	C	PI	LL	PL
OMC	.8792	.9021	.9596	.9417
γ_d	.8067	.9188	.9746	.9536
P_c	.9639	.7585	.7696	.7186
S_c	.9517	.8290	.8091	.7221
S_{cs}	.9591	.8264	.8150	.7366
P_i	.8778	.5433	.5265	.4281

Table 5.13 Comparison of Regressions Without and With Activity.

Property	<u>ORG, Z, C</u>		<u>ORG, Z, C, A</u>	
	F	Significance, %	F	Significance, %
OMC	41.1	0.1 * * *	40.6	0.1 * * *
	30.1	0.1 * * *	20.0	1.0 *
P _c	43.8	0.1 * * *	42.0	0.1 * * *
S _c	24.7	0.1 * * *	13.0	1.0 *
S _{cs}	27.9	0.1 * * *	17.6	1.0 *

Note :- Levels of Significance were read from Statistical Tables (Murdoch and Barnes, 1970); they are shown approximately because accurate estimates involved extrapolation. In the regressions without A the F values are higher, the degrees of freedom are lower and therefore the significance is greater than the regressions with A.

- * Significant
- * * Highly Significant
- * * * Very Highly Significant

matter, whilst permanent pasture would enrich it. Since some of the present soils have been in arable use for a very long period of time, whilst others had until recently been under permanent pasture for an equally long period of time, the effect of management would be expected to be large. The simple regression for organic matter against clay content shows an increasing trend as expected, Fig. 5.34, but failed to reach a statistical level of significance. The inclusion of silt content did not improve the level of significance, and the equation still remained insignificant. As can be seen from the predictive equation in Table 5.10, the effect of silt is to decrease the organic matter. As an alternative to the two variables clay and silt, the variable sand alone was considered, and this simple regression surprisingly gave correlation at 2.5% level of significance, although there is no improvement in the correlation coefficient, r^2 . This is thought to be due to more number of degrees of freedom. The correlation with sand content is as follows:

$$\text{Organic Matter} = 6.14 - 0.07S \quad (r^2 = 0.53) \quad (5.77)$$

When composition was used, the analysis was restricted to three variables since the sum of the texture is 100%. Clay was chosen as an independent variable because it was thought that this would be the best single variable. In every case except specific gravity and activity clay occurred in first or second place in the regressions and the coefficient for clay was higher than for silt. Organic matter was treated as more or less independent, and it appeared in many of the regressions as one of the more important variables. It was uncertain whether sand or silt should be used. Table

5.11 shows the result of comparing regressions against (1) silt, clay and organic matter; and (2) 'sand', clay and organic matter. For these regressions gravel content was included in the sand. The inclusion of silt was preferred because most of the F values were slightly better, although the improvement was marginal.

In order to see whether the plasticity index, plastic limit, or liquid limit would be useful, the regressions summarised in Table 5.12 (A) were made. Each contains organic matter and silt and either one of the Atterberg limits or clay. Since the number of degrees of freedom are the same throughout, the highest F value indicates the best regression. For these 10 natural Wootton Broadmead soils, plasticity index was always the best, except for swell pressure, for which the clay was the best. However, care should be taken in generalising this as the simple regression coefficients in Table 5.12 (B) show different trends in that liquid limit was best for compaction properties and clay for swell properties. The difference between the trends results from the interaction between the variables and the multiple regression equations are to be preferred.

Tables 5.12 (A) and 5.12 (B) show one interesting point in that the swell pressure, unlike the other properties, is primarily controlled by the clay both in multiple and simple regression. A simple explanation would be that all of optimum moisture content, optimum density, swell potential and swell amount are controlled by the "water-imbibing properties" of the clay, whereas in the swell pressure test the sample is prevented from imbibing water freely.

In these swell pressure tests, in which similar materials are compacted to similar conditions, it is approximately true to say that each clay particle has initially the same number of monolayers of water and each can exert the same force when free water is supplied. The resulting swell pressure is proportional to the sum of these forces, and thus to the number of clay particles. Note, however, that the most accurate model for swell pressure used plasticity index in preference to organic matter as the least important independent variable after clay and silt contents, see Table 5.9.

In order to investigate the usefulness of activity, F values were calculated for the regressions using composition alone (i.e. clay, silt and organic matter) adding activity to this composition, see Table 5.13. The inclusion of activity reduces the F value for all the properties, and therefore the levels of significance are all lower when activity is included. Thus activity seems not to be useful for these samples. However, it is necessary to test this conclusion on a larger sample before any conclusions are drawn to the usefulness of activity in predictive equations.

In the course of the above analysis, the question arose whether the effects of the clay and silt fractions were additive or not. In the equations based on composition alone in Table 5.10, the effects of the clay and silt fractions add for Atterberg limits and compaction properties, and subtract for swell properties. This trend is as might be expected as will now be explained. Both the clay

fraction and organic matter attract and hold water. During the determination of the liquid and plastic limits, the silt fraction presumably causes a minor disrupting effect, which results in small pores, which hold water. Thus the effects of clay, silt and organic matter are all additive for liquid and plastic limit. For plasticity index the positive effect of clay probably reflects the ability of clay to hold water more loosely (i.e. more layers of water for liquid limit than for plastic limit). The positive effect of silt probably associates with the filling of the larger pores which are caused by the silt, as the moisture tension falls to the lower values corresponding to the liquid limit. The negative effect of organic matter is not understood and might be an experimental error. For activity the general pattern follows the plasticity index except that the quantities differ numerically. Similarly for compaction properties, as all the samples were brought to optimum conditions, it is reasonable to expect that the effects of clay, silt and organic matter will add, as indeed they did. For swell pressure, the effects of clay and organic matter are positive, because the swell pressure is developed as these components attempt to swell. This trend is similar for both swell potential and volumetric swell amount in that both the effects of clay and organic matter are positive. However, in all cases of swelling the silt acts as an inert but disrupting material, because the double layer does not extend into the pores associated with the silt fraction. On this assumption, its net effect would be negative as indeed it is.

The role of silt in the various equations discussed above has one important implication, concerning the prediction of the swell properties from the Atterberg limits and placement properties. Predictions which ignore the silt fraction may be erroneous, because the silt has opposite effects on the dependent variables (swell) and on the independent variables (LL, PL, PI, OMC, etc). This may partly explain the impreciseness of many of the predictive theories suggested by earlier investigators. These earlier predictive theories will be discussed further in Part-III of this chapter.

For each property, the best predictive equation in Table 5.10 was used to make observed versus predicted plots for the various properties considered in this study. These are shown in Figs. 5.53 to 5.61 (A). These provide a visual check on the accuracy of the equations considered, and there are no outlying points in those of the regressions which were highly significant.

It was originally intended to test these predictive equations on the data of earlier investigators, however, no suitable data on natural soils has been found. The earlier investigators either published the data of artificial mixtures (Seed et al, 1962; Nayak and Christinsen, 1971, etc), or those who dealt with natural soils (Komornik and David, 1969; Vijayvergiya and Glazzaley, 1973; etc) concentrated on clay fraction and Atterberg limits.

5.4.5 Summary of Discussions on Natural Soils

It was found possible to establish accurate empirical

$$\text{ORG} = -0.0187 + 0.0667C - 0.0514Z$$

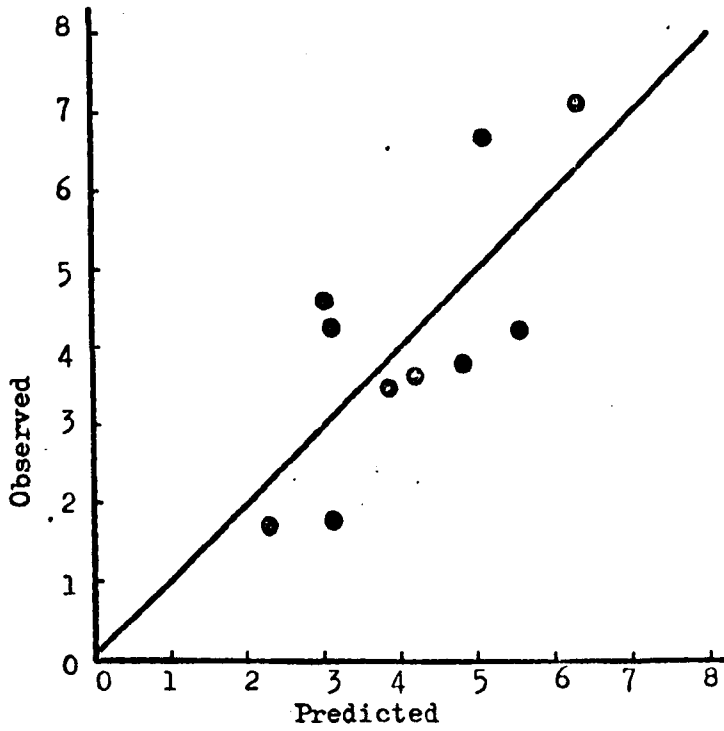


Fig.5.53 Organic Matter: Observed VS Predicted,
Natural Soils.

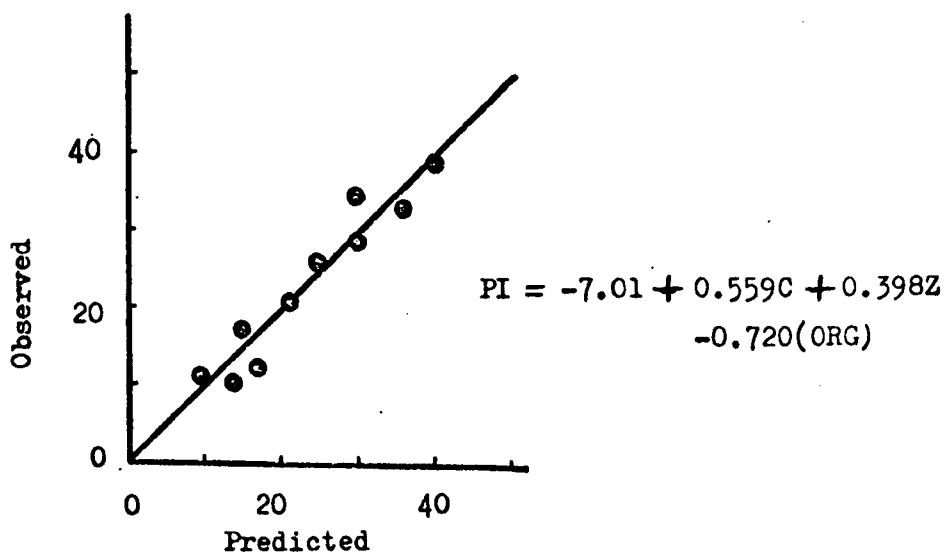
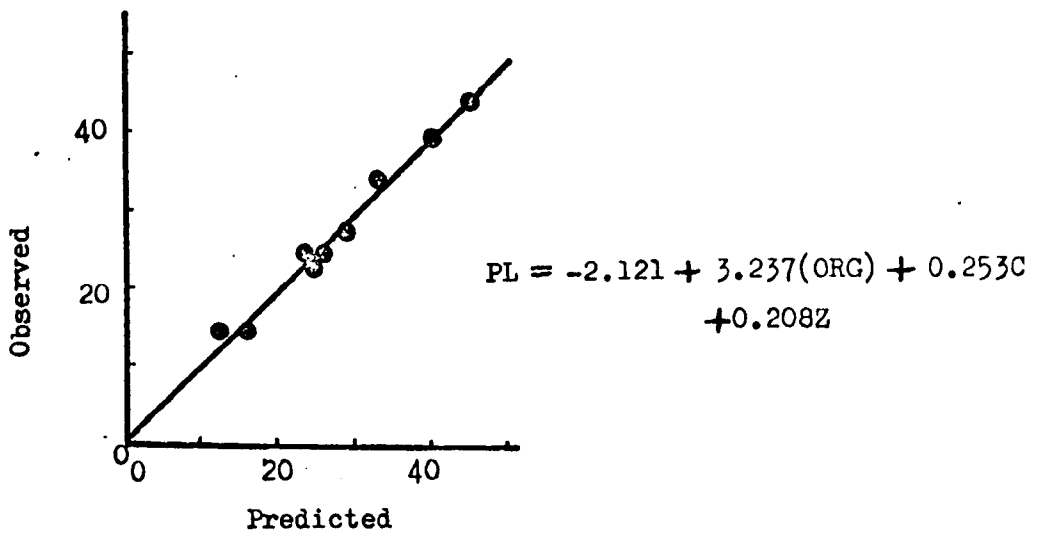
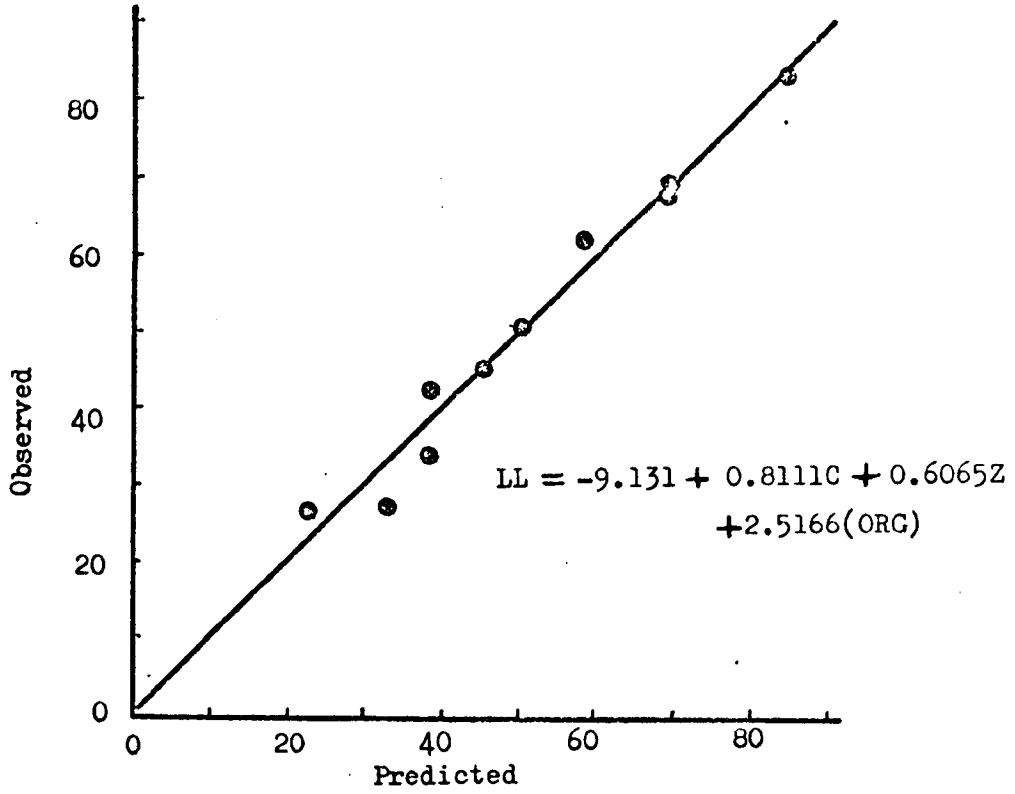


Fig.5.54 Atterberg Limits: Observed VS Predicted,
Natural Soils.

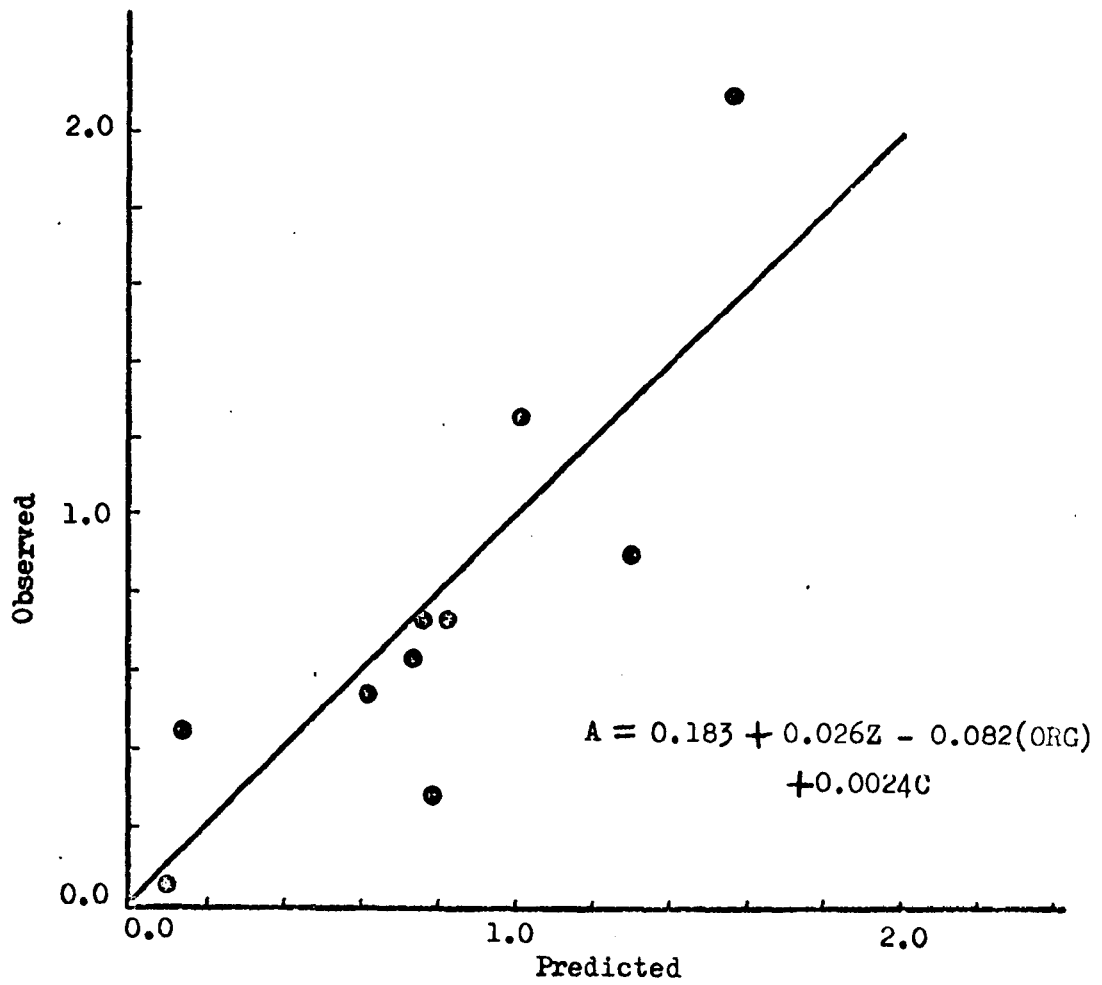


Fig.5.55 Activity: Observed VS Predicted, Natural Soils.

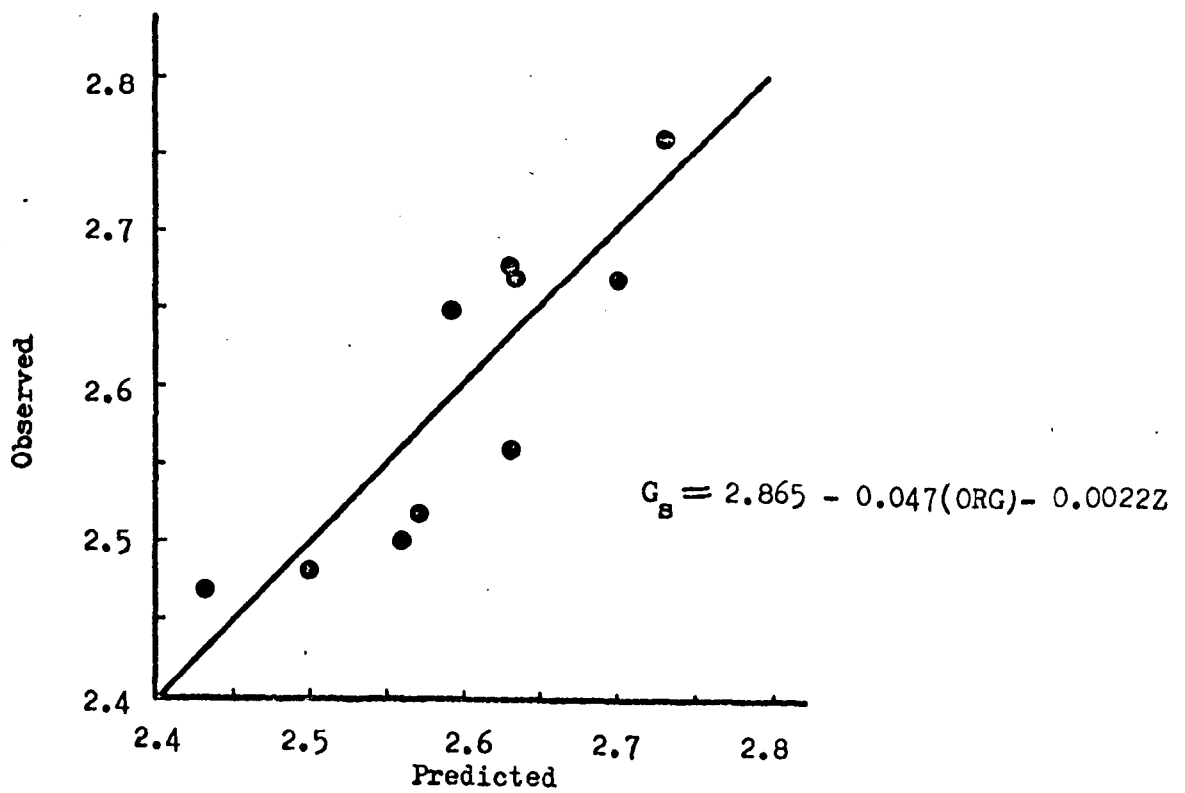


Fig.5.56 Specific Gravity: Observed VS Predicted, Natural Soils.

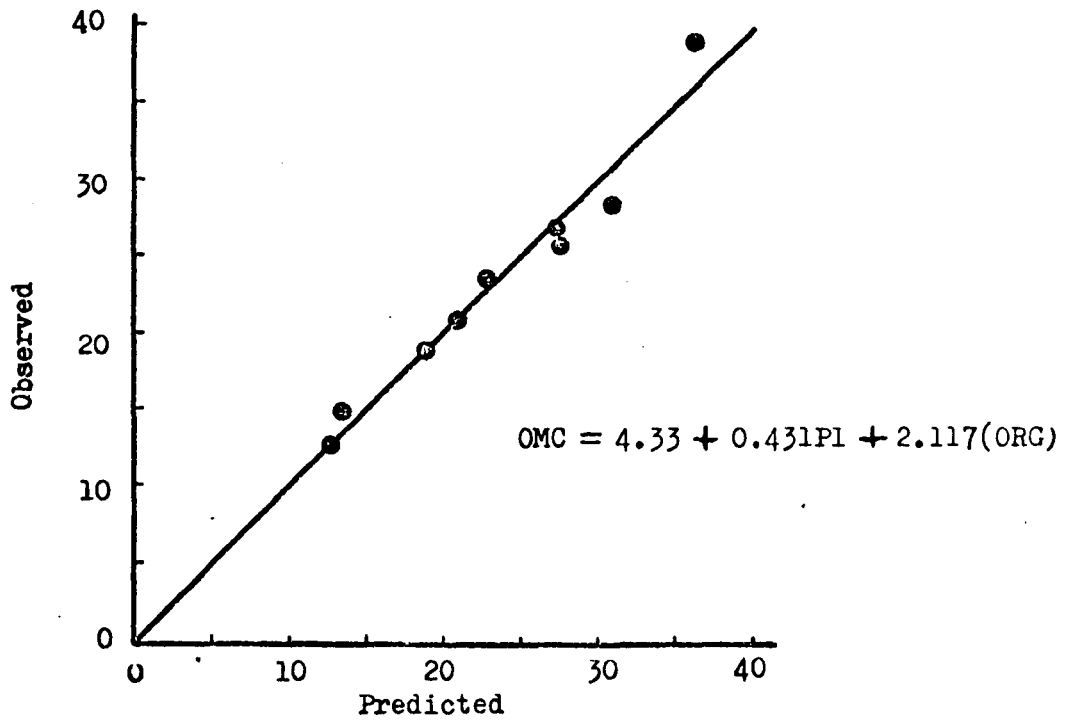


Fig.5.57 Optimum Moisture Content: Observed VS Predicted, Natural Soils.

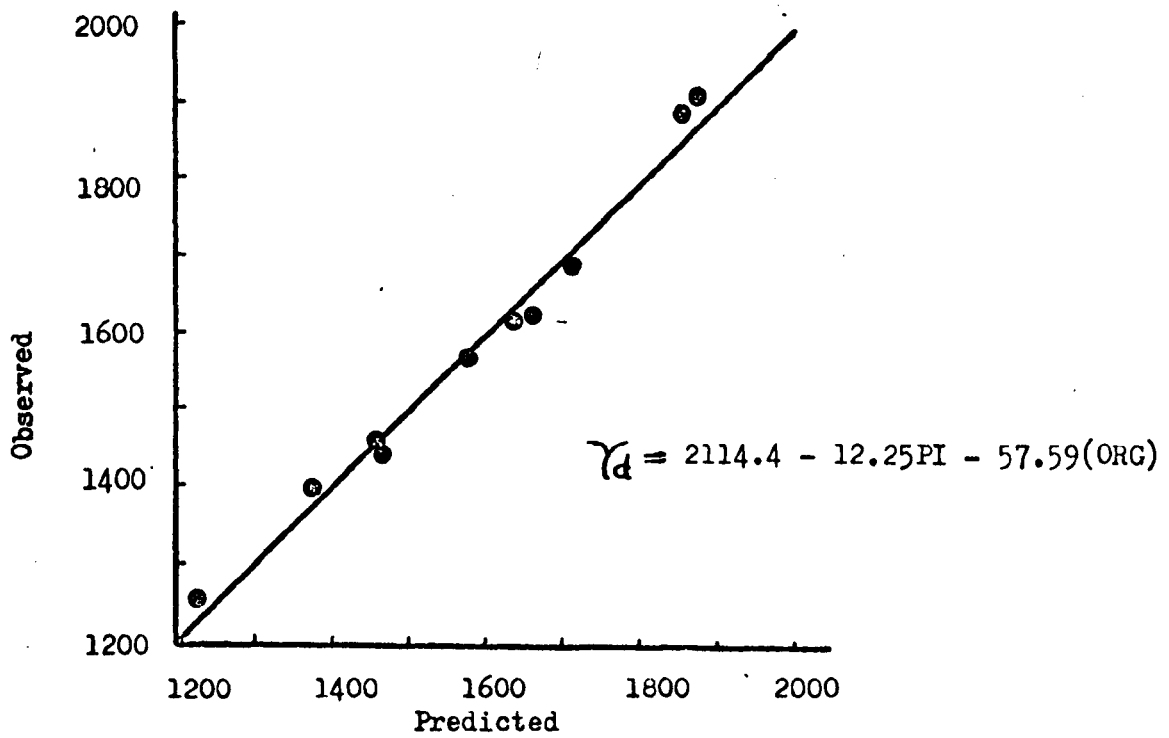


Fig. 5.58 Optimum Dry Density: Observed VS Predicted, Natural Soils.

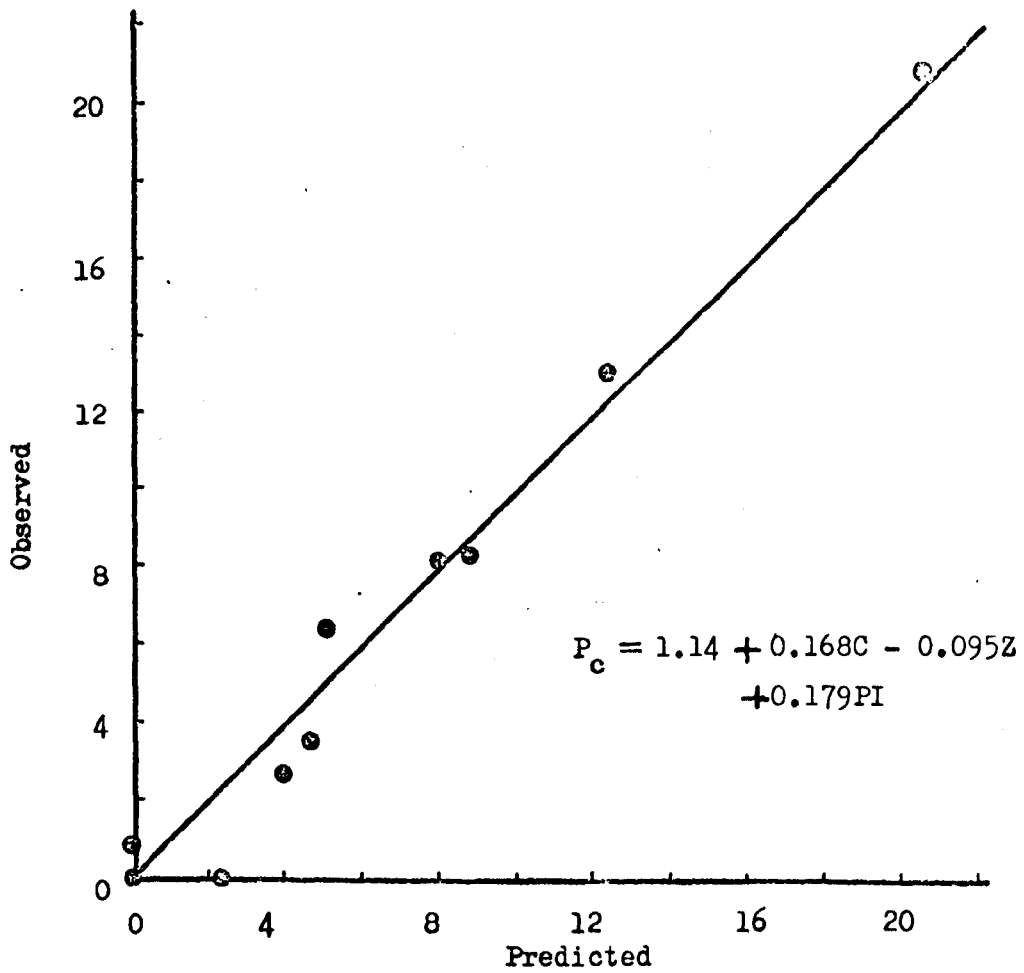


Fig.5.59 Laterally Confined Swell Pressure: Observed VS Predicted, Natural Soils.

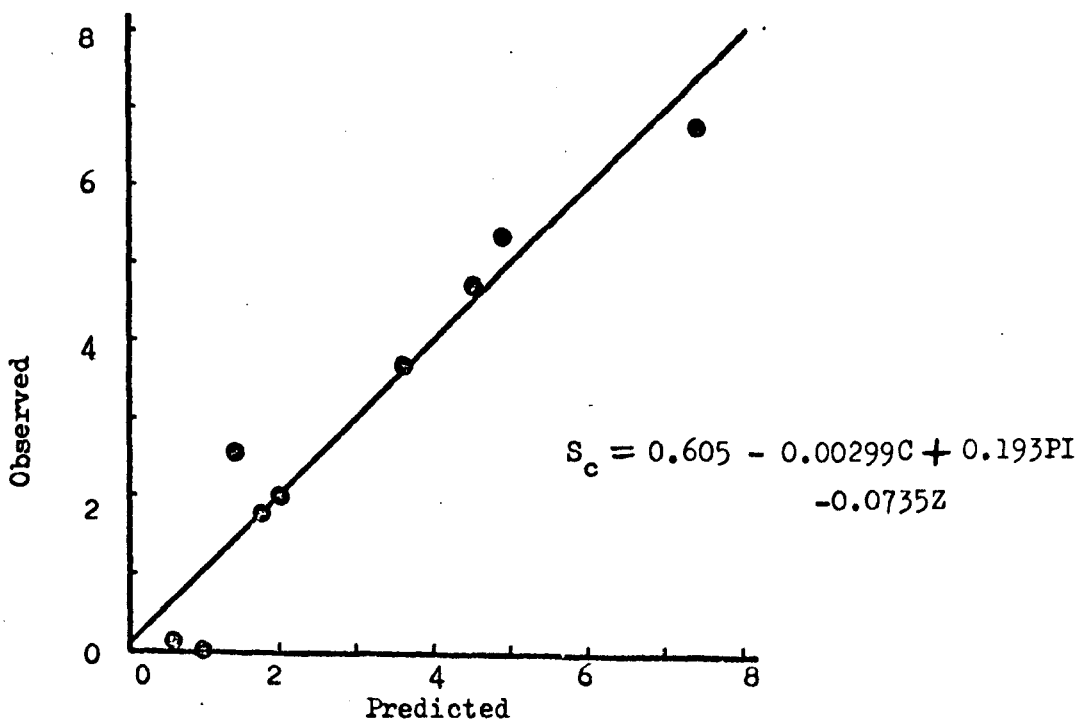


Fig.5.60 Laterally Confined Swell Potential: Observed VS Predicted, Natural Soils.

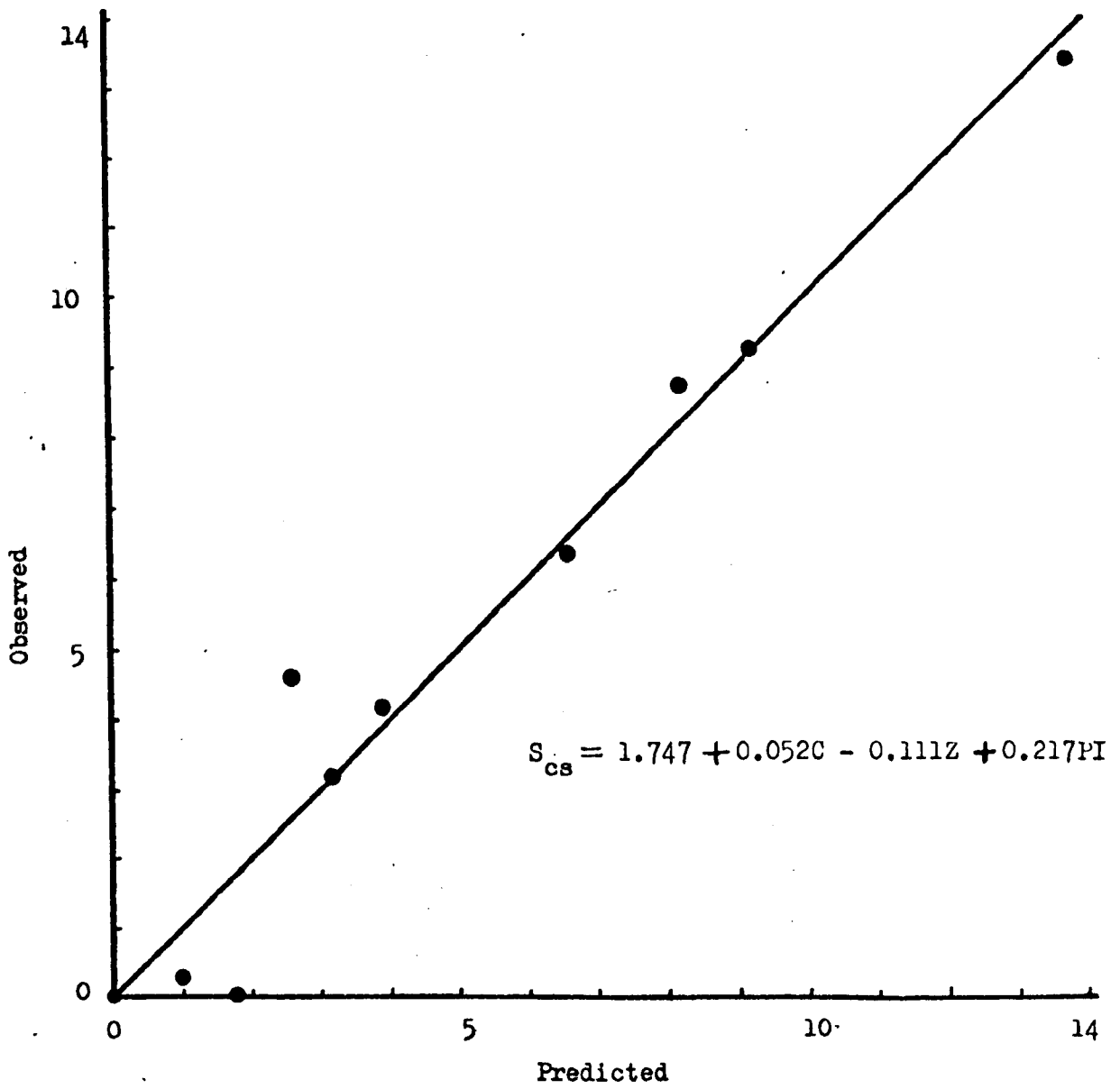


Fig.5.61 Swell Amount: Observed VS Predicted, Natural Soils.

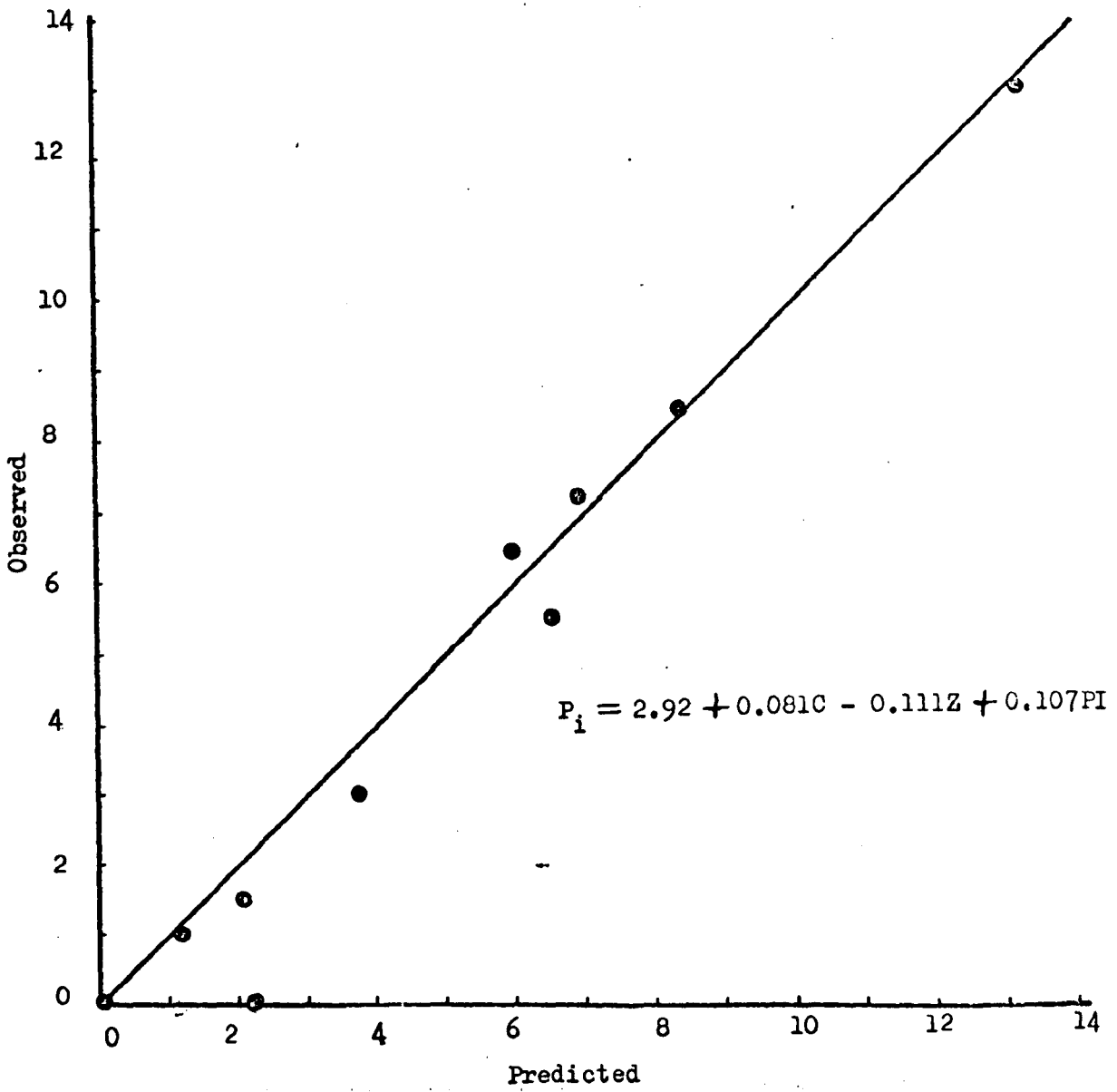


Fig. 5.61(A) Isotropic Swell Pressure: Observed VS Predicted,
 .Natural Soils.,

equations to predict the swell (and other) properties of soils in two quite different ways. In the case of the predictions based on clay content alone which were studied here, in addition to geological and mineralogical similarity, it was necessary for the soils to have a "family likeness" to each other, which was tested in terms of their particle size analysis. However, if the predictions were to be used for all the ten of the soils considered, it was found necessary to use independent variables additional to clay content. Two conclusions follow:

- (1) When working in a restricted area with a restricted range of soils, it is possible to make accurate predictions from equations whose validity is local.
- (2) When attempting to establish predictive equations for wide scale use, care must be taken to ensure that the samples on which the equations are based do contain representation of all types of soil to be found in the wide area of intended validity.

Predictive equations based on clay content, silt content, organic matter content, and plasticity index were found to be accurate. In general, plasticity index was found to be better than either liquid limit or plastic limit for this purpose. Somewhat surprisingly, clay content was found to be the most significant single variable to predict the swell pressure of natural soils, and the Atterberg limits were not required in the equation for swell pressure based on multiple regression. Although an explanation was advanced above, this point seems to

require further study using a wider range of soils.

In view of the absence of silt content from all the predictive equations in Chapter 4, the importance of silt content is remarkable. It was noticed that the contribution of silt to the Atterberg limits is opposite to its contribution to the swell properties. This must place a second restriction on the usefulness of the Atterberg limits in predicting swell properties in addition to the effect of clay type which was noted in Part-I. It is recommended that further consideration should be given to the use of silt content in these predictions, especially as it involves very little, if any, additional testing.

As expected from the tests on artificial mixtures in Part-I, it was found from the multiple regression analysis that the swell amount could be predicted with comparatively higher significance than could swell potential. (However, this improvement was not found for compaction, see Appendix 11.)

This discussion completes the main part of this thesis, the most important conclusions being:

1. the importance of silt in predictive equations;
2. the different patterns of behaviour of bentonite and illite, especially for swell pressure; and
3. the importance of swell amount rather than the swell potential.

Before presenting the conclusions formally in Chapter 6, the earlier predictive theories will be discussed in Part III

below.

Part-III: EARLIER PREDICTIVE THEORIES

5.5 INTRODUCTION

The data from Part-II (and Part-I) above are used here to reconsider the earlier predictive equations which were discussed in Chapter-4, taken in the same order.

5.5.1 Holtz and Gibbs (1956)

Using the limits in Table 4.1 as data for a regression analysis, Holtz and Gibbs (1956) probable expansion is given by:

$$\text{Probable Expansion} = 5.2814 + 0.9091 \text{ PI} - 0.4762C \quad (R^2 = 0.90) \quad (5.8)$$

where C is the clay content less than one micron. A similar regression for the natural soils of the present study yields the following equation for swell potential:

$$S_c = -0.7537 + 0.0117 \text{ PI} + 0.0888C \quad (R^2 = 0.91) \quad (5.9)$$

where C is the clay content less than two microns.

Although both the above equations (Eqns. 5.8 and 5.9) are highly significant, the trends of the parameters involved show an opposite effect in that the probable expansion decreases with clay fraction whereas swell potential increases. It is difficult to see why this difference should occur. In Holtz and Gibb's case plasticity index is more important than clay content whereas in the present study clay is more important than plasticity index. Therefore, it seems possible that these differences are due to the different

soils involved, and that different prediction equations are required for the two areas involved. The biggest calculated discrepancy is 56% at 100% clay content; viz, -47.62% for probable expansion and +8.88% for swell potential.

5.5.2 Williams (1957)

The values of swell potential measured in the present study both on artificial mixtures and natural soils were plotted in William's Chart, see Fig. 5.62. The measured swell potential is shown beside each point. For each of William's four groups of soils, the extreme values of swell potential were noted and are shown below.

<u>Degree of Swell</u>	<u>Swell Potential</u>
Low	0.0 - 2.6%
Medium	0.0 - 10.8%
High	1.8 - 17.5%
Very High	4.8 - 87.3%

Although the details are not fully satisfactory, the trends are as expected. Thus, Williams Chart appears to be useful for a preliminary classification of expansive soils.

5.5.3 Dinesh Mohan (1957)

In order to investigate the dependence of the swell characteristics on the liquidity index and liquid limit as suggested by the work of Dinesh Mohan (1957), these two variables were regressed separately with swell potential, swell amount and swell pressure. The swell characteristics did not correlate with liquidity index, presumably because

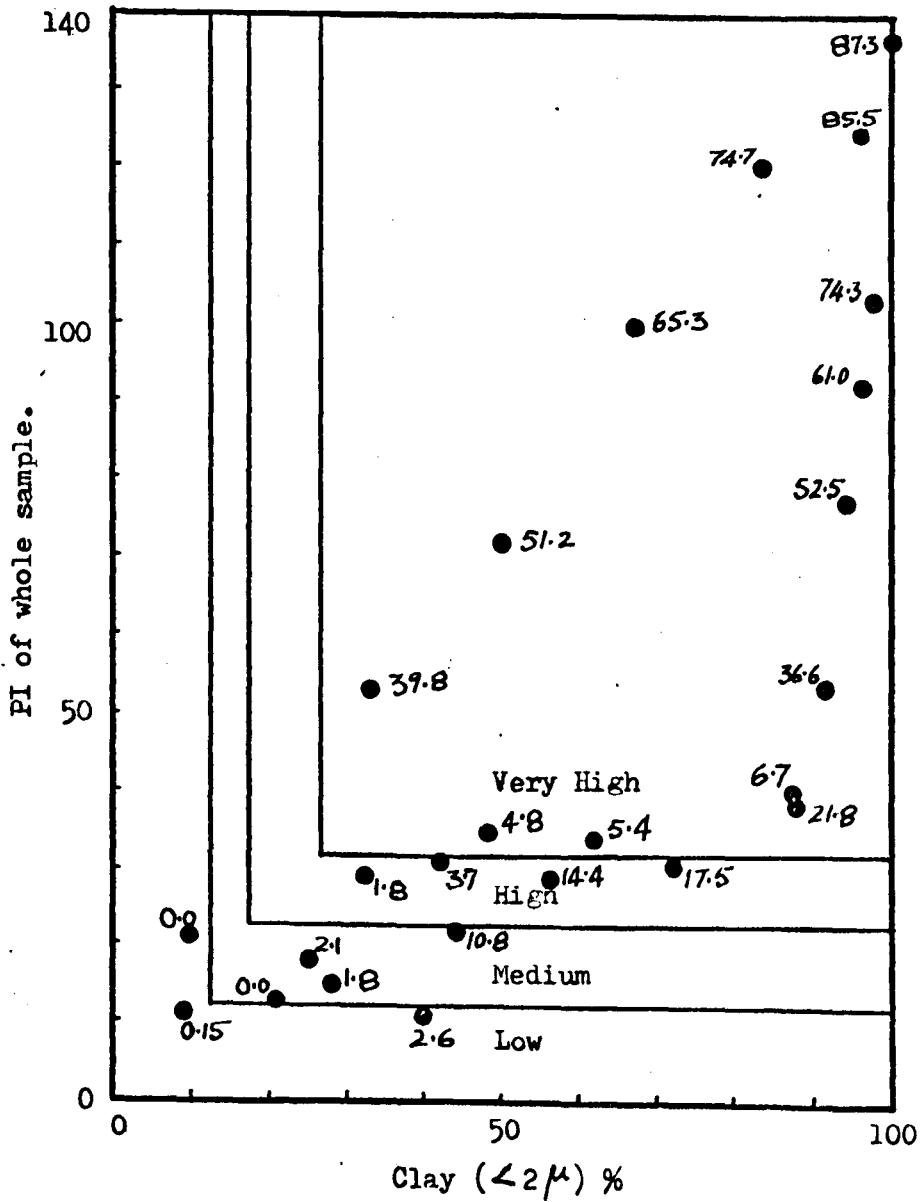


Fig. 5.62 William's (1957) Chart (Points show the Swell Potential Values measured in the Present Study)

the present experiment had been designed in effect to eliminate the effect of liquidity index. All the swell properties did correlate well at 1% level of significance with liquid limit, so the idea was at least partly correct. However, it was shown in Part-II that in the present samples plasticity index is a better parameter than liquid limit.

5.5.4 Seed et al (1962)

Seed et al (1962) gave their final equation for swell potential, Eqn. 4.11, in terms of plasticity index and clay fraction, viz:-

$$S_c = 3.6 \times 10^{-5} PI^{2.44} C \quad (5.10)$$

The predicted values of swell potential using this equation are shown in Table 5.14, and are plotted against the observed values for the natural soils in Fig. 5.63. It can be seen from Table 5.14 that Seed et al's equation overestimates the values to an unacceptable limit for both the artificial and natural samples. By using the data of the present natural samples, a multiple regression of $\log S_c$ against $\log PI$ and $\log C$ yielded:

$$\log S_c = -0.7291 + 0.3561 \log PI + 1.10 \log C \quad (R^2 = 0.93) \quad (5.11)$$

i.e.

$$S_c = 0.187 PI^{0.3561} C^{1.10} \quad (5.12)$$

The above equation is significant at the 1% level only, this being less satisfactory than those in Table 5.9, which are linear. Further, the numerical values of the coefficients are different from Seed et al's. In view

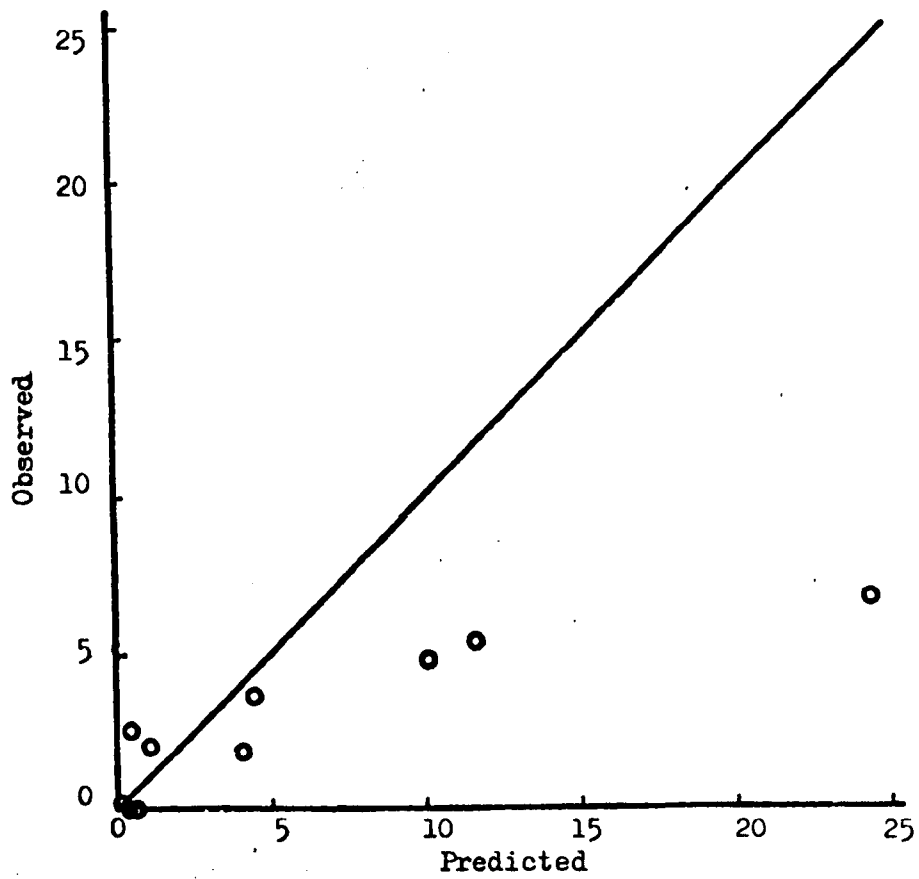


Fig. 5.63 Prediction of Swell Potential by Seed et al's Equation (eqn.4.11), Natural Soils.

Table 5.14 Prediction of Swell Potential.

Series	Composition	Observed Value of S_c (%)	Seed et al (1962) Eqn. (4.11)	Nayak & Chris-tinsen Eqn. (4.24)	Vijay-vergiya & Ghaz-zaley (1973) Eqn. (4.26)	Chen (1975) Eqn. (4.27)	From Multiple Regression Equation †
Bent - Sand	Bent. 100%	79.4	591	53.4	61.7	25185	27.2
	Bent. 83.3%	74.7	354	46.2	47.9	6009	23.8
	Bent. 66.7%	65.4	180	35.9	24.0	1060	20.1
	Bent. 50.0%	51.3	51	24.6	18.6	71	14.7
	Bent. 33.3%	39.9	19	18.6	9.6	22	10.9
	Bent. 16.7%	22.2	4	10.6	3.0	5	0.6
Illite - Sand	Illite 100%	21.8	23.6	21.2	3.5	6.5	8.5
	Illite 82%	17.5	11.3	16.2	2.4	3.4	6.8
	Illite 64%	14.4	7.4	14.3	2.1	2.9	6.2
	Illite 50%	10.8	3.0	11.3	1.7	1.6	5.0
	Illite 32%	1.8	0.8	8.7	1.8	0.9	3.5
	Illite 14%	0.5	0.1	7.0	1.3	0.6	0.6
Bent - Illite	Bent. 100%	88.3	588	62.1	437	25185	27.2
	Bent. 83.3%	85.5	454	67.8	513	8473	24.6
	Bent. 66.7%	74.3	283	58.5	214	1446	20.5
	Bent. 50.0%	61.1	210	52.0	112	575	18.4
	Bent. 33.3%	52.4	133	41.4	49	166	15.5
	Bent. 16.7%	36.6	56	28.9	9	24	11.0
Natural Soils (arranged in decreasing Clay Content)	350 - 8	6.7	24.3	16.7	0.6	6.9	7.4
	5	5.4	11.7	15.4	3.9	4.2	4.9
	4	4.8	10.1	13.4	2.0	4.8	4.5
	1	3.7	4.5	10.9	1.5	2.3	3.6
	7	2.6	0.5	7.9	1.0	0.7	1.4
	9	1.8	4.1	9.7	2.3	2.8	1.8
	3	2.1	1.1	8.2	1.4	1.2	2.1
	2	0.0	0.4	7.6	1.3	0.7	1.0
	10	0.0	0.6	7.3	1.9	1.5	0.1
6	0.2	0.1	6.9	1.9	0.7	0.6	

† Multiple Regression Equation with higher significance for S_c was used from Table 5.10.

of this it is thought that Seed et al's predictive equation should be restricted to the region from which the samples on which it was based were obtained.

5.5.5 Da Nilov (1964)

The index suggested by Da Nilov (1964) was calculated for the natural soils and tabulated in a decreasing order in Table 5.15 . The index values show that four of the ten natural Wootton Broadmead soils fall in the swelling group and the other six in the slumping group. None of the soils can be classified as ordinary soils, in Da Nilov's system. Values of swell pressure, swell potential and swell amount for the present natural samples are also shown in Table 5.15. From these it appears that although the trend of results is correct, the ranking achieved is imperfect especially for samples 7, 3 and 9. The imperfection is presumably because the only soil property considered by Da Nilov is liquid limit.

5.5.6 Ranganatham and Satyanarayana (1965)

Although no rigorous test of Ranganatham and Satyanarayana's (1965) predictive equation was possible in the present study, the results of making the approximation that plasticity index is equal to shrinkage index is shown in Fig. 5.64, the trend is correct but there is large scatter for low swelling soils, perhaps because the approximation is a bad one. It is of interest to note here that Seed et al (1962) and Ranganatham and Satyanarayana (1965) made a similar approach with the only difference that the former used plasticity index, whilst the latter used shrinkage index.

Table 5.15 Da Nilov's Index For Natural Soils.

Soil No.	Da Nilov's Index, %	P _c (psi)	S _c %	S _{cs} %	Da Nilov's Classification
350-8	-57	21.00	6.73	13.3	'SWELLING'
350-5	-57	13.10	5.40	9.3	
350-9	-52	2.55	1.82	3.2	
350-4	-45	8.30	4.80	8.8	
350-1	-39	8.20	3.70	6.3	'SLUMPING'
350-10	-38	0.00	0.00	0.0	
350-3	-31	3.50	2.10	4.2	
350-7	-24	6.40	2.60	4.7	
350-2	-22	0.00	0.00	0.0	
350-6	-20	0.96	0.15	0.2	

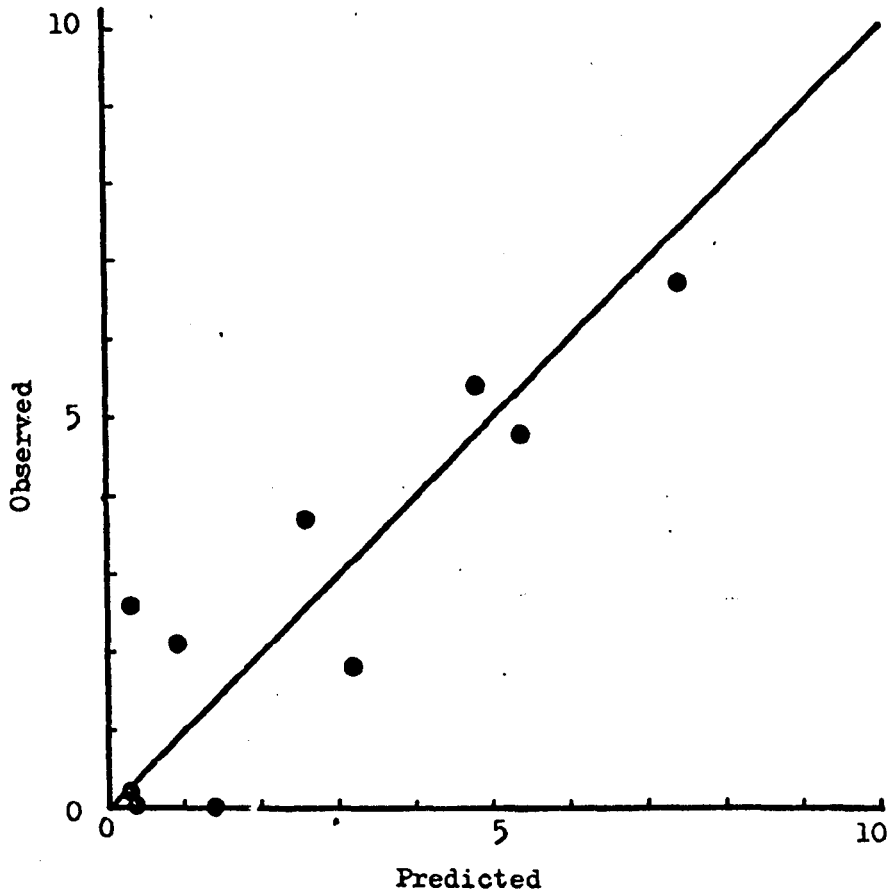


Fig. 5.64 Prediction of Swell Potential by Ranganatham and Satyanarayana's Equation (eqn. 4.19) assuming $PI=SI$, Natural Soils.

Nayak and Christinsen (1971) compared both these methods using the soils tested by Seed et al, and concluded that Ranganatham and Satyanarayana's method gives comparatively less scatter. They noticed that by suitable but undisclosed adjustment of the constant in Ranganatham and Satyanarayana's original equation, viz:-

$$S_c = 41.13 \times 10^{-5} \text{ SI}^{2.67} \quad (5.13),$$

the agreement would be better than that obtained by any of the equations proposed by Seed et al. They concluded that for the soils studied by Seed et al, shrinkage index is a considerably better indicator for swell potential than plasticity index.

5.5.7 Komornik and David (1969); Livneh et al (1969)

Predicted values of swell pressure from Komornik and David's (1969) equation are shown in Table 5.16, and are unsatisfactory when compared with the observed values. A multiple regression on the Wootton Broadmead soils using the same variables as Komornik and David, yielded:

$$\log P_c = 3.135 - 0.0017 \gamma_d + 0.0346 W_i - 0.01242 \text{ LL} \quad (R^2=0.61) \quad (5.14)$$

Komornik and David's equation, Eqn. 4.20, was:

$$\log P_c = \bar{2}.132 + 0.00065 \gamma_d - 0.0269 W_i + 0.0208 \text{ LL} \quad (5.15)$$

These two equations are different in their trends and numerical coefficients. The equation for Wootton Broadmead soils is statistically insignificant which indicates that

dry density, initial moisture content and liquid limit are not the correct choice for the present samples. Nayak and Christinsen (1971) tested Komornik and David's equation and found it unsuitable for their samples.

Table 5.16 also shows the predictions given by Livneh et al's modification of Komornik and David's method. (This uses the graph in Fig. 4.3). These seem to be unsatisfactory for both the natural and artificial soils. No calculations could be made for most of the bentonite soils because the value of λ for these soils is beyond the range suggested by Livneh et al.

Both Komornik and David's and Livneh et al's equations require modification to incorporate soil properties other than liquid limit, e.g. clay fraction, silt fraction, cementing agents like organic matter and plasticity index (see section 5.4.4).

5.5.8 Nayak and Christinsen (1971)

Nayak and Christinsen's (1971) semi-empirical equation for swell pressure,

$$P_c = 3.5817 \times 10^{-2} \text{ PI}^{1.12} \frac{C}{W_1^2} + 3.7912 \quad (5.16)$$

was found to be the nearest in predicting the observed values, see Table 5.16 and Fig. 5.65. However, their equation for swell potential,

$$S_c = 2.29 \times 10^{-2} \text{ PI}^{1.45} \frac{C}{W_1} + 6.38 \quad (5.17)$$

overestimates the observations (see Table 5.15) and is unsatisfactory for practical use. Their success with their swell pressure equation may result from the fact that they

Table 5.16 Prediction of Swell Pressure.

Series	Composition	Observed Value of P_c (psi)	Komonik and David (1969) Eqn. (4.20)	Livneh et al (1969)	Nayak & Christensen (1971) Eqn. (4.23)	Vijay-vergiya & Ghaz-zaley (1973) Eqn. (4.25)	From Multiple Regression Equation †
Bent - Sand	Bent.100%	42.8	189.9	--	27.4	311.2	42.4
	Bent.83.3%	38.8	102.2	--	25.3	241.2	36.5
	Bent.66.7%	33.7	52.6	--	20.3	121.4	30.1
	Bent.50.0%	28.0	25.0	--	16.5	93.8	22.2
	Bent.33.3%	20.6	13.7	56.6	12.4	48.2	16.2
	Bent.16.7%	11.2	6.4	28.3	5.8	15.2	4.0
Illite - Sand	Illite 100%	39.9	10.0	30.2	26.2	17.4	21.8
	Illite 82%	36.6	7.3	9.2	18.3	11.8	17.8
	Illite 64%	23.6	6.3	15.9	14.6	10.7	14.9
	Illite 50%	18.7	5.1	6.2	10.5	8.7	11.9
	Illite 32%	9.2	4.8	11.9	6.7	9.2	8.1
	Illite 14%	3.5	2.9	0.0	4.3	6.5	3.0
Bent - Illite	Bent.100%	52.2	212.5	--	37.2	2194	42.4
	Bent.83.3%	51.8	271.8	--	52.0	2583	37.3
	Bent.66.7%	50.5	153.9	--	52.3	1052	30.8
	Bent.50.0%	49.8	99.7	--	49.2	565	26.0
	Bent.33.3%	46.7	49.0	--	40.4	247	20.5
	Bent.16.7%	43.7	18.7	--	32.1	47	13.7
Natural Soils (arranged in decreasing Clay Content.	350 - 8	21.00	6.2	30.6	14.4	4.7	20.5
	5	13.10	9.1	45.0	14.6	19.60	12.4
	4	8.30	6.4	7.5	9.8	10.3	8.8
	1	8.20	5.2	6.0	8.1	7.2	8.0
	7	6.40	3.8	13.5	6.2	5.1	5.2
	9	2.60	7.1	30.0	5.7	11.8	3.9
	3	3.50	4.7	6.0	5.1	7.2	4.4
	2	0.00	4.7	--	4.9	6.5	2.1
	10	0.00	5.5	10.5	4.1	9.3	0.0
6	0.96	5.4	18.2	4.1	9.3	0.0	

† Multiple Regression Equation with higher significance for P_c was used from Table 5.10.

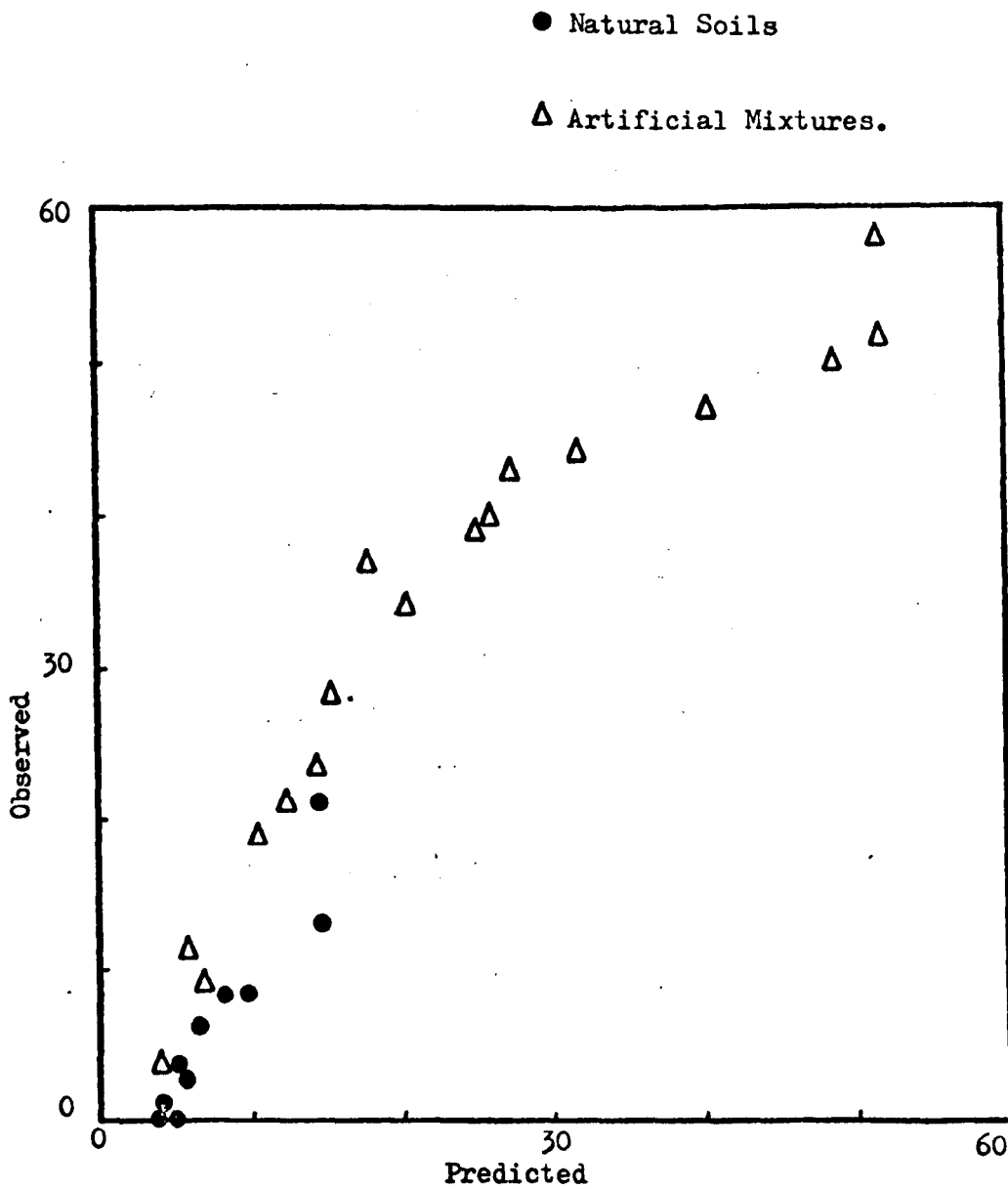


Fig.5.65 Prediction of Swell Pressure by Nayak and Christinsen's Equation (eqn. 4.23), All Soils.

consider clay content, which is the single most important variable that controls swell pressure, as has been found in the present study. However, Fig. 5.65 does suggest that there is a small systematic error in this prediction.

5.5.9 Vijayvergiya and Ghazzaley (1973)

Predictions from Vijayvergiya and Ghazzaley's equations,

$$\log S_c = \frac{1}{12} (0.4LL - W_i + 5.5) \quad (5.18)$$

$$\log P_c = \frac{1}{12} (0.4LL - W_i - 0.4) \quad (5.19)$$

are shown in Tables 5.15 and 5.16, and are not satisfactory. For Wootton Broadmead soils the following equation was obtained for swell potential, viz:-

$$\log S_c = -0.3467 + 0.0212 W_i + 0.0046LL (R^2=0.61) \quad (5.20)$$

The above equation is statistically insignificant. No equation was obtained for swell pressure because the computer rejected Vijayvergiya and Glazzaley's form of equation as insignificant before completing the calculations. Again it appears that soil properties other than liquid limit are necessary.

5.5.10 Chen (1975)

The predicted values using Chen's equation,

$$S_c = 0.2558 \exp (0.0838 PI) \quad (5.21)$$

are shown in Table 5.14. As the equation is an exponential type, it predicts unacceptably high values for the bentonite soils whose plasticity index is very high, and underestimates for the illitic soils. However, the predictions for the Wootton Broadmead soils are in reasonable agreement with the observed values see Fig. 5.66. However, for the low

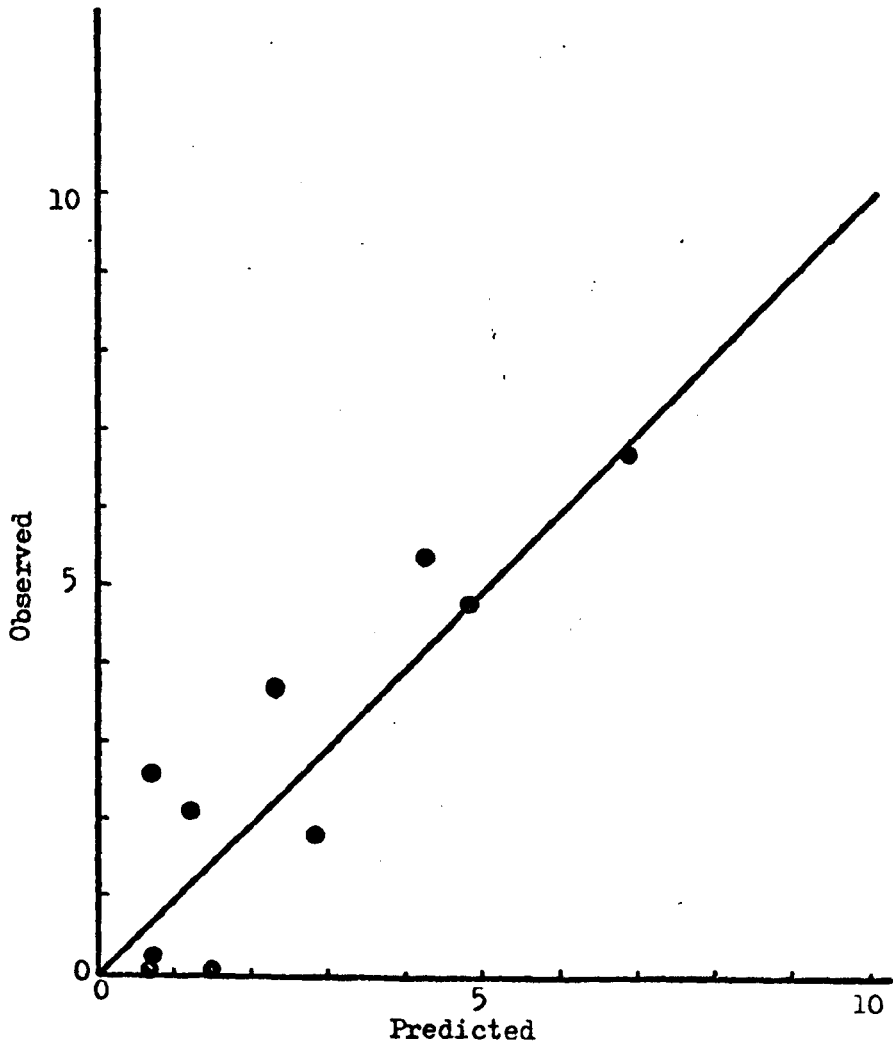


Fig.5.66 Prediction of Swell Potential by Chen's Equation (eqn. 4.27), Natural Soils.

swelling soils, the error in swell potential is $\pm 2\%$, which could represent an error of several hundred percent of the true value. Fig. 5.60 shows a better prediction on the basis of linear multiple regression.

5.5.11 Summary of Earlier Predictive Theories

Of the earlier predictive theories considered above, Nayak and Christinsen's (1971) equation for swell pressure gave a reasonably accurate prediction for both the natural and artificial soils considered here. None of the theories for swell potential was entirely satisfactory, although Chen's (1975) and Ranganatham et al's (1965) equations were reasonably satisfactory for the natural soils studied here. Nayak and Christinsen's (1971) approach was based on clay content, plasticity index and initial water content; Chen's (1975) approach on plasticity index; and Ranganatham et al's (1965) approach on shrinkage index. As the natural soils in the present study were few in number, closely related to each other, and basically illitic, it is not known whether the above agreement obtained here is real or fortuitous. There is also the problem that these earlier theories differ amongst themselves, for example, even though Seed et al (1962) and Chen (1975) both used plasticity index alone, Seed et al's predictions for the soils studied here were inaccurate. Apart from any differences which may result from differences in the method of measuring the swell properties, the work presented here suggests that there are three factors contributing to these inaccuracies: (1) the different patterns of behaviour associated with the different clay minerals; (2) the complexity

of the effect of texture, as shown by the importance of silt content; (3) the possibility that all of the correlations found so far are of local validity only, as shown indirectly by the improvement obtained when samples 6, 7, 9, and 10 were excluded in Part-II. In general, a fourth factor would be expected to contribute, viz; the effect of cementing agents. The immediate conclusion, therefore, is that it is possible to establish predictive equations which are accurate; but in the present state of knowledge it is necessary to check that any such equations which are used in practice are not used outside the sphere of their validity and are, in fact, accurate for the soils for which they are used.

In a wider context, if predictive equations which are accurate for a wide range of soils are to be obtained, further research will be required. Two immediate steps are recommended:

1. If the data can be obtained, to reconsider the data collected by earlier workers paying particular attention to silt content.
2. To extend the present work on natural soils to a series of closely related montmorillonitic soils.

Chapter 6

CONCLUSIONS AND RECOMMENDATIONS

6.1. INTRODUCTION

It is recognised that the following factors influence the swell properties of soils:-

- (a) type of clay
- (b) texture:
 - clay content,
 - silt content,
 - sand content,
 - gravel content.
- (c) organic matter content
- (d) initial conditions:
 - soil structure,
 - moisture content.
- (e) shape of sand particles
- (f) cementing agents
- (g) composition of pore fluid,
 - including absorbed ions.

In this study attention was concentrated on type of clay, texture and organic matter content. The other factors were not measured on natural soils, since they were not required for the analyses presented in Chapter 5. It is considered that the influence of these factors, (d) to (g), was minimal for the reasons discussed below.

The initial conditions were standardised. The influence of the shape of the sand particles was definitely eliminated in the artificial mixtures, since they all contained the same sand. It was probably eliminated in the natural soils, since they were all selected from a similar source. All the samples were remoulded, thereby minimising the effects of any cementing agents which may have been present. All the samples were mixed using distilled water, so that the composition of the pore fluid was controlled mainly by the salts associated with the clay and organic matter, which were definitely similar in the artificial mixtures, and probably similar in the natural ones.

The more important conclusions of the thesis and recommendations for further research have been presented in this Chapter.

6.2 CONCLUSIONS

(A) The following conclusions were reached with regard to the apparatus which was designed and used in the present study to measure the swell properties:

(1) Swell pressure measurements are subject to a systematic underestimate resulting from bedding and other errors. In the apparatus used here, it was estimated that the samples due to these errors expanded by approximately 1.0 to 1.5% volumetric strain, which resulted in an underestimate of the swell pressure of say 15% or more. Similar errors are thought to occur in all other apparatus.

(2) Calculations showed that the use of strain gauges

instead of proving bars for swell pressure measurement would decrease the volumetric expansion of the sample. This method of measurement was found to be satisfactory.

- (3) Observations showed that the apparatus for isotropic swell pressure measurement was subject to temperature effects. Calculations indicated that apparatus for laterally confined swell pressure measurement are also affected by temperature fluctuations. Swell pressure tests should therefore be conducted in a temperature controlled environment. The temperature effect is relatively more severe for the low swelling soils.

(B) The following conclusion was reached regarding the development of swell pressure:

- (4) In all the swell pressure tests, the observed swell pressure dropped after reaching a maximum. In one extra-long term test it was found that the swell pressure rose to a maximum and then fell to a steady value. Of three hypotheses considered, stress relaxation was thought to be the most likely reason for this behaviour.

(C) The following conclusions were reached with regard to the study of artificial mixtures comprising illite-sand, bentonite-sand, and bentonite-illite:

- (5) For the mixtures studied the Atterberg limits show a linear variation with clay content, below about 70% sand content. Skempton's activity, A , was also found to vary with sand content, so that it was not

a function of clay type alone as is often suggested.

- (6) In the clay-sand mixtures, both optimum moulding water content and maximum dry density, as measured in the standard compaction test, approximated to linear functions of composition, when all quantities were expressed volumetrically. However, there were weak interaction effects between clay and sand in the illite-sand mixtures.
- (7) In the clay-sand mixtures, whilst the swell potential itself was found to be non-linear with composition, the transformation of data to a volumetric basis (i.e. swell amount) enabled the variation with composition to be represented by a linear model. There were again weak interaction effects in the illite-sand mixtures.
- (8) In the clay-sand mixtures, the swell pressure variation was essentially non-linear. In the bentonite-sand mixtures, the bentonite dominated the behaviour over the entire range of the composition, whilst in the illite-sand mixtures the predominant component in the mixture dominated the behaviour. This pattern of behaviour was found to be similar to that shown by Kenny's (1967) results for $\tan \phi_r$. It was suggested that the differences in behaviour between the bentonite and the illite were due to the relative importance of physico-chemical effects and mechanical-friction effects for the two clays.

(9) In the bentonite-illite mixtures, the dependence on composition of all the properties considered here was exactly or almost linear, although some slight interaction effects may have been present for some of the properties.

(D) The following conclusions were reached with regard to the study of natural soils in this investigation:

(10) Prediction of various geotechnical properties of natural soils can be based on clay content alone only in severely limited circumstances, in which there is close similarity (geological, mineralogical, textural, etc) between the samples.

(11) Linear multiple regressions were sufficient to accurately predict the soil properties, when the correct choice of the independent parameters was made. For the present samples, clay content, silt content, organic matter content and plasticity index were found to be important.

(12) Whereas for the Atterberg limits and the compaction properties, the effect of silt reinforced the effect of clay, the opposite was found for the swell properties.

(13) Plasticity Index was better than any of liquid limit, plastic limit, or activity for representing the effect of the plasticity of the soil on both the compaction and swell properties as found from multiple regressions. However, for the natural

soils studied here, plasticity index was found to be less important than clay content to predict swell pressure.

- (E) The following conclusions were reached with regard to the test of earlier predictive theories on the data of the present samples:
- (14) Of the earlier predictive theories, only Nayak and Christinsen's (1971) equation for swell pressure gave a reasonably accurate prediction for both the natural and artificial soils considered here, and Ranganatham et al's (1965) and Chen's (1975) equations for swell potential were satisfactory for the natural soils.
 - (15) The differences between the earlier predictive equations were attributed mainly to the different patterns of behaviour of the different clay minerals, the effect of silt, and the possibility that the equations were of local validity only.

6.3 RECOMMENDATIONS

- (1) The present work should be extended to a series of closely related montmorillonitic soils.
- (2) Further attention should be paid to the importance of silt content.
- (3) For predictions for natural soils, consideration should be given to both the accuracy and significance of the predictions, and statistical methods should be used for this purpose.

- (4) For predictions for natural soils, consideration should be given to the sphere of validity of the predictions, i.e. to whether they are of local validity only.
- (5) Consideration should be given to the effect of cementing agents in undisturbed natural soils.
- (6) Further attention should be given to the problem of measurement of isotropic swell potential.
- (7) A further study should be made of stress relaxation effects on the development of swell pressure.
- (8) The effect of the shape of sand particles should be studied in artificial mixtures.

APPENDIX - 1

DESIGN CALCULATIONS

A1.1 Introduction

In designing the equipment for the measurement of both isotropic swell pressure and laterally confined swell pressure, it is of fundamental importance to keep the volumetric strain of the sample to the lowest possible value throughout the test. To achieve this objective and to estimate the value of the volumetric strain, it is necessary first to identify the sources of error in the apparatus, and then to calculate the magnitude of the components of volumetric strain of the sample introduced by each source of error. Realising that the volumetric strain of the sample will be dependent on the magnitude of swell pressure exerted by the sample, it is necessary to choose a value of anticipated swell pressure when making the design calculations. The literature shows that swell pressures as high as 140 psi (965 KN/m^2) [Ward et al, 1959 as quoted by Yong and Warkentin, 1966] could be developed depending on the type of soil and its placement structure. With this in view, a pressure of 100 psi was chosen as the design swell pressure. This value of 100 psi was used for all subsequent calculations, made for both swell pressure apparatus.

As the designs were made in imperial units, all the subsequent calculations are presented in the same units.

A1.2 ISOTROPIC SWELL PRESSURE

A1.2.1 Introduction

The apparatus designed for measuring the isotropic swell pressure is described earlier in section 2.4.3 and is shown in Fig. 2.27.. The possible sources of error that may effect the volumetric strain of the sample in such an apparatus are:-

- (a) Compressibility of water;
- (b) Expansion of chamber;
- (c) Compressibility of membrane;
- (d) Expansion of O-ring;
- (e) Compressibility and bedding error of porous stone;
- (f) Compressibility of filter paper.

Each source of error is considered in turn in the following sections, and the magnitude of the components of volumetric strain due to each source of error is calculated.

A.1.2.2 Compressibility of water

Normal practice is to consider water as an incompressible material as its value of compressibility is as low as $3 \times 10^{-6} \frac{1}{\text{psi}}$ (Handbook of Chemistry and Physics, 1974-75). However, it is necessary to consider even this 'negligible' compressibility of water, as we require the volumetric strain of the sample due to a combination of various sources, which also tend to be in the same range.

Bulk modulus of water, k

= Inverse of compressibility of water

$$= \frac{1}{3 \times 10^{-6} \left(\frac{1}{\text{psi}} \right)} = 0.33 \times 10^6 (\text{psi}).$$

Swell Pressure, P = 100(psi).

Volume of water in the chamber, V

= Internal volume of chamber - volume of sample

$$= 58.93 - 31.43 (\text{in}^3)$$

$$= 27.50 (\text{in}^3).$$

Change in volume of water, ΔV

$$= \frac{P}{K} V$$

$$= \frac{100 (\text{psi})}{0.33 \times 10^6 (\text{psi})} \times 27.50 (\text{in}^3)$$

$$= 8333.33 \times 10^{-6} (\text{in}^3).$$

Volumetric strain of the sample

$$= \frac{\text{change in volume of water}}{\text{volume of the sample}}$$

$$= \frac{8333.33 \times 10^{-6} (\text{in}^3)}{31.43 (\text{in}^3)}$$

$$= 265 \times 10^{-6}.$$

A1.2.3 Expansion of Chamber

Precautions were taken in the design of this pressure chamber in order to make the chamber as rigid as possible by

(i) constructing the chamber with steel, and (ii) making the chamber wall thickness as great as 0.5 in all around as well^{as} at the top. However, for an internal swell pressure of 100 psi there will still be a slight expansion. In the present context, where an attempt is made to keep the sample as closely as possible to a 'true no volume change condition', it becomes essential to consider the chamber expansion.

The pressure chamber is treated as a thick walled cylinder with internal radius, a , equal to 2.4 in and external radius, b , equal to 2.9 in. Considering the equation for symmetrical stress distribution to obtain displacements (Timoshenko and Goodier, 1951):

$$u = \frac{P a^2}{E (b^2 - a^2)} \left[(1 + \mu) \frac{b^2}{a} + (1 - \mu) a \right]$$

where,

u = the radial displacement on the inner face of the pressure chamber,

P = internal swell pressure = 100 psi,

E = Young's modulus for steel = 30×10^6 psi,

μ = Poisson's ratio for steel = 0.3.

The above equation can be rearranged as:

$$u = \frac{P a^2}{Et} \left[\frac{t}{a(b^2 - a^2)} \left\{ (1 + \mu) b^2 + (1 - \mu) a^2 \right\} \right]$$

where t is the thickness of the chamber wall equal to 0.5 in. Substituting for the values of a , b , t and μ in the parenthesis of the above equation, we can rewrite the

equation as:

$$u = \frac{1.17 P a^2}{Et} .$$

Change in cross-sectional area of the chamber on the inner face due to internal pressure

$$= \pi (a + u)^2 - \pi a^2$$

$$\approx 2\pi a u ,$$

since a is the inner radius of the pressure chamber,
Substituting for u in the above equation,

Change in cross-sectional area

$$= 2.34 \pi a \frac{Pa^2}{Et} .$$

∴ Change in volume

$$= 2.34 \pi a \frac{Pa^2}{Et} . L .$$

The above volume change is the component due to the hoop stresses developed on the inner face of the chamber.

Considering the change in volume due to the axial stress separately,

$$\text{axial force} = \pi a^2 P .$$

$$\text{axial stress} = \frac{\pi a^2 P}{\pi (b^2 - a^2)} .$$

$$\text{axial strain} = \frac{\pi a^2 P}{\pi (b^2 - a^2) . E}$$

$$= \frac{a^2 P}{E(b^2 - a^2)} .$$

$$\therefore \text{Change in length} = \frac{a^2 P}{E(b^2 - a^2)} . L .$$

$$\text{Change in volume} = \frac{PL a^2}{E(b^2 - a^2)} . \pi a^2 .$$

Total change in volume

$$= 2.34 \pi \frac{Pa^3L}{Et} + \pi \frac{Pa^4L}{E(b^2-a^2)}.$$

∴ Volumetric strain of the chamber

$$= \frac{2.34 \pi \frac{Pa^3L}{Et} + \pi \frac{Pa^4L}{E(b^2-a^2)}}{\pi a^2L}$$

$$= 2.34 \frac{Pa}{Et} + \frac{Pa^2}{E(b^2-a^2)}$$

$$= 2.34 \frac{100(\text{psi}) \times 2.4 (\text{in})}{30 \times 10^6 (\text{psi}) \times 0.5 (\text{in})} + \frac{100(\text{psi}) \times 2.4^2 (\text{in}^2)}{30 \times 10^6 (\text{psi}) \times (2.9^2 - 2.4^2) (\text{in}^2)}$$

$$= 44.69 \times 10^{-6}.$$

Volumetric strain of the sample due to Expansion of Chamber

$$= \frac{\text{volumetric strain of chamber} \times \text{volume of chamber}}{\text{volume of sample}}$$

$$= \frac{44.69 \times 10^{-6} \times 54.31 (\text{in}^3)}{31.43 (\text{in}^3)}$$

$$= 77.22 \times 10^{-6}.$$

A1.2.4 Compressibility of Membrane

The rubber membrane enclosing the sample is itself liable to compress, and hence may permit some volumetric expansion of the sample. According to Bishop and Henkel (1962), the compressibility of the membrane will be too small to be important, but it was decided to confirm this for the worst possible circumstances.

Yarwood and Castle (1959) quote values of Young's modulus, E , varying between 1420 psi and 1,000,000 psi, and ~~the~~ values of Poisson's ratio, μ , varying between 0.46 and 0.49. The Polymer Handbook (1965) give values of Young's modulus, E , varying between 188 psi (pure-gum vulcanizate) and 435000 psi (hard rubber, Ebonite). Bishop and Henkel (1962) quote an extension modulus of 2.0 lb/inch for a rubber membrane of 0.01 inch thickness, which would correspond to a Young's modulus of 200 psi. Due to this extremely large variation in the quoted value of Young's modulus, it was decided to conduct laboratory tests on strips cut from one of the batch of rubber membranes actually used in this work, following the test procedure described by Bishop and Henkel (1962, pp 168). The tests yielded a value for E equal to 120 psi. The lowest of these values (i.e. $E = 120$ psi) was used because it applied to the rubber actually used and because it gave the safest estimate. For Poisson's ratio, the lowest value of 0.46 quoted by Yarwood and Castle (1959) was used.

Let Δ_v = change in volume of membrane,

$$\Delta_v = \frac{P}{K} V$$

where, P is the internal swell pressure (psi),
 K is the bulk modulus of rubber (psi),
 V is the total volume of membrane (in³).

Bulk modulus, K

$$\begin{aligned}
 &= \frac{E}{(1-2\mu)^3} \\
 &= \frac{120 \text{ (psi)}}{(1-2 \times 0.46)^3} \\
 &= 500 \text{ (psi)}.
 \end{aligned}$$

∴ Change in volume of membrane, Δ_v

$$\begin{aligned}
 &= \frac{P}{K} V \\
 &= \frac{100 \text{ (psi)}}{500 \text{ (psi)}} \times 0.439 \text{ (in}^3\text{)} \\
 &= 0.0878 \text{ (in}^3\text{)}.
 \end{aligned}$$

Volumetric strain of the sample

$$\begin{aligned}
 &= \frac{\text{change in volume of membrane}}{\text{volume of sample}} \\
 &= \frac{0.0878 \text{ (in}^3\text{)}}{31.43 \text{ (in}^3\text{)}} \\
 &= 2800 \times 10^{-6}.
 \end{aligned}$$

A1.2.5 Expansion of 'O'-ring

An O-ring is placed in the apparatus between the top chamber and the base plate in order to provide a good seal. However, this O-ring may be subjected to tensile stresses due to the water pressure developed within the water chamber, thus resulting in tensile expansion of the O-ring.

Design swell pressure, $P = 100$ psi.

Diameter of O-ring, $d = 4.5$ inches.

Thickness of O-ring, $2Y = 0.24$ inch.

Radial force due to

$$\begin{aligned} \text{internal swell pressure} &= Pd \cdot 2Y \\ &= 100 \text{ (psi)} \times 4.5 \text{ (inch)} \times 0.24 \text{ (inch)} \\ &= 108 \text{ lbs.} \end{aligned}$$

Let, t be the tensile stress in the O-ring

Then,

$$\begin{aligned} t &= \frac{\text{Radial force}}{2 \pi r^2} \\ &= \frac{108 \text{ (lbs)}}{2 \pi (0.12)^2 \text{ (in}^2\text{)}} \end{aligned}$$

$$\doteq 1194 \text{ psi.}$$

As seen in the earlier section the value of Young's modulus, E , for soft rubber varies from 120 psi to 1000000 psi. As the O-ring is made with a rubber harder than the type used for membranes, it is thought justified to take the upper value of E for further calculations.

$$\therefore E = 1.0 \times 10^6 \text{ psi}$$

Tensile extension

$$\begin{aligned}
 &= \frac{t}{E} \\
 &= \frac{1194 \text{ (psi)}}{1.0 \times 10^6 \text{ (psi)}} \\
 &= 1194 \times 10^{-6} \\
 &= \frac{\Delta d}{d} .
 \end{aligned}$$

$$\begin{aligned}
 \therefore \Delta d &= 1194 \times 10^{-6} \times 4.5 \text{ (inch)} \\
 &= 5373 \times 10^{-6} \text{ (inch)}.
 \end{aligned}$$

Change in volume of O-ring

$$\begin{aligned}
 &= \Delta \left(\frac{\pi d^2}{4} \right) \times 2v \\
 &= \frac{\pi}{4} 2 d \Delta d \times 2v \\
 &= \frac{\pi}{4} 2 (4.5 \text{ inch}) \times 5373 \times 10^{-6} \text{ (in)} \times 0.24 \text{ (in)} \\
 &\doteq 9120.00 \times 10^{-6} \text{ (in}^3\text{)}.
 \end{aligned}$$

\(\therefore\) Volumetric strain of the sample

$$\begin{aligned}
 &= \frac{\text{Change in volume of O-ring (in}^3\text{)}}{\text{volume of the soil sample (in}^3\text{)}} \\
 &= \frac{9120 \times 10^{-6} \text{ (in}^3\text{)}}{31.42 \text{ (in}^3\text{)}} \\
 &= 290 \times 10^{-6} .
 \end{aligned}$$

If the O-ring obtains lateral support from the outside of the groove some or all of this volumetric strain will be unable to develop.

A1.2.6 Compressibility and Bedding Error
Of Porous Stones

In order to estimate the compressibility and bedding error of the porous stone on the volumetric changes of the sample, four tests were conducted. The details of these tests are given below.

The first two tests were carried out by using a conventional consolidometer. In the first test the porous stone was placed between a brass dummy sample and the loading cap in a consolidometer cell and a maximum load of 16 lbs was placed in increments on the hanger. Due to a lever arm ratio of 1:11, this represents a load of 176 lb on the stone. The reading of the deflection under each load was taken after 24 hours. This test yielded an average value of deflection per unit pressure of 5.0×10^{-5} inch/psi, see Fig. A1-1.

The same set-up described above was used for the second test with the only difference that the load on the hanger was increased in increments to 120 lbs, representing a maximum load of 1320 lbs on the porous stone. This load was chosen as it is comparatively much higher than that used in the first test. The graph of deflection against pressure on the stone is shown in Fig. A1-2, which yielded a deflection per unit pressure of 6.0×10^{-5} inch/psi at 100 psi pressure.

In the third test, the porous stone was placed in a consolidometer cell sandwiched between a dummy sample and loading cap as in the first two tests, but was directly loaded with the help of a loading yoke (Fig. A1-3), without the use of the consolidometer lever. A load of 15 lb was

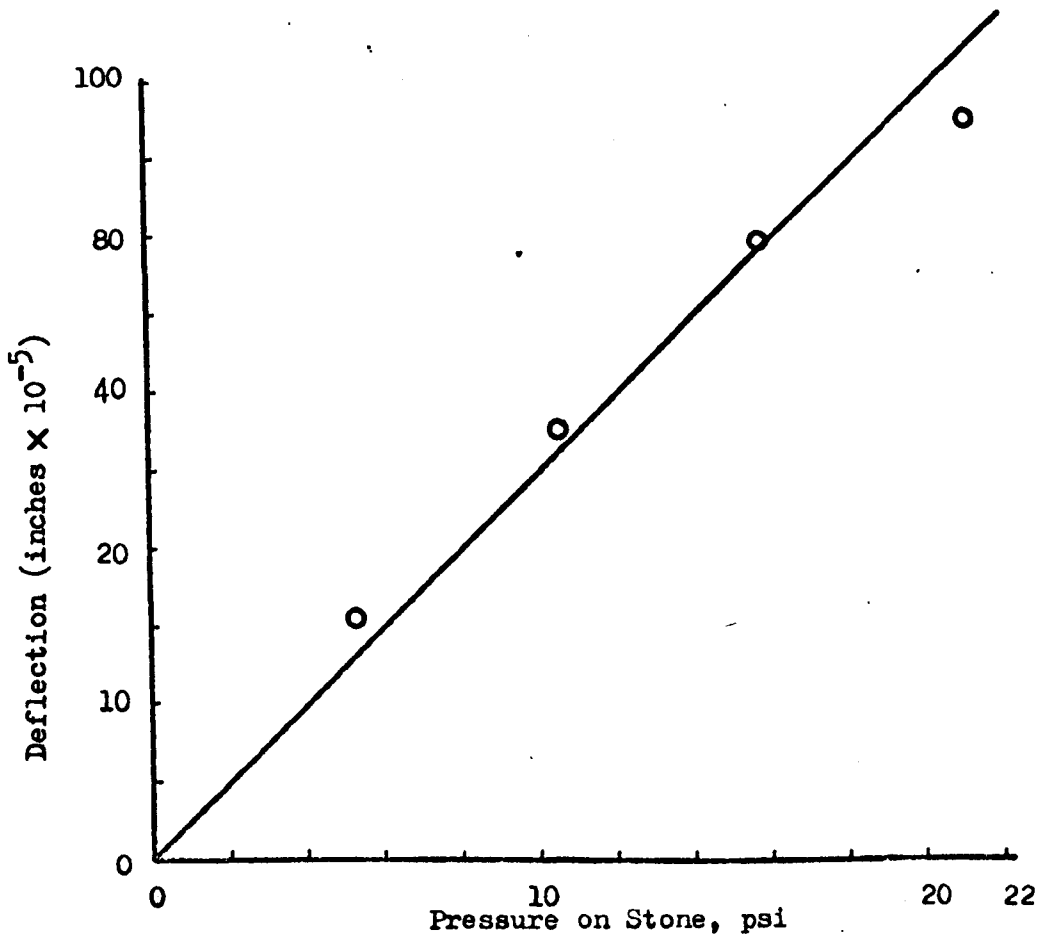


Fig. A1-1 Deflection against Pressure on Porous Stone,
Consolidometer Low order Loading.

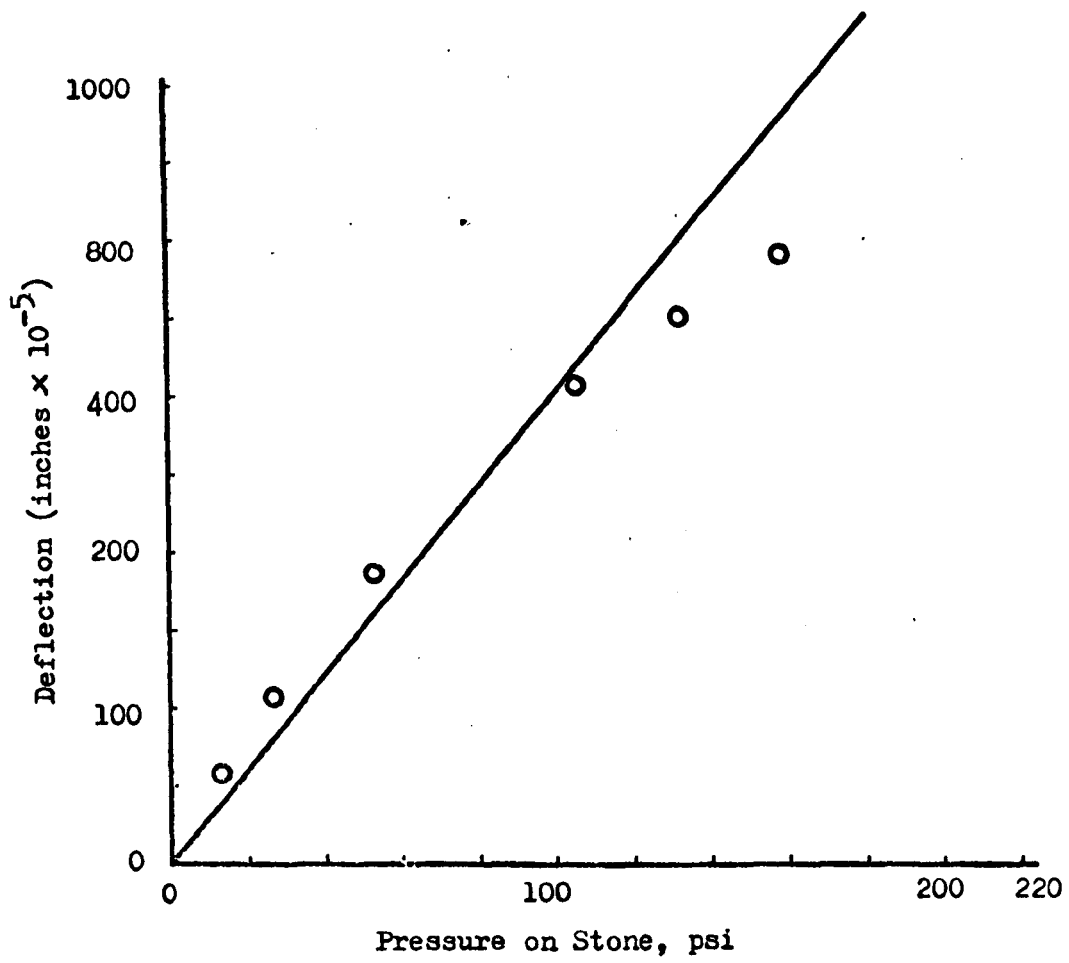


Fig. A1-2 Deflection against Pressure on Porous Stone,
Consolidometer High order Loading.

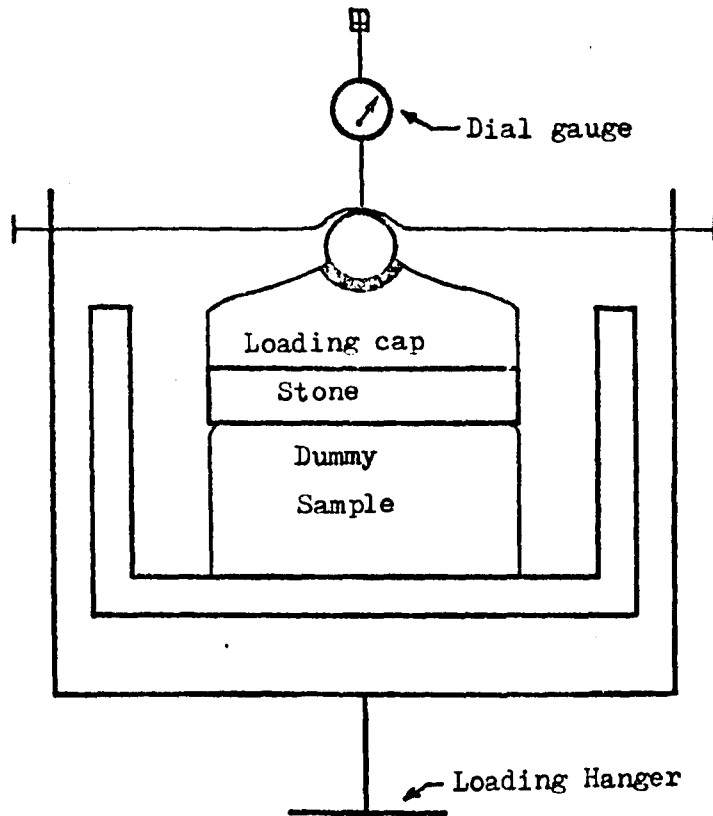


Fig. A1-3 Compressibility and Bedding Error of Porous Stone,
Set-Up For Test No.3.

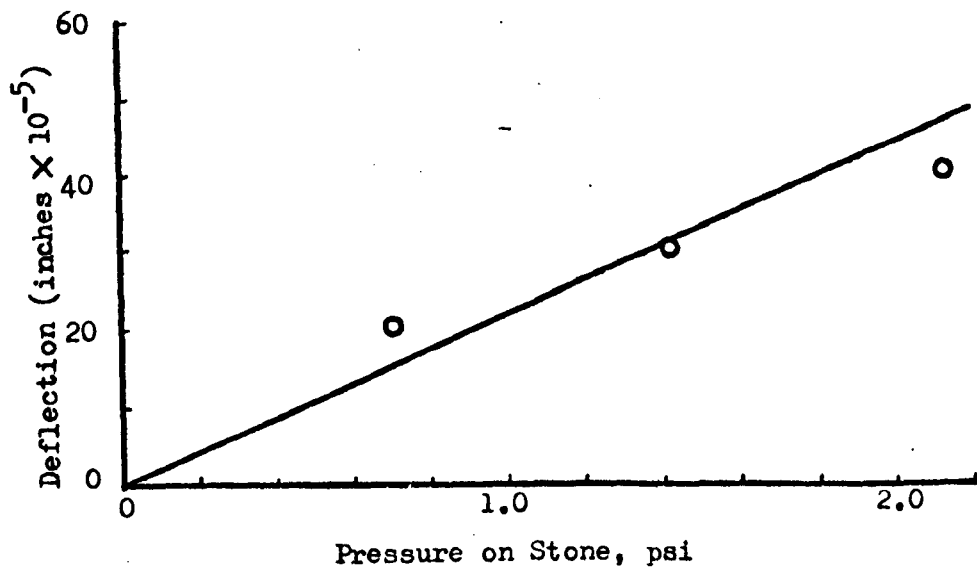


Fig. A1-4 Deflection against Pressure on Porous Stone, Cell
with Loading Yoke.

applied in three increments of 5 lbs and the deflection was measured 24 hrs after placing each load. The results of this test are shown in Fig. A1-4, which yielded an average value of deflection per unit pressure of 22.6×10^{-5} inch/psi.

The fourth test was performed on a surface plate (a perfectly plane and smooth cast iron sheet), see Fig. A1-5. A load of 15 lbs was placed in three equal increments on the porous stone and the deflection under each load was recorded after 24 hrs. This test yielded a deflection per unit pressure of 28.0×10^{-5} inch/psi, see Fig. A1-6.

The results of the four tests are summarised in Table A1-1, the last column shows the pressure at which the deflection is fitted to the observations. Tests 3 and 4, which were at low pressures yielded much higher values than tests 1 and 2 at higher pressures. This is not surprising due to the curvature of the graphs for tests 1 and 2 (Figs. A1-1 and A1-2) and the non-zero intercept of graph for test 3, see Fig. A1-4. Despite the fact that the design pressure was 100 psi, it was expected that most samples will be tested would develop lower pressures, and the average value of 15.40×10^{-5} inch/psi was adopted when calculating the volumetric strain of the sample due to the presence of porous stones.

Thus,

$$\begin{aligned} \text{Deflection per 100 psi of pressure} \\ &= 15.40 \times 10^{-5} \left(\frac{\text{in}}{\text{psi}} \right) \times 100(\text{psi}) \\ &= 1540 \times 10^{-5} \text{ (inches)}. \end{aligned}$$

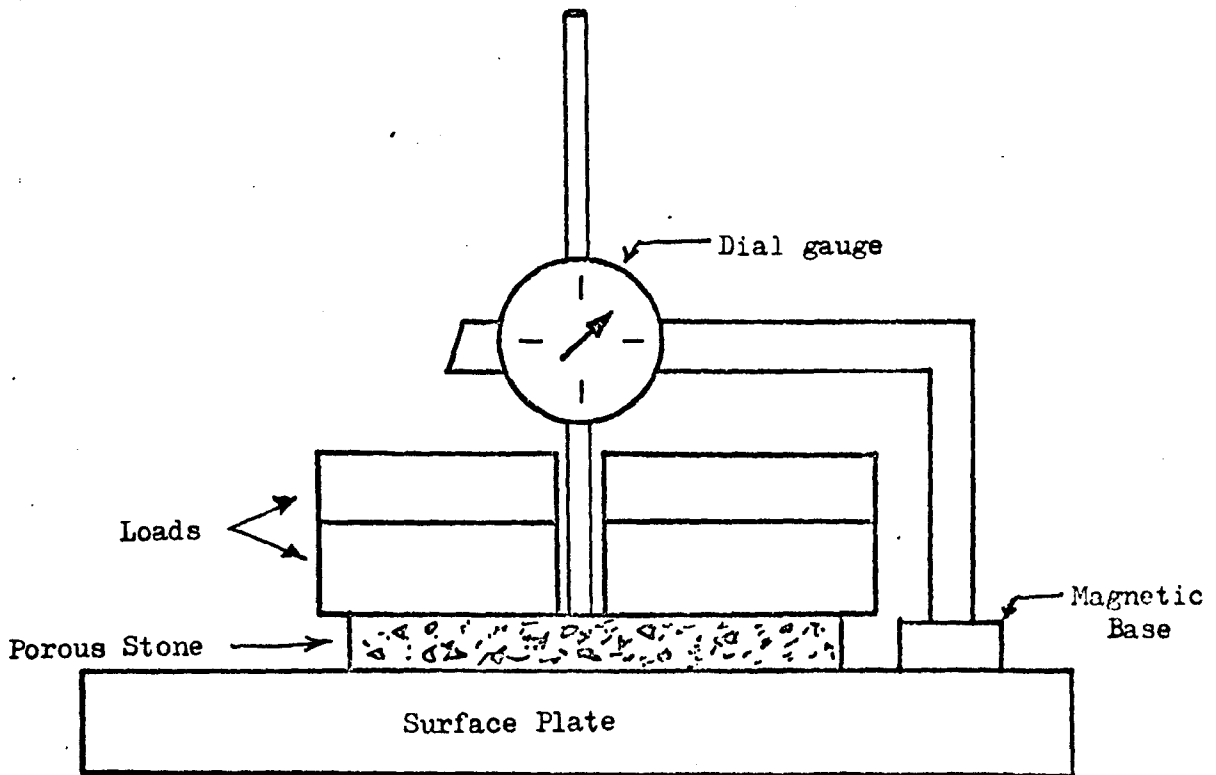


Fig. A1-5 Compressibility and Bedding Error of Porous Stone, Set-Up For Test No.4.

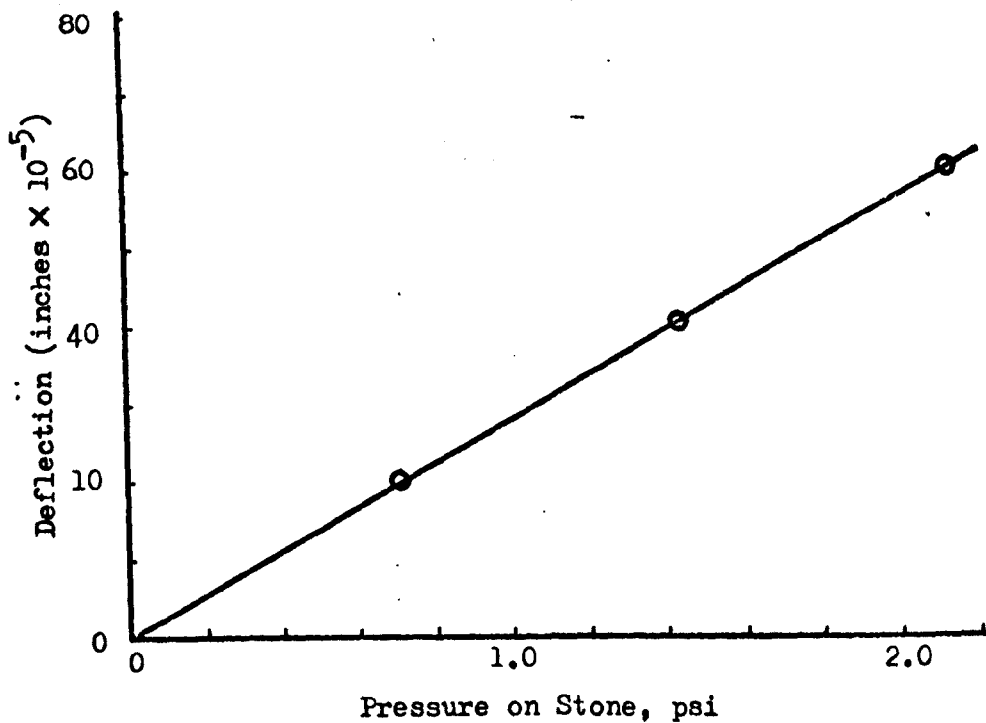


Fig. A1-6 Deflection against Pressure on Porous Stone, Surface Plate.

Table A.1-1 Compressibility and Bedding

Error of Porous Stones

S1 No.	Type of Test	Deflection (inch/psi)	Pressure (psi)
1.	Consolidometer, Low order Loading.	5.0×10^{-5}	16
2.	Consolidometer, High order Loading.	6.0×10^{-5}	100
3.	Cell with Loading Yoke	22.6×10^{-5}	1.4
4.	Surface Plate	28.0×10^{-5}	1.4
		<u>Average = 15.4×10^{-5}</u>	

Volumetric Strain of the Sample

$$\begin{aligned}
 & \dagger \text{ axial strain} \\
 & = \frac{\text{deflection}}{\text{height of sample}} \\
 & = \frac{1540 \times 10^{-5} (\text{in})}{2.5 (\text{in})} \\
 & = 6160 \times 10^{-6}
 \end{aligned}$$

Since this value of volumetric strain appeared to be very high, it was decided to use it to calculate the Young's modulus, E , of the stone. A value of 6.0×10^3 psi was obtained. But the value of E for a ceramic stone would be expected to be very nearly equal to that of concrete and should therefore be of the order of 3000×10^3 psi. This suggests that the results are due mainly to the bedding errors of the stone, and not due to the compression of the stone itself. The non-linear curves and non-zero intercepts mentioned above in connection with Figs. A1-1, A1.2 and A1.4 and the dependence of deflection on pressure shown in Table A.1-1 will all be explained by this conclusion. With a view to halve the bedding error, the porous stone was cemented to the pedestal of the chamber using araldite. Presumably, the remaining part of the bedding error could be eliminated by compacting the soil directly on to the porous stone, but this idea was thought to be impracticable, because of the risk of shattering the stone.

In accordance with the above, taking half the previous value, the volumetric strain of the sample for an internal pressure of 100 psi will now be equal to 3080×10^{-6} .

A1.2.7 Compressibility of Filter Papers

According to Fredlund (1969, Fig 12) the initial compression of a pair of filter papers at 100 psi is approximately 0.01 in. It is reasonable to expect that one or more cycles of preloading and unloading of the assembly before the beginning of the swell pressure test would improve the initial bedding of the set up so that the effects of the porous stone and filter paper were mutually compensating. However, in the isotropic swell pressure tests of the present study, no such preloading was given. Therefore, it was decided to estimate the volumetric strain of the sample due to the compressibility of filter paper.

In the present apparatus one filter paper was used, and therefore an allowance of 0.005 inch was adopted. The height of the sample was 2.5 inch.

∴ Volumetric Strain of Sample

$$\begin{aligned}
 &= \frac{\text{compression of filter paper}}{\text{height of sample}} \\
 &= \frac{0.005 \text{ (in)}}{2.5 \text{ (in)}} \\
 &= 2000 \times 10^{-6}.
 \end{aligned}$$

A1.2.8 Preliminary Test of Apparatus

According to the design calculations, the total percentage volumetric strain in the isotropic swell pressure apparatus amounted to 0.85%, see Table A1-2. This has been discussed in section A1.2.10. In order to make an

Table A.1-2 Volumetric Strain of Sample in
Isotropic Swell Pressure Apparatus

Sl No.	Source of Error	Volumetric Strain of Sample
1.	Compressibility of Water	265×10^{-6}
2.	Expansion of Chamber	77×10^{-6}
3.	Compressibility of Membrane	2800×10^{-6}
4.	Expansion of O-ring	290×10^{-6}
5.	Bedding Error of Stone	3080×10^{-6}
6.	Compressibility of filter paper	2000×10^{-6}
Total =		8512×10^{-6}
		= 0.85%

experimental verification of this, the apparatus was assembled using a dummy mild steel sample with a single membrane around it. The air vent valve on the top of the pressure chamber was connected to a pressure burette (Bishop and Henkel, 1962). After the pressure chamber had been filled with water and deaired, the water inlet valve at the bottom was closed and various pressures up to 4 bars (58 psi) were applied to the burette. The corresponding volumetric expansion of the apparatus was measured. After extrapolation to 100 psi the corresponding volumetric strain of the sample was found to be 0.125%, see Fig. A1-7. It was reassuring that this measured expansion was less than that predicted in the design calculations.

A1.2.9 Expansion of a Typical Sample

After the completion of an isotropic swell pressure test on a pure illite sample, the dimensions of the sample were measured in order to calculate the sample expansion in the apparatus. The value obtained was 1.5%. The measurements were made with Calipers and were therefore crude and approximate. Furthermore, there is a possibility for the sample to swell by absorbing water from the wet porous stone after the release of the swell pressure and during the process of dismantling the apparatus to remove the sample. In view of this, it was thought that the performance of the apparatus was similar to that which had been predicted.

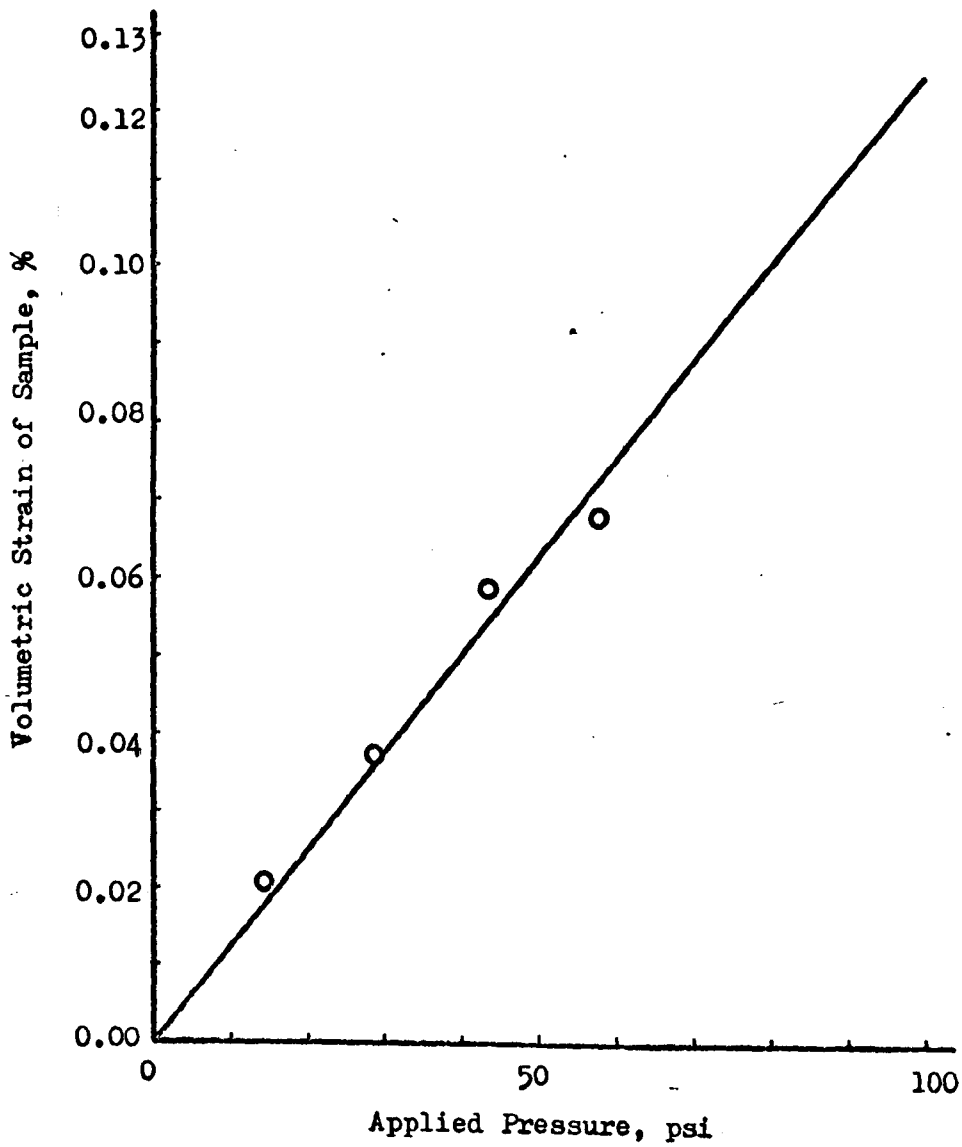


Fig. A1-7 Preliminary Test of Apparatus.

A1.2.10 Discussion

Three values of volumetric strain of the sample at 100 psi swell pressure have been obtained, viz; 0.85% by design calculations, 0.125% by a preliminary test using a dummy sample, and 1.5% by an approximate measurement on a typical illite sample. The consequent error in swell pressure measurement due to the presence of volumetric strain of the sample would be very difficult to estimate accurately. However, it can be noticed, from the data of McCormack and Wilding (1975, Fig 3) on two low swelling soils, that up to 10% swell of the sample the percentage loss in swell pressure would be around 10 times the actual value of swell. Accepting the highest figure of volumetric strain of the sample, ie 1.5%, and assuming that the effect of volumetric strain on swell pressure would be 10 times greater suggests that there might be a 15% under-estimate in the measured swell pressures. This would apply over the entire range of swell pressures, except that the non-linearity of some of the intermediate results (eg, see Fig. A1-2) suggests that the percentage error might be somewhat greater than 15% for low values of swell pressure.

A1.3 LATERALLY CONFINED SWELL PRESSURE

A1.3.1 Introduction

The apparatus designed for measuring the laterally confined swell pressure was described in Section 2.4.4 and is shown in Fig.2.28 . This apparatus is a modification of the one used by Seed et al (1962)^a. The modifications were made in order to eliminate as far as possible the sources of systematic error and to reduce the amount of volumetric expansion of the sample. Seed et al (loc. cit.) measured swell pressure by using a proving bar. They recorded that the deflection of the bar was equivalent to 0.04 inch per 100 psi, when a proving bar of $\frac{1}{4}$ in thickness was used. The following sources of error should be considered:

- (a) deflection of stem ;
- (b) bedding error, porous stone;
- (c) bedding error, jack;
- (d) volumetric change in sample before actuation of dial gauge;
- (e) reading error of dial gauge;
- (f) compressibility of filter papers.

The modifications made when designing the present apparatus are given below:-

- (1) Strain gauges on the tie rods were used to measure the swell pressure thereby eliminating the use of a proving

bar and dial gauge.

- (2) The screw and the sample base were designed as a single unit, and the porous stone in the swell pot was cemented to the sample base. This eliminated the bedding errors that could be caused by the jack and the porous stone, apart from the bedding of the sample on the stone.
- (3) The vertical stem, connecting the perforated plate and top clamping bar, was made large in diameter (0.5 in) and small in length (1.0 in) and was brazed to the perforated plate at the bottom and screwed at the top to the clamping bar. This was done in order to make the stem as rigid as possible.
- (4) In order to eliminate backlash in the screw, the threads were machined carefully to be a tight fit. It is recommended that any future apparatus should incorporate a backlash eliminator, e.g. some form of split nut arrangement.
- (5) Preloading of the assembly was used to eliminate the compressibility of the filter papers.

The following two sections show the design calculations.

A1.3.2 Use of Strain Gauges

In order to design a load measuring system, the cross bar was made 11 inch long x 2 inch wide x 2 inch thick, and was assumed not to deflect under load. The length

of the tie bars was controlled by the height of the apparatus and was 8 inches. The area of the tie bars was a compromise between restricting the expansion of the tie bars and the sample and extending the strain gauges sufficiently to produce readings large enough to be read. The tie bars were $\frac{1}{2}$ inch in diameter and the design calculations are as follows:

Design swell pressure, $P = 100$ psi.

Area of sample inside the swell pot

$$\begin{aligned} &= \pi r^2 \\ &= \pi (2)^2 \text{ (in)}^2 \\ &= 12.56 \text{ sq.in.} \end{aligned}$$

Total force on tie rods due to development of maximum swell pressure

$$\begin{aligned} &= P \cdot A \\ &= 100 \text{ (psi)} \times 12.56 \text{ (sq. in)} \\ &= 1256 \text{ lbs.} \end{aligned}$$

Total force on each tie rod,

$$W = 628 \text{ lbs.}$$

Cross-sectional area of tie bar, A_t

$$\begin{aligned} &= \pi (0.25)^2 \text{ (in)}^2 \\ &= 0.2 \text{ sq. in.} \end{aligned}$$

Length of tie bar, L

$$= 8 \text{ in.}$$

Young's modulus of steel, E

$$= 30 \times 10^6 \text{ psi.}$$

Extension of tie bar, δ

$$\begin{aligned} &= \frac{WL}{A_t E} \\ &= \frac{628 \text{ (lb)} \times 8 \text{ (in)}}{0.2 \text{ (sq. in)} \times 30 \times 10^6 \text{ (psi)}} \\ &= 837 \times 10^{-6} \text{ (in).} \end{aligned}$$

Strain in the bar

$$\begin{aligned} &= \frac{\delta}{L} \\ &= \frac{837 \times 10^{-6} \text{ (in)}}{8 \text{ (in)}} \\ &\div 105 \times 10^{-6}. \end{aligned}$$

The strain gauges used on the tie bars were $\frac{1}{2}$ inch long with a gauge factor of $2.10 \pm 0.5\%$ at 75°F (24°C), and were provided with self compensation for temperature. The strain was measured in microinch/inch using a strain-indicator, Model No P-350 of Budd Instruments Division. At the design pressure of 100 psi, the strain of 105×10^{-6} on each tie bar corresponded to about 200 divisions when the strain-indicator was used at full sensitivity. Thus, it was expected that the calibration would be approximately 2 divisions per 1 psi. At first sight this will be satisfactory, however it was thought that by running the system at full sensitivity random errors would be incurred. The alternative would have been to use more flexible tie bars, however it was decided to accept any

random errors which did occur, since these would be expected to average out in a series of tests, and it was necessary to keep the systematic error, which would not average out, as low as possible.

A1.3.3. Use of Proving Bar

Provision was made in the laterally confined swell pressure apparatus to measure swell pressure using a proving bar, as an alternative to the strain gauge system. The two tie rods of $\frac{1}{2}$ in dia. were replaced (see Fig.2.29) by two tie rods of $1\frac{1}{4}$ in diameter. This was to ensure that there is negligible extension of the tie bars. Instead, there is a deflection of the proving bar, which can be calibrated to measure the swell pressure. The design calculations were made choosing a proving bar of 11 inch x 1 inch x 1 inch.

Moment of Inertia, I

$$\begin{aligned}
 &= \frac{bd^3}{12} \\
 &= \frac{1 \text{ (in)} \times 1^3 \text{ (in}^3\text{)}}{12} \\
 &= \frac{1}{12} \text{ (in}^4\text{)}.
 \end{aligned}$$

Total force coming to the proving bar, W

$$= 1256 \text{ (lbs).}$$

Length of proving bar, L

$$= 11 \text{ (in).}$$

Young's modulus of steel, E

$$= 30 \times 10^6 \text{ psi.}$$

The proving bar was treated as fixed at both ends, thus

Deflection of proving bar, δ

$$\begin{aligned}
 &= \frac{WL^3}{48 EI} \\
 &= \frac{1256 \text{ (lbs)} \times 11^3 \text{ (in}^3\text{)}}{48 \times 30 \times 10^6 \text{ (psi)} \times \frac{1}{2} \text{ (in}^4\text{)}} \\
 &= 0.014 \text{ inches.}
 \end{aligned}$$

This deflection is for a design pressure of 100 psi, and the deflection per 1 psi will be approximately 0.0001 inch. In order to measure this deflection, a dial gauge sensitive to 0.0001 inch has to be used, the deflection of each division representing an expansion pressure of the order of 1 psi. This choice of values again leads to some random errors in the measurement of swell pressure, but the choice was made in order to keep the systematic error resulting from expansion of the sample as low as possible.

It can be seen from the above calculations that the deflection of the proving bar (0.014 inch) is much larger than the extension of tie bars (0.00084 inch) in the strain gauge system. Furthermore, the deflection in the former case will be larger still if perfect end fixing of the proving bar is not achieved. Therefore, once it was seen that the strain gauge system was working satisfactorily, it was decided to use the strain gauge system for the entire series of tests in the present study.

A1.3.4 Compressibility and Bedding Error of Porous Stones

Two porous stones were used in the laterally confined swell pressure apparatus. It was estimated in section A1.2.6 that at 100 psi swell pressure, each porous stone would deflect by 15.40×10^{-3} inches. However, in order to minimise this deflection by reducing the bedding error, the porous stone underneath the soil sample was cemented to the base and the sample was loaded and unloaded four or five times before the test began. Assuming that the net effect of these precautions would be to reduce the bedding error by 50%, the net bedding error in the apparatus becomes 15.40×10^{-3} inches.

A1.3.5 Summary

From the figures given above, the total percentage strain of the sample in the laterally confined swell pressure apparatus was estimated to be 1.6%, see Table A1-3. This figure was accepted without experimental verification because methods of measuring the dimensions of the sample before and after the tests seemed to be too crude for a worthwhile comparison. Most of the expansion resulted from the bedding errors of the porous stones and would not necessarily be eliminated by using a servomechanism to obtain a null reading force measuring system (Agarwal and Sharma, 1973). Either a predetermined positive compensation or a signal from the face of the sample itself would be required.

The comments in section A1.2.10 relating to the error

Table A.1-3 Volumetric Strain of Sample in Laterally

Confined Swell Pressure Apparatus.

(Sample thickness = 1.0inch)

Sl No.	Source of Error	Deflection (inches)	Percentage Strain of Sample at 100 psi Swell Pressure
1.	Extension of tie bars	0.837×10^{-3}	0.0837
2.	Bedding Error of Stones	15.40×10^{-3}	1.5400
			Total = 1.6%

in swell pressure would apply here also except that in this case the error will be somewhat greater, say 20 to 25%.

A.1.4 CONCLUSIONS

From the calculations made in this appendix on both swell pressure apparatus it seems that after all reasonable precautions have been taken there would be a volumetric expansion of 1.0% to 1.5% in 'constant volume' swell pressure tests, leading to underestimates in the swell pressure of the order of 15% to 25% say. If an accurate value of the absolute value of swell pressure was required, then consideration should be given to methods such as the use of a novel servomechanism or compacting the sample directly into a rigid pressure chamber, in which the swell pressure was measured by stiff load cells. However, the development of either system would be a major task in its own right. Since absolute values of swell pressure were not required in this study, it was decided that the simpler apparatus described above could be used here.

APPENDIX 2

SPECIFIC GRAVITY

A2.1 Introduction

Accurate values of the specific gravity of the various soils studied in this investigation were needed in the calculations. The specific gravity was determined in accordance with Test No 6 (B) BS 1377:1975. The results for the artificial mixtures and for the natural soils are in the next two sections.

A2.2 Artificial Mixtures

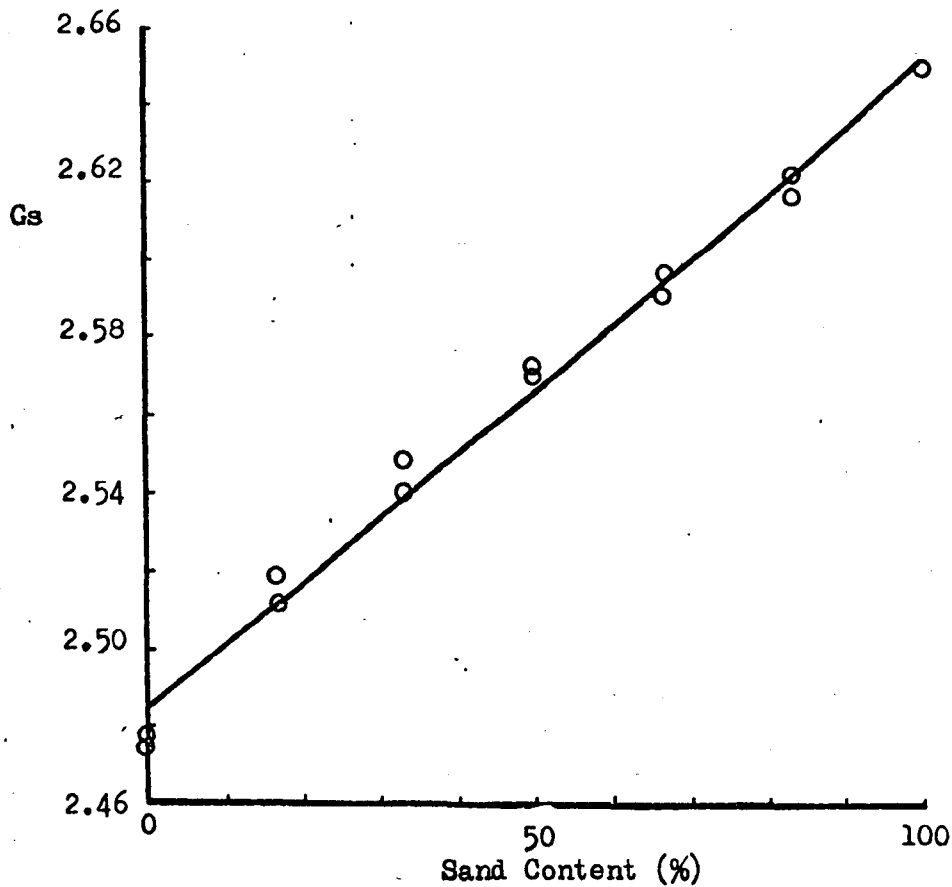
For the mixtures, the specific gravity was measured in duplicate, and the results were smoothed by regression analysis, based on the theoretical equation:

$$\frac{1}{G} = \frac{X}{G_a} + \frac{1 - X}{G_b} \quad (\text{A2-1})$$

where, X is the fraction of one phase in the 2-phase mixture; G_a and G_b are the specific gravities of the two phases. The Eq. A2-1 can be rearranged in the form:

$$G = \frac{1}{a + bX} \quad (\text{A2-2})$$

where a and b are constants. The results for the mixtures of illite - sand, and bentonite - sand, and bentonite - illite are in Figures A2-1 to A2-3. As the data for each set of mixtures was used independently for the regression

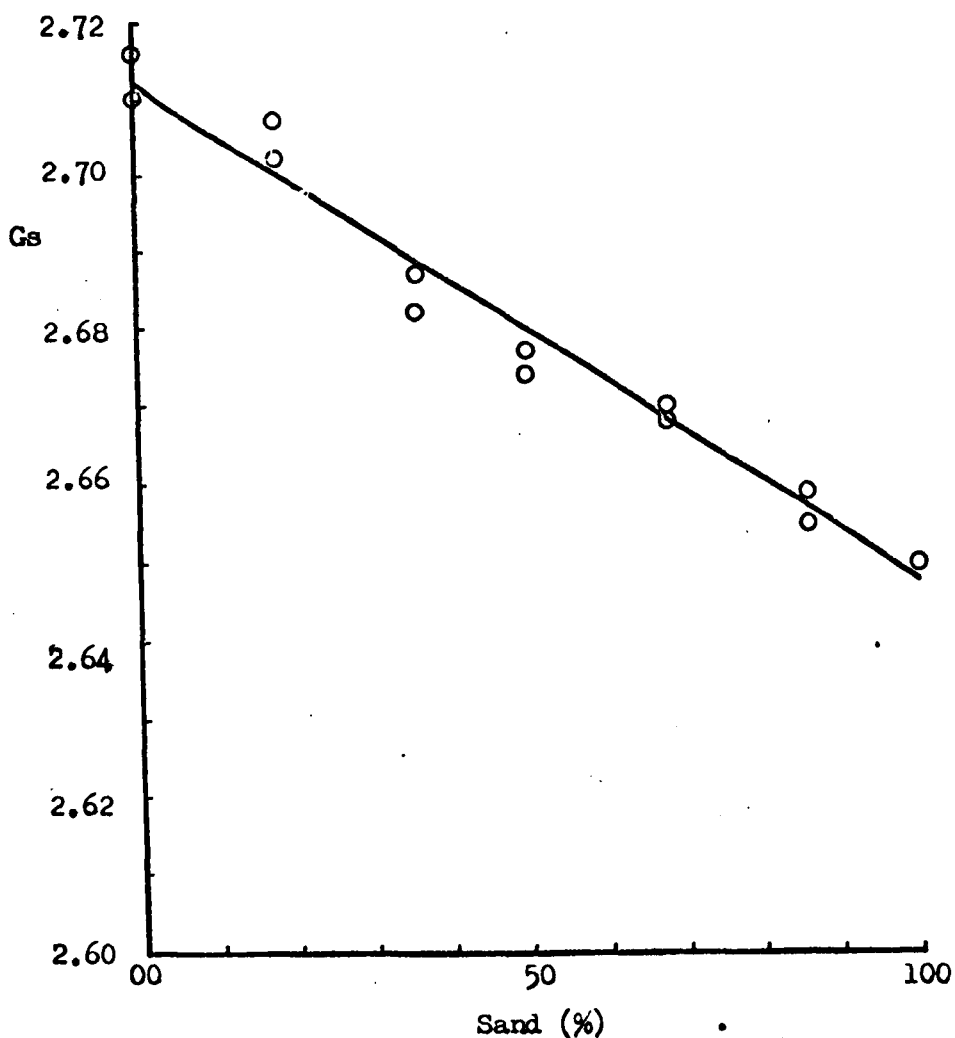


$$G_s = \frac{1}{0.4025 - 0.0255S} \quad (r^2 = 0.9912)$$

Where S is the sand fraction.

Sand (%)	Observed values of G _s 1st Obser.	2nd Obser.	Calculated value of G _s
0	2.474	2.477	2.485
16.7	2.519	2.511	2.511
33.3	2.548	2.540	2.538
50.0	2.569	2.572	2.566
66.7	2.597	2.591	2.594
83.3	2.622	2.617	2.623
100	2.650	--	2.653

Fig. A2-1 Specific Gravity of Bentonite-Sand Mixtures.

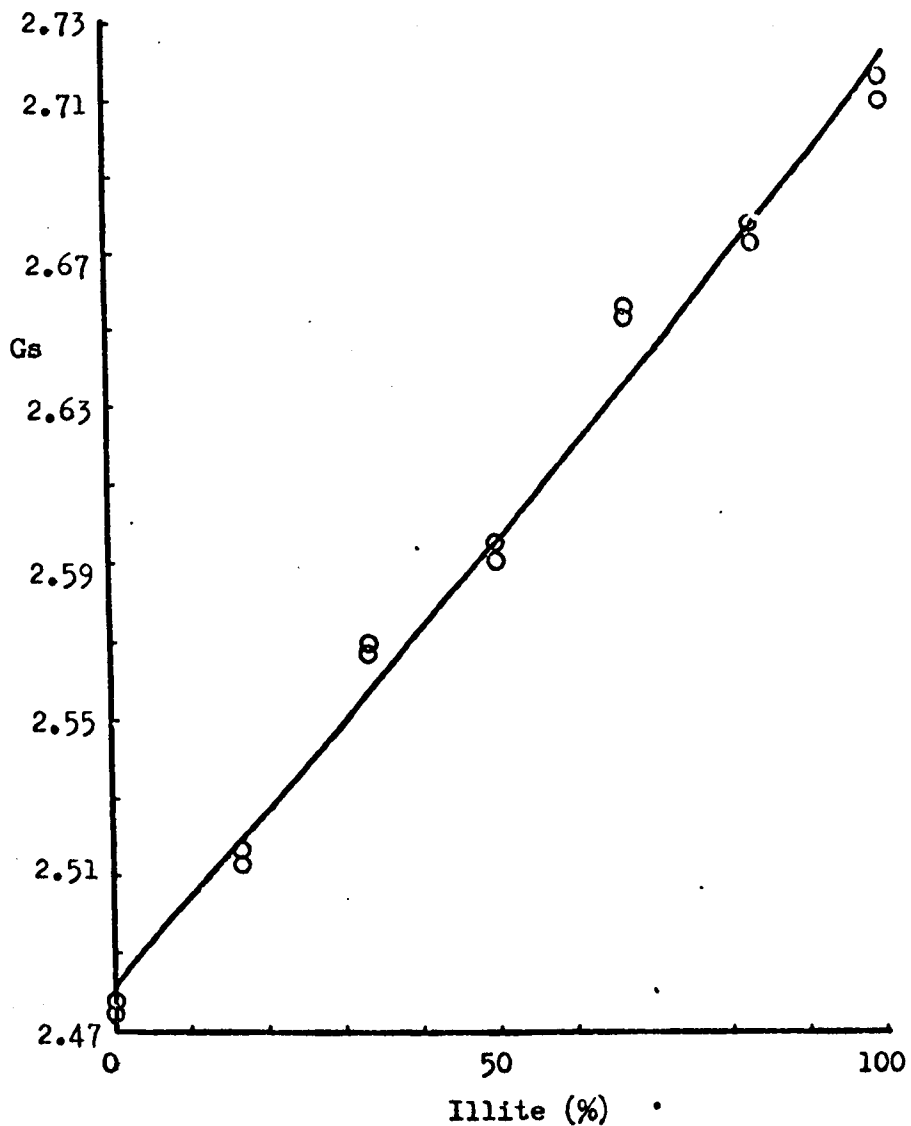


$$G_s = \frac{1}{0.3687 - 0.0089S} \quad (r^2 = 0.98)$$

Where, S is the sand fraction.

Sand Content (%)	Observed values of G _s		Calculated values of G _s
	1st Obser.	2nd Obser.	
0	2.716	2.710	2.712
18	2.707	2.702	2.701
36	2.682	2.687	2.689
50	2.674	2.677	2.680
68	2.668	2.670	2.668
86	2.659	2.655	2.657
100	2.650	2.650	2.648

Fig. A2-2 Specific Gravity of Illite-Sand Mixtures.



$$G_s = \frac{1}{0.4030 - 0.0357I} \quad (r^2 = 0.99)$$

Where I is the illite fraction in the mixture.

Type of Mixture	Observed values		Calculated Values of G
	No.1	No.2	
Illite 100%	2.710	2.716	2.723
Illite 83.3%	2.678	2.673	2.679
Illite 66.7%	2.653	2.655	2.637
Illite 50%	2.590	2.594	2.596
Illite 33.3%	2.567	2.569	2.557
Illite 16.7%	2.512	2.516	2.519
Bentonite 100%	2.474	2.477	2.481

Fig. A2-3 Specific Gravity of Bentonite-Illite Mixtures.

analysis, two final values were obtained for each of illite, bentonite, and sand. The worst difference was 0.011, and it was decided to use these different predicted values in the calculations for the corresponding sets of mixtures.

A2.3 Natural Soils

The specific gravity values of the 10 natural samples are reported in Chapter 3, see Table 3.6. The specific gravity of these natural soils was found to correlate primarily with the organic matter present at 1% level of significance. The correlation is as follows:

$$G_s = 2.7815 - 0.04489 (\text{ORG}) \quad (\text{A2-3})$$

$$(R = 0.7745)$$

where,

ORG= organic matter expressed as a percentage.

However, it is logical to expect that the specific gravity will be partly dependent on the texture of the soil. With this in view, multiple regression was performed by including silt and clay in addition to the organic matter. Although the multiple regression coefficient showed a slight improvement, the correlation was found to be significant only at the 5% level of significance, presumably because there are now less degrees of freedom. The prediction equation with these three variables is as follows:

$$G_s = 2.9240 - 0.0330 (\text{ORG}) - 0.00373 (\text{silt}) - \\ 0.00181 (\text{clay}) \quad (\text{A2-4})$$

$$(R = 0.8346)$$

where, organic matter, silt, and clay are expressed as percentages by weight.

The measured values of specific gravity were used in the calculations.

APPENDIX - 3

CATION EXCHANGE CAPACITY

A3.1 Introduction

The process of replacing cations of one kind by those of another in an adsorption complex is known as 'base exchange'. The quantity of such exchangeable cations in a soil is termed 'Cation Exchange Capacity' and is usually expressed in milli-equivalents (meq) per 100 gms dry soil. The cation exchange capacity of the three important clay minerals kaolinite, illite, and montmorillonite are 10 to 15 meq/100 gms, 30 to 40 meq/100 gms, and 90 to 110 meq/100 gms respectively (Kelley, 1948).

In this investigation, the cation exchange capacity of two natural soils was determined in accordance with the procedure suggested by Bear (1955). These two soils were selected on the basis of the highest and lowest clay contents (350 - 8 and 350 - 6). The object of the determination was to provide an indication of the range of cation exchange capacity of the natural soils used here, and to compare this with the x-ray results (see Chapter-3, Table 3.6), for clay mineral identification, of these soils.

A3.2 Experimental Procedure

A 10 gm sample of air-dry 2 mm sieved soil was placed on a 12.5 cm Whatman No 2 filter paper, and was leached with successive portions of Neutral Barium Sulphate ($BaSO_4$)

solution to 500 ml. Then 10 ml of a 10% Barium Chloride (Ba Cl_2) solution was poured over the sample in the filter paper. The excess Barium was washed out with distilled water, until the washed solution indicates the absence of chlorides. Next, the Barium adsorbed by the soil was displaced using 0.05 N HCl to a volume of 500 ml, and was collected in a clean jar. The jar was heated on a Bunsen burner flame, and the Barium was precipitated by adding 2% $\text{H}_2 \text{SO}_4$ to the hot solution. The precipitate was collected on a gravimetric filter paper. The filter paper was ashed inside a silicon crucible of known weight. The difference in weights of crucible in the empty state and after ashing the filter paper is equal to the weight of the precipitate. The weights were taken using a balance accurate to 0.0001 g.

The weight of the precipitate is the weight^{of} Barium Sulphate, from which the total cation exchange capacity was calculated as follows:

$$\text{Weight of Ba SO}_4 = \alpha \text{ mg}$$

$$\text{Weight of Barium} = \frac{\alpha \times 56}{152} \text{ mg}$$

Cation Exchange Capacity

$$= \frac{\alpha \times 56}{152 \times 56} \times 10 \frac{\text{meq}}{100 \text{ gm}}$$

A3.3 Results

The cation exchange capacity of soils 350-8 and

350 - 6 were observed to be 30.15 meq/100 gm and 2.33 meq/100 gm respectively. Dividing these values by the appropriate percentages of clay in the soils, the cation exchange capacity of soils 350 - 8 and 350 - 6 per clay become 34.6 meq/100 gm and 25.9 meq/100 gm respectively. These figures are slight overestimates because the effect of organic matter has been ignored. This low range of cation exchange capacity suggests that the soils are essentially either Kaolinitic or illitic without any montmorillonite group minerals. This was in line with the x-ray results of these soils shown in Chapter - 3 (see Table 3.6).

APPENDIX - 4

ISOTROPIC SWELL POTENTIAL

A4.1 Definition and Principle

The isotropic swell potential is defined in the present study as the percentage swell under an allround back pressure of 1 psi (6.895 kN/m²) of an unconfined sample compacted at optimum conditions in a standard A.A.S.H.O. compaction test. An attempt to measure this property was based on the principle that a sample enclosed in a rubber membrane and surrounded by water in a closed cell, when given access to free water, swells freely in all directions and displaces water from the cell equivalent to the increase in volume of the sample.

A4.2 Apparatus

A Triaxial cell of the type used for testing 4 in (102 mm) diameter samples was selected in the present study to measure the isotropic swell potential. This cell has four valves on its base, two valves leading to the pedestal on which the sample is seated, and the other two leading to the surrounding part of the cell. One of the valves leading to the pedestal was used to supply free water to the sample, and the other to permit air to escape from the apparatus. One of the other pair of valves was used to fill the cell with water, and the second was connected to a horizontal glass tube, 0.25 in. (6.4 mm) in diameter and 60 in. (1524 mm) long. The height of the

supply point of free water above the base of the triaxial cell and the height of the glass tube were arranged so that the sample in the cell is under a back pressure of 1 psi throughout the period of testing. The displaced water due to swelling of the sample is collected in a measuring jar from the end point of the glass tube.

A4.3 Test Procedure

The extruded compacted sample was placed on a dry porous stone, which in turn was placed on the pedestal of the triaxial cell. A rubber membrane similar to the one used in the isotropic swell pressure test (see section 2.5.1) was used to enclose the sample. Rubber O-rings were used to seal the sample from contact with the cell water. The top piece of the triaxial cell was rigidly attached to its base and the system was checked for any possible leaks. Next, the cell was filled with water keeping both the air outlet from the pedestal and air vent on the top of the cell open, and the valve leading to the glass tube closed. After the cell was completely filled with water, the air vent on the top of the cell was closed. Then, free water was flushed through the base of the pedestal by opening the valve supplying free water to the sample in order to drive out the entrapped air between the pedestal and the porous stone. Then, both the valve supplying free water and the valve for air release were closed, and the valve leading to the glass tube was opened, Water was run into the cell until the horizontal glass tube was completely

filled with water without any air bubbles in the tube. The system was left in this state for about 60 minutes to attain equilibrium. Next, free water was supplied to the sample to initiate the swelling process. The water displaced due to the increase in the volume of the soil was collected from the end of the glass tube in a graduated jar, the readings of the graduated jar being taken at regular intervals of time. An aluminium foil cover was placed on the graduated jar to reduce evaporation. The swelling was taken as completed when there was no difference between two successive readings of the graduated jar taken at an interval of 24 hours.

The ratio of the volume of water collected in the measuring jar to the initial volume of the sample, expressed as a percentage, is designated as the isotropic swell potential (S_i).

A4.4 Results and Comments

Fig. A4-1 shows the graphs of the isotropic swell potential against time for the illite sand series. Whilst the shape of the curves is similar to that of the variation of laterally confined swell potential (see section 3.4.5.1), it was observed that after reaching 'maximum', the water level at the end point of the glass tube receded. For this reason it was decided that these results should be treated with caution.

The results in volumetric terms are summarised in Table A4-1. Fig. A4-2 shows both water uptake, DW , and isotropic swell amount, S_{iS} , against sand content. Quadratic curves are fitted to both these sets of data up to 68% sand, although the fits are not as good as for

- × Illite 100%
- Illite 82%
- △ Illite 64%
- Illite 50%
- Illite 32%

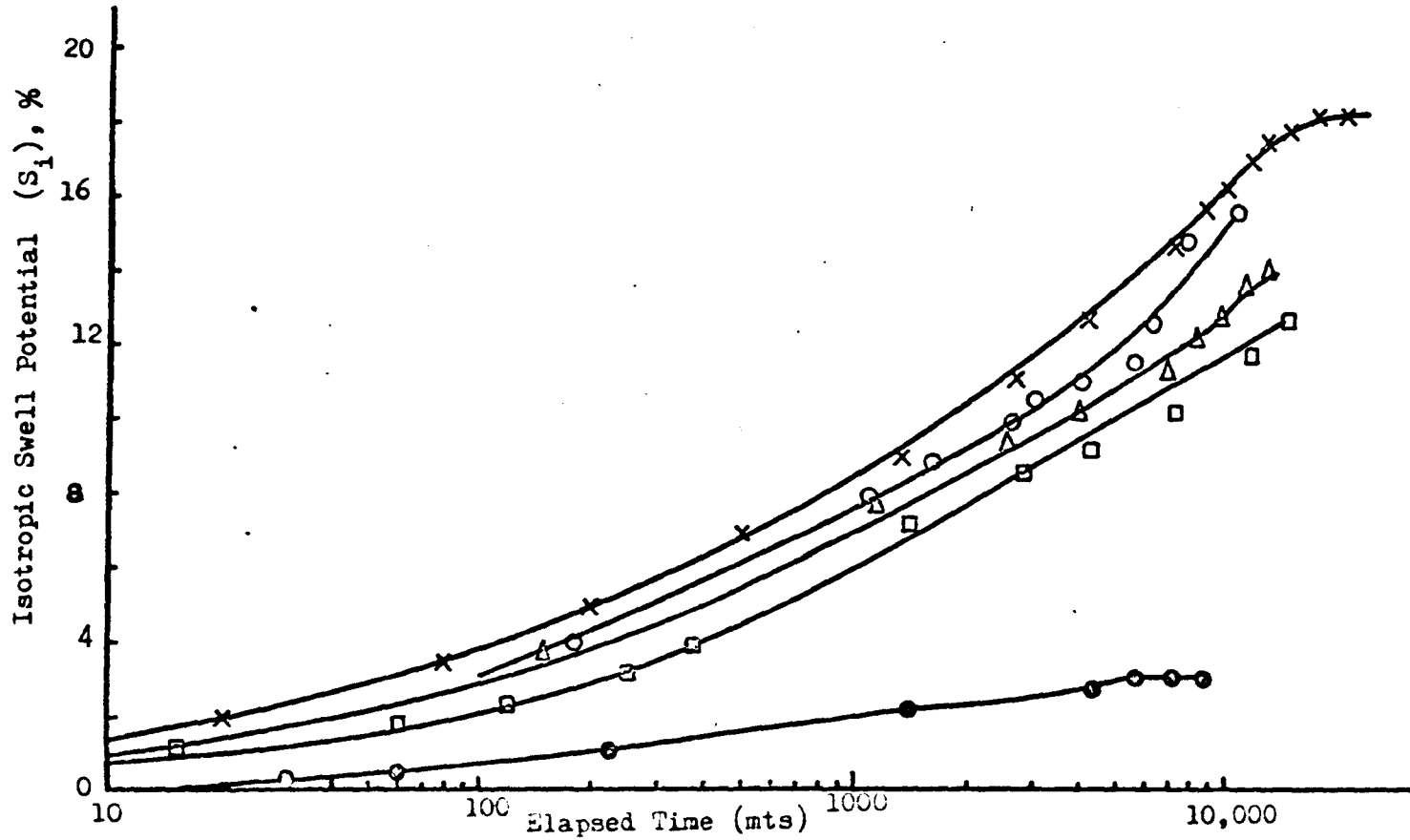


Fig. A4-1 Isotropic Swell Potential versus Time, Illite-Sand Mixtures.

Table A4-1. Illite - Sand: Isotropic Swell Potential Tests

All quantities are referred to the volume of Solids.

Clay %	\mathcal{V}_i %	α_i %	e_i %	S_{is} %	\mathcal{V}_f %	α_f %	e_f %
100.0	74	6	80	33	110	3	113
82.0	66	8	74	27	98	3	101
64.0	57	8	65	23	84	4	88
50.0	49	9	58	20	71	7	78
32.0	37	11	48	4	44	8	52
14.0	31	27	58	1.5	34	25	59.5
00.0	33	28	61	-	-	-	-

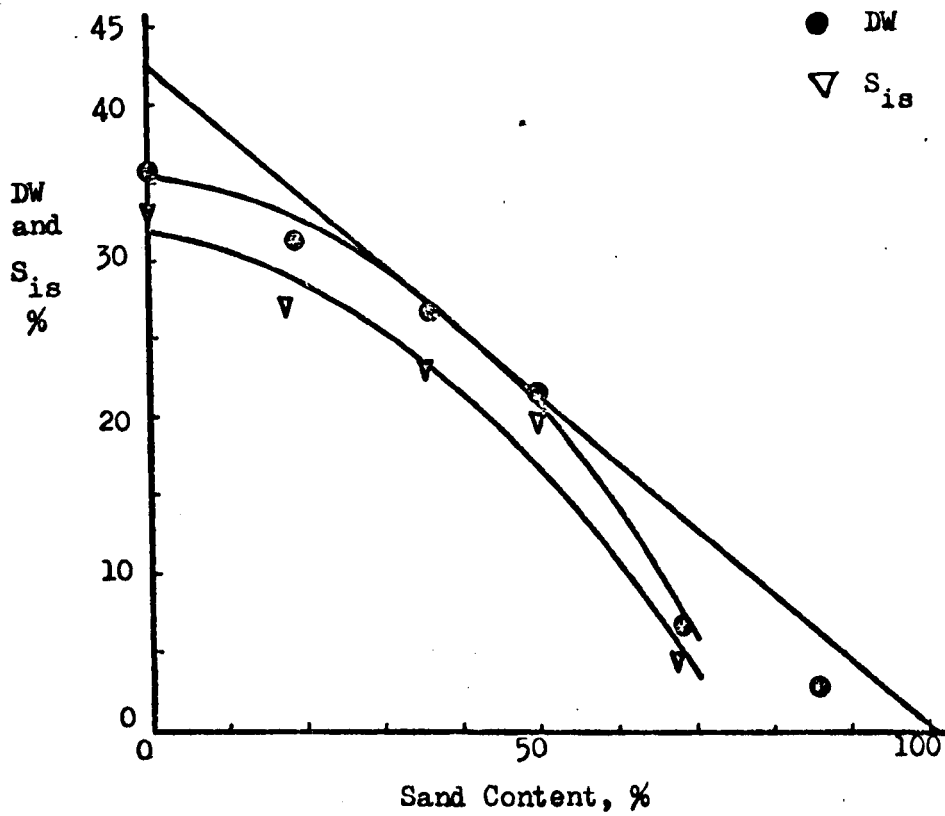


Fig. A4-2 Water Uptake and Isotropic Swell Amount
versus Sand Content, Illite-Sand Mixtures.

the laterally confined case, see Fig. 5.21. . The values of isotropic swell amount, S_{is} , when plotted against the water uptake, DW , fall close to the 1:1 line, Fig. A4-3. This behaviour is similar to that of the laterally confined samples, Fig. 5.22 . However, the behaviour of both quantities did seem to differ from that of the laterally confined case as is evident when Fig. A4-2 is compared in detail with Fig. 5.21 . In the laterally confined case, water uptake was fitted by a quadratic curve, whose tangent at 100% clay content passed through the no-clay content origin. This tangent is replotted in Fig. A4-2. The observed values of water uptake for the isotropic case are approximately tangential to this straight line at about 40% sand, but this may well be fortuitous. In particular both water uptake and swell amount for the isotropic case were less than the corresponding values for the laterally confined case at high clay contents. This is illustrated in Fig. A4-4, in which the ratio $\frac{S_i}{S_c}$ is plotted against the sand content. The values of S_i and S_c are very small at high sand content, and therefore the value of the ratio $\frac{S_i}{S_c}$ may be somewhat in error towards the right of the graph in Fig. A4-4. It is not clear why the isotropic swell potential, S_i is less than the laterally confined swell potential, S_c , at high clay contents. In Chapter-5 it was reported that the isotropic swell pressure is less than the laterally confined swell pressure for high clay contents, and it was suggested that this was because the unconfined sample is able to adjust its shape to relieve the stresses acting on it. This

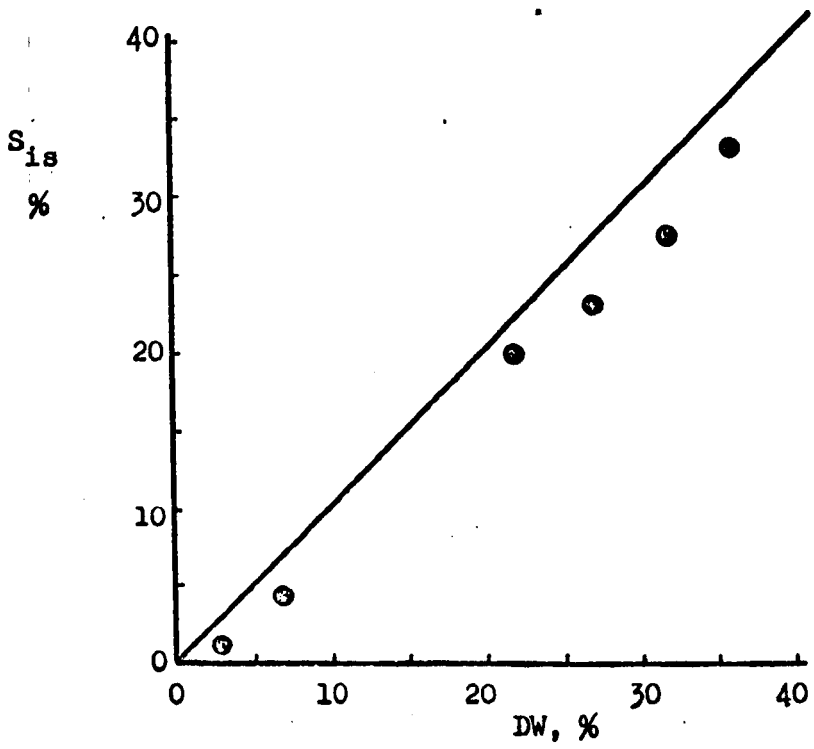


Fig. A4-3 Isotropic Swell Amount versus Water Uptake, Illite-Sand Mixtures.

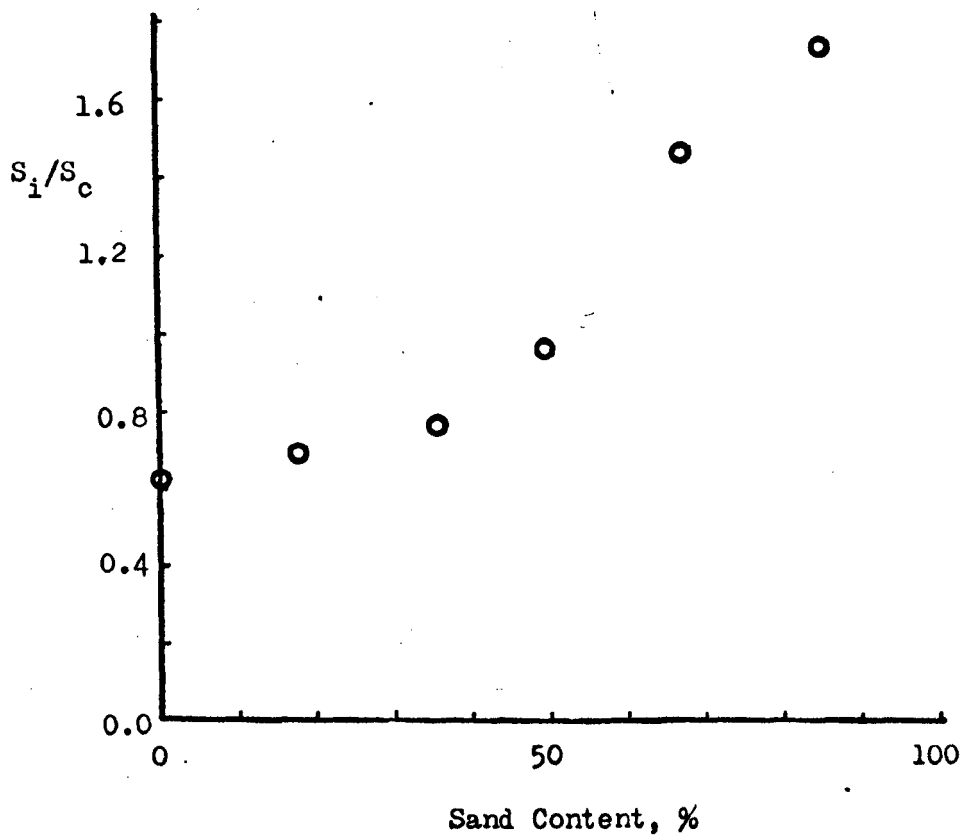


Fig. A4-4 Ratio of Isotropic to Laterally Confined Swell Potential VS Sand Content, Illite-Sand Mixtures.

explanation would not hold for swell potential. It was therefore feared that some experimental error associated with the recession of the water level in the glass tube has crept in. This may be due to (1) the sample shrinking, or (2) loss of water from the apparatus or (3) bedding corrections under the 1 psi back pressure as the sample wets and becomes softer.

It is recommended that further research is necessary to estimate the isotropic swell potential more satisfactorily.

APPENDIX - 5

NON-DIMENSIONAL COMPACTION CURVES

It is customary to present the results of compaction tests by plotting dry density γ_d against gravimetric water content w . As an aid to interpretation, a few contours of air voids content are often plotted; the location of these contours depends on the density of the solids γ_s . If results for several soils are to be plotted on the same diagram for comparative purposes, several sets of contours of air voids content are required, and confusion results. For such purposes it would be preferable to plot relative dry density y against volumetric water content x , where:-

$$y = \gamma_d / \gamma_s.$$

On such a diagram, there are unique sets of contours, which are independent of γ_s , for all of the following five quantities;

$$\text{Voids ratio} = e = \frac{V_a + V_w}{V_s} = \frac{1}{y} - 1 \quad (\text{A5-1})$$

$$\text{Porosity} = n = \frac{V_a + V_w}{V_t} = 1 - y \quad (\text{A5-2})$$

$$\text{Air voids content} = a = \frac{V_a}{V_t} = 1 - y - xy \quad (\text{A5-3})$$

$$\text{Degree of saturation} = S_r = \frac{V_w}{V_a + V_w} = \frac{xy}{1 - y} \quad (\text{A5-4})$$

$$\text{Degree of aeration} = S_a = \frac{V_a}{V_a + V_w} = \frac{1 - y - xy}{1 - y} \quad (\text{A5-5})$$

$$\text{Relative dry density} = y = \frac{V_s}{V_t} \quad (\text{A5-6})$$

$$\text{Volumetric water content} = x = \frac{V_w}{V_s} \quad (\text{A5-7})$$

The last two equations have been added for convenience; V_a , V_w , V_s , V_t are the volumes of air, water, and solids, and total volume, respectively. The various sets of contours may be plotted by calculating y from:-

$$\text{Voids ratio} \quad y = \frac{1}{1 + e} \quad (\text{A5-8})$$

$$\text{Porosity} \quad y = 1 - n \quad (\text{A5-9})$$

$$\text{Air voids content} \quad y = \frac{1 - a}{1 + x} \quad (\text{A5-10})$$

$$\text{Degree of saturation} \quad y = \frac{S_r}{x + S_r} \quad (\text{A5-11})$$

Since porosity and voids ratio are linear and non-linear functions of y , and since:-

$$S_a = 1 - S_r \quad (\text{A5-12})$$

there are only two sets of contours of importance, those for a and S_r .

Values of y for plotting contours of a and S_r are in Tables A5-1 and A5-2 respectively; values of y for various e are in Table A5-3.

TABLE A5-1 RELATIVE BULK DENSITY

PAK 1

W/V%	0.00	0.05	0.10	0.15	0.20	0.25	0.30	0.35	0.40
1.00	0.9500	0.9500	0.9500	0.9500	0.9500	0.9500	0.9500	0.9500	0.9500
0.98	0.9504	0.9514	0.9524	0.9533	0.9543	0.9553	0.9563	0.9573	0.9582
0.96	0.9508	0.9519	0.9529	0.9539	0.9549	0.9559	0.9569	0.9579	0.9588
0.94	0.9512	0.9523	0.9533	0.9543	0.9553	0.9563	0.9573	0.9583	0.9592
0.92	0.9516	0.9527	0.9537	0.9547	0.9557	0.9567	0.9577	0.9587	0.9596
0.90	0.9520	0.9531	0.9541	0.9551	0.9561	0.9571	0.9581	0.9591	0.9600
0.88	0.9524	0.9535	0.9545	0.9555	0.9565	0.9575	0.9585	0.9595	0.9604
0.86	0.9528	0.9539	0.9549	0.9559	0.9569	0.9579	0.9589	0.9599	0.9608
0.84	0.9532	0.9543	0.9553	0.9563	0.9573	0.9583	0.9593	0.9603	0.9612
0.82	0.9536	0.9547	0.9557	0.9567	0.9577	0.9587	0.9597	0.9607	0.9616
0.80	0.9540	0.9551	0.9561	0.9571	0.9581	0.9591	0.9601	0.9611	0.9620
0.78	0.9544	0.9555	0.9565	0.9575	0.9585	0.9595	0.9605	0.9615	0.9624
0.76	0.9548	0.9559	0.9569	0.9579	0.9589	0.9599	0.9609	0.9619	0.9628
0.74	0.9552	0.9563	0.9573	0.9583	0.9593	0.9603	0.9613	0.9623	0.9632
0.72	0.9556	0.9567	0.9577	0.9587	0.9597	0.9607	0.9617	0.9627	0.9636
0.70	0.9560	0.9571	0.9581	0.9591	0.9601	0.9611	0.9621	0.9631	0.9640
0.68	0.9564	0.9575	0.9585	0.9595	0.9605	0.9615	0.9625	0.9635	0.9644
0.66	0.9568	0.9579	0.9589	0.9599	0.9609	0.9619	0.9629	0.9639	0.9648
0.64	0.9572	0.9583	0.9593	0.9603	0.9613	0.9623	0.9633	0.9643	0.9652
0.62	0.9576	0.9587	0.9597	0.9607	0.9617	0.9627	0.9637	0.9647	0.9656
0.60	0.9580	0.9591	0.9601	0.9611	0.9621	0.9631	0.9641	0.9651	0.9660
0.58	0.9584	0.9595	0.9605	0.9615	0.9625	0.9635	0.9645	0.9655	0.9664
0.56	0.9588	0.9599	0.9609	0.9619	0.9629	0.9639	0.9649	0.9659	0.9668
0.54	0.9592	0.9603	0.9613	0.9623	0.9633	0.9643	0.9653	0.9663	0.9672
0.52	0.9596	0.9607	0.9617	0.9627	0.9637	0.9647	0.9657	0.9667	0.9676
0.50	0.9600	0.9611	0.9621	0.9631	0.9641	0.9651	0.9661	0.9671	0.9680
0.48	0.9604	0.9615	0.9625	0.9635	0.9645	0.9655	0.9665	0.9675	0.9684
0.46	0.9608	0.9619	0.9629	0.9639	0.9649	0.9659	0.9669	0.9679	0.9688
0.44	0.9612	0.9623	0.9633	0.9643	0.9653	0.9663	0.9673	0.9683	0.9692
0.42	0.9616	0.9627	0.9637	0.9647	0.9657	0.9667	0.9677	0.9687	0.9696
0.40	0.9620	0.9631	0.9641	0.9651	0.9661	0.9671	0.9681	0.9691	0.9700
0.38	0.9624	0.9635	0.9645	0.9655	0.9665	0.9675	0.9685	0.9695	0.9704
0.36	0.9628	0.9639	0.9649	0.9659	0.9669	0.9679	0.9689	0.9699	0.9708
0.34	0.9632	0.9643	0.9653	0.9663	0.9673	0.9683	0.9693	0.9703	0.9712
0.32	0.9636	0.9647	0.9657	0.9667	0.9677	0.9687	0.9697	0.9707	0.9716
0.30	0.9640	0.9651	0.9661	0.9671	0.9681	0.9691	0.9701	0.9711	0.9720
0.28	0.9644	0.9655	0.9665	0.9675	0.9685	0.9695	0.9705	0.9715	0.9724
0.26	0.9648	0.9659	0.9669	0.9679	0.9689	0.9699	0.9709	0.9719	0.9728
0.24	0.9652	0.9663	0.9673	0.9683	0.9693	0.9703	0.9713	0.9723	0.9732
0.22	0.9656	0.9667	0.9677	0.9687	0.9697	0.9707	0.9717	0.9727	0.9736
0.20	0.9660	0.9671	0.9681	0.9691	0.9701	0.9711	0.9721	0.9731	0.9740
0.18	0.9664	0.9675	0.9685	0.9695	0.9705	0.9715	0.9725	0.9735	0.9744
0.16	0.9668	0.9679	0.9689	0.9699	0.9709	0.9719	0.9729	0.9739	0.9748
0.14	0.9672	0.9683	0.9693	0.9703	0.9713	0.9723	0.9733	0.9743	0.9752
0.12	0.9676	0.9687	0.9697	0.9707	0.9717	0.9727	0.9737	0.9747	0.9756
0.10	0.9680	0.9691	0.9701	0.9711	0.9721	0.9731	0.9741	0.9751	0.9760
0.08	0.9684	0.9695	0.9705	0.9715	0.9725	0.9735	0.9745	0.9755	0.9764
0.06	0.9688	0.9699	0.9709	0.9719	0.9729	0.9739	0.9749	0.9759	0.9768
0.04	0.9692	0.9703	0.9713	0.9723	0.9733	0.9743	0.9753	0.9763	0.9772
0.02	0.9696	0.9707	0.9717	0.9727	0.9737	0.9747	0.9757	0.9767	0.9776
0.00	0.9700	0.9711	0.9721	0.9731	0.9741	0.9751	0.9761	0.9771	0.9780

TABLE A5-1

RELATIVE BULK DENSITY

PART 2

	A=0.50	0.55	0.60	0.65	0.70	0.75	0.80	0.85	0.90
VW/VS									
0.00	0.5000	0.4500	0.4000	0.3500	0.3000	0.2500	0.2000	0.1500	0.1000
0.02	0.4902	0.4412	0.3922	0.3431	0.2941	0.2451	0.1961	0.1471	0.0980
0.04	0.4808	0.4327	0.3846	0.3365	0.2885	0.2404	0.1923	0.1442	0.0962
0.06	0.4717	0.4245	0.3774	0.3302	0.2830	0.2358	0.1887	0.1415	0.0943
0.08	0.4630	0.4167	0.3704	0.3241	0.2778	0.2315	0.1852	0.1389	0.0926
0.10	0.4545	0.4091	0.3638	0.3182	0.2727	0.2273	0.1818	0.1354	0.0909
0.12	0.4464	0.4018	0.3571	0.3125	0.2679	0.2232	0.1780	0.1339	0.0893
0.14	0.4386	0.3947	0.3509	0.3070	0.2632	0.2193	0.1754	0.1316	0.0877
0.16	0.4310	0.3879	0.3448	0.3017	0.2586	0.2155	0.1724	0.1293	0.0862
0.18	0.4237	0.3814	0.3390	0.2966	0.2542	0.2119	0.1695	0.1271	0.0847
0.20	0.4167	0.3750	0.3333	0.2917	0.2500	0.2083	0.1667	0.1250	0.0833
0.22	0.4098	0.3689	0.3279	0.2869	0.2459	0.2049	0.1639	0.1230	0.0820
0.24	0.4032	0.3629	0.3226	0.2823	0.2419	0.2016	0.1613	0.1210	0.0806
0.26	0.3966	0.3571	0.3175	0.2778	0.2381	0.1984	0.1587	0.1190	0.0794
0.28	0.3906	0.3516	0.3125	0.2734	0.2344	0.1953	0.1563	0.1172	0.0781
0.30	0.3846	0.3462	0.3077	0.2692	0.2308	0.1923	0.1538	0.1154	0.0769
0.32	0.3788	0.3409	0.3030	0.2652	0.2273	0.1894	0.1515	0.1136	0.0758
0.34	0.3731	0.3358	0.2985	0.2612	0.2239	0.1866	0.1493	0.1119	0.0746
0.36	0.3676	0.3309	0.2941	0.2574	0.2206	0.1838	0.1471	0.1103	0.0735
0.38	0.3623	0.3261	0.2899	0.2536	0.2174	0.1812	0.1449	0.1087	0.0725
0.40	0.3571	0.3214	0.2857	0.2500	0.2143	0.1786	0.1429	0.1071	0.0714
0.42	0.3521	0.3169	0.2817	0.2465	0.2113	0.1761	0.1408	0.1056	0.0704
0.44	0.3472	0.3125	0.2778	0.2431	0.2083	0.1736	0.1389	0.1042	0.0694
0.46	0.3425	0.3082	0.2740	0.2397	0.2055	0.1712	0.1370	0.1027	0.0685
0.48	0.3378	0.3041	0.2703	0.2365	0.2027	0.1689	0.1351	0.1014	0.0676
0.50	0.3333	0.3000	0.2667	0.2333	0.2000	0.1667	0.1333	0.1000	0.0667
0.52	0.3289	0.2961	0.2632	0.2303	0.1974	0.1645	0.1316	0.0987	0.0658
0.54	0.3247	0.2922	0.2597	0.2273	0.1948	0.1623	0.1299	0.0974	0.0649
0.56	0.3205	0.2885	0.2564	0.2244	0.1923	0.1603	0.1282	0.0962	0.0641
0.58	0.3165	0.2848	0.2532	0.2215	0.1899	0.1582	0.1266	0.0949	0.0633
0.60	0.3125	0.2813	0.2500	0.2188	0.1875	0.1563	0.1250	0.0938	0.0625
0.62	0.3086	0.2778	0.2469	0.2160	0.1852	0.1543	0.1233	0.0926	0.0617
0.64	0.3049	0.2744	0.2439	0.2134	0.1829	0.1524	0.1220	0.0915	0.0610
0.66	0.3012	0.2711	0.2410	0.2108	0.1807	0.1506	0.1205	0.0904	0.0602
0.68	0.2976	0.2679	0.2381	0.2083	0.1786	0.1488	0.1190	0.0893	0.0595
0.70	0.2941	0.2647	0.2353	0.2059	0.1765	0.1471	0.1176	0.0882	0.0588
0.72	0.2907	0.2616	0.2326	0.2035	0.1744	0.1453	0.1163	0.0872	0.0581
0.74	0.2874	0.2586	0.2299	0.2011	0.1724	0.1437	0.1149	0.0862	0.0575
0.76	0.2841	0.2557	0.2273	0.1989	0.1705	0.1420	0.1136	0.0852	0.0568
0.78	0.2809	0.2528	0.2247	0.1966	0.1685	0.1404	0.1124	0.0843	0.0562
0.80	0.2778	0.2500	0.2222	0.1944	0.1667	0.1389	0.1111	0.0833	0.0556
0.82	0.2747	0.2473	0.2198	0.1923	0.1648	0.1374	0.1099	0.0824	0.0549
0.84	0.2717	0.2446	0.2174	0.1902	0.1630	0.1359	0.1087	0.0815	0.0543
0.86	0.2688	0.2419	0.2151	0.1882	0.1613	0.1344	0.1075	0.0806	0.0538
0.88	0.2660	0.2394	0.2128	0.1862	0.1596	0.1330	0.1064	0.0798	0.0532
0.90	0.2632	0.2368	0.2105	0.1842	0.1579	0.1316	0.1053	0.0789	0.0526
0.92	0.2604	0.2344	0.2083	0.1823	0.1563	0.1302	0.1042	0.0781	0.0521
0.94	0.2577	0.2320	0.2062	0.1804	0.1548	0.1289	0.1031	0.0773	0.0515
0.96	0.2551	0.2296	0.2041	0.1786	0.1531	0.1276	0.1020	0.0765	0.0510
0.98	0.2525	0.2273	0.2020	0.1768	0.1515	0.1263	0.1010	0.0758	0.0505
1.00	0.2500	0.2250	0.2000	0.1750	0.1500	0.1250	0.1000	0.0750	0.0500

TABLE A5-2 RELATIVE BULK DENSITY

PART 1

	SR=1.00	0.95	0.90	0.85	0.80	0.75	0.70	0.65	0.60
VW/VS									
0.00	1.0000	1.0000	1.0000	1.0000	1.0000	1.0000	1.0000	1.0000	1.0000
0.02	0.9804	0.9794	0.9783	0.9770	0.9756	0.9740	0.9722	0.9701	0.9677
0.04	0.9615	0.9596	0.9574	0.9551	0.9524	0.9494	0.9459	0.9420	0.9375
0.06	0.9434	0.9406	0.9375	0.9341	0.9302	0.9259	0.9211	0.9155	0.9091
0.08	0.9259	0.9223	0.9184	0.9140	0.9091	0.9036	0.8974	0.8904	0.8824
0.10	0.9091	0.9048	0.9000	0.8947	0.8889	0.8824	0.8750	0.8667	0.8571
0.12	0.8929	0.8879	0.8824	0.8763	0.8696	0.8621	0.8537	0.8442	0.8333
0.14	0.8772	0.8716	0.8654	0.8586	0.8511	0.8427	0.8333	0.8228	0.8108
0.16	0.8621	0.8559	0.8491	0.8416	0.8333	0.8242	0.8140	0.8025	0.7895
0.18	0.8475	0.8407	0.8333	0.8252	0.8163	0.8065	0.7955	0.7831	0.7692
0.20	0.8333	0.8261	0.8182	0.8095	0.8000	0.7895	0.7776	0.7647	0.7500
0.22	0.8197	0.8120	0.8036	0.7944	0.7843	0.7732	0.7609	0.7471	0.7317
0.24	0.8065	0.7983	0.7895	0.7798	0.7692	0.7576	0.7447	0.7303	0.7143
0.26	0.7937	0.7851	0.7759	0.7658	0.7547	0.7426	0.7292	0.7143	0.6977
0.28	0.7813	0.7724	0.7627	0.7522	0.7407	0.7282	0.7143	0.6989	0.6818
0.30	0.7692	0.7600	0.7500	0.7391	0.7273	0.7143	0.7000	0.6842	0.6667
0.32	0.7576	0.7480	0.7377	0.7265	0.7143	0.7009	0.6863	0.6701	0.6522
0.34	0.7463	0.7364	0.7258	0.7143	0.7018	0.6881	0.6731	0.6566	0.6383
0.36	0.7353	0.7252	0.7143	0.7025	0.6897	0.6757	0.6604	0.6436	0.6250
0.38	0.7246	0.7143	0.7031	0.6911	0.6780	0.6637	0.6481	0.6311	0.6122
0.40	0.7143	0.7037	0.6923	0.6800	0.6667	0.6522	0.6364	0.6190	0.6000
0.42	0.7042	0.6934	0.6818	0.6693	0.6557	0.6410	0.6250	0.6075	0.5882
0.44	0.6944	0.6835	0.6716	0.6589	0.6452	0.6303	0.6140	0.5963	0.5769
0.46	0.6849	0.6738	0.6618	0.6489	0.6349	0.6198	0.6034	0.5856	0.5660
0.48	0.6757	0.6643	0.6522	0.6391	0.6250	0.6098	0.5932	0.5752	0.5556
0.50	0.6667	0.6552	0.6429	0.6296	0.6154	0.6000	0.5833	0.5652	0.5455
0.52	0.6579	0.6463	0.6338	0.6204	0.6061	0.5906	0.5738	0.5556	0.5357
0.54	0.6494	0.6376	0.6250	0.6115	0.5970	0.5814	0.5645	0.5462	0.5263
0.56	0.6410	0.6291	0.6164	0.6028	0.5882	0.5725	0.5556	0.5372	0.5172
0.58	0.6329	0.6209	0.6081	0.5944	0.5797	0.5639	0.5469	0.5285	0.5085
0.60	0.6250	0.6129	0.6000	0.5862	0.5714	0.5556	0.5385	0.5200	0.5000
0.62	0.6173	0.6051	0.5921	0.5782	0.5634	0.5474	0.5303	0.5118	0.4918
0.64	0.6098	0.5975	0.5844	0.5705	0.5556	0.5396	0.5224	0.5039	0.4839
0.66	0.6024	0.5901	0.5769	0.5629	0.5479	0.5319	0.5147	0.4962	0.4762
0.68	0.5952	0.5828	0.5696	0.5556	0.5405	0.5245	0.5072	0.4887	0.4688
0.70	0.5882	0.5758	0.5625	0.5484	0.5333	0.5172	0.5000	0.4815	0.4615
0.72	0.5814	0.5689	0.5556	0.5414	0.5263	0.5102	0.4930	0.4745	0.4545
0.74	0.5747	0.5621	0.5488	0.5346	0.5195	0.5034	0.4861	0.4676	0.4476
0.76	0.5682	0.5556	0.5422	0.5280	0.5128	0.4967	0.4795	0.4610	0.4412
0.78	0.5618	0.5491	0.5357	0.5215	0.5063	0.4902	0.4730	0.4545	0.4346
0.80	0.5556	0.5429	0.5294	0.5152	0.5000	0.4839	0.4667	0.4483	0.4286
0.82	0.5495	0.5367	0.5233	0.5090	0.4938	0.4777	0.4605	0.4422	0.4225
0.84	0.5435	0.5307	0.5172	0.5030	0.4878	0.4717	0.4545	0.4362	0.4167
0.86	0.5376	0.5249	0.5114	0.4971	0.4819	0.4658	0.4487	0.4305	0.4110
0.88	0.5319	0.5191	0.5056	0.4913	0.4762	0.4601	0.4430	0.4248	0.4054
0.90	0.5263	0.5135	0.5000	0.4857	0.4706	0.4545	0.4375	0.4194	0.4000
0.92	0.5208	0.5080	0.4945	0.4802	0.4651	0.4491	0.4321	0.4140	0.3947
0.94	0.5155	0.5026	0.4891	0.4749	0.4598	0.4438	0.4268	0.4088	0.3896
0.96	0.5102	0.4974	0.4839	0.4696	0.4545	0.4386	0.4217	0.4037	0.3845
0.98	0.5051	0.4922	0.4787	0.4645	0.4494	0.4335	0.4167	0.3988	0.3797
1.00	0.5000	0.4872	0.4737	0.4595	0.4444	0.4286	0.4118	0.3939	0.3750

TABLE A5-2

RELATIVE BULK DENSITY

PART 2

	SR=0.50	0.45	0.40	0.35	0.30	0.25	0.20	0.15	0.10
VW/VS									
0.00	1.0000	1.0000	1.0000	1.0000	1.0000	1.0000	1.0000	1.0000	1.0000
0.02	0.9615	0.9574	0.9524	0.9459	0.9375	0.9259	0.9091	0.8824	0.8333
0.04	0.9259	0.9184	0.9091	0.8974	0.8824	0.8621	0.8333	0.7895	0.7143
0.06	0.8929	0.8824	0.8696	0.8537	0.8333	0.8065	0.7692	0.7143	0.6250
0.08	0.8621	0.8491	0.8333	0.8140	0.7895	0.7576	0.7143	0.6522	0.5556
0.10	0.8333	0.8182	0.8000	0.7778	0.7500	0.7143	0.6667	0.6000	0.5000
0.12	0.8065	0.7895	0.7692	0.7447	0.7143	0.6757	0.6250	0.5556	0.4545
0.14	0.7812	0.7627	0.7407	0.7143	0.6818	0.6410	0.5882	0.5172	0.4167
0.16	0.7576	0.7377	0.7143	0.6863	0.6522	0.6098	0.5556	0.4839	0.3846
0.18	0.7353	0.7143	0.6897	0.6604	0.6250	0.5814	0.5263	0.4545	0.3571
0.20	0.7143	0.6923	0.6667	0.6364	0.6000	0.5556	0.5000	0.4286	0.3333
0.22	0.6944	0.6716	0.6452	0.6140	0.5769	0.5319	0.4762	0.4054	0.3125
0.24	0.6757	0.6522	0.6250	0.5932	0.5556	0.5102	0.4545	0.3846	0.2941
0.26	0.6579	0.6338	0.6061	0.5738	0.5357	0.4902	0.4348	0.3659	0.2778
0.28	0.6410	0.6164	0.5882	0.5556	0.5172	0.4717	0.4167	0.3488	0.2632
0.30	0.6250	0.6000	0.5714	0.5385	0.5000	0.4545	0.4000	0.3333	0.2500
0.32	0.6098	0.5844	0.5556	0.5224	0.4839	0.4386	0.3846	0.3191	0.2381
0.34	0.5952	0.5696	0.5405	0.5072	0.4687	0.4237	0.3704	0.3061	0.2273
0.36	0.5814	0.5556	0.5263	0.4930	0.4545	0.4098	0.3571	0.2941	0.2174
0.38	0.5682	0.5422	0.5128	0.4795	0.4412	0.3968	0.3448	0.2830	0.2083
0.40	0.5556	0.5294	0.5000	0.4667	0.4286	0.3846	0.3333	0.2727	0.2000
0.42	0.5435	0.5172	0.4878	0.4545	0.4167	0.3731	0.3226	0.2632	0.1923
0.44	0.5319	0.5056	0.4762	0.4430	0.4054	0.3623	0.3125	0.2542	0.1852
0.46	0.5208	0.4945	0.4651	0.4321	0.3947	0.3521	0.3030	0.2459	0.1786
0.48	0.5102	0.4839	0.4545	0.4217	0.3846	0.3425	0.2941	0.2381	0.1724
0.50	0.5000	0.4737	0.4444	0.4118	0.3750	0.3333	0.2857	0.2308	0.1667
0.52	0.4902	0.4639	0.4348	0.4023	0.3659	0.3247	0.2778	0.2239	0.1613
0.54	0.4808	0.4545	0.4255	0.3933	0.3571	0.3165	0.2703	0.2174	0.1562
0.56	0.4717	0.4455	0.4167	0.3846	0.3488	0.3086	0.2632	0.2113	0.1515
0.58	0.4630	0.4369	0.4082	0.3763	0.3409	0.3012	0.2564	0.2055	0.1471
0.60	0.4545	0.4286	0.4000	0.3634	0.3333	0.2941	0.2500	0.2000	0.1429
0.62	0.4464	0.4206	0.3922	0.3608	0.3261	0.2874	0.2439	0.1948	0.1389
0.64	0.4386	0.4128	0.3846	0.3535	0.3191	0.2809	0.2381	0.1899	0.1351
0.66	0.4310	0.4054	0.3774	0.3465	0.3125	0.2747	0.2326	0.1852	0.1316
0.68	0.4237	0.3982	0.3704	0.3398	0.3061	0.2688	0.2273	0.1807	0.1282
0.70	0.4167	0.3913	0.3636	0.3333	0.3000	0.2632	0.2222	0.1765	0.1250
0.72	0.4098	0.3846	0.3571	0.3271	0.2941	0.2577	0.2174	0.1724	0.1220
0.74	0.4032	0.3782	0.3509	0.3211	0.2885	0.2525	0.2128	0.1685	0.1190
0.76	0.3968	0.3719	0.3448	0.3153	0.2830	0.2475	0.2083	0.1648	0.1163
0.78	0.3906	0.3659	0.3390	0.3097	0.2778	0.2427	0.2041	0.1613	0.1136
0.80	0.3846	0.3600	0.3333	0.3043	0.2727	0.2381	0.2000	0.1579	0.1111
0.82	0.3788	0.3543	0.3279	0.2991	0.2679	0.2336	0.1961	0.1546	0.1087
0.84	0.3731	0.3488	0.3226	0.2941	0.2632	0.2294	0.1923	0.1515	0.1064
0.86	0.3676	0.3435	0.3175	0.2893	0.2586	0.2252	0.1887	0.1485	0.1042
0.88	0.3623	0.3383	0.3125	0.2846	0.2542	0.2212	0.1852	0.1456	0.1020
0.90	0.3571	0.3333	0.3077	0.2800	0.2500	0.2174	0.1818	0.1429	0.1000
0.92	0.3521	0.3285	0.3030	0.2756	0.2459	0.2137	0.1786	0.1402	0.0980
0.94	0.3472	0.3237	0.2985	0.2713	0.2419	0.2101	0.1754	0.1376	0.0962
0.96	0.3425	0.3191	0.2941	0.2672	0.2381	0.2066	0.1724	0.1351	0.0943
0.98	0.3378	0.3147	0.2899	0.2632	0.2344	0.2033	0.1695	0.1327	0.0926
1.00	0.3333	0.3103	0.2857	0.2593	0.2308	0.2000	0.1667	0.1304	0.0909

Table - A5-3

e	γ_d/γ_s
0.00	1.00
0.05	0.9524
0.10	0.9091
0.15	0.8696
0.20	0.8333
0.25	0.8000
0.30	0.7692
0.35	0.7407
0.40	0.7143
0.45	0.6897
0.50	0.6667
0.55	0.6452
0.60	0.625
0.65	0.6061
0.70	0.5882
0.75	0.5714
0.80	0.5556
0.85	0.5405
0.90	0.5263
0.95	0.5128
1.00	0.5000

APPENDIX. 6

ELASTIC MIXING LAWS

A6.1 Introduction

Several workers in the past have attempted to develop suitable mixing laws for the prediction of the elastic constants of 2-phase mixtures of metals and polymer materials. These laws were considered here as a semi-empirical approach to the problem of predicting the swell properties from the corresponding properties of the soil components, such as sand and clay. Throughout this section, the soil is assumed to be composed of two solid phases, eg. sand and clay; and v_1 and v_2 are the parts by volume of these phases.

A6.2 Voigt and Reuss

According to Gray and McCrum (1969), Voigt (1910) suggested a linear mixing law of the form:

$$K = v_1 K_1 + v_2 K_2 \quad (\text{A6-1})$$

where K is the bulk modulus of the mixture, and K_1 and K_2 are the bulk moduli of phases 1 & 2 respectively.

Whilst Voigt suggested the above relation assuming that the strain throughout the composite mixture is uniform, Reuss (1929) (quoted by Gray and McCrum, 1969), based on the assumption of constant stress throughout the mass, suggested the relation:

$$\frac{1}{K} = \frac{v_1}{K_1} + \frac{v_2}{K_2} \quad (\text{A6-2})$$

Comparison of Equations (A6-1) and (A6-2) draws attention to the importance of defining the property of interest in the most suitable way, eg. if Reuss were correct $\frac{1}{K}$ would be more suitable than K.

A6.3 Paul's Theory

Paul (1960) put forward the following two laws as the upper and lower bounds on Young's modulus (E), by making use of the strain energy theorems of elasticity:

$$E = E_1 v_1 + E_2 v_2 \quad (\text{A6-3})$$

$$\frac{1}{E} = \frac{1}{E_1} v_1 + \frac{1}{E_2} v_2 \quad (\text{A6-4})$$

It can be noticed that these bounds have the same form as the equations proposed by Voigt and Reuss respectively.

A6.4 HSH Bounds

According to Gray and McCrum (1969), Hill (1963) and Hashin and Shtrikman (1963) tightened the above laws by recommending the following bounds, usually called as HSH bounds:

$$K_1 + \frac{v_2}{\frac{1}{k_2 - k_1} + \frac{3v_1}{3K_1 + 4G_1}} \leq K \leq K_2 + \frac{v_1}{\frac{1}{K_1 - K_2} + \frac{3v_2}{3K_2 + 4G_2}} \quad (\text{A6-5})$$

where G denotes shear modulus. The HSH bounds use two material properties K and G, of both phases to predict a single property of the composite mixture.

A6.5 Logarithmic Mixing Law

Gray and McCrum (1969) considered the implications of a logarithmic mixing law of the following form for elastic shear modulus, G , viz:-

$$\log G = v_1 \log G_1 + v_2 \log G_2 \quad (\text{A6-6})$$

They observed that this mixing law falls well within the HSH bounds, and they suggest it as a law of mixing.

Because of the agreement with the HSH bounds it has been included here, but strictly it is empirical.

A6.6 Summary

The equations above were considered to discover whether satisfactory mixing laws could be generated by substituting P_c say for the elastic constants E, G or K . In practice, only the linear mixing law of Voigt (1910) has proved useful, and in particular many of the swell pressure measurements lay outside the Voigt-Reuss bounds, which are themselves wider than the HSH bounds.

APPENDIX 7

LATERALLY CONFINED SWELL PRESSURE OF
BENTONITE-ILLITE MIXTURES

The time versus laterally confined swell pressure relationships for the bentonite-illite series are shown in Figs. A7-1 to A7-5. They are somewhat erratic, with the swell pressure falling and rising before the maximum value was reached. The only reason for this appears to be that the strain gauge indicator was shared with another person working in a different room, whilst these readings were being taken. It is feared that some of the adjustments were altered as the instrument was moved from place to place, thus altering the initial calibration. The whole system was recalibrated after this series had been completed.

(Calibration involves dismantling the swell pressure apparatus in order to apply known loads to the tie bars; thus, a recalibration can not be made once a test is in progress). For the other series of tests made in this study the readings were taken without moving the instrument, thus avoiding any distortion of the initial calibration. These tests yielded well behaved and reliable results, see Chapter 3.

Consideration was given to the idea of repeating the bentonite-illite series of swell pressure tests. However, the original mixtures had been expended. The bentonite varied from bag to bag, and it would have been necessary to make a complete set of five new mixtures, and to make compaction tests on these. However, only one swell

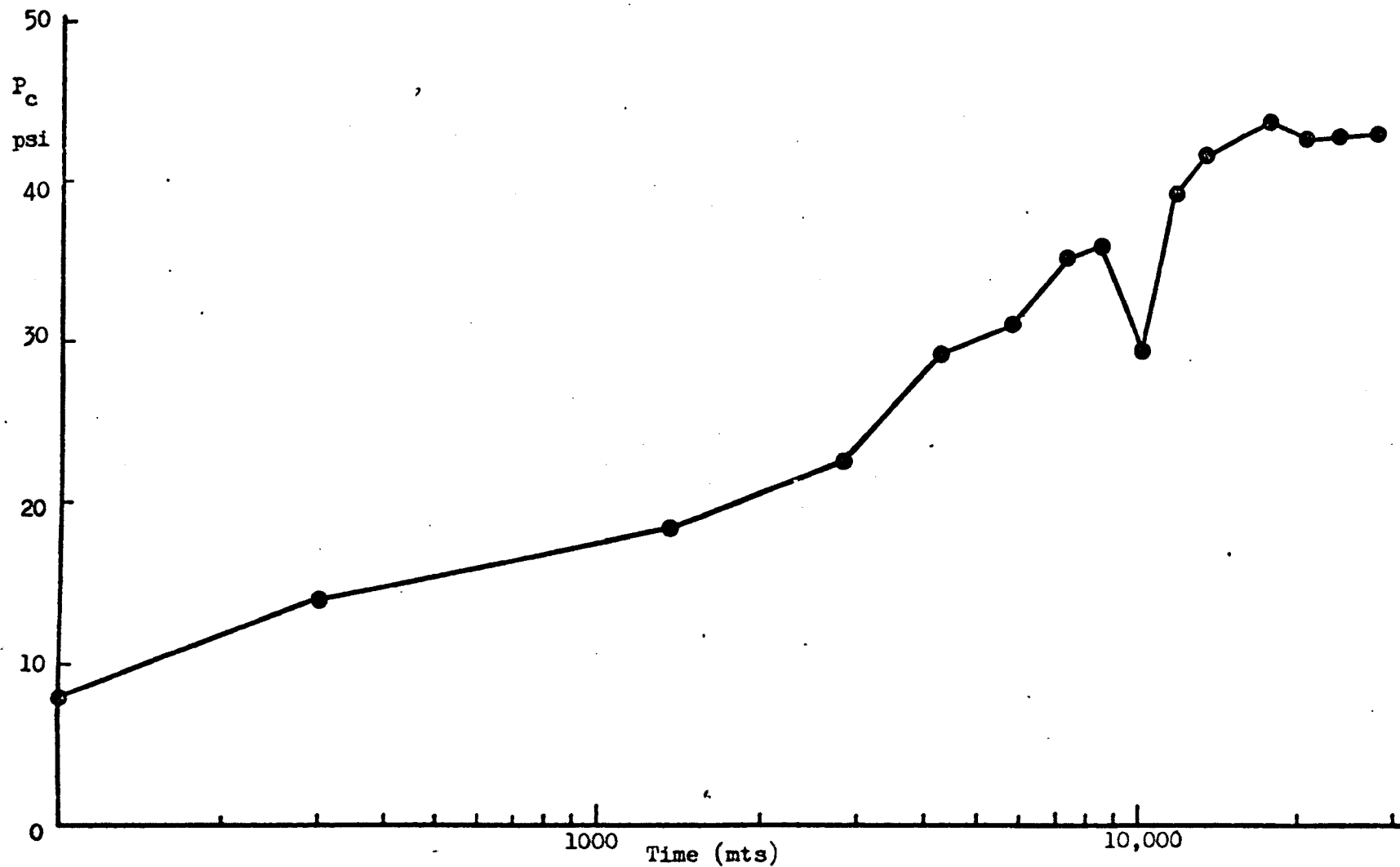


Fig. A7-1 Laterally Confined Swell Pressure versus Time, Bentonite 16.7% - Illite 83.3%

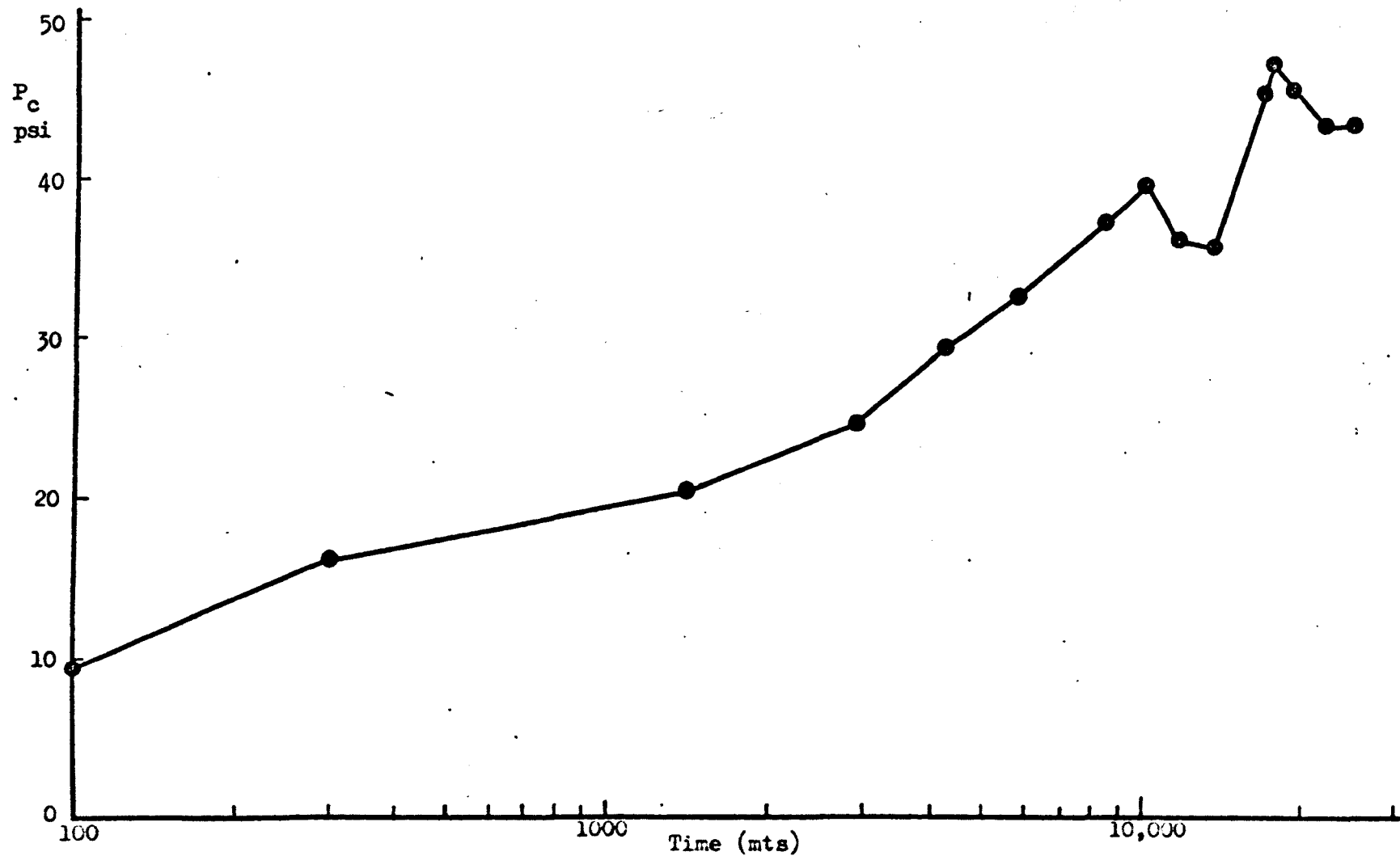


Fig. A7-2 Laterally Confined Swell Pressure versus Time, Bentonite 33.3% - Illite 66.7%

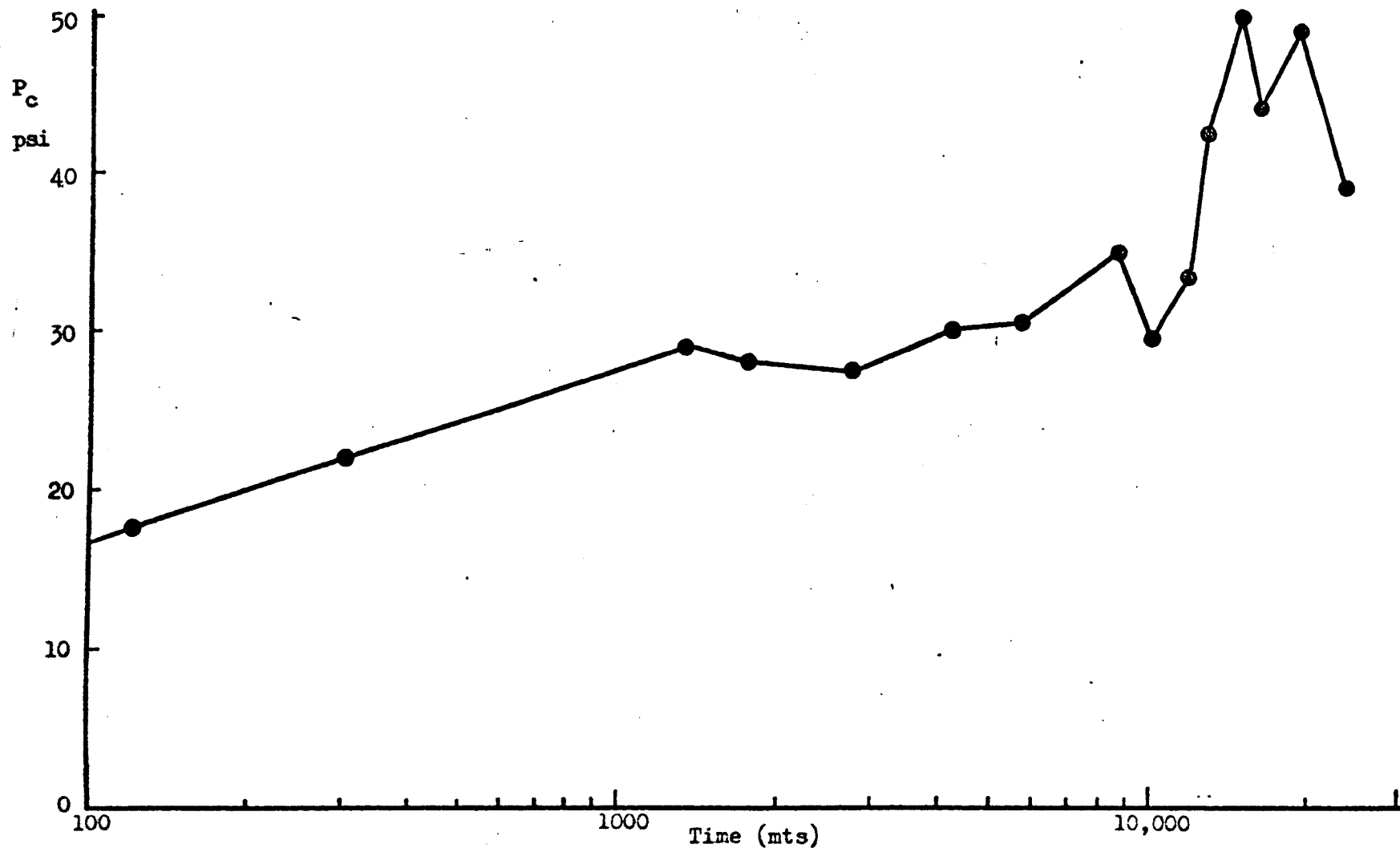


Fig. A7-3 Laterally Confined Swell Pressure versus Time, Bentonite 50% — Illite 50%

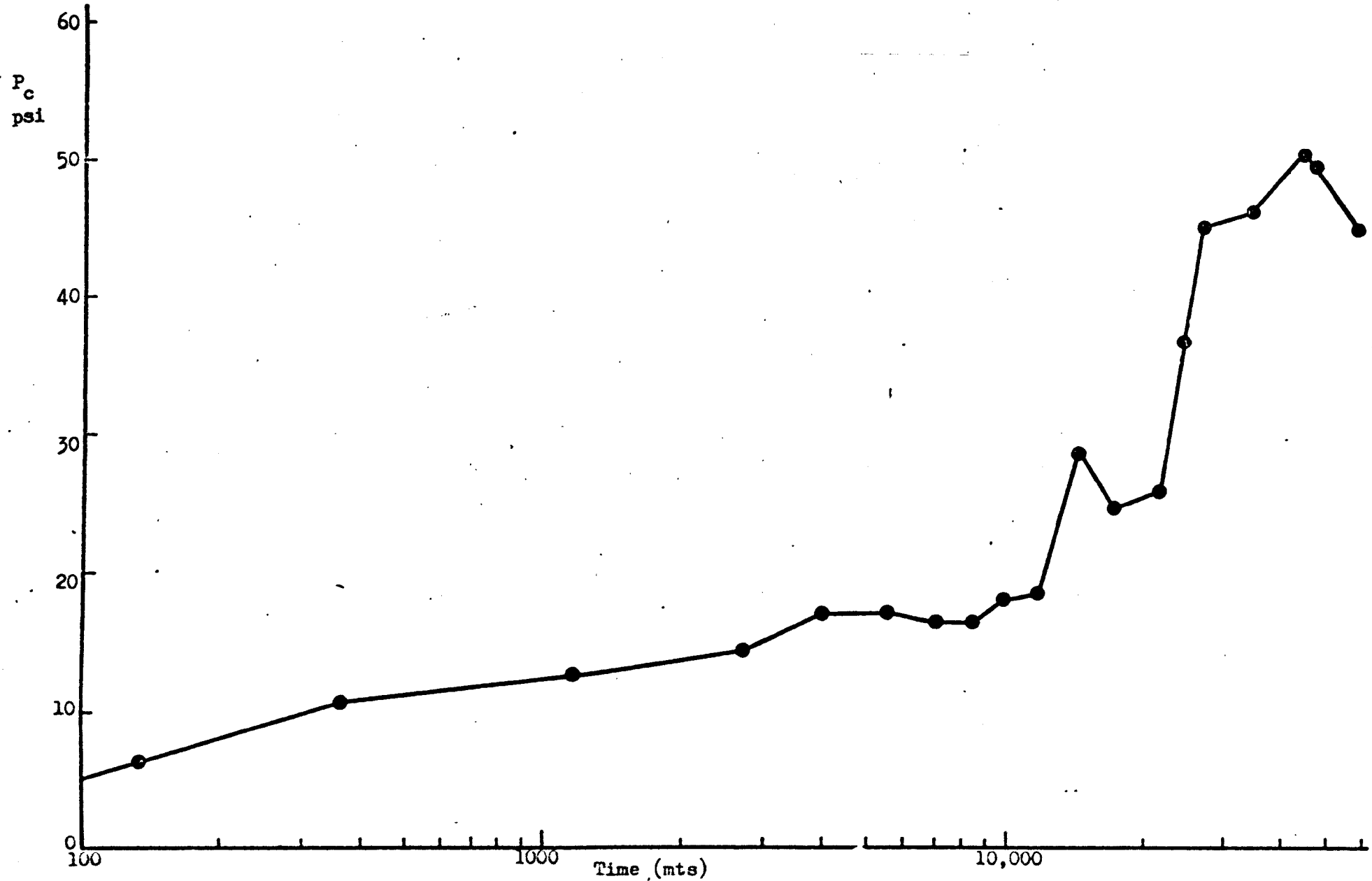


Fig. A7-4 Laterally Confined Swell Pressure versus Time, Bentonite 66.7% - Illite 33.3%

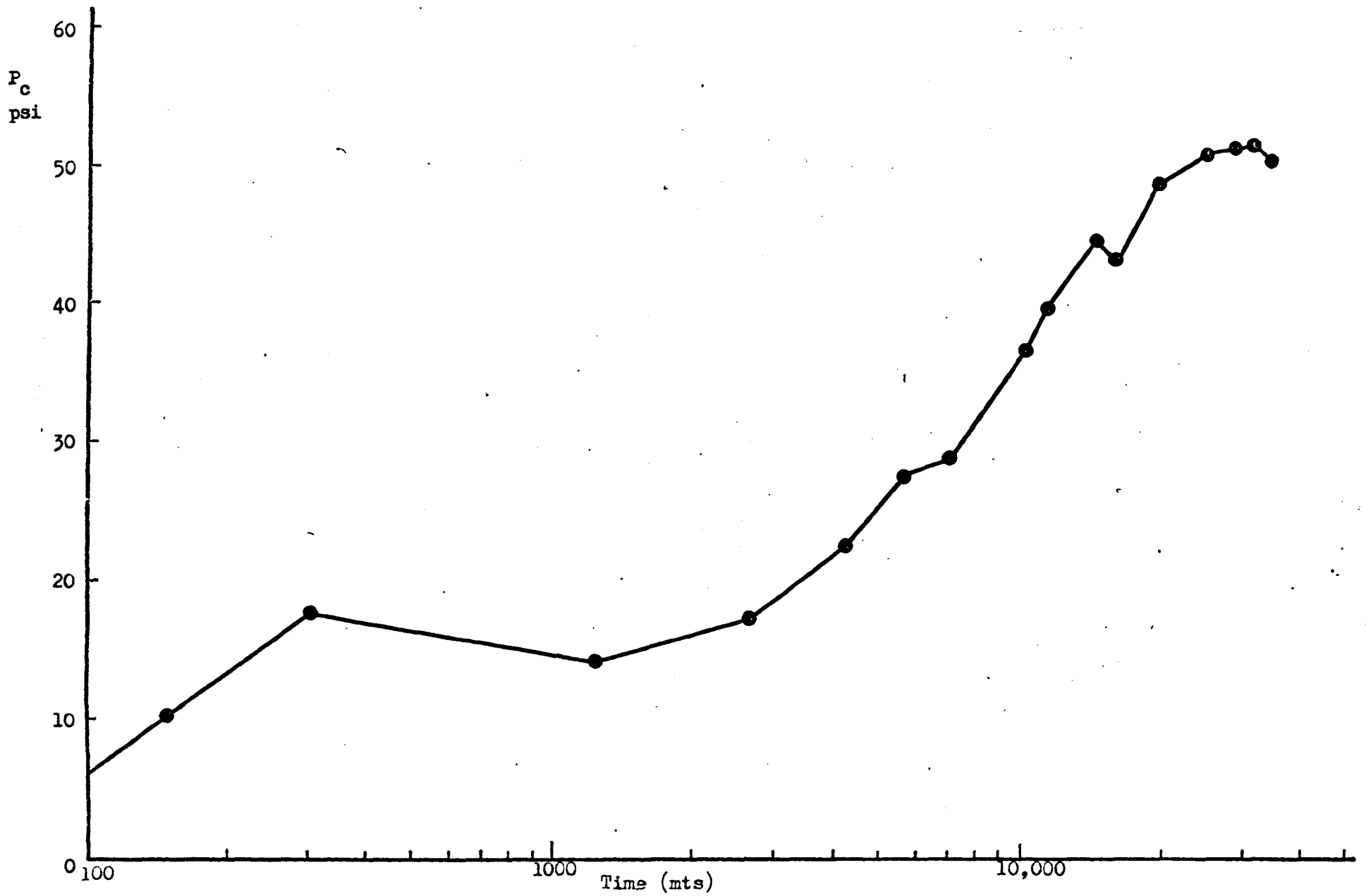


Fig. A7-5 Laterally Confined Swell Pressure versus Time, Bentonite 83.3% — Illite 16.7%

pressure apparatus was available, and five tests at about 4 weeks per test would have taken too long after the main programme had been completed. Since these tests were less important than those on the clay + sand mixtures, and since this series of tests was not expected to show large variability, it was decided not to repeat these tests. Furthermore, the tests at the end points (pure bentonite and pure illite) yielded satisfactory results, and the maximum swell pressures of the mixtures fall between the values for the two pure clays in a linear manner as could be expected, see section 5.3.4.

APPENDIX 8

ANALYSIS OF PARTICLE SIZE DISTRIBUTION CURVES

Assume that soil x is a mixture of a fraction F of soil A and a fraction (1-F) of soil B. Then any given particle size fraction of soil x, P_x , is given by:-

$$P_x = F P_a + (1-F) P_b \quad (\text{A8.1})$$

where, P_a = Particle size fraction of A,

P_b = Particle size fraction of B.

Hence, the fraction F may be calculated from:-

$$F = \frac{P_x - P_b}{P_a - P_b} \quad (\text{A8.2})$$

The particle size distributions were split into seven size fractions, clay, fine silt, medium silt, coarse silt, fine sand, medium sand and coarse sand, which seemed suitable for these particular samples. The method of analysis is outlined below:

1. Calculate the values of F for each of the seven fractions in turn using equation (A8.2)
2. Find the weighted average of these seven values of F, where the weighted average is proportional to the difference between the two soil sources involved.

$$\text{Weight, } W = |P_a - P_b| \quad (\text{A8.3})$$

Find the mean of the seven fractions calculated in Step 1, by using the formula:

$$\text{Mean Fraction, FM} = \frac{\sum_1 (F \times W)}{\sum_1 W} \quad (\text{A8.4})$$

3. Calculate the error in fractions using:

$$\text{error, E} = (F - FM) \quad (\text{A8.5})$$

4. Calculate the mean square error in fractions using the formula:

$$\text{Mean Square Error, EM} = \frac{\sum_1 E^2 \times W}{\sum_1 W} \quad (\text{A8.6})$$

5. Using the following formula, calculate in turn the seven predicted proportions of particle size distributions of soil x :

$$Q = P_b + \left[FM \times (P_a - P_b) \right] \quad (\text{A8.7})$$

where Q is the proportion of predicted particle size for any size fraction under consideration.

In this method of analysis, the mean square error in fractions calculated by eq . (A8.6) was used to measure the goodness of fit. However, the main method of assessment used was to compare the observed against predicted particle size distributions graphically. The final results of this analysis are reported in Chapter 5 (Figs.5.41 to 45), and are discussed in section 5.4.2 .

Appendix 9

CALCULATION OF SAMPLE EXPANSION, etc.

α_i and α_f in Tables 5.1, 5.4 and 5.5 were calculated to one place of decimals by subtracting \mathcal{V}_i and \mathcal{V}_f from e_i respectively. The small discrepancies in the Tables are due to rounding off.

The expansion in the Tables 5.1, 5.4 and 5.5 was calculated by using the final measured water content at the end of swell pressure test, W_f , in the following way:

$$W_w = W_s \times W_f \quad , \quad \therefore \quad W_f = \frac{W_w}{W_s}$$

$$V_w = \frac{W_w}{\gamma_w}$$

$$V_s = \frac{W_s}{G \gamma_w}$$

Assuming full saturation, it follows:

$$V_{\text{final}} = V_w + V_s$$

If $V_w + V_s \leq V_{\text{initial}}$, it was assumed that the expansion was zero. Otherwise, expansion = $(V_w + V_s) - V_{\text{initial}}$.

The expansion is expressed as percentage with respect to the original volume.

The expansion (%) could also be calculated by using the formula:

$$\text{Expansion, \%} = \frac{V_f - e_i}{100 + e_i} \times 100,$$

but note that the figures in the Tables have been rounded, so their use in this equation will be slightly inaccurate.

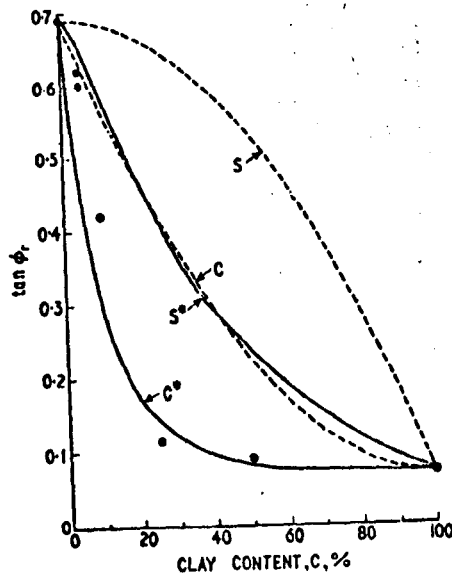
In the Tables 5.2 and 5.3 the calculations were made before they were rounded off by using the following formulae:

$$\alpha_i = e_i - \mathcal{J}_i$$

$$e_f = e_i + S_{cs}$$

$$\alpha_f = e_f - \mathcal{J}_f.$$

Appendix 10

Tan ϕ_r vs CLAY CONTENT, MONTMORILLONITE

TAN ϕ_r VERSUS CLAY CONTENT FOR Na-MONTMORILLONITE, $< 2\mu$, 0 G NaCl
 PER 1 (Points: Kenney's observations; C and S—predicted limits based on clay mineral
 content; and C* and S*—predicted limits based on clay plasma content)

Fig. A10-1 (Reproduced from Smart, 1970)

Smart (1970) suggested that for softer and more active clays, it may be that clay content should be based on the volume of clay plasma, which is conceived as a single phase comprising the clay mineral and its adsorbed water. In other words C was replaced by C*, where,

$$C^* = \frac{V_c + V_{abs}}{V_c + V_s + V_{abs}}$$

where,

V_c = volume of clay solids,

V_s = volume of sand solids,

V_{abs} = volume of adsorbed water.

Smart (1970) assumed $V_{abs} = 5 V_c$.

Appendix 11

ADDITIONAL REGRESSION EQUATIONS

The following regressions for the optimum compaction conditions, i.e. initial volumetric water content, v_i , and initial void ratio, e_i , supplement those in Tables 5.9 and 5.10.

$$(1) v_i = 0.172 + 0.0056C + 0.038(\text{ORG}) + 0.002 Z$$

$$(R^2 = 0.93) \text{ (0.1\% level of significance)}$$

$$(2) v_i = 0.157 + 0.011 \text{ PI} + 0.043(\text{ORG})$$

$$(R^2 = 0.94) \text{ (0.1\% level of significance)}$$

$$(3) e_i = 0.232 + 0.0058C + 0.031(\text{ORG}) + 0.0024 Z$$

$$(R^2 = 0.85) \text{ (1.0\% level of significance)}$$

$$(4) e_i = 0.22 + 0.013 \text{ PI} + 0.033(\text{ORG})$$

$$(R^2 = 0.94) \text{ (0.1\% level of significance)}$$

REFERENCES

Agarwal, K.B. and Sharma, S.C. (1973),

"A Method For Measuring the Swelling Pressure of an Expansive Soil,"

Proceedings of 3rd International Conference on Expansive Soils, Haifa, Vol.I, pp 155-160.

Aitchison, G.D (1969),

"A Statement of The Problems The Engineer Faces With Expansive Soils",

Proceedings of 2nd International Conference on Expansive Soils, Texas, Vol. I, pp18-23.

Alpan, .I.(1957),

"An Apparatus For Measuring The Swelling Pressure in Expansive Soils,"

Proceedings of 4th International Conference in S.M. & F.E., London, Vol.I, pp 3-5

Baracos, A. (1976),

"Clogged Filter Discs",

Geotechnique, Vol. 26, No.4, pp 634-36

Bear, F.E. (1955),

"Chemistry of The Soil,"

Monograph Series No 126, Reinhold Publishing Corporation, New York

Bishop, A.W. and Henkel, D.J. (1962),

"The Measurement of Soil Properties in the Triaxial Cell,"

Edward Arnold Books, London

British Standard Institution. British Standard 1377 : 1975:

"Methods of Testing Soil for Civil engineering purposes, London, 1975

Brown, G. (1961),

"The X-Ray Identification and Crystal Structures of Clay Minerals",

Mineralogical Society Publication, London.

Chen, F.H. (1975),

"Foundations on Expansive Clays",

Elsevier Scientific Publishing Company, Amsterdam.

Chu, T.Y. and Mou, C.H. (1973),

"Volume Change Characteristics of Expansive Soils Determined by Controlled Suction Tests",

Proceedings of 3rd International Conference on Expansive Soils, Haifa, Vol. I, pp 177-185.

Da Nilov (1964),

"Diagram For Dividing Soils into Ordinary, Slumping and Swelling Soils",

Translated from Osnobaniya, fundamental Mekhianik O Grunter, No/5.

Davidson, D.T. and Sheeler, J.B. (1952),

"Clay Fraction in Engineering Soils, III : Influence of Amount on Properties",

Proceedings of Highway Research Board, Washington, pp 558-563

Dawson, R.F. (1956),

"Discussion of Engineering Properties of Expansive Clays",

Transactions of A.S.C.E., Vol. 121.

Dinesh Mohan (1957),

"Strength and Consolidation Characteristics of Remoulded Black Cotton Soils",

Proceedings of 4th International Conference on S.M. & F.E., London, Vol.I, pp 72-74.

Dinesh Mohan (1973),

"Foundation Practice in Expansive Soils of India",
 Proceedings of 3rd International Conference on
 Expansive Soils, Haifa, Vol. I, pp 319-324.

Dixon, W.J. (1971),

"Biomedical Computer Programmes",
 Publication in Automatic Computation No 2,
 University of California Press, Berkeley, pp 233-47.

DSIR Publication, (1972),

"Soil Mechanics for Road Engineers",
 Road Research Laboratory, 7th Edition, London.

Dumbleton, M.J. and West, G (1966),

"The Influence of Coarse Fraction On The Plastic
 Properties of Clay Soils",
 Transport and Road Research Laboratory Report.No 36,
 2090, pp 1-17.

Finn, F.N. (1951),

"The Effect of Temperature on the Consolidation
 Characteristics of Remoulded Clay",
 Symposium on Consolidation Testing of Soils, American
 Society For Testing Materials, Special Technical
 Publication No 126, pp 65 -71.

Finn, W.D. and Strom, B, (1958),

"Nature and Magnitude of Swell Pressure",
 Proceedings of Highway Research Board, 37th Annual
 Meeting, No 313, pp 493-505.

Fredlund, D.G. (1969),

"Consolidometer Test Procedural Factors Affecting
 Swell Properties,"
 Proceedings of 2nd International Conference on
 Expansive Soils, Texas, Vol. I, pp 435-454.

Gray, R.W. and McCrum, N.G. (1969),

"Origin of the γ Relaxations in Polyethylene and Polytetrafluoroethylene,"

Journal of Polymer Science, Part A.2, Vol. 7,
pp 1329-55.

Gromko, G.J. (1974),

"Review of Expansive Soils",

Journal of The Geotechnical Engineering Division,
Proc. of A.S.C.E., Vol. 100, No. GT6, Proc Paper
10609, pp 667-687.

Hamilton, J.J. and Crawford, C.B. (1959),

"Improved Determination of Preconsolidation Pressure
of a Sensitive Clay",

American Society of Testing Materials, Special
Technical Publication No 254, pp 254-271.

Hardy, R.M. (1965),

"Identification and Performance of Swelling Soil
Types",

Canadian Geotechnical Journal, Vol. 11, No. 2,
pp 141-153.

Hashin, Z and Shtrikman, S,

J. Mech. Phys. Solids, 11, 127.

(Cited in Gray and McCrum, 1969)

Hilf, J.W. (1948),

"Estimating Construction Pore Pressures in Rolled
Earth Dams",

Proceedings of 2nd International Conference on
S.M. & F.E., Rotterdam, Vol. III, pp 234-240.

Hill, R (1963),

J. Mech. Phys. Solids, 11, 357.

(Cited in Gray and McCrum, 1969).

Holland, J.E. (1968),

"Some Considerations in the Behaviour of Quasi-Saturated Expansive Clays",

Ph.D Thesis, Monash University, Melbourne, Australia, (Cited in Kassiff, 1973)

Holtz, W.G. and Gibbs, H.J. (1956),

"Engineering Properties of Expansive Clays",

Transactions of A.S.C.E., Vol. 121.

Hveem, F.N. (1958),

"Suggested Method of Test For Expansion Pressure of Remoulded Soils",

Procedures For Testing Soils, American Society For Testing Materials, pp 285-286.

Jennings, J.E. (1961),

"A Comparison Between Laboratory Prediction and Field Observation of Heave of Buildings on Desiccated Subsoils,"

Proceedings of 5th International Conference on S.M. & F.E., Paris.

Jennings, J.E. and Knight, K (1958),

"The Prediction of Total Heave From The Double Oedometer Tests",

Symposium on Expansive Clays, South African Institution of Civil Engineers, Johannesburg, pp 13-19.

Kassiff, G. (1961),

"Swell Pressures Exerted on Asbestos-Cement Conduits,"

D.Sc (Tech) Thesis, Technion Israel Inst. of Tech., Haifa (Cited in Kassiff, 1973)

Kassiff, G (1973),

"General Report on Swelling Potential",

Proceedings of 3rd International Conference on Expansive Soils, Haifa, Vol. 2, pp 119-122.

Kassiff, G., Komornik, A., Wiseman, G., and Zeitlen, J.G. (1965).

"Studies and Design Criteria for Structures on Expansive Clays",

International Research and Engineering Conference on Expansive Clays, College Station, Texas.

Katti, R.K., Kulkarni, S.K., and Fotedar, S.K. (1969),

"Shear Strength And Swelling Pressure Characteristics of Expansive Soils, .

Proceedings of 2nd International Conference on Expansive Clays, Texas, pp 334-347

Kelley, W.P. (1948),

"Cation Exchange in Soils,"

Monograph Series No. 109, Reinhold Publishing Corporation, New York.

Kenny, T.C. (1967),

"The Influence of Mineral Composition on the Residual Strength of Natural Soils,"

Proceedings of the Geotechnical Conference, Oslo, Norwegian Geotechnical Institute, Vol. I, pp 123-129.

King, D.W. (1969),

"Soils of The Luton and Bedford District",

Special Soil Survey No 1, Agricultural Research Council Soil Survey, Harpenden, pp 1-39.

Komornik, A and David, D (1969),

"Prediction of Swelling Pressure of Clays",

Proceedings of A.S.C.E., S.M & F.E. Division, SM1, January, pp 209-225.

Lambe, T.W. (1960),

"A Report Completed for the Technical Studies Programme of the Federal Housing Administration".

(Cited in Chen, 1975)

Lashley, R and Lindsay, N.C. (1978),

"A Troublesome Soil",

Final Year Project Submitted to Dept. of Civil
Engg., Glasgow University.

Leonards, G.A. and Girault, P. (1961),

"A Study of the One-Dimensional Consolidation Test",

Proceedings of 5th International Conference on
S.M. & F.E., Vol. I, pp 213-218.

Livneh, M., Kassiff, G., and Wiseman, G. (1969)

"The Use of Index Properties in The Design of
Pavements on Expansive Clays",

Proceedings of 2nd International Conference on
Exoansive Soils, Texas, Vol. I, pp 218-234.

Matlock, H and Dawson, R.F. (1951),

"Aids in The Interpretation of the Consolidation
Tests",

Symposium on Consolidation Testing of Soils,
American Society for Testing Materials, Special
Technical Publication No. 126, pp 43-52.

McCormack, D.E. and Wilding. L.P. (1975),

"Soil Properties Influencing Swelling in Canfield
and Geeburg Soils",

Soil Science Society of America Proceedings, Vol.
39, No. 3, pp 496-502.

Means, R.E. and Parcher, J.V. (1963),

"Physical Properties of Soils",

Charles E. Merrill Books, Inc., Columbus, Ohio.

Mielenz, R.C. and King, M.E. (1955),

"Phsyical-Chemical Properties and Engineering
Performance of Clays",

Bulletin, California, Division of Mines, No. 169.

Murdoch, J and Barnes, J.A. (1970),

"Statistical Tables,"

MacMillan Publication, London, 2nd Edition, pp 18-20.

Nayak, N.V. and Christinsen, R.W. (1971),

"Swelling Characteristics of Compacted, Expansive Soils",

Clays and Clay Minerals, Vol. 19, pp 251-261.

Noble, C.A. (1966),

"Swelling Measurements and Prediction of Heave For a Lacustrine Clay",

Canadian Geotechnical Journal, Vol. III, No.1, pp 32-41.

Norman H.Nie., Hadlai Hull, C., Jenkins, J.G.
Steinbrenner, K., Bent, D.H. (1975),

"Statistical Package For The Social Sciences",

McGraw-Hill Book Company, London.

Novaris-Ferreria, H. (1967),

"Influence of Clay Content on the Plasticity of Soils",

Fourth Regional Conference for Africa on S.M. & F.E., Cape Town, Vol. I, December, pp 261-266.

Olson, R.E. and Mesri, G (1970),

"Mechanism Controlling The Compressibility of Clays",

Journal of S.M. & F.E., Proceedings of A.S.C.E., SM6, 96, pp 1863-78.

Paul, B. (1960),

"Prediction of Elastic Constants of Multiphase Materials",

Transactions of the Metallurgical Society of AIME, vol. 218, pp 36-41.

Polymer Handbook (1965) : Interscience Publishers,
New York.

- Ranganatham, B.V. and Satyanarayana, B (1965),
 "A Rational Method of Predicting Swelling Potential",
 Proceedings of VI International Conference on S.M.
 & F.E., Montreal, Vol. I, pp 92-97.
- Reuss, A (1929),,
 "Z. Angew. Math. Mech., "
 9,49 (Cited in Gray and McCrum, 1969)
- Roderick, G.L. and Jin, J.S. (1963),
 "Characteristics of Some Clays From Wisconsin",
 Highway Research Board, Bulletin No 463, pp 51-62.
- Rowe, P.W. and Barden, L (1966),
 "A New Consolidation Cell,"
 Geotechnique, Vol. 16, pp 162-170.
- Seed, H.B., Woodward, R.J., and Lundgren, R. (1962),
 "Prediction of Swelling Potential For Compacted Clays",
 Proceedings of A.S.C.E., S.M & F.E. Division, SM3, June,
 pp 53-87.
- Seed, H.B., Mitchell, J.K., and Chan, C.K.(1962)^a,
 "Studies of Swell and Swell Pressure Characteristics
 of Compacted Clays,"
 Highway Research Board, Bulletin No 313, pp 12-39.
- Seed, H.B., Woodward, R.J. and Lundgren, R (1964),
 "Clay Mineralogical Aspects of The Atterberg Limits",
 Journal of S.M. & F.E., Proceedings of A.S.C.E.,
 SM4, 90, pp 107-131.
- Skempton, A.W. (1961),
 "Horizontal Stresses in an Over-Consolidated Eocene
 Clay",
 Proceedings of 5th International Conference on S.M. &
 F.E., Vol. I, pp 351-357.

Smart, P (1970),

"Residual Shear Strength,"

Journal of S.M. & F.E., Proceedings of A.S.C.E.,
Vol. 96, No SM6, pp 2181-2183.

Smart, P, (1975)

"The Double Oedometer Test",

Lecture Notes, Unpublished.

Terzaghi, K and Peck, R.B. (1967),

"Soil Mechanics in Engineering Practice",

John Wiley and Sons, Inc, 2nd Edition, New York.

Timoshenko, S and Goodier, J.N. (1951),

"Theory of Elasticity",

McGraw-Hill Book Company, New York.

Uppal, H.L. and Palit, R.M. (1969),

"Measurement of Swelling Pressure of Expansive Clays"

Proceedings of 2nd International Conference on
Expansive Clays, Texas, pp 250-255.

Vijayvergiya, V.N. and Ghazzaly, O,I, (1973),

"Prediction of Swelling Potential For Natural Clays",

Proceedings of 3rd International Conference on
Expansive Soils, Haifa, Vol. I, pp 227-236.

Voigt, W, (1910),

"Lehrbuch der Kristallphysik",

Teubner, Leipzig, (Cited in Gray and McCrum, 1969)

Ward, W.H., Samuels, S.C. and Butler, M.E. (1959),

"Further Studies of The Properties of London Clay",

Geotechnique, Vol. 9, pp 33.

Williams, A.A.B. (1957),

"Discussion on Jennings's Paper",

Transactions South African Institute of Civil
Engineers, Vol. 8.

Yarwood, T.M. and Castle, F (1959),

"Physical and Mathematical Tables",

London (MacMillan).

Yong, R.N. and Warkentin, B.P. (1966),

"Introduction To Soil Behaviour",

The MacMillan Publishing Company, New York.